

Functional characterization of the gene
schlappohr (CG7739) during development of
Drosophila

Dissertation
for the award of the degree
“doctor rerum naturalium”
of the Georg-August-University Göttingen

Submitted by
Nils Halbsgut
from Lüneburg

Göttingen, 2010

Referent: Prof. Dr. Andreas Wodarz

Korreferent: Prof. Dr. Ernst Wimmer

Tag der mündlichen Prüfung: 05.07.2010

Table of contents

A Functional characterization of the gene <i>schlappohr</i> (CG7739) during development of <i>Drosophila</i>	4
A Summary.....	4
A.1 Introduction.....	6
A.1.1 Cell polarity and Par/aPKC complex	6
A1.1.1 Domain structure of Baz and identification of Schlappohr in a yeast-two-hybrid screen against the conserved N-terminal region of Baz.....	7
A.1.2 Eclosion in <i>Drosophila</i>	8
A.1.2.1 Neuropeptides and the hormonal regulation of eclosion.....	8
A.1.2.2 Bursicon and its role in cuticle tanning and wing expansion in <i>Drosophila</i>	9
A.1.3 T-cell immunomodulatory protein, the mammalian orthologue of Shlp plays a regulatory role in the adaptive immune system	15
A.1.4 Innate immunity in <i>Drosophila</i>	16
A.1.4.1 Humoral immunity.....	16
A.1.4.2 Cellular immunity.....	21
A.1.5 Aim of this thesis	23
A.2 Results	25
A.2.1 Molecular characterization of Schlappohr (Shlp).....	25
A.2.1.1 Organization of the <i>shlp</i> gene	25
A.2.1.2 Domain structure of the Schlappohr (Shlp) protein	25
A.2.1.3 Phylogenetic analysis of Shlp	26
A.2.2 Expression and subcellular localization of Shlp.....	29
A.2.2.1 Generation of Shlp antibodies.....	29
A.2.3 Localization of <i>shlp</i> mRNA.....	34
A.2.4 Generation of <i>shlp</i> mutant alleles	36
A.2.5 Phenotypic analysis of <i>shlp</i> mutant alleles	38
A.2.5.1 Viability of <i>shlp</i> mutants.....	38
A.2.5.2 Apicobasal cell polarity of <i>shlp</i> mutant embryos.....	39
A.2.5.2 Wing defects of <i>shlp</i> mutant flies and rescue of the mutant phenotype.....	40
A.2.5.3 Overexpression of Shlp-eGFP in flies mimics the defects seen in <i>shlp</i> ¹³¹ mutant flies.....	49
A.2.5.4 Functional analysis of Shlp protein domains	50
A.2.6 Infection and survival experiments to test a potential role of Shlp in immunity	51
A.2.7 Biochemical characterization of Shlp protein.....	53
A.2.6.1 Glycosylation of Shlp	53
A.2.6.2 Secretion of Shlp in <i>Drosophila</i> S2r cells.....	54
A.2.6.3 Screen for interaction partner of Shlp by a yeast two-hybrid-screen	55
A.2.6.4 Screen for interaction partners of Shlp by mass spectrometry.....	56
A.3 Discussion.....	59
A.3.1 Domain structure and phylogenetic analysis of Shlp.....	60
A.3.2 Expression and subcellular localization of Shlp protein and <i>shlp</i> mRNA	60

A Table of contents

A.3.2.1	Localization of Shlp protein	60
A.3.2.2	Localization of <i>shlp</i> mRNA	61
A.3.3	Phenotypic analysis of <i>shlp</i> mutants	61
A.3.4	Overexpression of Shlp-eGFP in flies mimics the defects seen in <i>shlp</i> ¹³¹ mutant flies	63
A.3.5	Structure-function analysis of the Shlp protein	64
A.3.6	Biochemical characterization of Shlp protein.....	64
A.3.6.1	Secretion of Shlp in <i>Drosophila</i> S2r cells.....	64
A.3.6.2	Glycosylation of Shlp	65
A.3.6.3	Screen for interaction partners of Shlp	65
A.3.7	Infection experiments to test a potential role of Shlp in immunity.....	66
B	The role of vesicle trafficking for cell polarity of <i>Drosophila</i> neuroblasts.....	67
B	Summary	67
B.1	Introduction	68
B.1.1	Cell polarity and asymmetric division of NBs	68
B.1.2	Polarity and vesicle trafficking.....	75
B.1.3	Vesicle trafficking and asymmetric cell division of NBs	80
B.2	Results	82
B.2.1	Influence of a general block of endocytosis on neuroblast cell polarity	82
B.2.2	The influence of exocyst function on embryonic NB cell polarity.....	84
B.2.3	The influence of a general block of endocytosis on larval NB polarity	86
B.2.4	Mosaic analysis with a repressible cell marker (MARCM) screen to analyze the influence of vesicle trafficking on NB polarity	87
B.2.4.1	Role of exocyst function for larval NB polarity.....	90
B.2.4.2	Role of α -Adaptin function for larval NB polarity.....	93
B.2.4.3	Role of Rab 5 function for larval NB polarity	94
B.2.4.4	Role of ESCRT function for larval NB polarity.....	95
B.3	Discussion	96
B.3.1	Influence of a general block in endocytosis on embryonic and larval neuroblast cell polarity	96
B.3.2	The influence of exocyst function on embryonic neuroblast cell polarity	97
B.3.3	Mosaic analysis with a repressible cell marker (MARCM) screen to analyze the influence of vesicle trafficking on neuroblast polarity.	98
B.3.3.1	Role of exocyst function for larval neuroblast polarity.....	98
B.3.3.2	Role of α -Adaptin function for larval neuroblast polarity.....	99
B.3.3.3	Role of Rab 5 function for larval neuroblast polarity	100
B.3.3.4	Role of ESCRT function for larval neuroblast polarity.....	100
B.3.4	Does vesicle trafficking play a role in NB polarity?.....	101
C	Material and Methods.....	103
C.1	Chemicals and reagents	103
C.1.1	Microscopy and Image Acquisition	103
C.1.2	DNA sequence analysis.....	103
C.2	Genetic methods	103

C.2.1 Fly breeding and fly stocks	103
C.2.2 Generation of <i>shlp</i> mutant alleles by imprecise excision of P-elements	107
C.2.3 Generation of transgenic flies	110
C.2.4 Mosaic analysis with a repressible cell marker (MARCM) in <i>Drosophila</i> larval brains	110
C.2.5 Generation of embryos maternally and zygotically mutant for <i>onion rings</i> ¹⁴²⁻⁵ (<i>exo84^{omr}</i>)	113
C.2.6 Analysis of embryos lacking <i>shibire</i> gene function during neuroblast division	114
C.2.7 Analysis of L3 larvae lacking <i>shibire</i> gene function during neuroblast division	114
C.3 Immunohistochemistry	114
C.3.1 Antibodies	114
C.3.2 Embryo fixation and immunofluorescent antibody staining	116
C.3.3 Fixation and antibody staining on brains of wandering third instar larvae	117
C.3.4 Cell fixation and staining	117
C.3.5 Fluorescent <i>in situ</i> hybridization (FISH) on embryos and brains of wandering third instar larvae	117
C.3.6 DAPI staining of adult wings	119
C.4 Cell culture	119
C.4.1 Cell transfection	119
C.5 Molecular biology methods	119
C.5.1 List of plasmid vectors	119
C.5.2 List of oligonucleotides	120
C.5.3 Sequencing of plasmids and PCR products	122
C.5.4 Generation of <i>shlp</i> expression constructs	123
C.5.5 Generation of Shlp deletion constructs by site directed mutagenesis	125
C.5.6 Generation of pGEX-4T-1- <i>shlp</i> -exDom	126
C.5.7 Single fly genomic DNA preparation	126
C.5.8 Extraction of genomic DNA from flies	127
C.5.9 Long-template PCR	127
C.6 Biochemical methods	128
C.6.1 Western Blot and Immunoprecipitation	128
C.6.2 Deglycosylation of Shlp-GFP	128
C.6.3 Secretion assay in S2r cells	128
C.6.4 Purification of GST-Shlp-exDom for antibody production	129
C.6.5 Pull down with Shlp-intra beads	130
C.7 Infection and Survival experiments	131
D References	132
Danksagung	152
Curriculum Vitae	153

A Functional characterization of the gene *schlappohr* (CG7739) during development of *Drosophila*

A Summary

In this study the role the gene *schlappohr* (*shlp*) during development of *Drosophila melanogaster* (*Drosophila*) was investigated. *shlp* encodes a evolutionary highly conserved protein with unknown function. Structure prediction based on the SMART algorithm suggests that Shlp is a single pass transmembrane protein with a classical amino terminal signal peptide followed by a large extracellular domain. Furthermore, a C-terminal only 22 amino acid long intracellular domain is predicted. An alignment of this domain with orthologues from different species reveals high sequence conservation with the very last eight carboxy terminal amino acids even being identical between all animal orthologues.

This highly conserved C-terminal domain of Shlp was identified in a yeast-two-hybrid screen with the N-terminus of the polarity protein Bazooka (Baz) as bait. Initially the subcellular localization of Shlp in embryonic neuroblasts (NBs) pointed to a role during the establishment of cortical localization of Baz in NBs, a process which is until now poorly understood. However, further analysis of a *shlp* mutant that was generated in the course of this study provided evidence that Shlp is not required for cortical recruitment of Baz. Analysis of the *shlp* mutant also revealed that the cortical localization of Shlp in NBs was an artifact caused by the antibody used in immunofluorescence stainings.

shlp mutant flies are viable and fertile but show defects in wing expansion and cuticle tanning that are strikingly similar to defects found in flies with defective Bursicon (Burs) signaling, however with a much lower penetrance. Therefore, we checked for genetic interaction between *shlp* and *rickets* (*rk*), the gene encoding the presumptive Bursicon receptor DLRG2. Despite striking similarities in the observed defects, it was not possible to show that these two genes genetically interact in the same pathway. In unexpanded wings of *shlp* mutant flies apoptosis of epithelial cells, which is a process that is necessary for proper wing maturation, was severely delayed. In the central nervous system of third instar larvae mutant for *shlp* the expression pattern of the molting hormone Burs was disturbed with some neurons especially in the thoracic region lacking Burs expression. This suggests that the observed defects in adults might be caused by a reduced number of Burs expressing neurons. Overexpression of a C-terminally eGFP

tagged version of Shlp completely inhibited wing expansion, suggesting that this protein has a dominant negative function.

Since, TIP, the mammalian homologue of Shlp has a role in immunity, we analyzed if the humoral immune response is affected in *shlp* mutant flies. However, neither the humoral response to infection with Gram-negative nor the response to Gram-positive bacteria was affected.

Additionally, we provide evidence that N-terminally eGFP-tagged Shlp (eGFP-Shlp) is secreted in *Drosophila* Schneider cells and that Shlp is glycosylated. This is in agreement with the biochemical properties of the mammalian homologue. In order to identify interacting proteins of Shlp, pull down experiments coupled with mass spectrometric analysis of the precipitated proteins were performed.

A.1 Introduction

In this study I analyzed the role of the gene *schlappohr* (*shlp*, CG7739) during development of *Drosophila melanogaster* (*Drosophila*). It was identified as a potential interaction partner of the polarity regulator Bazooka. Because of a potential role of *shlp* during wing development of the adult fly and a potential involvement in the innate immune response, I will also give a short introduction into these processes.

A.1.1 Cell polarity and Par/aPKC complex

Polarity is characteristic for most cells. It is defined as asymmetry in cell shape, protein distribution and cell function. One cell type that displays extreme polarity is the epithelial cell, which has an important function in multicellular organisms by forming physiological and mechanical barriers and organizing tissue architecture (Suzuki and Ohno, 2006). Epithelial cells show an apico-basal polarity that is reflected by the shape of the cell, the oriented alignment of the cytoskeletal networks and the uneven distribution of organelles and molecules (Knust and Bossinger, 2002). Even the plasma membrane of epithelial cells is polarized, being divided into two distinct regions: the apical domain, facing the external environment or the lumen; and the basolateral domain, that is in contact with other cells or the basal substratum (Knust and Bossinger, 2002).

Another highly polarized cell type is the neuronal stem cell of the ventral neurogenic region of the *Drosophila* embryo, the so called neuroblast (NB). Embryonic NBs give rise to the nervous system of the larva. NBs delaminate as individual cells from the neuroectodermal epithelium into the interior of the embryo where they are positioned between the ectoderm and the mesoderm, enter mitosis and divide repeatedly in an asymmetric fashion (Fig. A.1-1) (Wodarz and Huttner, 2003; Wodarz, 2005). In each division another NB and a smaller ganglion mother cell (GMC) is generated. NBs will continue dividing while the GMCs divide only once more to generate a pair of neurons or glial cells (Wodarz, 2005). During delamination and division NBs retain the pronounced polarity they inherited from the neuroectodermal epithelium (Wodarz, 2005).

Apico-basal polarity of the neuroectodermal epithelium and NBs is controlled by the highly conserved PAR/aPKC complex. During NB divisions this complex additionally controls correct spindle orientation and asymmetric segregation of cell fate determinants (Wodarz *et al.*, 2000; Petronczki and Knoblich, 2001). The complex consisting of the proteins Bazooka (Baz), *Drosophila* atypical Protein Kinase C (DaPKC) and *Drosophila* Partitioning defective

protein 6 (DPar6), localizes to the subapical region in epithelial cells and forms an apical crescent in NBs (Wodarz *et al.*, 1999). Mutations in the genes encoding the complex lead to loss of apico-basal polarity in epithelia and in NBs (Wodarz *et al.*, 2000; Petronczki and Knoblich, 2001; Wodarz, 2005).

How the PAR/aPKC complex localizes to the apical cortex in NBs is not known, since all subunits of the complex are cytoplasmic proteins. Recently, it has been shown that Baz can bind to phosphoinositide membrane lipids mediated by a conserved region in its C-terminal part. Therefore this region of Baz could mediate cortical localization by direct interaction with the plasma membrane (Krahn *et al.*, 2010). However, whether this is the only mechanism regulating cortical localization of the PAR/aPKC complex in NBs or if additional adaptor proteins aid in mediating its cortical localization is currently unknown.

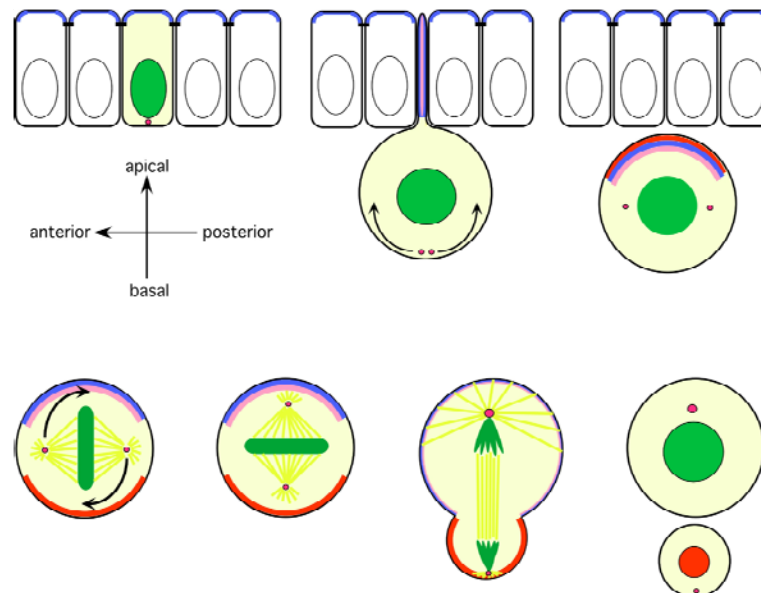


Figure A.1-1: A simulated time course of delamination and division of a single neuroblast in the ventral neurogenic region of a *Drosophila* embryo. The subcellular localization of several polarity regulators, cell fate determinants and their adaptor proteins is indicated in different colors. The PAR/aPKC complex is indicated in blue, Pins, Gai and Dlg in pink, the cell fate determinants and their adaptor proteins (Pros, Miranda, Numb, Pon, Brat) in red, DNA in green, microtubules in yellow. The red dots represent centrosomes. In the epithelium for simplicity, only the PAR/aPKC complex is shown. Pins = Partner of Inscuteable, Dlg = Discs large, Pros = Prospero, Pon = Partner of Numb, Brat = Brain tumor. Adapted after Wodarz and Huttner (2003).

A1.1.1 Domain structure of Baz and identification of Schlappohr in a yeast-two-hybrid screen against the conserved N-terminal region of Baz

Baz is an integral component of the PAR/aPKC complex. It is a large scaffolding protein containing an N-terminal conserved region 1 (CR1) that is required for homodimerization, three PDZ (Psd95, Discs large, ZO-1) domains in the central region of the protein, one aPKC

binding domain and a conserved region in the C-terminal part (Kuchinke *et al.*, 1998; Benton and St Johnston, 2003; Krahn *et al.*, 2010).

To identify novel adaptor proteins of the PAR/aPKC complex, a yeast-two-hybrid screen was carried out with the N-terminal region of Baz. This region was chosen because its high sequence similarity between *Drosophila*, *Caenorhabditis elegans* (*C. elegans*) and Vertebrates suggests a novel conserved function (Egger-Adam, 2005). One of the interaction partners, CG7739 or Schlappohr (Shlp) as we named it in this thesis because of its wing phenotype, is a novel transmembrane protein with a highly conserved, but so far undescribed intracellular domain that alone interacted with Baz in the yeast-two-hybrid screen. This interaction was particularly interesting because we speculated that Shlp might be a transmembrane protein that is needed to localize Baz to the plasma membrane in NBs and could therefore provide the missing link that tethers the PAR/aPKC complex to the cortex.

A.1.2 Eclosion in *Drosophila*

A.1.2.1 Neuropeptides and the hormonal regulation of eclosion

Neuropeptides regulate major developmental, physiological and behavioral changes both in invertebrates and vertebrates. Especially findings in the experimentally tractable nervous system of invertebrates have given valuable insights into neuropeptide biology. Continuous growth in arthropods requires the periodical shedding of the cuticle and replacement of the old with a new one. In the insect *Drosophila* the steroid hormone 20-hydroxy ecdysone (hereafter referred to as ecdysone) is released before all larval moults, pupation and eclosion and is responsible for the synthesis of a new cuticle (Riddiford, 1993; Luo *et al.*, 2005; Davis *et al.*, 2007). It also initiates the shedding of the old cuticle, a process that is called ecdysis and is controlled by a set of interacting neuropeptides (Fig. A.1-2), which ensure that this behavior only takes place at the end of each molt (Clark *et al.*, 2004). These neuropeptides act on tissues that had been ecdysone-primed before. It was shown in *Manduca sexta*, constant ecdysone levels block ecdysis (Davis *et al.*, 2007), indicating that a decline in hormone titer gives the signal to start ecdysis (Truman, 1996; Davis *et al.*, 2007). The first neuropeptide to be released after ecdysone levels have declined is ecdysis-triggering hormone (ETH) (Park *et al.*, 2002). ETH induces an increase in eclosion hormone (EH) levels (Clark *et al.*, 2004). EH functions in a positive feedback loop to further promote the release of ETH (Kingan *et al.*, 2001). While both ETH and EH promote pre-ecdysis behavior (Baker *et al.*, 1999), EH release within the central nervous system (CNS) additionally promotes the release of crustacean cardioactive peptide (CCAP) (Gammie and Truman, 1999; Clark *et al.*, 2004).

CCAP eventually starts the motor program that is needed for ecdysis behavior by activating Protein kinase A (PKA) (Gammie and Truman, 1999; Luan *et al.*, 2006). The post-eclosion hormone Bursicon colocalizes with most CCAP positive neurons and is secreted into the hemolymph following eclosion (Dewey *et al.*, 2004; Luo *et al.*, 2005; Mendive *et al.*, 2005; Luan *et al.*, 2006).

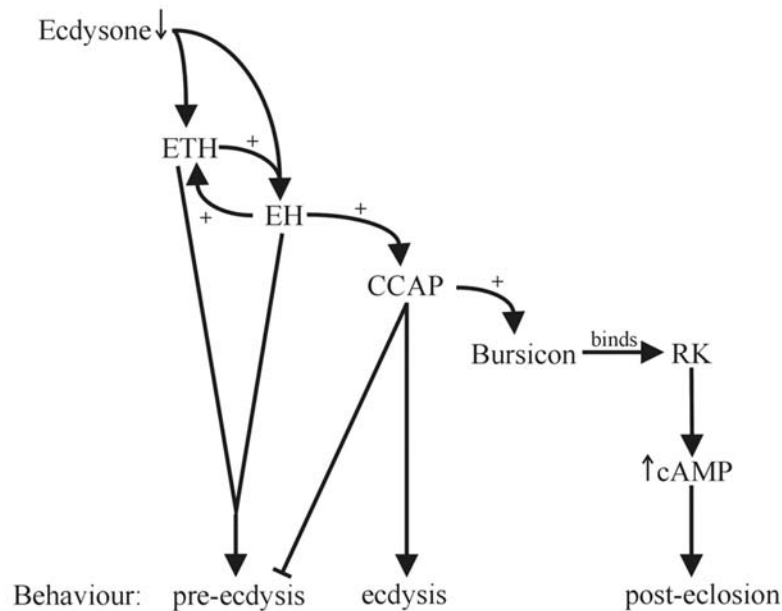


Figure A.1-2: Neuropeptide signaling during eclosion. Decreasing ecdysone levels trigger the release of ecdysis-triggering hormone (ETH), which causes the secretion of ecdysis hormone (EH). These hormones function together in a positive-feedback loop, amplifying the release of one another and regulate pre-eclosion behavior. In response to EH, crustacean cardioactive peptide (CCAP) is released, which ends pre-eclosion and promotes the eclosion motor program. During eclosion Bursicon is released in response to CCAP and binds to its receptor Ricketts (also DLGR2, see chapter A.1.2.2), which causes the induction of the post-eclosion motor program and subsequent tanning. Adapted after Davis *et al.* (2007).

A.1.2.2 Bursicon and its role in cuticle tanning and wing expansion in *Drosophila*

In addition to shedding the old cuticle, expand and harden a new one, which also happens during larval molts, adult eclosion in *Drosophila* requires the expansion of the, until this stage, folded wings. Therefore physiological changes in the wing cuticle must take place and internal pressure has to be increased to force hemolymph into the wings which will result in wing expansion (Peabody *et al.*, 2008). Wing expansion is followed by hardening of the cuticle and extensive cell death in the nervous and muscular system that aids eclosion (Kimura and Truman, 1990).

One of the key molecules regulating post-eclosion events is the neurohormone Bursicon (Burs). Burs was identified already in 1965 as a peptide neurohormone that initiates the

tanning of the insect cuticle (Fraenkel and Hsiao, 1965). It took almost 40 years until the molecular nature of Burs was discovered and it was shown that it is not only responsible for tanning and hardening of the cuticle but also for expansion of the wings during the final stages of insect morphogenesis (Dewey *et al.*, 2004; Luo *et al.*, 2005; Mendive *et al.*, 2005).

Dewey *et al.* (2004) discovered that one of the Burs subunits, called BURS is a 15 kDa protein encoded by the *Drosophila* gene *CG13419* and in 2005 it was shown simultaneously by two independent groups that Burs is a heterodimer formed by two cysteine knot proteins (Luo *et al.*, 2005; Mendive *et al.*, 2005), and serves as a ligand for the *Drosophila* Leucine-rich repeats-containing G-protein-coupled receptor 2 (DLGR2) encoded by the gene *ricketts* (*rk*) as predicted before (Baker and Truman, 2002). Luo *et al.* (2005) could also demonstrate that the second Burs subunit (Partner of bursicon) is encoded by the *Drosophila* gene *CG15284*. Since different nomenclatures were suggested for the two Burs subunits, we refer to the nomenclature of Mendive *et al.* (2005) who named *CG15284 bursicon β* (*bur β*) and the corresponding protein Bursicon β (Burs β). *CG13419* will therefore be named *bursicon α* (*burs α*) and the corresponding protein Bursicon α (Burs α).

Burs α and Burs β belong to the cysteine knot protein family (CKP), a class of vertebrate signal proteins that contain a consensus framework formed by six conserved cysteine residues (Honegger *et al.*, 2008). The cysteines establish disulphide bonds and form a ring. Three distinct domains form the typical three-dimensional structure of CKPs with two antiparallel β-strands (fingers) and an α-helical structure (heel). The exposure of hydrophobic residues to the aqueous surrounding leads to the formation of dimers (Honegger *et al.*, 2008). The CKP family of proteins contains the vertebrate glycoprotein hormones, growth factors, mucins and bone morphogenetic protein (BMP) antagonists (Honegger *et al.*, 2008). Burs α and β are most closely related to the BMP antagonists (Luo *et al.*, 2005). Members of the BMP antagonist family like Cerberus or Gremlin have been shown to antagonize the actions of BMP ligands during embryonic development and tissue differentiation in Vertebrates (Canalis *et al.*, 2003; Sudo *et al.*, 2004; Luo *et al.*, 2005).

Burs is a conserved peptide hormone that can be found in many arthropods. In the mid sixties Fraenkel and Hsiao (1965) could demonstrate this using the “ligated fly assay”: flies that were ligated around the neck immediately upon emergence remained white and soft. When a test solution, containing either hemolymph from a fly that just had darkened or active bursicon, was injected into the neck ligated flies, their cuticle darkened (Fraenkel and Hsiao, 1965; Honegger *et al.*, 2008). Hemolymph from three different fly species as well as hemolymph from four other insect orders was as well able to induce tanning in neck ligated flies

demonstrating a conserved function. Homologues of Burs α and Burs β can be found in many arthropods, including insects (Dewey *et al.*, 2004; Luo *et al.*, 2005; Mendive *et al.*, 2005; Robertson *et al.*, 2007; Van Loy *et al.*, 2007), crustaceans (Wilcockson and Webster, 2008) and arachnids (Robertson *et al.*, 2007). Both subunits in all species tested so far contain a predicted signal peptide, indicative of secreted proteins. In addition they contain eleven conserved cysteine residues. In analogy to the common structure of CKPs described above, it was suggested that Burs α and Burs β form a similar three dimensional structure with two antiparallel β -strands and one α -helical structure (Honegger *et al.*, 2008) (Fig. A.1-3).

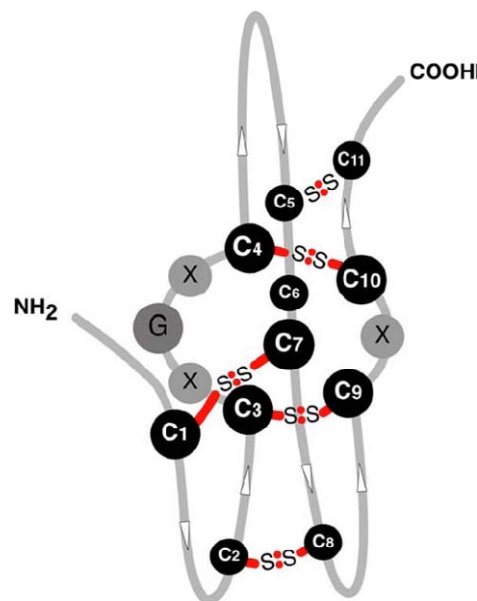


Figure A.1-3 Predicted cysteine knot structure of Burs α and Burs β . See text for details. Adapted after Honegger *et al.* (2008).

The bursicon heterodimer has been shown to bind to the DLGR2 receptor with high specificity (Luo *et al.*, 2005). DLGR2 belongs to the Leucine-rich repeat containing G-protein-coupled receptors (LGRs), a subgroup of G-protein coupled receptors (GPCRs). Characteristic for LGRs is an N-terminal region that contains multiple leucine-rich repeats, which are important for ligand binding (Honegger *et al.*, 2008; Van Loy *et al.*, 2008).

In cell culture experiments Luo *et al.* (2005) could show that binding of the Burs heterodimer to DLGR2 induces the production of cAMP. *rk* mutants in which no functional DLGR2 is produced do not tan and melanize and do not expand their wings either (Baker and Truman, 2002).

Different point mutations in the *burs* α gene were identified by Dewey *et al.* (2004) in a screen for mutations that affect wing expansion in *Drosophila*. In addition, flies homozygous for these mutant *burs* α alleles showed defective tanning. By introducing a *wildtype burs* α transgene into the mutant background, which was expressed under the control of *CCAP-*

GAL4, a GAL4 line that drives expression exclusively in CCAP expressing neurons (Park *et al.*, 2003), the defects could be rescued (Honegger *et al.*, 2008). These results together with the *rk* mutant wing phenotype strongly argue that Burs is essential both for cuticle tanning and wing expansion.

Wing expansion and maturation in *Drosophila*

As stated above, Burs signaling is essential for the final stages of wing development. Therefore a short overview of the processes leading to wing unfolding and maturation will be given here.

Freshly hatched flies unfold their wings by an increase in blood pressure that forces hemolymph into the wings. This increase in blood pressure is achieved by ingestion of air and tonic contraction of abdominal muscles (Baker and Truman, 2002). Recently, Tögel *et al.* (2008) showed that wing maturation additionally requires the pumping activity of wing hearts. Wing hearts are two bilateral muscular pumps that originate from eight embryonic progenitor cells arising in two pairs in parasegments 4 and 5 (Togel *et al.*, 2008). Flies lacking wing hearts show a severe wing phenotype which results in inability to fly.

The mature wing forms by the fusion of the ventral and dorsal layers of cuticle, which are secreted by the underlying epidermis (Honegger *et al.*, 2008). After approximately one hour both cuticular layers fuse and sclerotize to form a mature wing. For proper fusion and sclerotization of the cuticular layers most of the epithelial wing cells need to be removed. Kimura *et al.* (2004) showed that during wing spreading after eclosion, all cell of the wing except for the cells associated with the veins enter programmed cell death, delaminate from the epithelium and disappear into the thorax. Ectopic expression of a viral anti-apoptotic gene, *p35*, inhibited cell death suggesting that cysteine proteases, also known as caspases are involved in this process. Experimental evidence that Burs could be the signal to induce cell death comes from experiments based on the above mentioned “neck ligation assay”. Cell death of wing epithelial cells was inhibited in flies that had been neck ligated immediately after hatching, while cell death was normal when ligation occurred 20 min after hatching. In flies homozygous for the *rk^l* allele cell death also failed to happen, while injection of 8-Br-cAMP, a membrane permeable analogue of the second messenger for Burs, into these *rk^l* mutants restored cell death (Kimura *et al.*, 2004). They could further show that G-proteins and PKA are required for cell death in the wing, indicating that Burs signals through the cAMP/PKA pathway. Contradictory results were reported by Natzle *et al.* (2008), who still observed chromatin condensation, fragmentation and loss of nuclei in *rk^l/rk^t* trans-

heterozygous flies, suggesting that an independent or redundant pathway might exist to trigger cell death in the wing after eclosion. They proposed that this discrepancy between their data and that of Kimura *et al.* might be explained by a second site mutation in the original *rk^l* stock used by Kimura *et al.* that perturbs cell death.

Studies conducted with a GFP-tagged Armadillo (*Drosophila* β -catenin) transgene used to follow the changes of cell shape and adhesion in the wing suggested that clearance of the cells involves an epithelial-mesenchymal transition (EMT) (Kiger *et al.*, 2007). One hour after eclosion Armadillo-GFP was lost from the membrane and became cytoplasmic; the epithelial cells of the wing rounded up, lost contact with each other and changed shape. Finally, they acquired a fibroblast-like phenotype and moved from the wing into the thoracic cavity (Kiger *et al.*, 2007). It has been suggested that EMT is regulated by bursicon, since in *burs a* and *rk* mutant alleles delamination of cells did not happen and Armadillo-GFP was still membrane-localized even 24 hours after eclosion (Natzle *et al.*, 2008). Tögel *et al.* (2008) reported contradictory results. They reported as mentioned above that cell clearance during wing maturation requires the hemolymph flow generated by the wing hearts and is therefore a passive process. In *in vivo* time-lapse studies they demonstrated that ablation of wing hearts resulted in abundance of delaminated cells in the wing, which prevented proper bonding of the two cuticle layers. A few years earlier it had also been proposed that hemocytes, cells that are responsible for phagocytosis of apoptotic cells as well as bacteria (Franc *et al.*, 1999; Zettervall *et al.*, 2004), participate in wing maturation by phagocytosis of apoptotic cells and secretion of extracellular matrix material that is needed for fusion of the two cuticular layers (Kiger *et al.*, 2001).

The epithelial cells of the wing secrete molecules of the extracellular matrix, including the Tissue-inhibitor-of-metalloproteinases (Timp), that are needed for the two epithelial cell layers to fuse (Kiger *et al.*, 2007). The final process in wing maturation is the sclerotization of the two wing cuticles, which is controlled by Burs (Honegger *et al.*, 2008).

Sclerotization and tanning of the insect cuticle

The cuticle of insects has to change its chemical properties to become stiff, pigmented and waterproof. This process is called cuticle maturation and can be subdivided into two processes, termed sclerotization (or hardening of the cuticle) and melanization, which is the tanning of the cuticle. The cuticle is composed of the procuticle, which is primarily composed of chitin and proteins and a thin hydrophobic, waxy, chitin-free layer, the epicuticle (Locke, 2001; Honegger *et al.*, 2008). The procuticle consists of two parts of which one is secreted

before ecdysis termed exocuticle and one which is secreted after ecdysis termed endocuticle. Both parts differ in their protein and chitin content. In many insects only the parts of the exocuticle become sclerotized (Andersen, 2010).

The central molecule both for sclerotization and tanning is dopamine, the synthesis of which is initiated by the hydroxylation of Tyrosine by tyrosine hydroxylase (TH) (encoded by the *pale* (*ple*) gene in *Drosophila*) to 3,4-dihydroxyphenylalanine (DOPA). DOPA is then decarboxylated by Dopa decarboxylase (encoded by *dopa decarboxylase* (*ddc*) in *Drosophila*) to dopamine (Davis *et al.*, 2007) (Fig. A.1-4). Davis *et al.* were the first to show that Burs plays a role in cuticle tanning by regulating phosphorylation of TH via PKA. The main site of activational control of *Drosophila* TH is the PKA phosphorylation site at serine 32 (Ser32) (Vie *et al.*, 1999). In *burs α* or *rk* mutant flies TH phosphorylation at this site was undetectable. Injection of 8-Br-cAMP restored TH phosphorylation at Ser32 and tanning, indicating that Burs signaling acts on the cAMP/PKA signaling pathway to control tanning of the insect (Davis *et al.*, 2007; Honegger *et al.*, 2008). While TH activation was controlled by Burs after eclosion, TH translation was controlled by EH and CCAP which are secreted before eclosion (Horodyski *et al.*, 1993; Ewer and Truman, 1996; Clark *et al.*, 2004; Davis *et al.*, 2007).

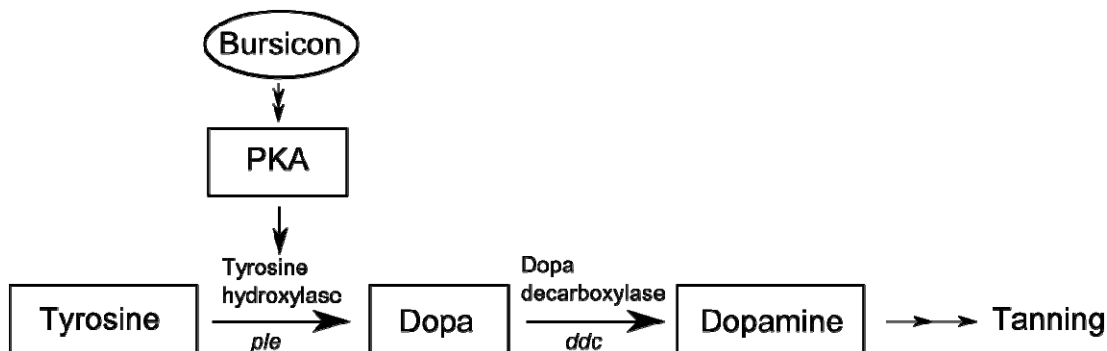


Figure A.1-4: Burs induces cuticle tanning by regulating phosphorylation of Tyrosine hydroxylase via PKA. Metabolites of Dopamine are required for tanning. Tyrosine hydroxylase (encoded by *ple*) converts Tyrosine into Dopa and Dopa hydroxylase catalyses the conversion of Dopa into Dopamine. PKA, which is activated in response to Burs signaling, activates Tyrosine hydroxylase by phosphorylation of Ser32. Adapted after Davis *et al.* (2007).

Burs expression in the insect nervous system

In the larval third instar stage Burs α is expressed quite broadly and includes two pairs of neurons in the subesophageal, thoracic and abdominal neuromeres (Fig. A.1-5) (Dewey *et al.*, 2004; Peabody *et al.*, 2008; Zhao *et al.*, 2008). Weak expression is also reported in a pair of

neurons in the brain (Peabody *et al.*, 2008). The expression pattern of Burs β is more restricted to a subset of neurons in the abdominal segments indicating that the functional dimeric hormone is also more restricted at this stage (Luo *et al.*, 2005; Peabody *et al.*, 2008). During pupal development (Fig. A.1-5), Burs α expression becomes increasingly restricted and in pharate adults the pattern of Burs α coincides completely with the expression pattern of Burs β (Luan *et al.*, 2006; Peabody *et al.*, 2008). At this stage, which directly precedes wing expansion, Burs α is usually expressed in 14 neurons in the abdominal ganglion and in two neurons in the subesophageal ganglion (Peabody *et al.*, 2008).

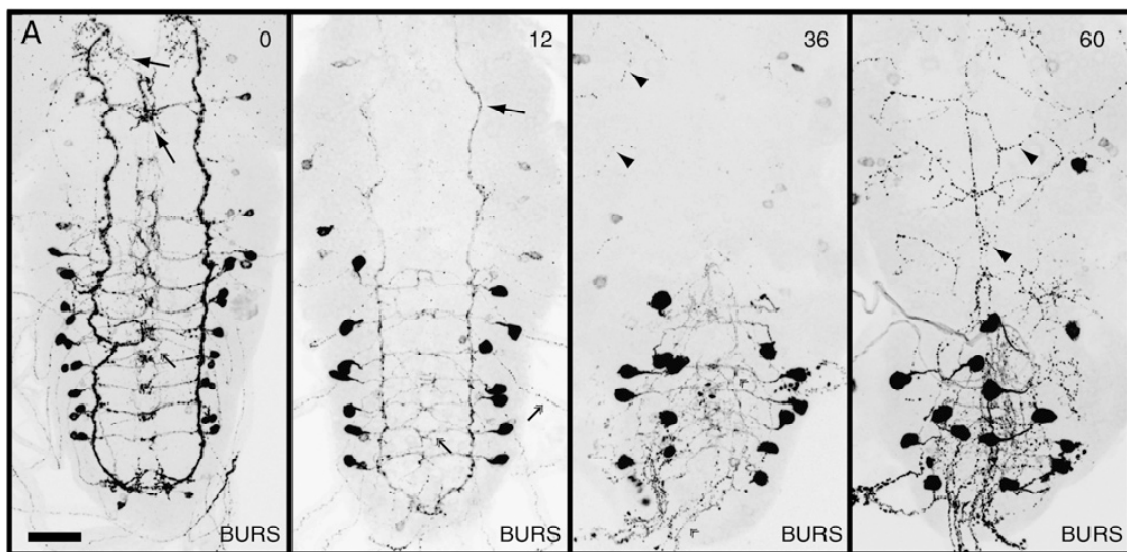


Figure A.1-5: Immunofluorescent antibody staining with anti-Burs α antibody (BURS) in the ventral nerve cord 0, 12, 36 and 60 hours after puparium formation (APF). In the course of development the expression of Burs α gets more restricted. 60 hours APF Burs α is only expressed in 14 neurons in the abdominal ganglion and in two neurons in the subesophageal ganglion (only one is shown) Arrows point to neurites that were pruned back by the next stage shown. Arrowheads represent new adult specific neurites and double feathered arrows point to abdominal neurites that were pruned back by the next stage shown. Scale bar is 50 μ m. Adapted from Zhao *et al.* (2008).

A.1.3 T-cell immunomodulatory protein, the mammalian orthologue of Shlp plays a regulatory role in the adaptive immune system

T-cell immunomodulatory protein (TIP), the mammalian orthologue of Shlp, was identified in a screen for novel secreted factors involved in T-cell biology. A cDNA library containing both novel secreted and transmembrane proteins was transiently transfected into mammalian 293T cells and the cell supernatant was tested in a number of cell-based high-throughput assays on primary human T-cells, T-cell lines and reporter cell lines (Fiscella *et al.*, 2003). TIP was identified in this screen as an inducer of Interferon- γ (IFN- γ) in primary T-cells. TIP is a

protein of 612 amino acids that shares no homology with any other protein with known function (Fiscella *et al.*, 2003). Northern blot analysis revealed that *tip* mRNA was ubiquitously expressed, but the protein could not be detected in T-cells, B-cells or monocytes suggesting that proteins expression or secretion may be modulated by an unknown mechanism. Western Blot analysis using an anti-TIP rabbit polyclonal antibody indicated that the protein is glycosylated. Furthermore it was shown that treatment of human and murine T-cells with the purified extracellular domain of TIP resulted in the secretion of IFN- γ as well as two other cytokines, Interleukin-10 (IL-10) and Tumor necrosis factor- α (TNF- α) by the T cells. p44/p42 Mitogen-activated protein kinase (MAPK) phosphorylation was induced immediately after treating human T cells with the extracellular domain of TIP indicating activation of MAPK signaling. To elucidate the *in vivo* function of TIP, graft-versus-host disease (GVHD) was induced in mice by injecting lymph node cells (LNC) from another mouse line. GVHD becomes obvious by a decrease in leukocytes and a severe decrease in erythrocytes, resulting in death. When TIP was injected into mice that had been injected with LNC, 80 % of mice survived this treatment, whereas only 20 % of mice survived that had been injected with LNC only (Fiscella *et al.*, 2003). This demonstrated that TIP had a positive effect on survival in GVHD.

A.1.4 Innate immunity in *Drosophila*

Innate immunity is common to all metazoans and serves as the first line of defense against microbial invaders. The *Drosophila* innate immune response comprises two main components. The humoral response depends on the production of antimicrobial peptides in the fatbody, which is equivalent to the mammalian liver (Ferrandon *et al.*, 1998; Tzou *et al.*, 2002a; Hoffmann, 2003; Ferrandon *et al.*, 2007).

The cellular response involves mainly the phagocytosis by plasmatocytes, the predominant blood cells in *Drosophila*, but also the melanization of invading pathogens by crystal cells and encapsulation of parasites by lamellocytes (Rizki and Rizki, 1984; Braun *et al.*, 1998; Hoffmann, 2003; Williams, 2007).

A.1.4.1 Humoral immunity

The use of powerful genetics that can be carried out in *Drosophila* led to the discovery of two signaling pathways – the Toll and (Janeway and Medzhitov, 2002) pathways – that play essential roles in the production of antimicrobial peptides (AMPs) by activating two *Drosophila* members of the Nuclear factor- κ B (NF- κ B) family of inducible transactivators

(Tzou *et al.*, 2002a; Hoffmann, 2003; Kim and Kim, 2005; Ferrandon *et al.*, 2007). The Toll pathway is mainly stimulated by challenge with fungi or Gram-positive bacteria and activates the NF- κ B-like transactivator Dif (Dorsal-related immunity factor). Infection with Gram-negative bacteria leads preferentially to activation of the Imd pathway and nuclear translocation of the NF- κ B-like transactivator Relish in adult flies (Kim and Kim, 2005; Ferrandon *et al.*, 2007). Several factors that are involved in the Toll signaling pathway were initially discovered due to their role in dorsoventral patterning in the embryo (Moussian and Roth, 2005). Moreover, the Toll signaling pathway shares some similarities to the mammalian signaling cascades downstream of the Interleukin-1 receptor (IL-1R) and the Toll-like receptors (TLRs) (Ferrandon *et al.*, 2007). The Imd pathway by contrast has some parallels to the Tumor-necrosis factor-receptor (TNFR) pathway in mammals (Hoffmann, 2003). Overviews of both pathways are given in Fig. A.1-6 and A.1-7.

The Toll signaling pathway

As stated above the Toll receptor is preferentially activated by Gram-positive bacteria and fungi. Activation of the Toll receptor is achieved by binding of a cleaved form of the cytokine Spätzle, which is a cysteine knot protein related to neurotrophins, to the ectodomain of the receptor (Weber *et al.*, 2003; Hu *et al.*, 2004). Although the insect genome encodes a family of Toll receptors, which comprises nine members (Tauszig *et al.*, 2000), only Toll itself has been demonstrated to have an immune function while the other 8 Toll receptors seem to play a role during development (Kambris *et al.*, 2002). Spätzle, the ligand for Toll, is synthesized as an inactive dimeric precursor, linked by a disulphide bridge. To be able to bind and activate Toll, it requires proteolytic processing of its 106 amino-acid C-terminus fragment. In response to infection, Spätzle is cleaved and thereby activated by Spätzle-processing enzyme (SPE). SPE is secreted as an inactive zymogen and is specifically activated by fungi and Gram-positive bacteria as a result of a proteolytic cascade (Jang *et al.*, 2006). SPE contains an amino-terminal CLIP-domain, a disulphide-knotted protein-protein interaction domain that is present in several invertebrate serine proteases involved in immune zymogen cascades (Jiang and Kanost, 2000). How SPE is activated in response to fungal or bacterial infection has not been determined in detail yet. Two genes have been identified that are required for Toll activation by Gram-positive bacteria named *semmelweis* and *osiris* (Michel *et al.*, 2001; Gobert *et al.*, 2003). *semmelweis* encodes a member of the peptidoglycan-recognition proteins (PGRPs) family and *osiris* a member of the Gram-negative-binding proteins (GNBPs) family, that were initially characterized in larger insect species through their ability to bind either to intact bacteria or structural motifs of bacteria (Lee *et al.*, 1996; Yoshida *et al.*, 1996; Kang *et*

al., 1998; Hoffmann, 2003). Interestingly, loss-of function mutations in either *semmelweis* or *osiris* result in reduced survival to Gram-positive infections and activation of Toll. It is likely that these blood-borne proteins cooperate to bind to Gram-positive bacteria and to activate the proteolytic cascade that results in the cleavage of Spätzle. This view is sustained by the fact that simultaneous overexpression of PGRP-SA and GNBPI results in challenge-independent activation of the Toll pathway (Gobert *et al.*, 2003). PGRP-SA binds preferentially to lysine-type peptidoglycan, which is common for many Gram-positive bacteria (Chang *et al.*, 2004; Wang *et al.*, 2006b; Ferrandon *et al.*, 2007). GNBPI functions together with PGRP-SA in recognition of several Gram-positive bacterial strains (Wang *et al.*, 2006b).

The Toll pathway is also preferentially triggered by fungi as monitored by the sustained expression of Drosomycin, one of the antimicrobial peptides that is induced by the Toll pathway (Lemaitre *et al.*, 1997; Rutschmann *et al.*, 2000a). One soluble receptor in the hemolymph, GNBPI3 has a central role in the detection of the fungal cell wall, mainly by recognizing glucans (Gottar *et al.*, 2006). A fungal protease of the entomopathogenic fungus *Beauveria bassiana* was shown to activate the Toll pathway by inducing the cleavage of Persephone (Ligoxygakis *et al.*, 2002), a *Drosophila* hemolymph zymogen, that is thereby transformed into an active protease (Gottar *et al.*, 2006). Persephone then triggers the activation of a proteolytic cascade that activates the Toll ligand Spätzle.

How is the signal that infection with Gram-positive bacteria or fungi triggers then relayed into the cell by the Toll pathway? The NF- κ B transcription factor factor DIF is employed as activator of antimicrobial peptide expression in adult flies (Meng *et al.*, 1999; Ferrandon *et al.*, 2007). Activated Spätzle binds to the amino-terminal Toll ectodomain and leads to homodimerization of two Toll receptors (Weber *et al.*, 2003; Ferrandon *et al.*, 2007) (Fig. A6). Homodimerization of the Toll receptor induces the assembly of a multivalent complex called Toll-induced signaling complex (TISC) around the intracellular tail of the Toll receptor. The intracellular tail of Toll contains a 150-amino-acid TIR (Toll, IL-1 receptor, and Resistance genes) domain. TISC is composed of the three death-domain (DD) containing proteins Myeloid differentiation primary response gene 88 (MyD88), Tube and Pelle (Sun *et al.*, 2002; Sun *et al.*, 2004). While MyD88, which like Toll also contains a TIR domain, and Tube are adaptor proteins, Pelle is a serine-threonine kinase (Sun *et al.*, 2004; Ferrandon *et al.*, 2007). Cactus, a homologue of the mammalian inhibitor of NF- κ B, is rapidly phosphorylated and degraded upon Toll activation, possibly through polyubiquitylation (Belvin *et al.*, 1995; Fernandez *et al.*, 2001; Ferrandon *et al.*, 2007). Degradation of Cactus leads to the graded release of the NF- κ B transcription factor DIF. The mechanism by which TISC activation leads

to Cactus phosphorylation is still under debate. One model is that the Cactus-DIF complex is recruited at the TISC, where Cactus may be phosphorylated (Ferrandon *et al.*, 2007). Once DIF is released, it can be translocated to the nucleus where it binds to NF- κ B response elements and thereby induces expression of genes encoding antimicrobial peptides like Drosomycin, an antifungal peptide or Defensin, which is active against Gram-positive bacteria (Wu and Anderson, 1998; Meister *et al.*, 2000; Ferrandon *et al.*, 2007).

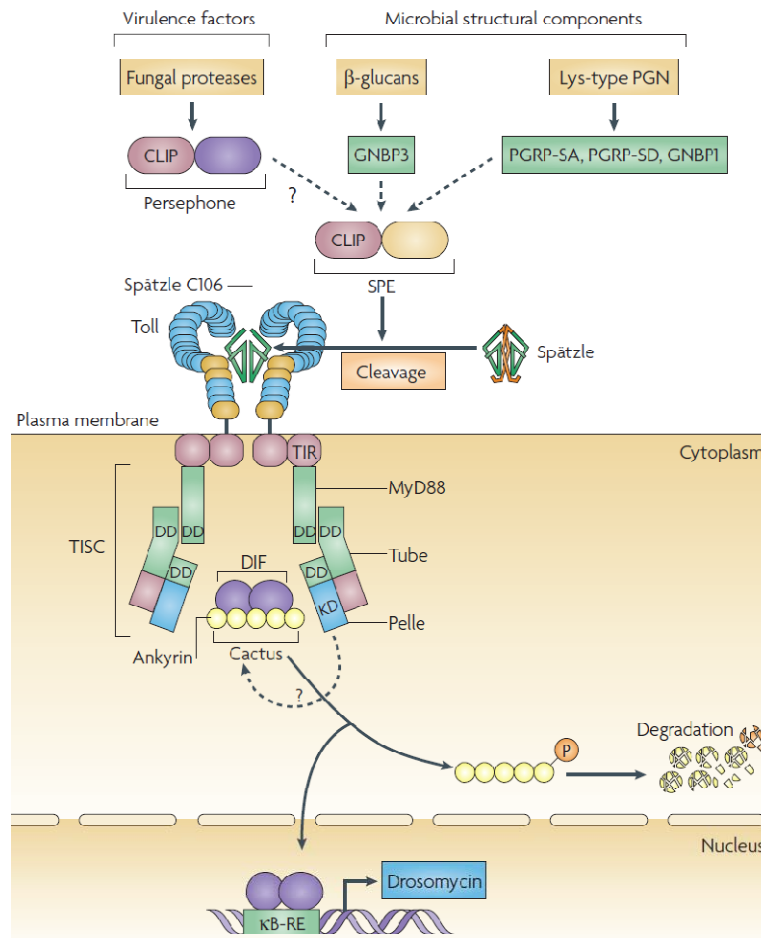


Figure A.1-6: The Toll pathway in adult *Drosophila*. Activation of the Toll pathway is mainly triggered by infection with fungi or Gram-positive bacteria. Activation of this signaling cascade results in the expression of antimicrobial peptides like Drosomycin. See text for details. Adapted after Ferrandon *et al.* (2008).

The Imd signaling pathway

A potent inducer of the Imd pathway is meso-diaminopimelic acid (DAP)-type peptidoglycan (PNG) derived from Gram-negative bacteria and certain Gram-positive bacteria, such as *Bacillus spp.* DAP-type PGN is recognized by the receptors PGRP-LC and PGRP-LE that also mediate the activation of the Imd pathway (Choe *et al.*, 2002; Gottar *et al.*, 2002;

Takehana *et al.*, 2002; Kaneko *et al.*, 2006; Aggarwal and Silverman, 2008). PGRP-LC is the main transmembrane (type II) receptor of the Imd pathway, while PGRP-LE is a cleaved secreted PGN sensor in the hemolymph. The genetic relationship between PGRP-LC and PGRP-LE is complex. PGRP-LC is partially required for the induction of the Imd pathway by challenge with Gram-negative bacteria, as shown by a decreased, but not absent, expression of antimicrobial peptides in loss-of-function mutants of the gene coding for PGRP-LC (Choe *et al.*, 2002; Gottar *et al.*, 2002; Ferrandon *et al.*, 2007). PGRP-LE mutants in contrast are not prone to most Gram-negative infections (Takehana *et al.*, 2004). Only double mutants for PGRP-LC and PGRP-LE have been shown to be susceptible to infection with Gram-negative bacteria suggesting that both PGRPs act synergistically in Imd pathway activation (Takehana *et al.*, 2004; Kaneko *et al.*, 2006; Ferrandon *et al.*, 2007). All in all, these experiments suggest that PGRP-LE activates the Imd pathway through PGRP-LC, probably by forming PGRP-LE/PGRP-LC heterodimers (Ferrandon *et al.*, 2007). The death domain containing protein Immune deficiency (Imd) has a central role in the Imd pathway (Fig. A7). It is required to transmit the signaling of active PGRP-LC and possibly that of non secreted PGRP-LE when it functions as a putative intracellular receptor (Gottar *et al.*, 2002; Kaneko *et al.*, 2006). The RHIM (RIP (receptor-interacting protein) homotypic interaction motive)-like motif in the N-terminal domain of both PGRP-LC and PGRP-LE is required to initiate signaling (Kaneko *et al.*, 2006). A domain mediating interaction between PGRP-LC and Imd has been shown to be dispensable for signaling and therefore it has been proposed that an unidentified factor might mediate the interaction between those two (Choe *et al.*, 2005; Kaneko *et al.*, 2006). Imd initiates two genetically different processes that ultimately target the NF- κ B transcription factor Relish (Fig. A7). After activation of Imd Relish is phosphorylated and thereafter cleaved by a second process (Silverman *et al.*, 2000; Stoven *et al.*, 2000). While the carboxy-terminal ankyrin repeats of the protein stay in the cytoplasm, the amino-terminal DNA-binding REL domain get translocated into the nucleus, where it activates mainly activates expression of AMP encoding genes (Stoven *et al.*, 2000). Imd signaling induces the phosphorylation of Relish through the activation of Transforming growth factor- β activated kinase 1 (TAK1) and I κ B kinase (IKK) complexes and cleavage of Relish through the Caspase homologue death-related ced-3/Nedd2-like protein (DREDD) (Rutschmann *et al.*, 2000b; Silverman *et al.*, 2000; Lu *et al.*, 2001). For the activation of TAK1 and IKK, several proteins are needed, including FAS-associated death domain (FADD), DREDD and molecules that are required in the conjunction of Lysine63 (K63)-linked polyubiquitin chains to unknown substrates (Leulier *et al.*, 2000; Naitza *et al.*, 2002; Zhou *et al.*, 2005). It has been

suggested that Imd could be such a substrate, because its mammalian orthologue Receptor-interacting protein 1 (RIP1) has been shown to be polyubiquitinated. Ligase function that is provided by the RING-finger of Tumor-necrosis-factor receptor associated factor (TRAF) in mammals may be mediated by the RING-finger containing *D. melanogaster* inhibitor-of-apoptosis protein 2 (DIAP2) in *Drosophila* (Ferrandon *et al.*, 2007). TAK1-binding protein 2 (TAB2) contains a zinc finger that binds to K63-linked polyubiquitin chains and therefore might participate in the assembly of a Kenny-Immune-response deficient 5 (IRD5) signaling complex (Ferrandon *et al.*, 2007).

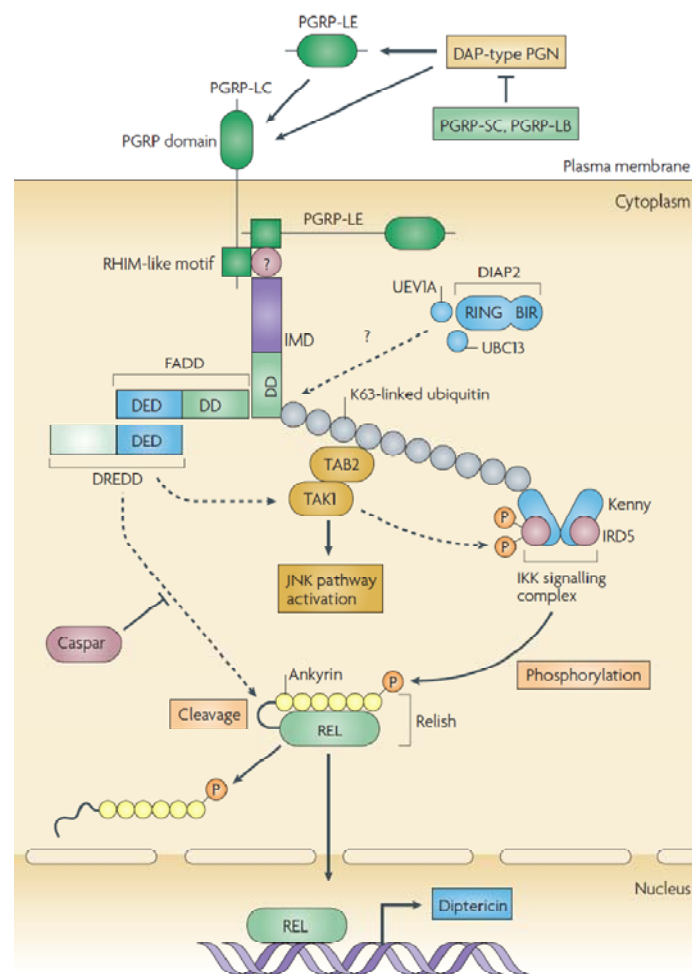


Figure A.1-7: The Imd pathway in *Drosophila*. Activation of the Imd pathway is predominantly initiated by infection with Gram-negative bacteria. Induction of this pathway leads to the expression of AMPs like Diptericin. See text for details. Adapted after Ferrandon *et al.* (2008).

A.1.4.2 Cellular immunity

Cellular immune responses in *Drosophila* larvae are carried out by three classes of circulating cellular immune surveillance cells, also known as hemocytes: Plasmatocytes, lamellocytes and crystal cells (Williams, 2007). Hematopoiesis, the generation of hemocytes, occurs in two distinct waves, one in embryos, the other one in larvae. Both lineages of hemocytes persist to

the adult stage (Stuart and Ezekowitz, 2008).

Plasmatocytes are phagocytic macrophage-like cells comprising about 90-95 % of the *Drosophila* hemocytes (Kim and Kim, 2005; Williams, 2007). Depending on the developmental stage, the main function of plasmatocytes is either the removal of effete cells and larval tissues, which happens in embryos and pupae, or in pathogen surveillance and clearance, as occurring in larvae and adults (Stuart and Ezekowitz, 2008). For phagocytosis to occur, receptors on the surface of the engulfing cell must recognize an invading organism or apoptotic cell. Several conserved proteins have been identified in insects that are required for proper phagocytosis, including complement-like factors, pathogen-recognition receptors and cytoskeletal proteins (Pearson *et al.*, 2003; Kocks *et al.*, 2005; Ulvila *et al.*, 2006; Williams, 2007).

Four classes of proteins are required for the recognition of pathogens: complement-like opsonins – opsonins are soluble molecules, that when bound to a particle enhance uptake of the particle –, scavenger receptors, Epidermal growth factor (EGF)-like-repeat-containing receptors and a highly variant receptor and opsonin, Down syndrome cell-adhesion molecule (DSCAM) (Stuart and Ezekowitz, 2008). The best characterized opsonins in *Drosophila* are a group of proteins, the Thioester-containing proteins (TEPs) (Stuart and Ezekowitz, 2008). A member of the TEP family, Macroglobulin-related protein (MCR), was found to bind and increase phagocytosis of *Candida albicans* (Stroschein-Stevenson *et al.*, 2006). Scavenger receptors are structurally unrelated multi-ligand receptors that are defined by their ability to bind to polyanionic ligands. An example for this receptor class is Croquemort, a *Drosophila* protein related to the CD36-like scavenger receptors that are conserved in mammals and flies. Croquemort is a receptor for apoptotic cells and in Croquemort-deficient embryos plasmatocytes have a very poor phagocytic activity for apoptotic cells, indicating its requirement for proper phagocytosis (Franc *et al.*, 1999). A well defined EGF-like-repeat-containing receptor is the *Drosophila* Eater protein. It is a type I membrane protein that contains 32 characteristic EGF-like repeats in its extracellular domain. Eater has been shown to directly bind to microbial ligands via its Amino-terminus and flies lacking Eater displayed impaired phagocytosis and decreased survival after bacterial infection although Toll and Imd signaling appeared normal (Kocks *et al.*, 2005). DSCAM is an immunoglobulin superfamily member and has been shown to bind to *E. coli* and potentially acts as both a phagocytic receptor and opsonin (Watson *et al.*, 2005; Stuart and Ezekowitz, 2008). It was predicted that DSCAM may have more than 38000 potential splice variants by combining constant and variable regions. (Schmucker *et al.*, 2000). Its role as phagocytic receptor and opsonin has

been supported by its identification in the phagosome proteome (Stuart *et al.*, 2007).

The other 5-10 % of circulating hemocytes are lamellocytes and crystal cells. Lamellocytes have a flattened shape and undertake the encapsulation of larger invaders such as parasite eggs and a third class of blood cells, crystal cells, secrete the components required for the melanization of invading organisms, as well as for wound repair (Rizki and Rizki, 1984; Lanot *et al.*, 2001; Kim and Kim, 2005; Williams, 2007).

A.1.5 Aim of this thesis

The aim of this thesis was to study the role of *shlp* (CG7739) in the development of *Drosophila*. Shlp was identified in a yeast-two-hybrid screen with the N-terminus of the polarity protein Baz. Since it is still not known how the Baz protein localizes to the apical cortex in neuroblasts, Shlp was a good candidate protein to achieve cortical localization of Baz because it is a highly conserved transmembrane protein. In a previous study a partial colocalization of Shlp with Baz at the apical cortex of embryonic neuroblasts as well as a redistribution of Shlp to the mitotic spindle in dividing neuroblasts was shown, which supported the hypothesis that Shlp might have a role in apical localization of Baz in neuroblasts and furthermore might provide a link between the PAR/aPKC complex and the spindle (Egger-Adam, 2005). In this thesis I generated a *null*-mutant of *shlp* (see chapter A.2) and provide evidence that localization of Bazooka and other polarity markers is not affected in these mutants arguing against a role for Shlp in localizing Bazooka to the apical cortex of neuroblasts. Furthermore I demonstrated by performing antibody stainings on *shlp* mutant embryos that the apical localization of Shlp in embryonic neuroblasts observed previously was an artifact due to the unspecific binding of the used antibody (data not shown).

shlp mutant flies are viable and fertile and display abnormal wing expansion and cuticle tanning. We named this gene *shlp* (*schlappohr*, german for “lop ear”) due to the characteristic wing defects displayed by mutant flies. These wing and cuticle phenotypes show striking similarities to defects observed in flies with impaired Burs signaling. Therefore our further studies in this thesis aimed in characterizing *shlp* particularly with regard to an involvement of this gene in Burs signaling.

For the mammalian homologue of *shlp*, TIP, it was shown that it has a regulatory role in the adaptive immune system (Fiscella *et al.*, 2003). To test if *shlp* has a role in the innate immune response of *Drosophila*, we checked *shlp* mutant flies for enhanced susceptibility to infection with bacterial pathogens in collaboration with the lab of Prof. Bruno Lemaitre, University of Lausanne.

A Introduction

To further gain insight into the molecular function of the Shlp protein, we performed assays to analyze the biochemical properties of Shlp and we performed pull down experiments to identify interacting proteins that might provide information in which molecular pathway Shlp is involved.

A.2 Results

A.2.1 Molecular characterization of Schlappohr (Shlp)

A.2.1.1 Organization of the *shlp* gene

The gene *CG7739* or *schlappohr* (*shlp*) as named in this thesis is located on the left arm of the third chromosome in 71D and is encoded on the reverse strand (Fig. A.2-1). It includes two exons of 320 bp and 1950 bp and encodes a protein of 596 aa. In the 5' UTR of *shlp* a P-element is inserted. P{EP}GE24395 (abbreviated GE24395) is located 103 bp upstream of the *shlp* start codon. This P-element is in the same orientation as *shlp* and its insertion is viable.

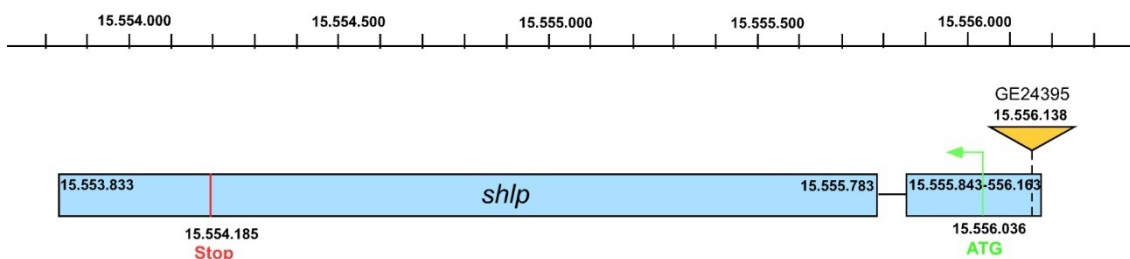


Figure A.2-8: Localization and organization of the *shlp* gene. *shlp* is located in 71D on the left arm of the third chromosome. It is encoded on the reverse strand and contains two exons (320 bp and 1950 bp, blue boxes). The start and stop codon is indicated with green or red color, respectively. Numbers denote the base pairs in the *Drosophila* genome. Yellow triangle marks the insertion of GE24395 that is located 103 bp upstream of the start codon in the 5'UTR of *shlp*. This P-element insertion is viable. The P-element is not drawn to scale.

A.2.1.2 Domain structure of the Schlappohr (Shlp) protein

Schlappohr (Shlp) is an evolutionary highly conserved protein, but its molecular function is unknown. A mammalian orthologue of Shlp, T-cell immunomodulatory protein (TIP), is implicated to play a role in the adaptive immune system. It was shown that treatment of T cells with purified TIP results in the secretion of INF- γ , TNF- α and IL-10 (Fiscella *et al.*, 2003). In a mouse acute graft-versus-host disease (GVHD) model, treatment with TIP had a protective effect. GVHD causes decrease in white blood cells and severe anemia, resulting in death. When treated with TIP, 80 % of animals survived, compared to only 20 % survivors in mock treated animals (Fiscella *et al.*, 2003).

To get a first idea on the domain structure of Shlp the amino acid sequence was analyzed

A Results

using SMART (Simple Modular Architecture Research Tool) sequence analysis tool (<http://smart.embl-heidelberg.de>) (Schultz *et al.*, 1998). Fig. A.2-2 is a schematic representation of the domain structure as predicted by SMART. Amino acids (aa) 1 to 20 of Shlp are predicted to be a classical signal peptide that is needed for membrane targeting and secretion of the protein. An Integrin alpha N-terminal domain is predicted for aa 80 to 334. Such domains are found in the amino terminus of integrin alpha subunits and are predicted to fold into a β -propeller structure that is involved in ligand binding (Springer, 1997; Leitinger *et al.*, 2000). Aa 396 to 437 are predicted to form a PAC (PAS-associated, C-terminal) motif. PAC motifs are found carboxy-terminally to PAS (Per, ARNT, Sim) motifs and contribute to the PAS structural domain (Ponting and Aravind, 1997). Animal PAS domains have protein-binding and dimerization functions (Lindebro *et al.*, 1995; Ponting and Aravind, 1997). Since PAC motifs are usually found together with PAS motifs and no PAS motif can be found in the Shlp protein sequence by the SMART program, it is not clear whether the predicted PAC domain is of any functional relevance. Aa 552 to 574 are predicted to form a single pass transmembrane domain. Topology prediction based on the TMHMM website <http://www.cbs.dtu.dk/services/TMHMM/> (Center for Biological Sequence Analysis, Technical University of Denmark) suggests that the amino terminal region (aa 1-551) of Shlp is extracellular while the short 22 amino acid long carboxy terminus is intracellular.

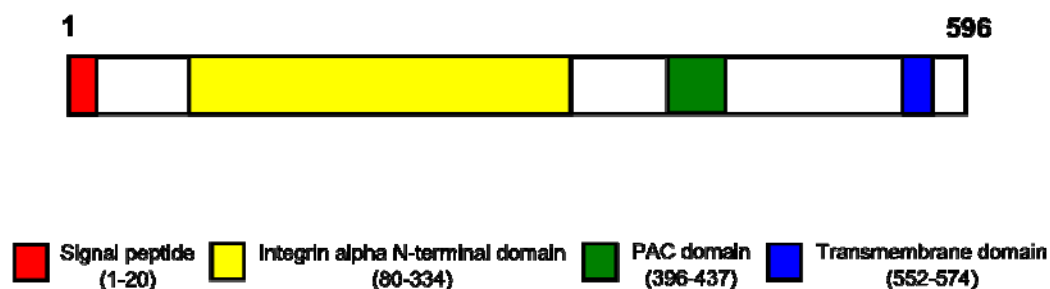


Figure A.2-9: Schematic representation of the domain structure of Shlp. The numbers below the legend indicate the amino acid position of the domains as predicted by the SMART sequence analysis tool. Different domains are color coded in the legend. Numbers in the legend represent the length of the indicated domains in aa.

A.2.1.3 Phylogenetic analysis of Shlp

To check whether Shlp is an evolutionary conserved protein and to identify similar proteins with known function, a BLAST (Basic Local Alignment Search Tool) search (Altschul *et*

al., 1990) was made using protein-protein BLAST from the National Center for Biotechnology Information (NCBI) homepage. The results reveal that Shlp is a highly conserved protein and orthologues of this protein exist in many phyla of the animal kingdom. Fig. A.2-3 shows a phylogenetic tree of Shlp orthologues with representatives of the phyla Chordata, Arthropoda and Nematoda. These proteins can therefore be grouped into a family of proteins termed TIP-like proteins after the chordate orthologues. Surprisingly, one protein and so far the only non-animal protein with sequence similarity to TIP-like proteins (Kaczanowski and Zielenkiewicz, 2003) can be found in the proteome of the Malaria parasite *Plasmodium falciparum* (see also Fig. A.2-3).

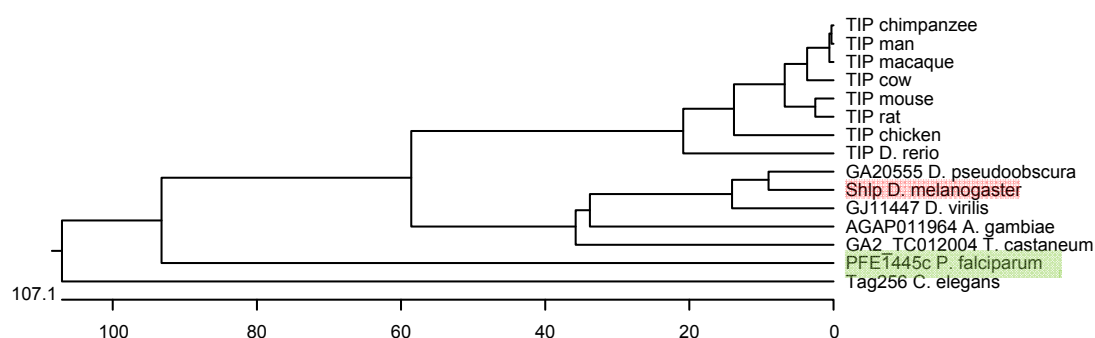


Figure A.2-10: Phylogenetic tree representation of an alignment of Shlp orthologues using ClustalW. *Drosophila melanogaster* Shlp is highlighted in pink. *Plasmodium falciparum* PFE1445c, the only non-animal orthologue is highlighted in green. Scale bar below represents amino acid substitutions (x100).

Next, we checked which proteins in the proteome of *Drosophila melanogaster* (*Drosophila*) have a similar protein sequence and thus could be related. BLAST searches were conducted and the four best fitting results from BLAST searches performed with BLAST from NCBI and SIB (Swiss Institute of Bioinformatics) were aligned together with their mouse orthologues using ClustalW. A phylogenetic tree representation of this alignment reveals that Shlp and TIP are more closely related than Shlp with the next related proteins in the *Drosophila* proteome (Fig. A.2-4). This is true for Inflated, gamma Tubulin and Importin alpha 3 as well as for Partner of Snf (Sans-fille). This strongly argues that Shlp is unique in the *Drosophila* proteome and therefore no paralogues of Shlp exist in the *Drosophila* proteome. Interestingly, by performing a protein-protein BLAST with TIP against the Human proteome, no TIP paralogue could be identified. This is surprising since many genes that exist as single copies in *D. melanogaster* are represented by several copies in vertebrates, most likely due to an extensive genomic duplication during early chordate evolution (McLysaght *et al.*, 2002).

A Results

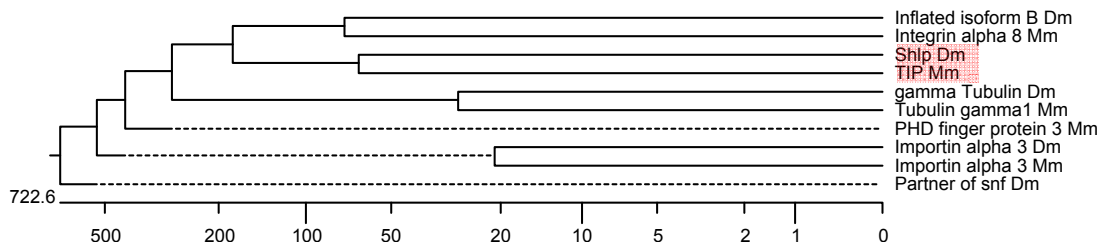


Figure A.2-11: Phylogenetic tree representation of an alignment of *Drosophila* Shlp, its only mouse orthologue TIP and other *D. melanogaster* proteins with sequence similarity to Shlp as well their mouse orthologues. Scale bar below represents amino acid substitutions (x100). Shlp and TIP are highlighted in pink. Dm = *Drosophila melanogaster*, Mm = *Mus musculus*.

One remarkable feature of Shlp and other proteins of the TIP-like protein family is the highly conserved potentially intracellular carboxy terminus (Fig. A.2-5). Its length is restricted to 22 aa in all animal species, it has a high content of charged aa and its last eight aa are the same in all animal orthologues examined so far (Fig. A.2-5). However, the function of this highly conserved 22 aa stretch is unknown.

Interestingly, although the overall amino acid sequence between Shlp and *Plasmodium falciparum* Q8I3H7 is better conserved than between *Caenorhabditis elegans* Tag256 and *D. melanogaster* Shlp (Fig. A.2-3), the amino acid sequence of the Q8I3H7 carboxy terminus differs substantially from the consensus seen in animal TIP like proteins (data not shown).

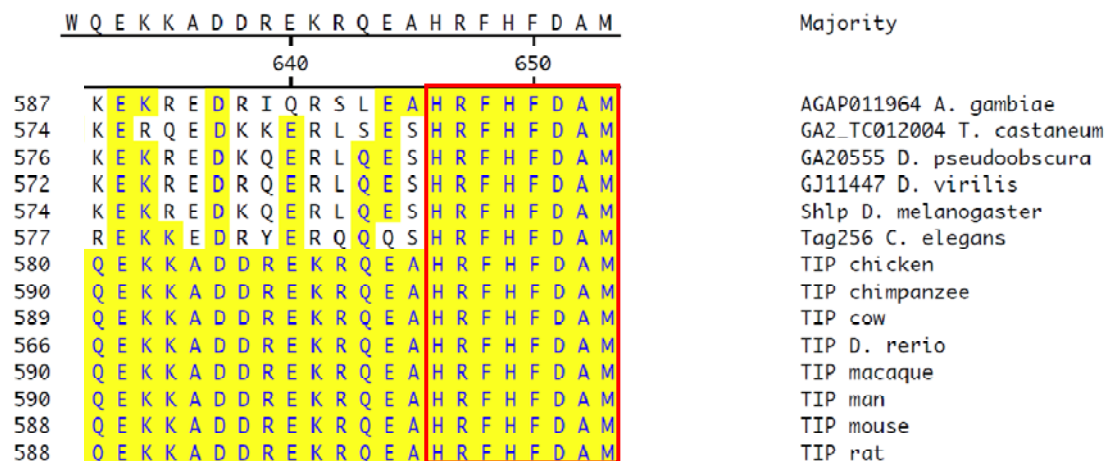


Figure A.2-12: Alignment of the highly conserved carboxy terminally intracellular region. Yellow coloring marks residues that match the consensus exactly. The red frame marks the last eight carboxy terminal aas.

A.2.2 Expression and subcellular localization of Shlp

A.2.2.1 Generation of Shlp antibodies

To further analyze the function of Shlp during development of *Drosophila*, antibodies against different peptides of Shlp were generated. Fig. A.2-6 schematically represents the epitopes in Shlp against which three different antibodies have been generated (CG7739 EP023003, CG7739 EP023004 and CG7739 SAC115).

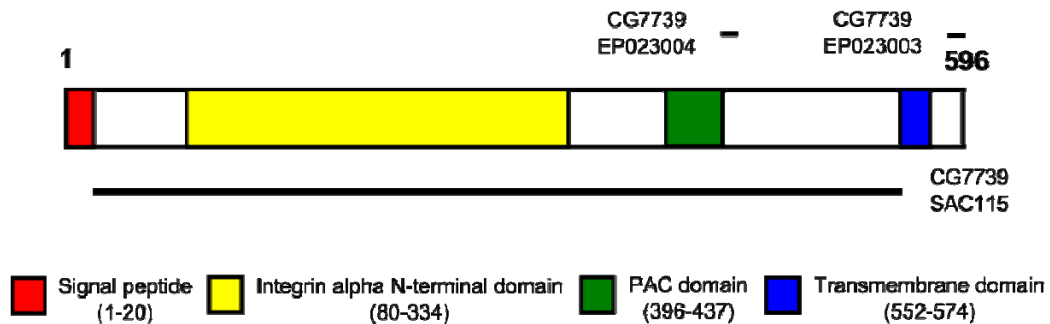


Figure A.2-13: Schematic representation of Shlp and the epitopes against which antibodies have been raised. Positions of epitopes are indicated by black bars. SAC115 was generated against aa 20-551, EP023004 was generated against aa 435-449 and EP023003 was generated against aa 580-596. Different domains are color coded in the legend. Numbers in the legend represent the length of the indicated domains in aa.

CG7739 EP023003 and CG7739 EP023004 are antibodies raised in rabbits against peptides with short amino acid sequences of Shlp. CG7739 EP023003 is directed against the most carboxy terminal region of Shlp (aa 580-596). Immunofluorescent antibody stainings with this antibody performed on *wildtype* embryos showed a ubiquitous staining. On the subcellular level a staining of the mitotic spindle of mitotic cells of *Drosophila* as well as of the apical region of epithelial cells and a blurry apical crescent of interphase neuroblasts could be observed (data not shown). Antibody staining performed on embryos lacking Shlp revealed that this staining represents artifacts (see A.2.5 and data not shown). When antibody staining was performed on *wildtype* embryos with the CG7739 EP023004 antibody no specific staining could be observed (data not shown). Therefore an antibody against a fusion between Glutathion-S-Transferase and the extracellular domain of Shlp termed CG7739 SAC115 was raised in guinea pig. When antibody staining with this antibody was performed on *wildtype* embryos, no difference could be observed between this staining and embryos stained with the according preimmune serum. The same results were observed when stainings were performed on brains of third instar larvae as well as on

A Results

ovaries (data not shown). We conclude from these observations that either the sensitivity of the generated antibodies for the endogenous Shlp epitopes is low or that the Shlp protein levels are very low during oogenesis, embryonic and larval brain development.

To investigate the subcellular distribution of Shlp in the embryo, *engrailed::GAL4* (*en::GAL4*) was used to drive expression of untagged Shlp under the control of a somatic promoter (*pUASst-shlp*) in the pattern of the segment polarity gene *engrailed*. Embryos were stained with CG7739 SAC115 and analyzed by confocal laser scanning microscopy. We found Shlp protein enriched in the *engrailed* expression domain (Fig. A.2-7 A). On the subcellular level, ectopic Shlp in the *engrailed* domain localized to the plasma membrane and it could also be detected in small intracellular vesicular structures (A7 B, arrow). Similar results could also be observed with the two above mentioned rabbit anti-Shlp antibodies (data not shown).

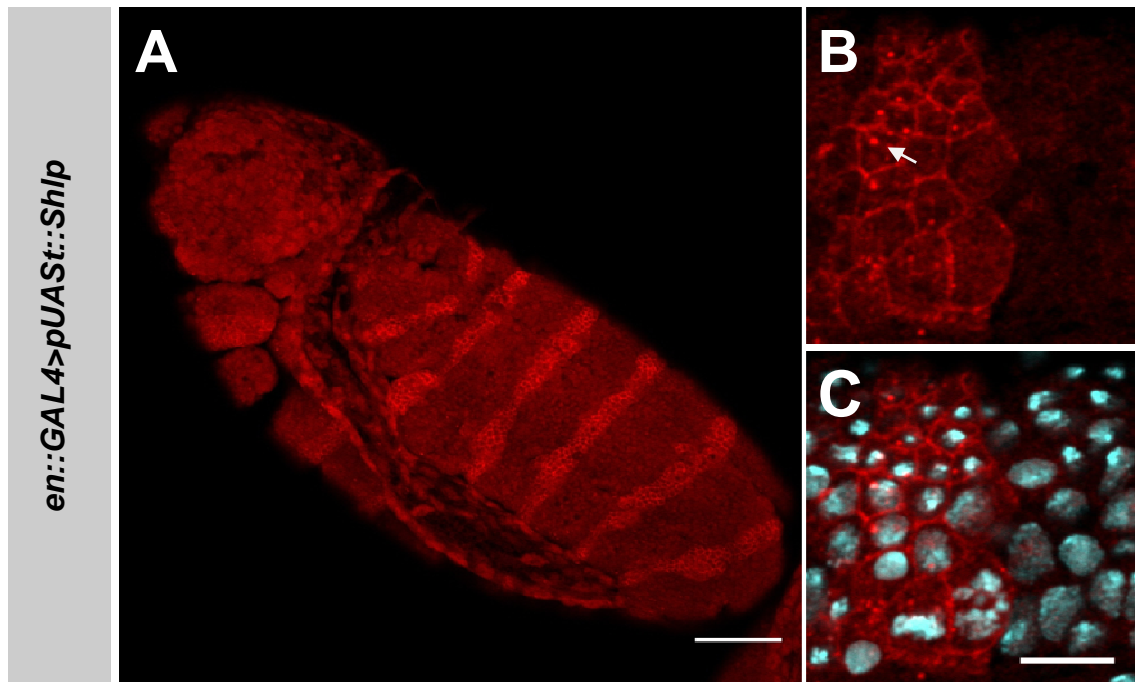


Figure A.2-14: Antibody staining with CG7739 SAC115 on embryos expressing pUASst-Shlp under *engrailed::GAL4* control. (A) CG7739 SAC115 detects Shlp specifically in the *engrailed* expression domain. (B-C) Shlp localizes to the plasma membrane and to intracellular vesicular structures (B, arrow). Scale bar is 50 μm in A and 10 μm in B and C. Embryo is stage 11. Anterior is to the left, dorsal is up.

Next, we analyzed the subcellular localization of ectopically expressed Shlp in epithelia and neuroblasts of the *Drosophila* embryo. Therefore, pUAS-Shlp was expressed under the control of *tubulin::GAL4* (*tub::GAL4*), a GAL4 line that expresses GAL4 in all cells. Embryos were stained with CG7739 SAC115 and with an antibody directed against Bazooka as marker for the subapical region of epithelial cells and the apical membrane of dividing neuroblasts. As shown in Fig. A.2-8 Shlp localizes to the basolateral plasma membrane in neuroectodermal cells when overexpressed ubiquitously. In these epithelial cells it localizes basally to Bazooka (Fig. A.2-8 D). In neuroblasts it localizes to the plasma membrane, however not in a polarized way (see Fig. A.2-9 D, asterisk).

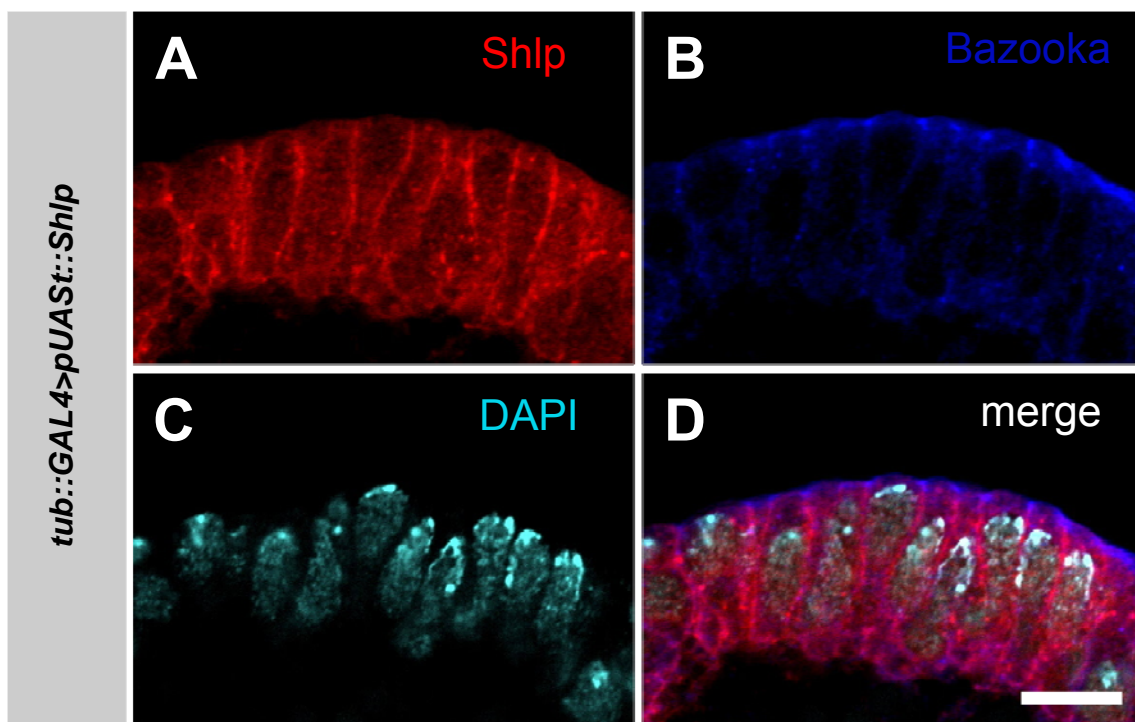


Figure A.2-15: Shlp localizes to basolateral membrane in the neuroectoderm. Embryos were stained with anti-Shlp SAC115 antibody (A), against Bazooka (B) and DAPI (C). (D) is a merge of all previous panels. Embryo is stage 11. Scale bar is 10 μ m.

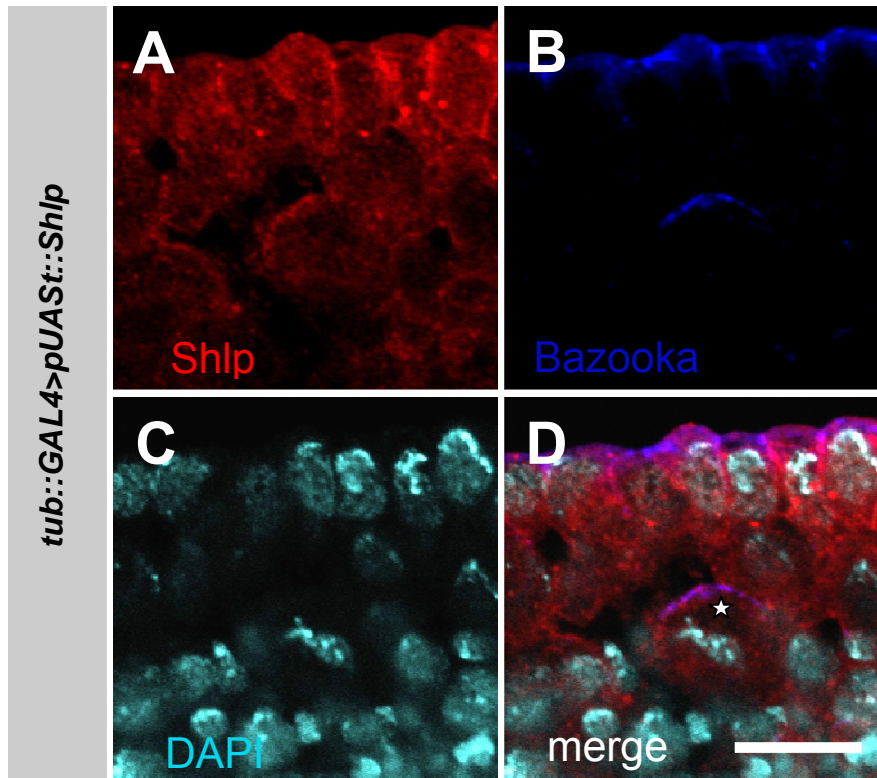


Figure A.2-16: Shlp localizes to the plasma membrane but not in a polarized way. Embryos were stained with anti-Shlp SAC115 antibody (A), against Bazooka (B) and DAPI (C). (D) is a merge of all previous panels. The white asterisk in (D) marks a metaphase neuroblast. Embryo is stage 11. Scale bar is 10 μ m.

As another approach to clarify the localization of Shlp in embryos we overexpressed a carboxy-terminally GFP-tagged Shlp protein with *daughterless::GAL4* (*da::GAL4*), another GAL4 line that ubiquitously activates expression in the embryo and stained for GFP and Bazooka (Fig. A.2-10). While Bazooka localizes to the subapical region in the neuroectoderm, Shlp-GFP localizes to the basolateral membrane, similar to untagged Shlp protein. In neuroblasts Shlp-GFP localizes ubiquitously to the plasma membrane, again similar to untagged Shlp.

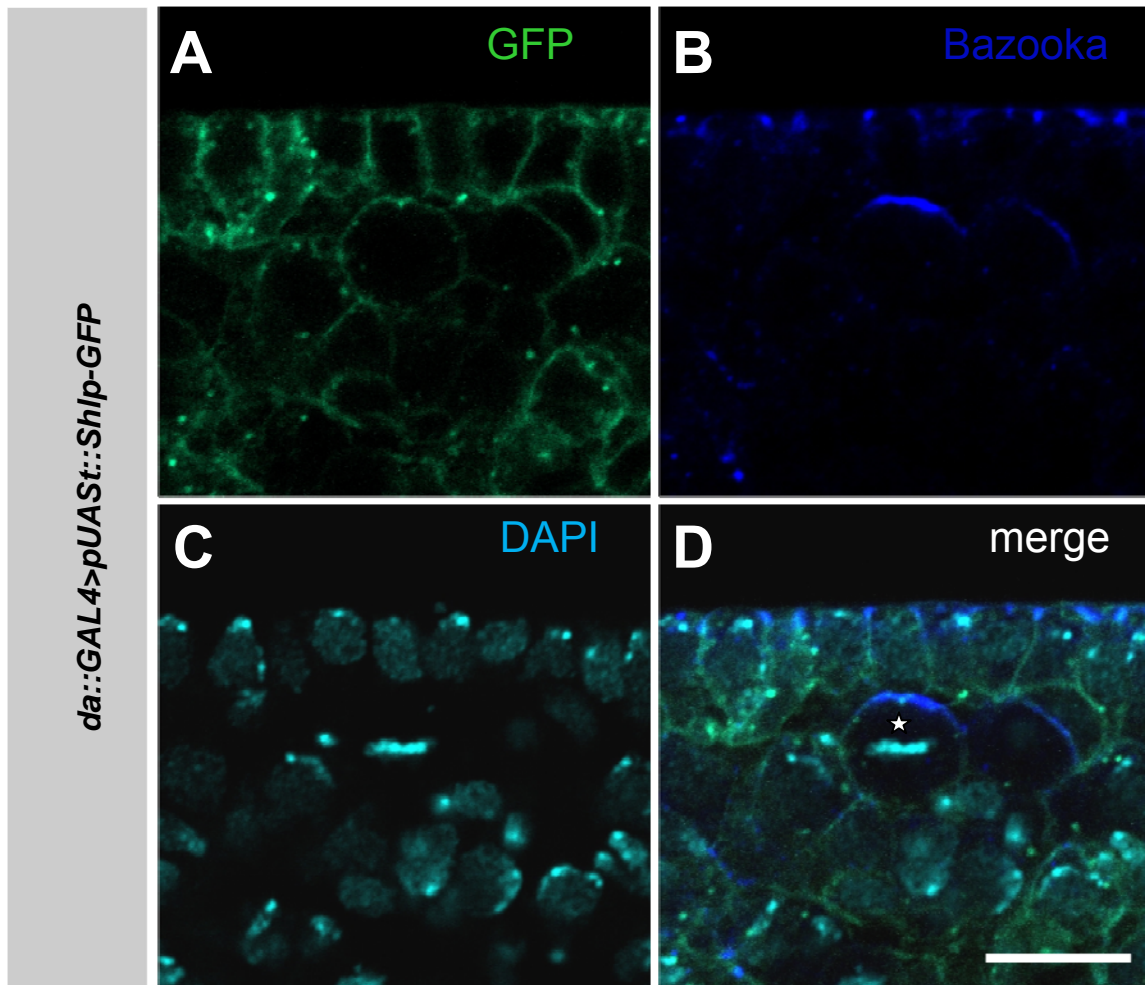


Figure A.2-17: Localization of Shlp-GFP in embryos. Embryos were stained with anti-GFP (A), anti-Bazooka (B) and DAPI (C). The asterisk marks a dividing neuroblast in metaphase. Embryo is stage 11. Scale bar is 10 μ m.

TIP, the mammalian orthologue of Shlp, was identified as a secreted factor (Fiscella *et al.*, 2003). Therefore, we also checked the localization of overexpressed untagged Shlp in a secretory epithelium, the salivary gland of the *Drosophila* embryo. In this experiment we overexpressed Shlp ubiquitously with *da::GAL4* and stained for Shlp as well as for the apical marker Bazooka and for the septate junction marker Discs Large (Dlg). In contrast to the neuroectodermal epithelium where Shlp localized to the basolateral membrane, ectopic Shlp was strongly enriched apically in the secretory cells of the salivary gland (Fig. A.2-11 A).

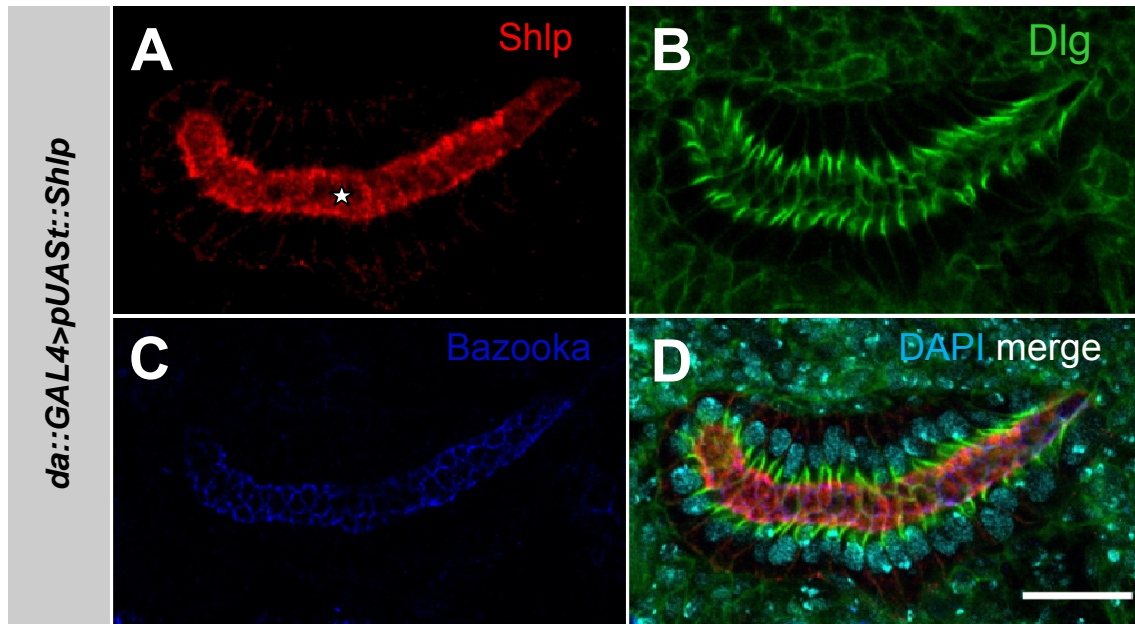


Figure A.2-18: Localization of overexpressed Shlp in the salivary glands of embryos. Embryos were stained with anti-Shlp EP023003, Discs Large (Dlg), a basolateral marker, Bazooka and DAPI. Note apical accumulation of Shlp close to the luminal space. Luminal space is marked with an asterisk. Embryo is stage 15. Scale bar is 20 μ m

A.2.3 Localization of *shlp* mRNA

Since it was not possible to detect endogenous Shlp protein levels with the available antibodies, we went on to determine the expression pattern of endogenous *shlp* mRNA in the *Drosophila* embryo and in the brain of wandering third instar larvae. To be able to detect the mRNA with subcellular resolution we used a protocol for fluorescent in situ hybridisation (FISH). Performing FISH on *wildtype* embryos with a *shlp* antisense RNA probe resulted in a staining that was indistinguishable from staining with a control sense RNA probe (data not shown). We therefore considered this staining to be unspecific. These results indicate that the levels of endogenous *shlp* mRNA are low during embryonic development, in agreement with low endogenous Shlp protein levels in the embryo as suggested by the staining with antibodies against Shlp.

Next, we did FISH on brains of wandering third instar larvae to check the expression of *shlp* during later development. Fig. A.2-12 A, B and A.2-13 A, B show an overview of a hemisphere of a third instar larval brain. As shown in Fig. A.2-12 *shlp* mRNA is expressed in the central brain (CB) and the optic lobe (OL) of the larval brain. Surprisingly, we were not able to detect *shlp* mRNA in the ventral nerve chord (data not shown). As shown in Fig. A.2-12 B-D *shlp* mRNA is enriched in large, rounded cells in the central brain region (Fig. A.2-12 D, asterisk), which are central brain neuroblasts, the neuroblast subtype that

will later give rise to most of the neurons present in the adult brain (Ito and Hotta, 1992).

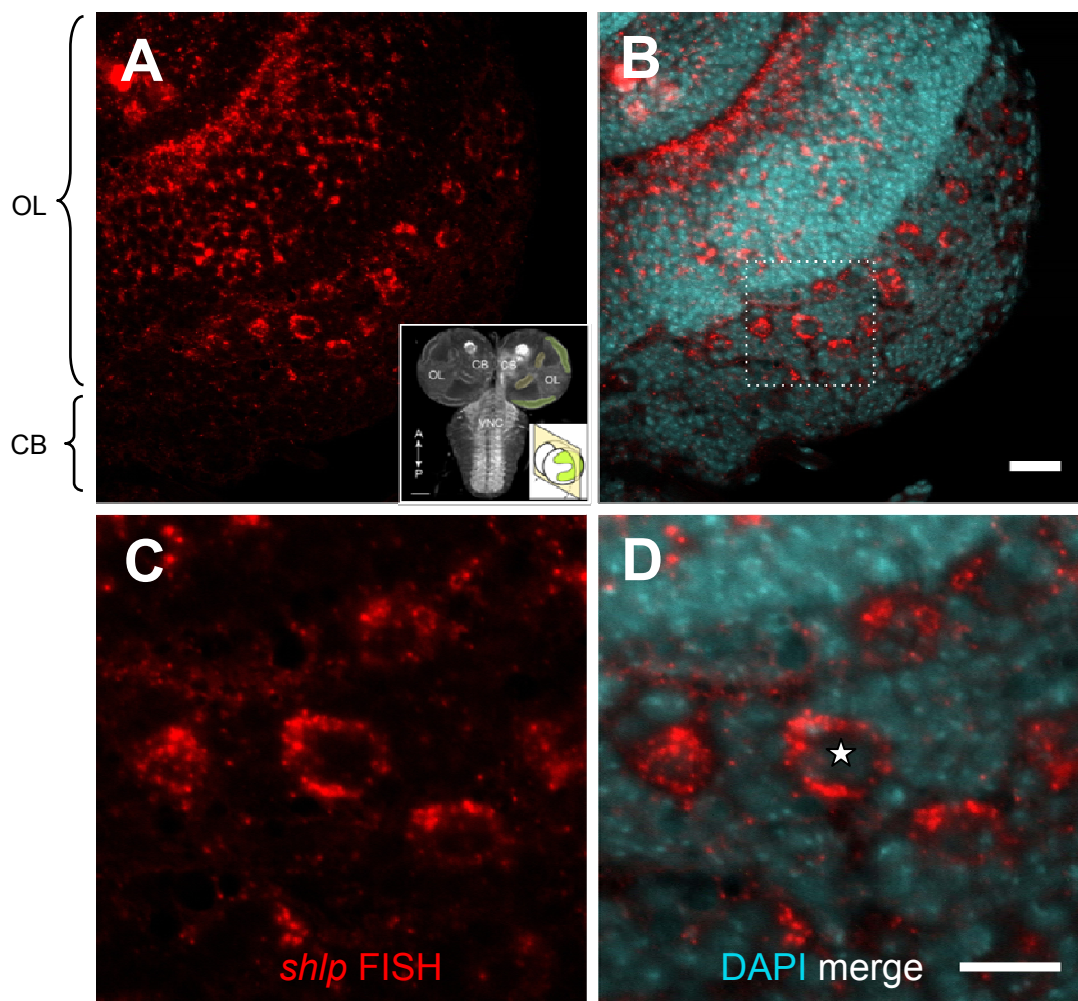


Figure A.2-19: Fluorescent in situ hybridisation with *shlp* antisense probe on *wildtype* wandering third instar larval brains. A and B show an overview of a hemisphere of a brain. Region marked by a rectangle in B is shown enlarged in C and D. Asterisk in D marks a neuroblast. Scale bar is 20 μm in A and B, 10 μm in C and D. The inset in A illustrates an overview of the larval brain. Adapted after (Egger *et al.*, 2007). OL = optic lobe, CB = central brain, VNC = ventral nerve cord, A = anterior and P = posterior.

Fig. A.2-13 shows FISH with the same *shlp* antisense RNA probe as in A12 but performed on brains of *shlp*¹³¹ mutant larvae (see also A.2.4) as a control. *shlp*¹³¹ mutant larval brains displayed no FISH signal in the hemisphere, strongly arguing that the FISH signal in the central nervous system is specific.

We conclude from this that *shlp* expression is low in the embryo and that *shlp* is specifically expressed in the optic lobe and central brain of third instar larvae.

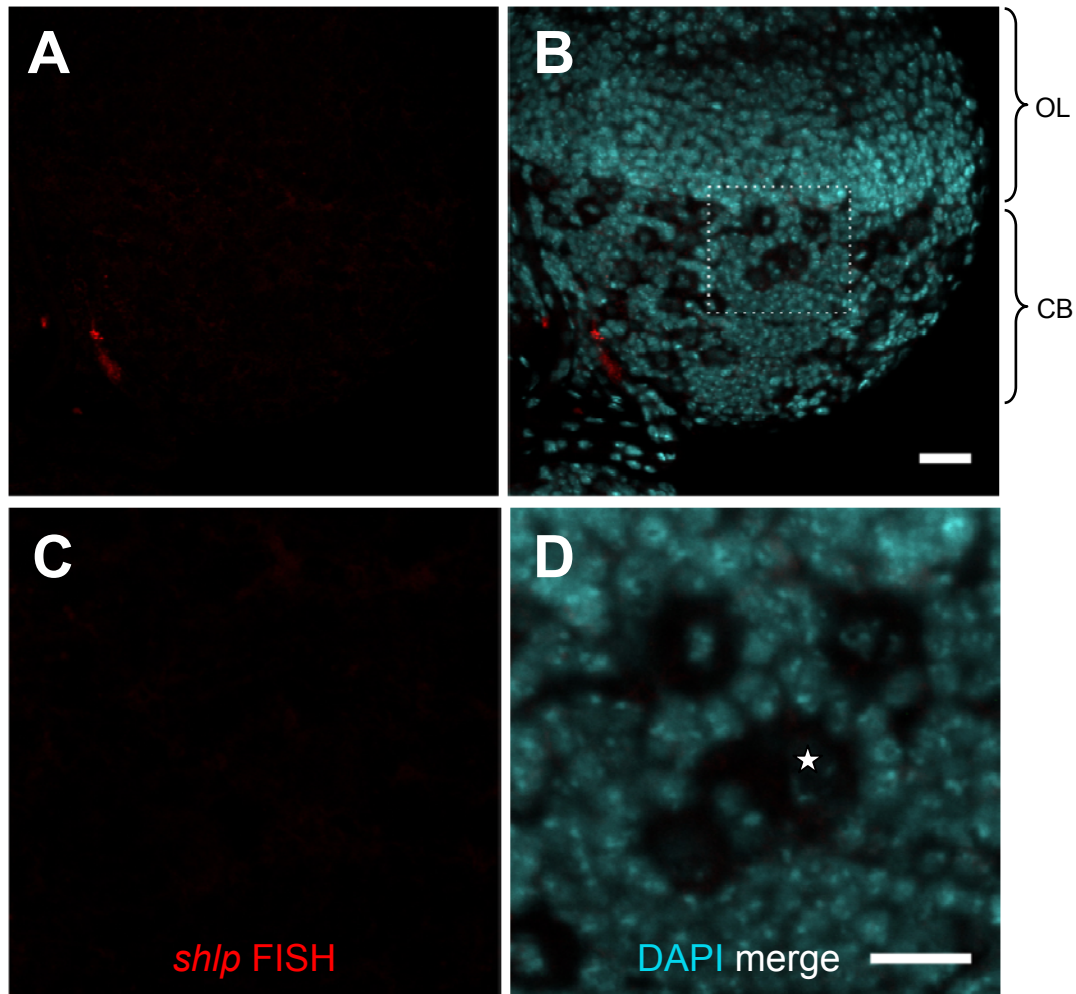


Figure A.2-20: Fluorescent in situ hybridisation with *shlp* antisense probe on *shlp*¹³¹ mutant wandering third instar larval brains. Region marked by a rectangle in B is shown enlarged in C and D. Star in D marks a neuroblast. Scale bar is 20 μ m in A and B, 10 μ m in C and D. OL = optic lobe, CB = central brain.

A.2.4 Generation of *shlp* mutant alleles

To investigate the developmental function of *shlp* we generated deletion mutants by imprecise P-element excision as described in Material and Methods, chapter C.2.2. By mobilizing the P-element GE24395, which is inserted in the 5'UTR of *shlp* as described in chapter A.2.1.1, two alleles were generated in which large parts of the coding region of *shlp* are deleted (Fig. A.2-14 A). Both alleles were molecularly characterized by PCR (Fig. A.2-14 B) and sequencing. In *shlp*⁵² 925 bp of the *shlp* gene locus were deleted downstream of GE24395. Molecular characterization of the mutant allele by PCR and sequencing revealed that 2162 bp of the originally inserted P-element are still present in this allele. Surprisingly, the orientation of this remaining P-element fragment is inverted relative to the orientation of the originally inserted P-element. In this allele the coding

region for the start codon, the signal peptide and a large part of the Integrin alpha N-terminal region are deleted.

In *shlp*¹³¹ 1842 bp downstream of GE24395 are removed. This deletion includes the coding region for the start codon, the signal peptide, the extracellular domain and parts of the transmembrane domain of Shlp. Since no start codon is present in the remaining 111 bp of coding sequence, it is very unlikely that any functional Shlp protein can be produced in *shlp*¹³¹. Therefore, we concluded that *shlp*¹³¹ represents a null allele of *shlp*.

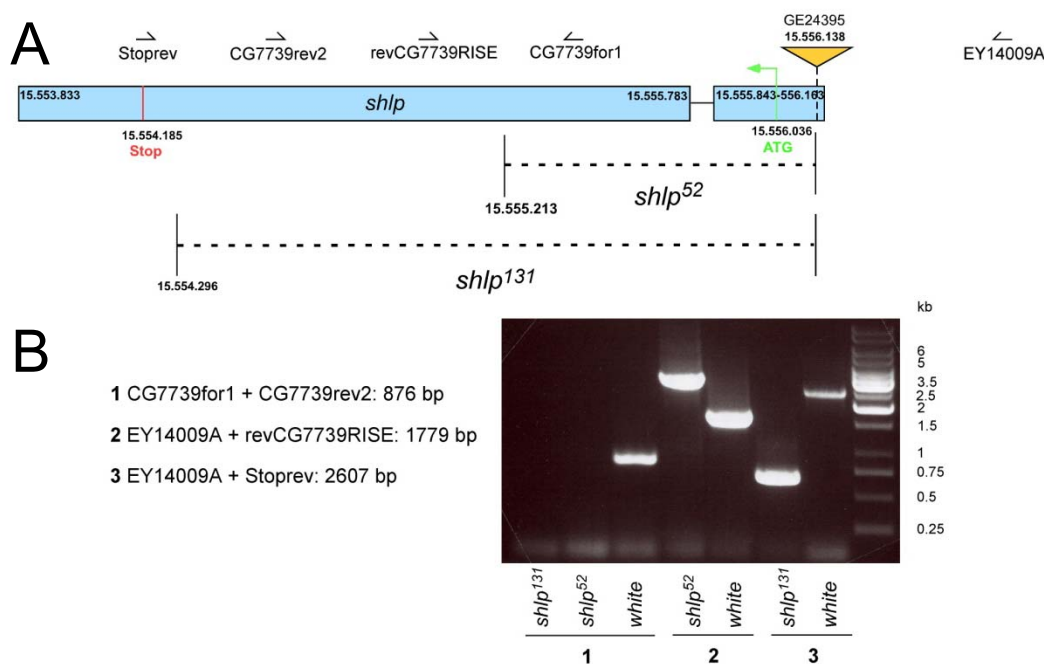


Figure A.2-14: Molecular characterization of *shlp* alleles. (A) Schematic representation of the *shlp* gene locus and of the mutant alleles. In two deletion mutants for *shlp*, *shlp*¹³¹ and *shlp*⁵² large regions of the *shlp* gene locus have been deleted. In *shlp*⁵² 925 bp, in *shlp*¹³¹ 1842 bp downstream of GE24395 are missing. Start and stop codons are denoted with green and red colour. The numbers denote the base pairs in the *Drosophila* genome. Yellow triangle marks the position of the P element GE24395 that is located 103 bp upstream of the start codon in the 5'UTR of *shlp* and was used to generate these mutants. The small arrows above the scheme depict the position of primers that were used to characterize the molecular lesions in *shlp*. (B) Primer combinations and PCR on genomic DNA to characterize the mutant alleles. kb = kilobase.

The original *shlp*^{131*} and *shlp*^{52*} alleles were semi lethal with few escapers. We analyzed the hatching rates of embryos laid by *shlp*^{131*} and *shlp*^{52*} homozygous parents, of embryos laid by females homozygous for *shlp*^{131*} mated to *shlp*^{52*} males and of *wildtype* embryos as control (Fig. A.2-15). Comparing the hatching rates of these embryos revealed that in *shlp*^{131*}/*shlp*^{52*} transheterozygous embryos the low hatching rate observed in *shlp*^{131*} (10,6

A Results

%) and *shlp*^{52*} (30,8 %) could be rescued to 85,3 % and therefore almost to control levels of *white* embryos (95,5 %). These results indicated that the reduced viability of *shlp*^{131*} and *shlp*^{52*} was either caused by additional mutations present on the *shlp*^{131*} and *shlp*^{52*} chromosomes or that the two alleles complement each other in an interallelic fashion. Adult escapers homozygous for *shlp*^{131*} also showed a strongly decreased locomotion activity compared to *wildtype* control flies. Complementation tests of *shlp*^{131*} and *shlp*^{52*} with deficiencies removing the genomic region of *shlp*, (*Df(3L)XG8* and *Df(3L)XG10*, revealed that the decreased viability of both alleles and the locomotion defects in *shlp*^{131*} are caused by a second mutation on the third chromosome. We removed this second mutation by recombination with an isogenic third chromosome and re-establishment of the mutant alleles. The newly established *shlp*¹³¹ and *shlp*⁵² stocks were fully viable and showed normal movement.

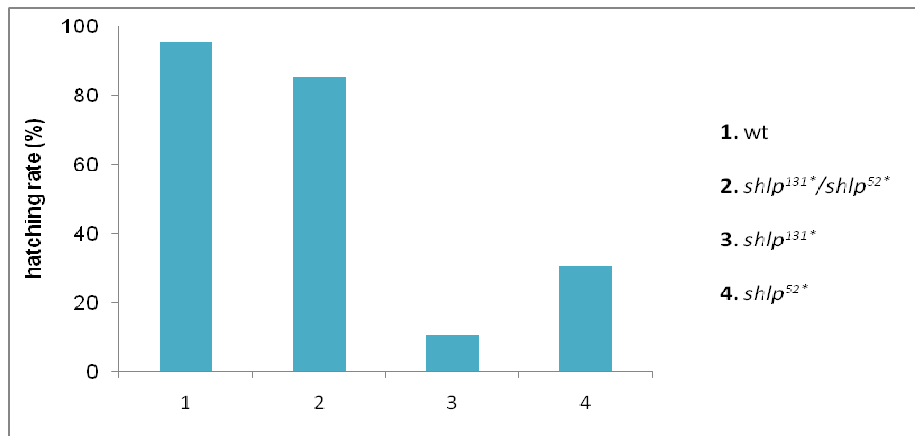


Figure A.2-15: Hatching rates were determined for embryos homozygous for the original *shlp* alleles. The low hatching rates (3, 4) of homozygous mutants could be improved for transheterozygous embryos (2). Therefore, additional mutants account for the reduced viability observed in homozygous embryos.

A.2.5 Phenotypic analysis of *shlp* mutant alleles

A.2.5.1 Viability of *shlp* mutants

To analyze if loss of *shlp* leads to defects that cause a decrease in viability we determined the hatching rate of mutant embryos (Fig. A.2-16). The average hatching rate of embryos homozygous for *shlp*¹³¹ (79 %) was comparable to that of *wildtype* embryos (88 %) and embryos homozygous for the original P-element insertion *shlp*^{GE24395} (82 %). So we concluded that *shlp* is not essential for embryonic development.

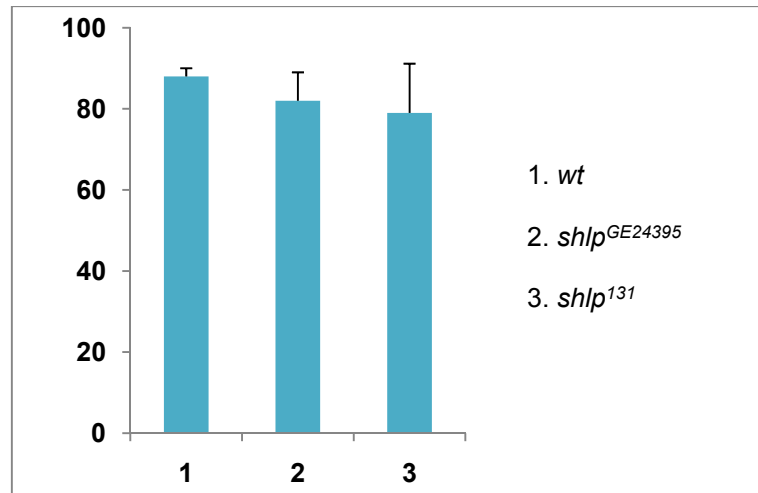


Figure A.2-16: *shlp*¹³¹ mutant embryos show hatching rates comparable to *wt* embryos. 100 embryos were collected and after two days time to develop at 25°C, the number of hatched embryos was determined. The experiment was repeated three times. *shlp*^{GE24395} is the original P-element insertion allele that was used to generate the mutants as described above.

A.2.5.2 Apicobasal cell polarity of *shlp* mutant embryos

The *shlp*¹³¹ and the *shlp*⁵² deletion mutants were viable and fertile and it was possible to establish a healthy stock from both mutants. Since *shlp* was identified in a yeast-two-hybrid screen as an interaction partner of the Bazooka protein, which is a key regulator of apicobasal cell polarity (Müller and Wieschaus, 1996; Wodarz *et al.*, 1999; Knoblich, 2008), we analyzed whether the *shlp* mutants displayed polarity defects in epithelial cells and in neuroblasts of the *Drosophila* embryo. We stained embryos mutant for *shlp* with the polarity markers Bazooka and Miranda and analyzed their polarity (Fig. A.2-17). The polarity both in epithelial cells and in neuroblasts of *shlp* mutant embryos was normal. We also checked the localization of other polarity markers like aPKC, which localizes to the subapical region in epithelial cells and to the apical cortex in neuroblasts and DE-Cadherin as an adherens junction marker in *shlp* mutants. As marker for septate junctions in epithelial cells Discs Large was tested and as a basal marker Dystrophin. All these markers were distributed as in the *wildtype* control and will therefore not be shown here.

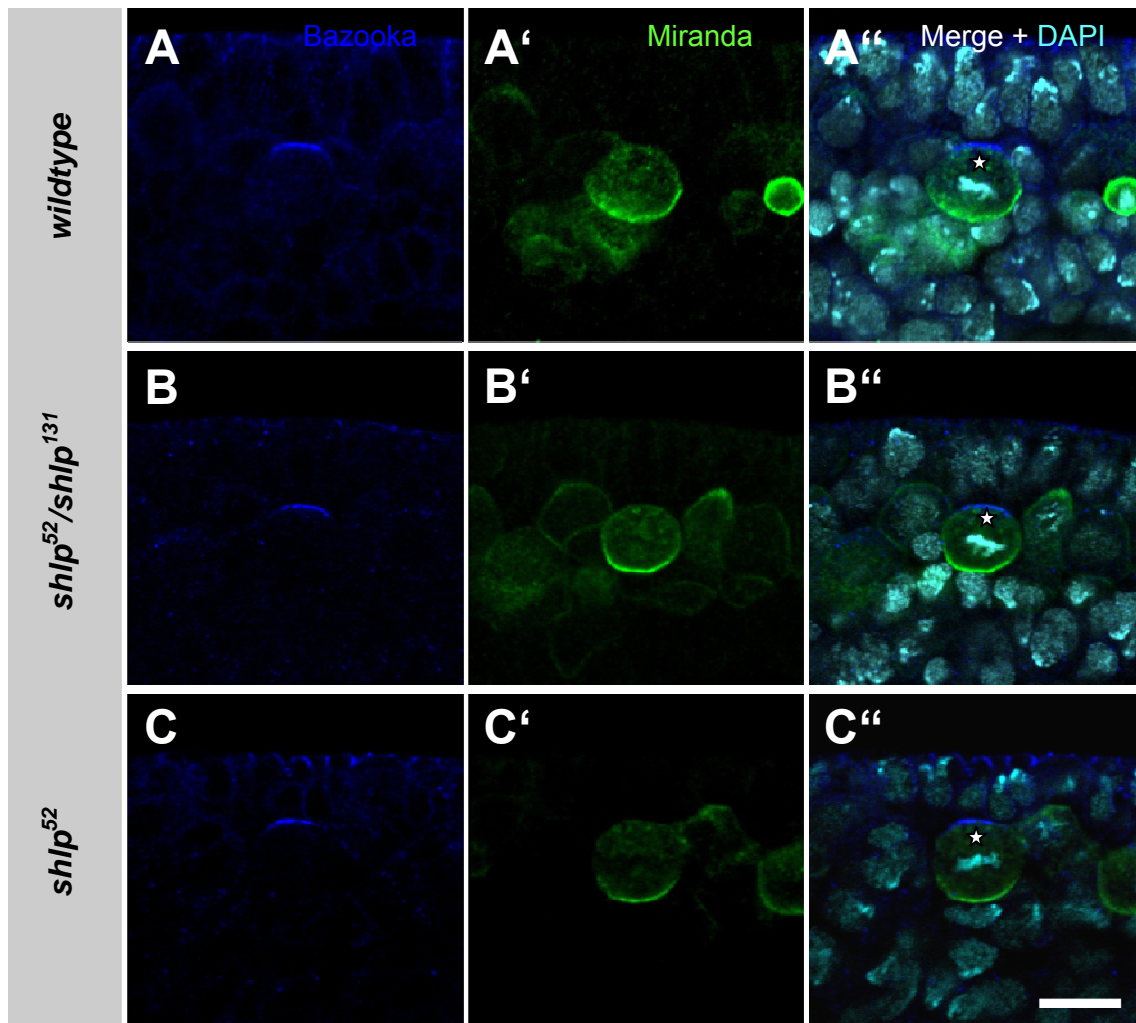


Figure A.2-17: Antibody staining on *shlp* mutant embryos with polarity markers does not reveal any polarity defects. Embryos were stained for Bazooka (blue), Miranda (green) and DAPI. (A-A'') *wildtype* control embryos. (B-B'') *shlp*⁵²/*shlp*¹³¹ transheterozygous embryos. (C-C'') *shlp*⁵² mutant embryos. Asterisks mark metaphase neuroblasts. Embryos are at stage 11. Scale bar is 10 μ m.

A.2.5.2 Wing defects of *shlp* mutant flies and rescue of the mutant phenotype

Since *shlp* mutant flies were viable and fertile, we next checked whether they showed some milder developmental defects. We observed an increased number of flies homozygous for *shlp*¹³¹ that did not unfold their wings compared to *wildtype* control flies. 29.1 % of *shlp*¹³¹ mutant flies (n = 385) had wings that were only partially expanded or completely unexpanded. *Wildtype* flies did not show this defect at all (n = 241) and *shlp*^{GE24395} flies, which carry the P-element insertion that was used to generate the mutant, showed this phenotype with a very low penetrance (0.4 %, n = 262).

In order to show that this defect is caused by the loss of *shlp* gene function only, we rescued it by ectopically expressing *shlp* in the mutant background. For this purpose, we introduced *pUAS-shlp* on the second chromosome in the *shlp*¹³¹ mutant background

(*pUAS-shlp; shlp¹³¹*) and crossed it to *arm::GAL4*, which itself had been crossed into the *shlp¹³¹* mutant background and determined the number of flies with normally unfolded wings (Fig. A.2-18).

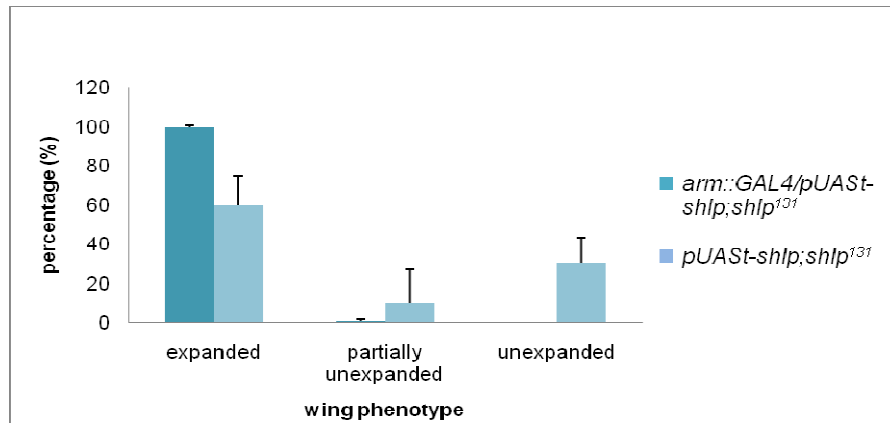


Figure A.2-18: Rescue of *shlp* mutant. Expression of untagged Shlp in the *shlp¹³¹* mutant background (*arm::GAL4/pUAS-shlp;shlp¹³¹*) results in a complete rescue of the wing unfolding defects. If only *pUAS-shlp* without *arm::GAL4* is present (*pUAS-shlp;shlp¹³¹*) no rescue was observed. The experiment was repeated three times. The experiments were performed at 25°C.

Expression of an untagged Shlp construct under the control of *armadillo::GAL4* resulted in an almost complete rescue (99.5 % expanded wings) of the wing phenotype (Fig. A.2-17, *arm::GAL4/pUAS-shlp; shlp¹³¹*). If only *pUAS-shlp* was present without transactivator, we observed no rescue (9.8 % partially expanded wings; 30.7 % unexpanded wings).

The wing unfolding phenotype we observed was variable since some flies had partially unexpanded wings (Fig. A.2-19 B, B'), while others had completely unexpanded wings (Fig. A.2-19 C, C'). Additionally, we observed other defects to the wing unfolding phenotype. *shlp¹³¹* mutant flies had postscutellar bristles that were frequently crossed (Fig. A.2-19 B', C', white arrow), while the bristles of control animals had an almost parallel orientation (Fig. A.2-19 A', white arrow). Pronounced crossing of postscutellar bristles has also been described for loss of function mutants of the α subunit of Bursicon (Bursicon α) and could indicate a failure in thoracic expansion (Dewey *et al.*, 2004). While the cuticle of control animals is smooth and shiny (Fig. A.2-19 A'), the cuticle of *shlp¹³¹* animals often appeared soft and blunt (Fig. A.2-19 B', C'), resembling the cuticle of freshly hatched flies. The thorax and notum of *shlp¹³¹* mutant flies were often darkened (Fig. A.2-19 C', white asterisk). Animals that showed the blunt cuticle phenotype often had wide clefts between the abdominal segments (Fig. A.2-19 C', white arrowhead) which sometimes occurred together with defects in abdominal segmentation (Fig. A.2-19 C, C', black

arrows).

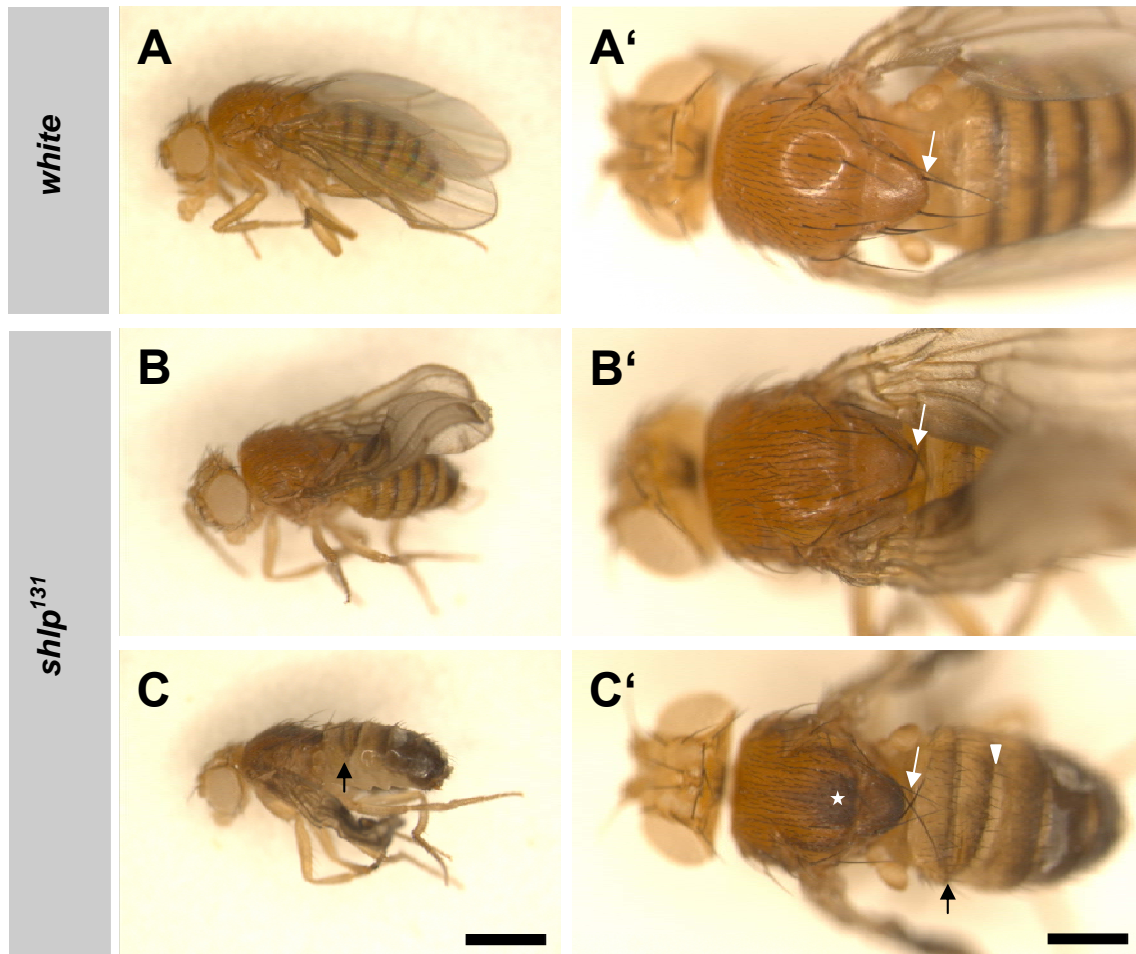


Figure A.2-19: *shlp*¹³¹ flies display defects in wing unfolding and cuticle tanning. (A and A') *white* female with unfolded wings and normally tanned cuticle. Postscutellar bristles are oriented in parallel (white arrow). (B and B') *shlp*¹³¹ female with partially expanded wings. Postscutellar bristles are crossed (white arrow). (C and C') *shlp*¹³¹ male with unexpanded wings. Postscutellar bristles are crossed (white arrow). Cuticle on thorax and notum is darkened (white asterisk). Wide clefts between abdominal segments are obvious (white arrowhead). Thoracic cuticle of *shlp*¹³¹ animals (B', C') appears blunt and soft compared to cuticle of control animals (A'). Some *shlp*¹³¹ animals showed segmentation defects in the abdomen (C, C', black arrows). Scale bar in A-C is 1000 μ m; 500 μ m in A'-C'.

We searched the literature for mutants that cause similar phenotypes and found one candidate pathway that leads to similar wing and cuticle defects when disturbed. Loss of function in Bursicon signaling causes defective wing expansion and cuticle tanning (Fraenkel and Hsiao, 1962; Baker and Truman, 2002; Dewey *et al.*, 2004; Peabody *et al.*, 2008). Also pronounced crossing of postscutellar bristles has been described for Bursicon mutants (Dewey *et al.*, 2004).

We therefore checked if there is any genetic interaction between *shlp*¹³¹ and the gene

ricketts (*rk*), which encodes for the supposed Bursicon receptor *Drosophila* Leu-rich repeats-containing G-protein-coupled receptor 2 (DLGR2) (Baker and Truman, 2002). Flies homozygous mutant for *rk* are viable and exhibits wing unfolding and cuticle tanning defects similar to what we observed for *shlp* loss of function. If both genes act in the same pathway and one introduces one mutant copy of *rk* into the *shlp*¹³¹ mutant background this will enhance the wing expansion defect even though animals with only one mutant copy of *rk*, do not exhibit wing expansion defects. Animals heterozygous for a null allele of *rk* and homozygous for *shlp*¹³¹ (*rk*⁴/+; *shlp*¹³¹) showed the low penetrance wing unfolding defect observed in *shlp*¹³¹ mutant flies. Surprisingly, animals homozygous for *rk*⁴ and *shlp*¹³¹ (*rk*⁴; *shlp*¹³¹) exhibited defects that indicated an enhancement of the *shlp*¹³¹ mutant phenotype (Fig. A.2-20 D and D'). As mentioned above, *shlp*¹³¹ mutant flies show a wing unfolding defect with low penetrance that was often connected to defects in cuticle morphology and intensive darkening especially of the thorax and notum (Fig. A.2-20 B and B'). Flies homozygous for *rk*⁴ did not expand their wings and their cuticle tanning was defective. Although their cuticle darkened similar to *white* control flies (Fig. A.2-20 C-C'), the timing of this process was delayed up to several hours (Baker and Truman, 2002). *rk*⁴ mutants also displayed extensive crossing of postscutellar bristles indicating a defect in thorax expansion. Similar to *shlp*¹³¹ mutants, their cuticle often appeared blunt and soft (Figure A.2-20 C'). Flies homozygous for both *rk*⁴ and *shlp*¹³¹ displayed a complete block in wing expansion like in *rk*⁴ mutant flies (Fig. A.2-20 D). Similar to the *shlp*¹³¹ or *rk*⁴ homozygous flies alone postscutellar bristles of these flies showed pronounced crossing and their cuticle appeared blunt and soft (Fig. A.2-20 D', white arrow). Unlike the *rk*⁴ homozygous flies, that never showed extensive darkening of the cuticle, and unlike the *shlp*¹³¹ homozygous flies, that showed extensive darkening of the cuticle only with moderate penetrance, the *rk*⁴; *shlp*¹³¹ flies showed this phenotype with high penetrance (Fig. A.2-20 D', white asterisk). Therefore the *rk*⁴; *shlp*¹³¹ double mutant displays defects that neither the *rk*⁴ nor the *shlp*¹³¹ single mutant shows. This additive effect indicates that the two genes rather act in parallel pathways than in the same pathway.

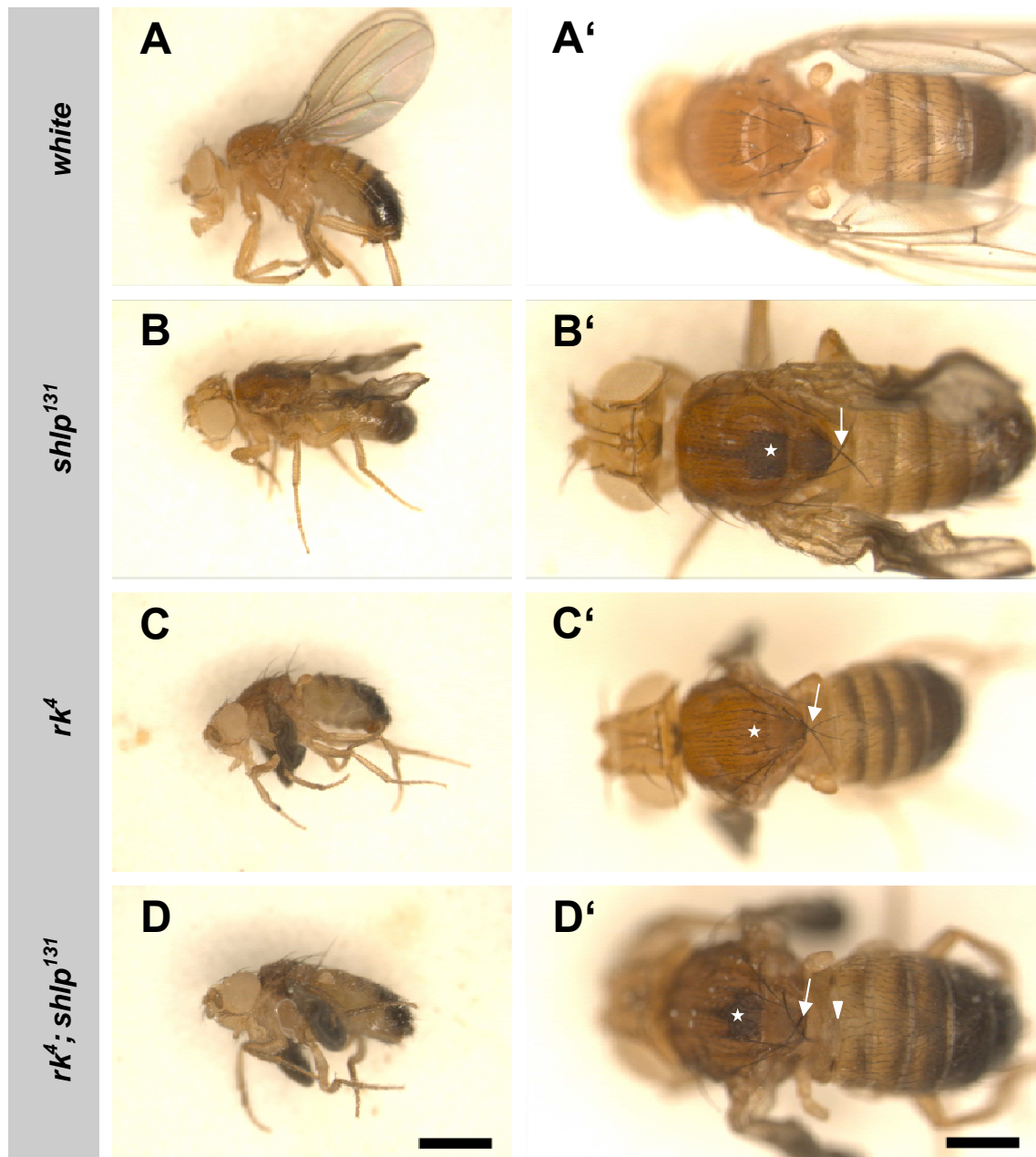


Figure A.2-20: The rk^4 allele enhances the $shlp^{131}$ phenotype. (A and A') *white* male with wildtype wings and cuticle tanning. Cuticle appears smooth and shiny. (B and B') $shlp^{131}$ male with partially expanded wings. Thorax shows abnormal darkening (white asterisk) and postscutellar bristles display prominent crossing (white arrow). (C and C') rk^4 male with unfolded wings and pronounced crossing of postscutellar bristles (white arrow). Cuticle appears blunt. Cuticle of the thorax is pigmented normally (white asterisk). (D and D') $rk^4; shlp^{131}$ male with unfolded wings, abnormal darkening of the thorax (white asterisk). Postscutellar bristles show prominent crossing (white arrow). Cuticle appears blunt. Animals often have wide clefts between abdominal segments (white arrowhead). Scale bar in A, B, C and D is 1000 μm ; 500 μm in A', B', C' and D'.

Bursicon signaling induces cuticle hardening and tanning and regulates wing expansion. Following wing expansion it is supposed to promote programmed cell death of epidermal cells of the wing (Kimura *et al.*, 2004). Since $shlp^{131}$ mutant flies displayed wing

expansion defects similar to mutants that affect Bursicon signalling, we checked whether *shlp*¹³¹ mutants had any defects in programmed cell death in the wing epithelium. Therefore, we collected freshly hatched flies and allowed them to develop for 30-60 min. After this period wings were dissected, fixed and subsequently stained with the DNA marker DAPI to visualize the morphology of the cell nuclei. During this 30-60 min time period most *wildtype* control flies expanded their wings (Fig. A.2-21 A, A'). DAPI staining revealed that most of the wing cells had disappeared from the wing while chromatin of the remaining cells was fragmented, indicating the onset of cell death (Fig. A.2-21 A', white arrows). In a subset of wing epithelial cells nuclei were still intact (Fig. A.2-21 A', white arrowheads). These cells represent the cells of the wing that are associated with veins. DAPI staining on *shlp*¹³¹ mutant flies that expanded wings normally revealed similar results as in *wildtype* animals (data not shown). DAPI staining on unexpanded wings of *shlp*¹³¹ mutant flies revealed an increased number of viable cells (Fig. A.2-21 B, B'). After 30-60 min wing epithelial cells were intact as shown by DAPI staining and nuclei did not display chromatin fragmentation as seen in *wildtype* wings (Fig. A.2-21 A'). Since it has been proposed that dying cells are cleared from the wing within 3 h after wing spreading (Togel *et al.*, 2008) we also analyzed the wing epithelium 5 h 30 min - 6 h after hatching (Fig. A.2-21 C, C' and D, D'). At this time point the wing blade should be free of cells except for the cells of the wing vein. While the wing of control flies was free of living cells except for the cells of the veins (Fig. A.2-21 C and C', white arrowheads), cells in unexpanded wings of *shlp*¹³¹ mutant flies were still alive as indicated by DAPI staining (Fig. A.2-21 D and D'). We also analyzed the wings of *shlp*¹³¹ mutant flies 24 h and 48 h after hatching (data not shown). While 24 h after hatching living cells were still present, no living cells could be observed after 48 h (data not shown). These results indicate that programmed cell death of wing epithelial cells is severely delayed in *shlp* mutant flies.

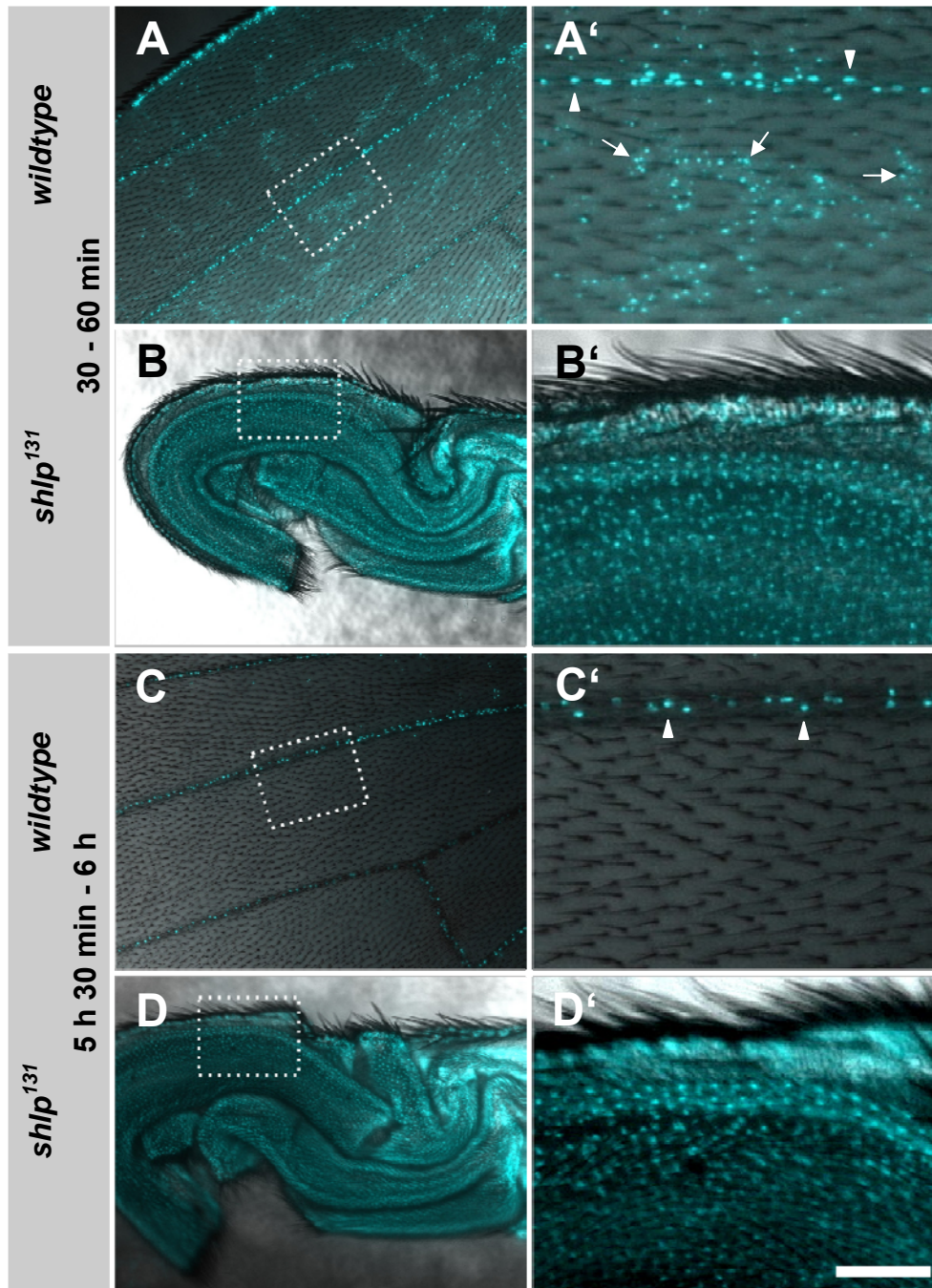


Figure A.2-21: Apoptosis of epithelial cells is delayed in wings of *shlp*¹³¹ mutant flies. (A and A') Wing of a *wildtype* fly 30 - 60 min after hatching. Only nuclei in wing veins are intact (A', white arrowheads). Nuclear staining in most other areas of the wing is absent or appears dispersed and fragmented (A', white arrows). (B and B') Unexpanded wing of *shlp*¹³¹ fly 30 - 60 min after hatching. DAPI staining reveals that the morphology of cell nuclei is intact. (C and C') In a wing of a *wildtype* fly nuclear staining is only present in the wing veins, indicating loss of all other cells. (D and D') Nuclei are still intact in a wing of a *shlp*¹³¹ mutant fly 5 h 30 min - 6 h after hatching. Area marked with a rectangle in A - D is magnified in A' - D'. All images are merges of DAPI and DIC channel. Scale bar is 100 μm in A - D and 50 μm in A' - D'.

The defects of *shlp*¹³¹ mutant flies in wing unfolding and cell death of wing epithelial cells show similarities to the defects in flies with disrupted Bursicon signalling. A major difference is the low penetrance of the defects of *shlp*¹³¹ mutant flies compared to the highly penetrant phenotypes seen for example in *rk*⁴ mutants, where wing expansion is completely blocked. One explanation for these observations could be lowered Bursicon levels in the *shlp*¹³¹ mutant. Previously, it has been reported that Bursicon α is expressed in pairs of neurons in the subesophageal, thoracic and abdominal neuromeres of the ventral nerve cord (Dewey *et al.*, 2004; Peabody *et al.*, 2008; Zhao *et al.*, 2008). To check whether the expression pattern of the heterodimeric neurohormone Bursicon is changed, we stained central nervous systems (CNS) of wandering third instar larvae with an antibody directed against Bursicon α . CNS of control *wildtype* larvae (A.2-22 A and A') stained with the Bursicon α antibody showed the previously reported pattern. The pattern of Bursicon α immunoreactivity on CNS of *shlp*¹³¹ mutant larvae differed from the *wildtype* pattern. While in *wildtype* CNS Bursicon α positive neurons were present in the thoracic neuromeres (Fig. A.2-22 A, white arrow), these neurons were often absent in *shlp*¹³¹ CNS (Fig. A.2-22 B, white arrow). We quantified the number of Bursicon α positive neurons in the CNS of *wildtype* and *shlp*¹³¹ wandering third instar larvae (Fig. A.2-22 C). In contrast to an average number of 33 neurons in *wildtype* CNS (n = 16), in *shlp*¹³¹ CNS we detected only 23 neurons on average (n = 15). These experiments demonstrate that the number of Bursicon α positive neurons is reduced in CNS of *shlp*¹³¹ mutant third instar larvae.

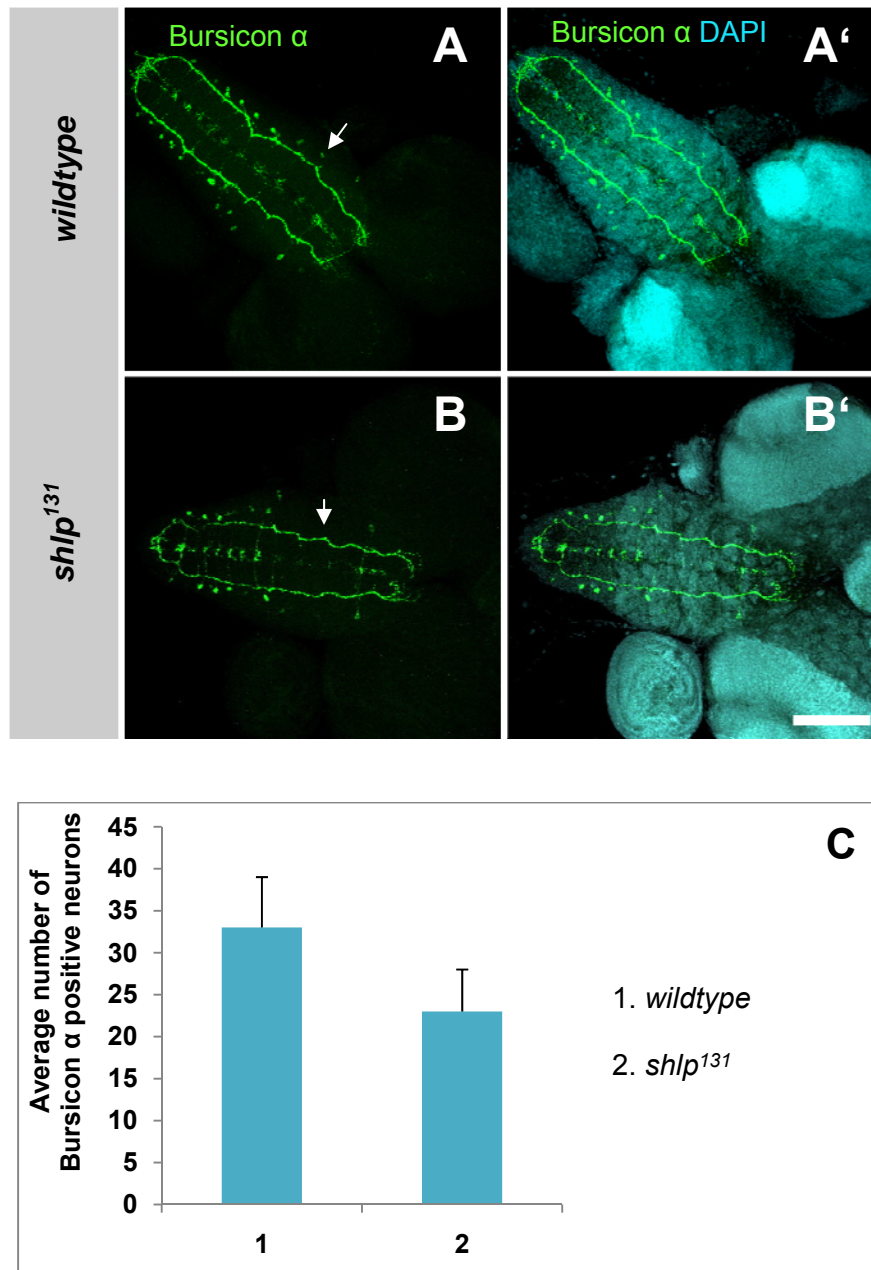


Figure A.2-22: The number of Bursicon α positive neurons is reduced in the ventral nerve cord of *shlp*¹³¹ L3 larvae. (A and A') In *wildtype* third instar larvae, Bursicon α is expressed in pairs of neurons in the subesophageal, thoracic and abdominal neuromeres of the ventral nerve cord. (B and B') In the CNS of *shlp*¹³¹ larvae, Bursicon α is often not expressed in the thoracic neuromeres (white arrow, compare with white arrow in A). Green = Bursicon α , turquoise = DAPI. A, A', B and B' are maximum intensity projections of single confocal planes. Scale bar is 100 μ m. (C) Quantification of the number of Bursicon α positive neurons reveals *shlp*¹³¹ larvae have on average less Bursicon α positive neurons (23 \pm 5, n=15) than *wildtype* larvae (33 \pm 6, n=16).

A.2.5.3 Overexpression of Shlp-eGFP in flies mimics the defects seen in *shlp*¹³¹ mutant flies

Embryos overexpressing Shlp-eGFP developed normally and the localization of Shlp-eGFP in the embryo was similar to untagged Shlp when overexpressed (see A.2.2). Surprisingly, when we overexpressed Shlp-eGFP with the strong ubiquitous GAL4 line *tub::GAL4* we observed wing and cuticle phenotypes that were comparable to those seen in the *shlp*¹³¹ mutant (Fig. A.2-23 A and A'). Interestingly, all flies that overexpressed Shlp-eGFP under the control of *tub::GAL4* showed the wing unfolding and cuticle defects (Fig. 4.2-23 B and B'). This effect seemed to be dosage dependent, since we only observed this fully penetrant phenotype when using *tub::GAL4*, while using other ubiquitous transactivator lines like *actin::GAL4* or *da::GAL4* resulted only in a moderate number of flies with wing defects (data not shown).

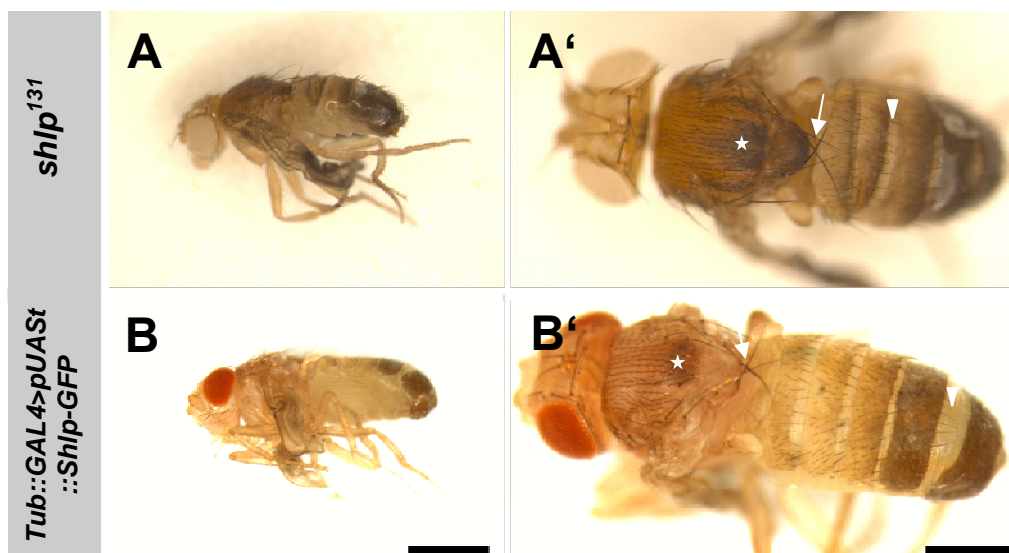


Figure A.2-23: Flies overexpressing Shlp-eGFP show defects in wing unfolding and cuticle tanning. (A and A') *shlp*¹³¹ male with unexpanded wings. (A') Postscutellar bristles are crossed (white arrow). Cuticle on thorax and notum is darkened (white asterisk) and there are wide clefts between abdominal segments (white arrowhead). (B and B') male fly expressing Shlp-eGFP under the control of *Tub::GAL4*. Wings are unexpanded, postscutellar bristles are crossed (white arrow), cuticle on notum is darkened (white asterisk) and there are wide clefts between abdominal segments (white arrowhead). Cuticle appears blunt. Scale bar in A, B is 1000 μ m; 500 μ m in A* and B*.

To check whether clearance of epithelial cells is defective just as in *shlp*¹³¹ mutant flies, we fixed and stained wings of flies overexpressing Shlp-eGFP 30 – 60 min and 5:30 – 6 h after hatching as described above. After 30 – 60 min, identical to wings of *shlp*¹³¹ mutant flies that did not unfold their wings, wings of Shlp-eGFP overexpressing flies were positive for

DAPI staining and no sign of chromatin fragmentation was visible (Fig. A.2-24 A and A'). Even after 5:30 – 6 h nuclei of wing epithelial cells, as revealed by DAPI staining, appeared to be intact (Fig. A.2-24 B and B').

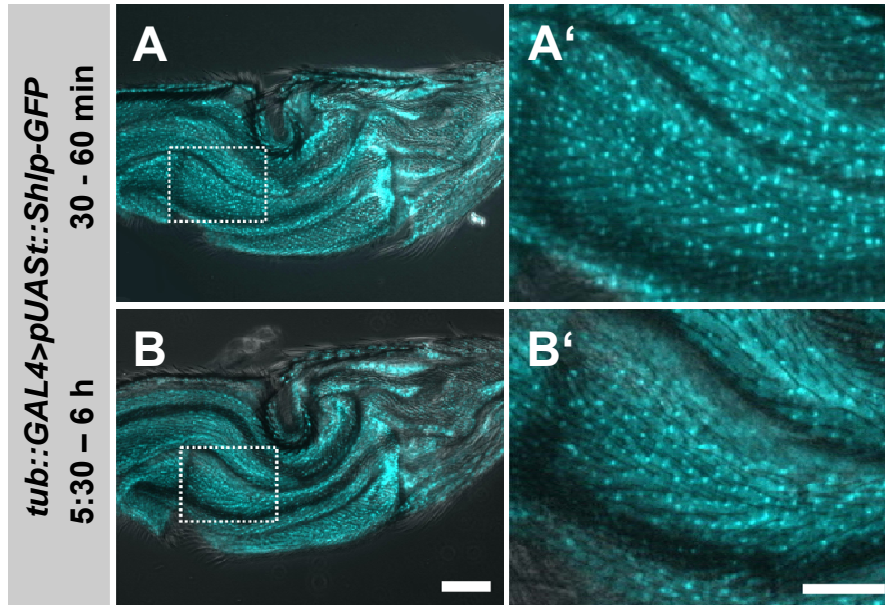


Figure A.2-24: Apoptosis of epithelial cells is delayed in the wing of flies that overexpress Shlp-eGFP. (A and A') Unexpanded wing of a fly overexpressing Shlp-eGFP under the control of *tub::GAL4* 30 – 60 min after hatching. DAPI staining reveals that wing cells are intact. (B and B') Cells are still intact after 5:30 – 6 h after hatching. Area marked with a rectangle in A and B is magnified in A' and B'. All images are merges of DAPI and DIC channel. Scale bars are 100 μ m in A and B and 50 μ m in A' and B'.

A.2.5.4 Functional analysis of Shlp protein domains

We have shown that the wing unfolding defects displayed by flies homozygous for *shlp*¹³¹ can be rescued by expressing an untagged form of Shlp (see chapter A.2.5.2). Overexpression of carboxy-terminally eGFP-tagged Shlp protein in the fly causes similar defects as *shlp*¹³¹, indicating a potential dominant negative function of this protein. To analyze which domains are needed to rescue the wing expansion defects of *shlp*¹³¹ flies, we generated a series of Shlp deletion constructs with an amino-terminally attached eGFP and generated transgenic flies (Fig. A.2-25). The transgenes inserted on the second chromosome were selected and crossed into the *shlp*¹³¹ background analogous as described in A.2.5.2. Like the *wildtype* protein, the deletion constructs were scored for rescue of the wing expansion and cuticle tanning defects seen in the *shlp*¹³¹ mutant. Final results of the rescue experiments are still in progress.

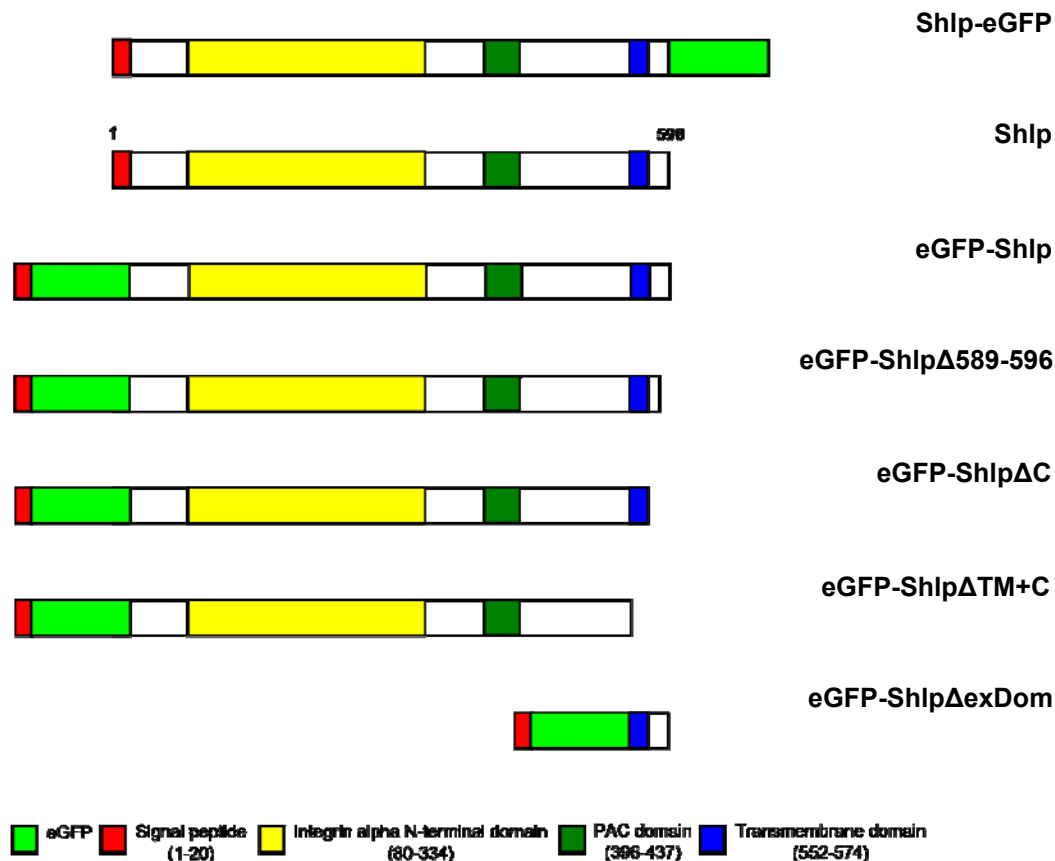


Figure A.2-25: Schematic representation of Shlp constructs used to generate transgenic flies. Shlp-eGFP is *wildtype* Shlp with an eGFP tag at the carboxy terminus. eGFP-Shlp is *wildtype* Shlp with an amino terminal eGFP tag. eGFP-Shlp Δ 589-596 lacks the last eight carboxy terminal aa of Shlp; eGFP-Shlp Δ C lacks the last 22 carboxy terminal aa; eGFP-Shlp Δ TM+C lacks the transmembrane domain and the intracellular domain; eGFP-Shlp Δ exDom lacks the extracellular domain of Shlp. For all amino-terminally eGFP tagged proteins, the Shlp signal peptide was placed in front of the eGFP tag to achieve membrane targeting of the proteins.

A.2.6 Infection and survival experiments to test a potential role of Shlp in immunity

In cooperation with the group of Bruno Lemaitre survival experiments after bacterial infection were conducted to test if Shlp has an influence on the humoral immune reaction. We conducted these experiments because TIP, the mammalian homologue of Shlp, has a modulatory role in adaptive immune responses (Fiscella *et al.*, 2003). Although *Drosophila* has no adaptive immune response, many of the mechanisms governing innate immunity are conserved between vertebrates and invertebrates and therefore one could speculate that Shlp, since it is not required for viability, might have a function during the innate immune

response. To test the role of Shlp in humoral immunity, *shlp*¹³¹ mutant flies were challenged by infection with the Gram-negative bacterium *Erwinia carotovora* (*E. carotovora*) (Fig. A.2-26 A) and the Gram-positive bacterium *Enterococcus faecalis* (*E. faecalis*) (Fig. A.2-26 B). It is known that infection of flies with *E. carotovora* activates the Toll pathway, while infection with *E. faecalis* activates the immune deficiency (Imd) pathway (Buchon *et al.*, 2009). In response to infection with *E. carotovora* *shlp*¹³¹ flies survived comparable to *wildtype* or *shlp*^{GE24395} flies (Fig. A.2-26 A). As a control a *relish* (*rel*) loss-of-function mutant (*rel*^{E20}) was included in the experiment. In the *rel*^{E20} mutant, Imd pathway mediated induction of antimicrobial peptides is impaired (Janeway and Medzhitov, 2002). *Rel*^{E20} flies in contrast to *wildtype*, *shlp*^{GE24395} and *shlp*¹³¹ flies rapidly succumbed infection with *E. carotovora*. *shlp*¹³¹ mutant flies survived infection with *E. faecalis* comparably well as *wildtype* flies, while null mutants for *spätzle* (*spl*^{m7}), died quickly after infection (Fig. A.2-26 B). *spätzle* encodes a ligand that is required to induce the Toll pathway and *spl* loss-of-function leads to loss of Toll pathway induction (Ferrandon *et al.*, 2007) and therefore flies mutant for *spl* are susceptible to infection with Gram-positive bacteria. The increased survival of *shlp*^{GE24395} flies in comparison to *wildtype* flies was not further considered here and may be a matter of statistical variation. We conclude from these experiments that *shlp* is not directly involved in the humoral immune reaction in response to bacterial infection.

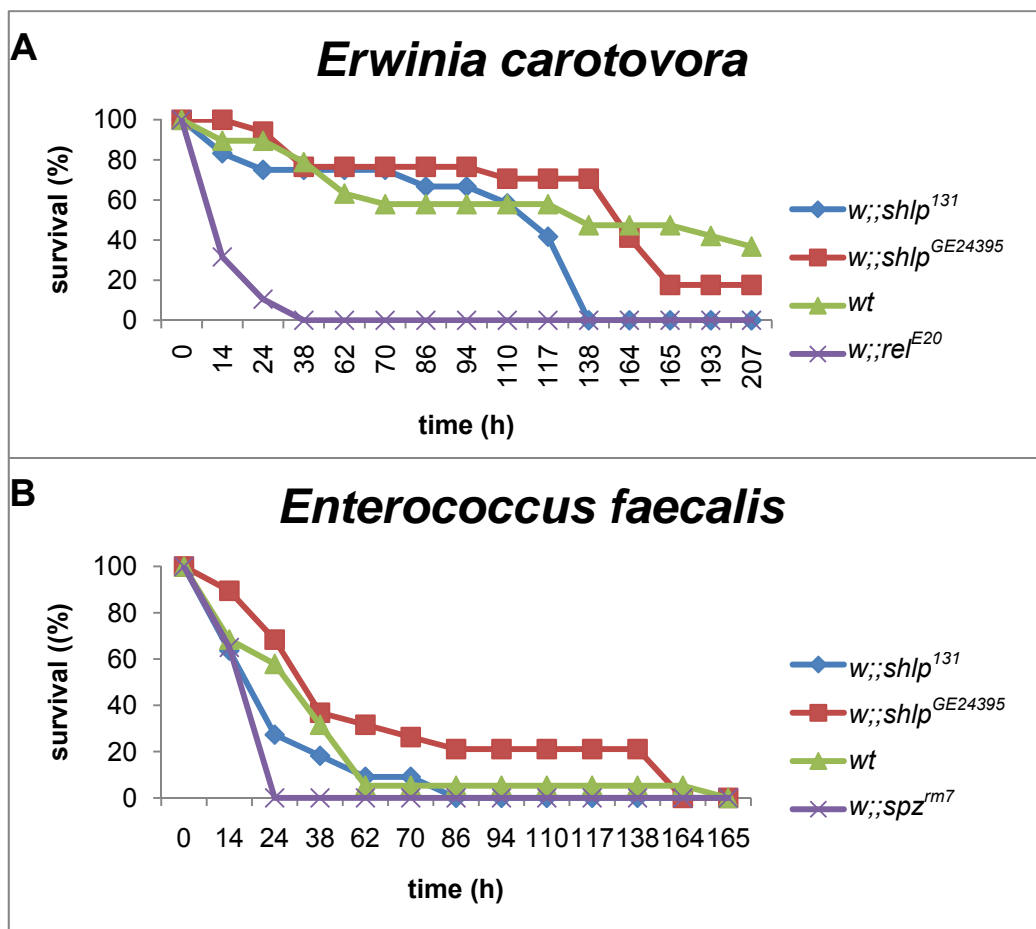


Figure A.2-26: *shlp*¹³¹ mutant flies do not show an increased susceptibility to infection with Gram-negative (A) or Gram-positive (B) bacteria. The survival rates (%) of *shlp*¹³¹ flies infected with the Gram-negative bacterium *Erwinia carotovora* (A) or the Gram-positive bacterium *Enterococcus faecalis* (B) were compared with *shlp*^{GE24395} flies, *wildtype* (*wt*) flies and flies mutant with in the Imd pathway (*rel*^{E20}) or the Toll pathway (*spz*^{m7}). Flies were infected by septic injury with a needle dipped in a concentrated bacterial pellet.

A.2.7 Biochemical characterization of Shlp protein

A.2.6.1 Glycosylation of Shlp

The mammalian homologue of Shlp, TIP, has been described to harbor twelve potential N-linked glycosylation sites. When performing Western Blot analysis with an antibody directed against TIP on the purified extracellular domain of TIP which had been expressed in 293T mammalian cell culture cells, the protein ran at a position higher than the predicted molecular weight (Fiscella *et al.*, 2003). Therefore, we analyzed the Shlp amino acid sequence for the presence of N-linked glycosylation sites using the program NetNGlyc 1.0 (<http://www.cbs.dtu.dk/services/NetNGlyc/>). Six asparagine residues at the amino acid positions 22, 129, 167, 187, 229 and 379 are predicted to be N-glycosylated according to

A Results

this algorithm, out of which glycosylation of residues 22, 129 and 187 is most likely. To test if Shlp is N-glycosylated, we performed a deglycosylation assay. Protein lysates were prepared from embryos expressing Shlp-eGFP ubiquitously under the control of *da::GAL4*. Then Shlp-eGFP was precipitated using GFP-Trap[®] as described in Material and Methods C.6.2 and treated with PNGase F. PNGase F, also known as N-Glycosidase F, is an amidase that cleaves between the innermost N-acetylglucosamin and asparagine residues of high mannose, hybrid and complex oligosaccharides from N-linked glycoproteins (Maley *et al.*, 1989). Shlp-eGFP has a predicted molecular weight of 94 kDa. But detection of Shlp-eGFP in Western Blot shows a molecular weight of approximately 115 kDa (Fig. A.2-26, second lane from left). Shlp-eGFP treated with PNGase F ran at a molecular weight of approximately 100 kDa (Fig. A.2-26, first lane from left). An eGFP-tagged cytoplasmic protein, Rings lost-eGFP (Rngo-eGFP) was also treated with PNGase F as control (Fig. A.2-26, first lane from right). In contrast to Shlp-eGFP, no band shift can be observed by PNGase F treatment. These results indicate that Shlp is an N-glycosylated protein.

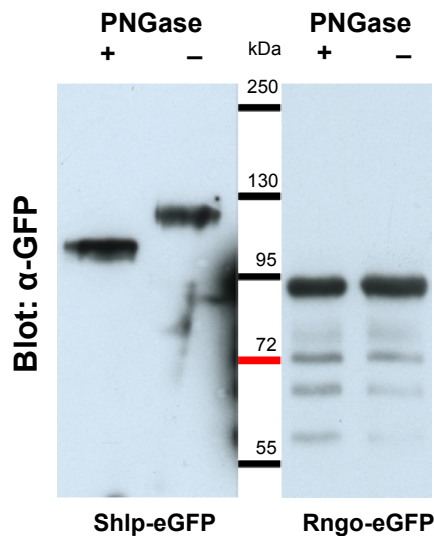


Figure A.2-27: Shlp is a N-glycosylated protein. Shlp-GFP was precipitated from embryonic protein lysates using GFP-Trap[®] and subsequently treated with PNGase F. Protein was eluted from GFP-Trap[®] beads, separated by SDS-PAGE and subjected to Western Blot analysis using a GFP antibody. When treated with PNGase F, Shlp-eGFP shifts to a lower molecular weight (+ PNGase, compare lane – PNGase as control without enzyme). When Rngo-eGFP, a cytoplasmic protein without predicted glycosylation sites, was treated with PNGase F, no bandshift could be observed (compare lane +PNGase with lane – PNGase).

A.2.6.2 Secretion of Shlp in *Drosophila* S2r cells

TIP, the mammalian homologue of Shlp has been described to be a secreted protein (Fiscella *et al.*, 2003). Therefore we checked if Shlp is secreted in *Drosophila* S2r cells. We

transfected S2r cells transiently with pAW-*shlp* and pAW-SP-eGFP-*shlp*, two transgenes which allow the expression of Shlp and eGFP-Shlp under the control of an actin-promotor. After four days, cells were treated as described in C.6.3. Then protein lysates were separated by SDS-PAGE and subjected to Western Blot analysis (Fig. A.2-27). In cell supernatants from untransfected cells we were not able to detect any Protein with the SAC115 Shlp antibody (Fig. A.2-27, lane 1). In cell supernatants from cells transfected with pAW-*shlp* it was not possible to detect a prominent band (Fig. A.2-27, lane 2). We were able to detect a very faint band by using longer expositions that corresponded to a lower molecular weight than the major bands observed on Western Blots performed on Cell lysates (Fig. A.2-27, lane 5) indicating a very low level of secretion. Western blot performed on cell supernatants of cells transfected with pAW-SP-eGFP-*shlp* resulted in a strong signal for Shlp protein, indicating a robust secretion of eGFP-Shlp (Fig. A.2-27, lane 3). The secreted protein has a lower molecular weight than full-length eGFP-Shlp detected in protein lysates from cells (Fig. A.2-27, lane 6), indicating that the secreted form of eGFP-Shlp needs to be cleaved.

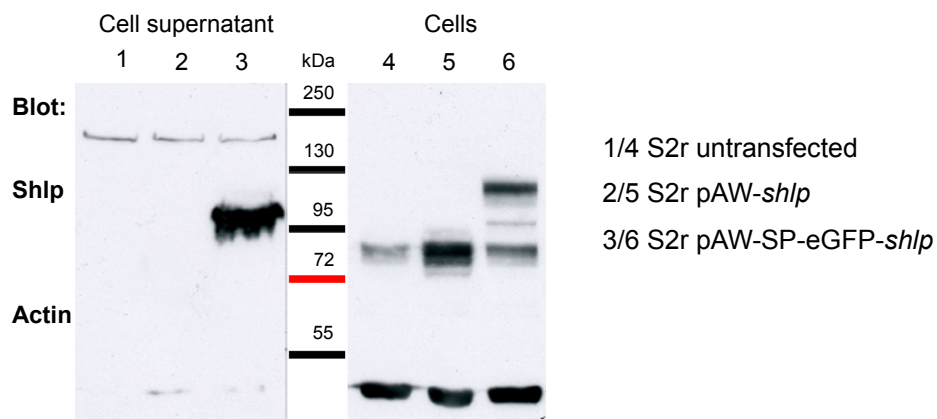


Figure A.2-28: eGFP-Shlp is secreted in S2r *Drosophila* cells. S2r cells were 1/4 not transfected, 2/5 transfected with pAW-*shlp* and 3/6 transfected with pAW-SP-eGFP-*shlp*. The supernatant of these S2r cells were then subjected to SDS-PAGE and Western Blot analysis with guinea pig SAC115 Shlp antibody (lane 1-3). As a control cell lysates were also subjected to SDS-PAGE and Western Blot analysis under the same conditions as the supernatants (lane 4-6). As a loading control the blot was cut at 55 kDa and incubated with an actin antibody.

A.2.6.3 Screen for interaction partner of Shlp by a yeast two-hybrid-screen

To get insights into the molecular function of Shlp we sought to identify novel interaction partners of the highly conserved intracellular carboxy terminus of Shlp. Therefore a yeast two-hybrid-screen was carried out by *Hybrigenics*, Paris, France, with the last 22 carboxy

terminal aa of Shlp as bait. The results of this screen are attached in the appendix of this thesis. *Hybrigenics* classifies the positive hits of a two hybrid screen regarding their confidence into 5 groups from A (very high confidence in the interaction) to E (non specific interaction). In summary no interactions were found that meet the requirements for the categories A (very high confidence in the interaction) to C (good confidence in the interaction). Of the 20 potential interaction partners 16 were grouped into category D (moderate confidence in interaction, including false positives and interactions that are difficult to detect in a two-hybrid-screen) and four were grouped into category E (non specific interactions). Since the found interaction between Shlp and the Bazooka amino-terminus, that was found in a previous yeast-two-hybrid-screen (Egger-Adam, 2005) could not be reproduced and because of the predicted low confidence of the found interactions, they were not further considered in this study.

A.2.6.4 Screen for interaction partners of Shlp by mass spectrometry

To gain further insights into the molecular function of Shlp during development of *Drosophila* we sought to identify interaction partners by mass spectrometry. Therefore protein extracts were prepared from embryos and L3 larvae that express Shlp-eGFP under the control of *da::GAL4*. As a negative control we used *w* embryos and L3 larvae. Shlp-eGFP was precipitated from these protein extracts using GFP-Trap[®] and the precipitated protein was separated and mass spectrometrically analyzed in the group of Dr. Olaf Jahn at the Max Planck Institute for Experimental Medicine. Unfortunately, the amount of soluble Shlp-eGFP that could be precipitated from lysates was low and it was not possible to identify any proteins from this approach by mass spectrometry. One result of such a precipitation is given in Fig. A.2-29. To circumvent the problems connected with solubilising a transmembrane protein, we used a peptide consisting of the last 22 highly conserved carboxy terminal aa covalently coupled to agarose beads (Shlp-intra beads) to perform pull downs on embryonic lysates and lysates of freshly hatched *white* flies (see Material and Methods C.6.5). When performing pull down experiments with Shlp-intra beads and control beads (see C.6.5), protein from the lysates bound unspecifically to the agarose gel matrix, which led to extensive background. It was not possible to identify differences between Shlp-intra beads and control beads. Therefore it was not possible to identify new interaction partners with this approach.

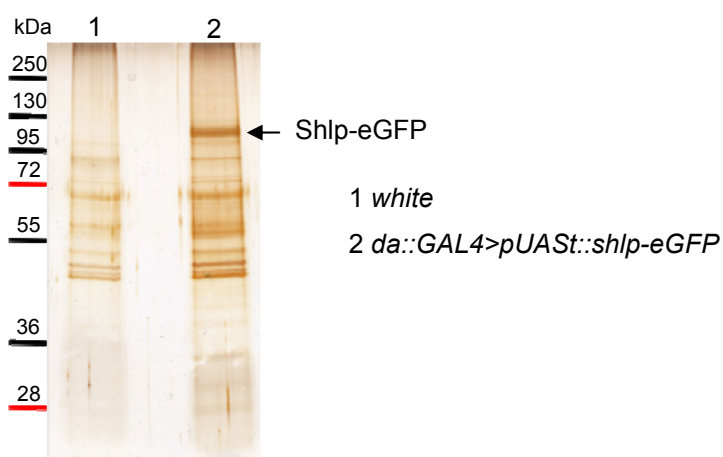


Figure A.2-29: Precipitation of Shlp-GFP from embryonic lysates using GFP-Trap[®]. Embryonic lysates were prepared from *white* embryos (1) or from embryos expressing Shlp-eGFP under the control of *da::GAL4* (2). Arrow marks Shlp-GFP. Gel was silver stained.

Recently we optimized our protocol for pull down experiments performed on embryonic protein lysates using Shlp-intra beads. In SDS-PAGE, a band of about 70 kDa that was not present when the pull down was performed with control beads, could reproducibly be detected in precipitates from pull downs with Shlp-intra beads (Fig. A.2-30). This band was cut out and analyzed by mass spectrometry in the group of Olaf Jahn, but unfortunately the protein amount was too low to confidently identify the corresponding protein or proteins. By repeating the experiment and pooling the precipitated protein, we will enlarge the amount of protein to finally be able to identify the potential Shlp interaction partners.

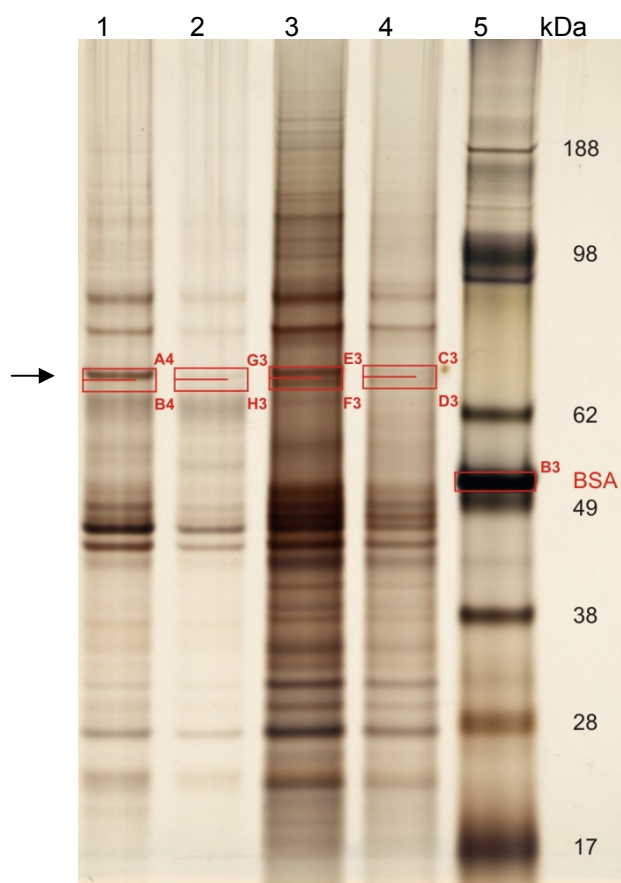


Figure A.2-30: Pull down with Shlp-intra and control beads performed on embryonic lysates. Lane 1: Pull down was performed with Shlp-intra beads and bound proteins were eluted by addition of 40 μ g Shlp-intra peptide. Lane 2: Pull down was performed with control beads, elution was performed with 40 μ g Shlp-intra peptide. Lane 3: Pull down was performed with Shlp-intra beads, elution was performed by boiling in 20 μ l 2XSDS sample buffer. Lane 4: Pull down was performed with control beads, elution was performed by boiling in 20 μ l 2XSDS sample buffer. Lane 5: Marker including 100 ng bovine serum albumin (BSA). Arrow marks a 70 kDa protein band that is absent in controls (Lane 2 and 4) and was used for mass spectrometry analysis. Red rectangles and number (A4, B4, G3, H3, E3, F3, C3, D3 and B3) mark gel pieces that were cut out and further processed for analysis.

A.3 Discussion

In this study the role the gene *schlappohr* (*shlp*) during development of *Drosophila* was investigated. Shlp was identified in a yeast-two-hybrid screen with the N-terminus of the polarity protein Bazooka (Baz) as bait. It was studied because initially its subcellular localization in embryonic NBs pointed to a role during the establishment of cortical localization of Baz in NBs, a process which is until now poorly understood. However, further analysis of a *shlp* mutant that was generated in the course of this study provided evidence that Shlp is not required for cortical recruitment of Baz. Analysis of the *shlp* mutant also revealed that the cortical localization of Shlp in NBs was an artifact caused by the used antibody.

shlp mutant flies are viable and fertile but show defects in wing expansion and cuticle tanning that are strikingly similar to defects found in flies with defective Bursicon (Burs) signaling, however with a much lower penetrance. Therefore, we checked for genetic interaction between *shlp* and *ricketts* (*rk*), the gene encoding the presumptive Bursicon receptor DLRG2. Despite striking similarities in the observed defects, it was not possible to show that these two genes genetically interact. In unexpanded wings of *shlp* mutant flies apoptosis of epithelial cells, which is a process that is necessary for proper wing maturation, was severely delayed. In the central nervous system of third instar larvae mutant for *shlp* the expression pattern of the molting hormone Burs was disturbed with some neurons especially in the thoracic region lacking Bursicon expression. This suggests that the observed defects in adults might be caused by a reduced number of Burs expressing neurons. Overexpression of a C-terminally eGFP tagged version of Shlp completely inhibited wing expansion, suggesting that this protein has a dominant negative function.

Since, TIP, the mammalian homologue of Shlp has a role in immunity, we analyzed if the humoral immune response is affected in *shlp* mutant flies. However, neither the humoral response to infection with Gram-negative nor the response to Gram-positive bacteria was affected.

Additionally, we provide evidence that N-terminally eGFP-tagged Shlp (eGFP-Shlp) is secreted in *Drosophila* Schneider cells and that Shlp is glycosylated. This is in agreement with the biochemical properties of the mammalian homologue. In order to identify interacting proteins of Shlp, pull down experiments coupled with mass spectrometric analysis of the precipitated proteins were performed.

A.3.1 Domain structure and phylogenetic analysis of Shlp

Shlp contains an amino-terminally localized signal peptide, an Integrin alpha N-terminal domain, a PAC motif and a single pass transmembrane domain. Amino acids 1-552 are predicted to be extracellular and amino acids 575-596 are predicted to be intracellular. In order to identify evolutionary related proteins that might help unravelling the molecular function of Shlp, we performed a protein-protein BLAST (NCBI) search and identified proteins with similarity to Shlp in many animal phyla. But based on its amino acid sequence no closely related protein with known function could be identified arguing that the closely related orthologues constitute a novel protein family of TIP-like proteins, which is named after its mammalian homologues. Surprisingly, we also identified one homologue of Shlp, termed Q8I3H7, in the proteome of the malaria parasite *Plasmodium falciparum* (*P. falciparum*). Kascanowski and Zielenkiewicz already described Q8I3H7 as the only non-animal homologue of the mammalian Shlp homologue TIP (Kaczanowski and Zielenkiewicz, 2003). They speculated that Q8I3H7 might either be an ancient secretory protein needed for the *P. falciparum* life cycle that had been adapted for T-cell function in mammals or it might be involved in the ability of *P. falciparum* to immunomodulate the host in order to escape the host's immune surveillance. Interestingly, the highly conserved carboxy-terminus of all animal TIP like proteins is not conserved in Q8I3H7. It is tempting to speculate that this potentially intracellular part of the protein might be required for cellular processes specific for animals.

A.3.2 Expression and subcellular localization of Shlp protein and *shlp* mRNA

A.3.2.1 Localization of Shlp protein

None of the Shlp antibodies that were generated was able to detect the endogenous protein in ovaries, embryos or larvae although we could show that they were able to detect overexpressed Shlp. These results indicate that either the sensitivity for Shlp protein of the generated antibodies is very low or that the endogenous Shlp levels are very low. When we ectopically expressed Shlp in embryos using the UAS-GAL4 system, it localized to the basolateral side of ectodermal epithelial cells and ubiquitously to the plasma membrane of NBs. Additionally, it localized to intracellular vesicles. When we ectopically expressed carboxy-terminally eGFP-tagged Shlp in embryos we observed similar results. Contrary to the basal localization in the ectodermal epithelial cells, Shlp was concentrated apically in the secretory cells of the salivary gland. This is in accordance with the previously described observation that Shlp is a secreted protein. This discrepancy in the localization of Shlp

between ectodermal epithelial cells and the epithelial cells of the salivary gland indicates cell type specific differences in the subcellular localization of the protein. The basolateral localization in ectodermal epithelial cells is surprising since Shlp is predicted to be N-glycosylated and we could show that Shlp-eGFP is N-glycosylated in a biochemical assay (see also 2.6.1). N-glycosylation has been implicated in apical targeting of transmembrane proteins (Scheiffele *et al.*, 1995; Schuck and Simons, 2004; Mellman and Nelson, 2008) and therefore one would expect apical sorting of Shlp. Since observation of Shlp and Shlp-eGFP localization was determined in an ectopic overexpression situation one cannot rule out the possibility that the observed distribution differs from the wildtype Shlp distribution.

A.3.2.2 Localization of *shlp* mRNA

Since it was not possible to determine the endogenous distribution of Shlp protein, we performed FISH to unravel the distribution of *shlp* mRNA in embryos and third instar larval brains. FISH with two independent *shlp* antisense RNAs on wildtype embryos was indistinguishable from FISH performed on *shlp*¹³¹ mutant embryos indicating that the *shlp* embryonic mRNA level is below our detection level. The same probes revealed a highly distinct *shlp* mRNA localization pattern in larval brains. Previously, it was described that *shlp* mRNA is ubiquitously expressed in early embryonic stages and becomes undetectable at embryonic stage 14 (Egger-Adam, 2005). These results are in contrast to our observation and might be caused by different mRNA detection methods used. Nevertheless, we consider our inability to detect *shlp* mRNA in embryos as another hint for overall low expression level of Shlp protein and *shlp* mRNA.

In the larval brain large cells in the central brain region, most likely central brain NBs, as well as cells of the optic lobe of unknown origin, were positive for *shlp* mRNA. We still need to verify the identity of the presumptive central brain NBs by co-staining with a NB marker like Mira.

A.3.3 Phenotypic analysis of *shlp* mutants

Flies homozygous for the two presumptive *shlp* null alleles *shlp*¹³¹ and *shlp*⁵² were viable and fertile. *shlp* mutant embryos displayed hatching rates comparable to the hatching rates of wildtype control embryos or embryos homozygous for the initial P-element insertion chromosome *shlp*^{GE24395}. Apicobasal polarity was not affected in *shlp* mutant embryos arguing against a role of *shlp* during establishment or maintenance of cell polarity.

29.1 % of *shlp*¹³¹ mutant flies had wing unfolding defects that were frequently connected with disturbed cuticle tanning. We considered this to be a specific defect, since by ectopical

expression of a Shlp transgene we could fully rescue the wing and cuticle defects. Similar wing and cuticle defects were also observed in flies mutant for Burs signaling (Baker and Truman, 2002; Dewey *et al.*, 2004; Luo *et al.*, 2005; Mendive *et al.*, 2005).

Loss of *rk* gene function leads to a failure in apoptosis of wing epithelial cells (Kimura *et al.*, 2004). *rk* encodes the Bursicon receptor DLGR2 and therefore Bursicon signaling seems to be required for the induction of post-ecdysal cell death of wing epithelial cells, which in turn is necessary for proper wing maturation. Staining the nuclei of unexpanded *shlp* mutant fly wings, we observed a severe delay in cell death of wing epithelial cells, equivalent to the *rk* mutant phenotype.

Because of these similar phenotypes, we checked if *shlp*¹³¹ and *rk*⁴, a loss of function allele of *rk*, genetically interacted. We hypothesized that if both genes act in the same pathway, than removal of one copy of *wildtype rk* might be able to amplify the wing expansion defect of the *shlp* mutant. Introducing one mutant copy of *rk*⁴ into the *shlp*¹³¹ homozygous mutant background did not enhance the wing defects of the *shlp* mutant arguing against a genetic interaction in the same pathway. Homozygous *rk*⁴; *shlp*¹³¹ double mutant flies were viable and they showed the wing expansion defects of the *rk*⁴ mutant, but the double mutants were often smaller and often displayed abnormal cuticle darkening that we occasionally observed in the *shlp*¹³¹ mutant flies. These observations do not conclusively hint to a genetic interaction between *shlp* and *rk*.

A difference to Bursicon signaling mutants is the comparatively low penetrance of the impaired wing expansion phenotype of *shlp* mutant flies. Null mutants for either *bursicon α* or *bursicon β*, the genes coding for the subunits of the Burs heterodimer or for *rk* display a complete block of wing expansion and a severe delay in cuticle tanning (Baker and Truman, 2002; Dewey *et al.*, 2004; Luo *et al.*, 2005; Mendive *et al.*, 2005).

Another gene that displays a partially penetrant wing expansion defect when mutated is the gene *unfulfilled (unf)*, which encodes a transcriptional repressor of the nuclear receptor family (Sung *et al.*, 2009). A proportion of *unf* mutant flies displays wing expansion defects, while the remaining flies expand wings but display severely compromised fertility. *unf* is expressed in mushroom body neurons and a small number of other cells of the central nervous system. Based on the expression pattern of *unf* the authors speculate that the observed wing defects and the impaired fertility might be caused by a neuronal defect. Based on the neuronal localization of *unf* transcripts Sung *et al.* hypothesized that the subsets of peptidergic neurons that produce the neuropeptides of the neuroendocrine cascade might be candidates responsible for the *unf* mutant phenotype. These peptidergic neurons include the eclosion hormone

neurons (EH neurons) that express and release eclosion hormone (McNabb *et al.*, 1997), the crustacean cardioactive peptide (CCAP) neurons that express and release CCAP but do not express Bursicon (CCAP neurons) and a subset of CCAP expressing neurons that co-express Bursicon (Bursicon neurons, (Park *et al.*, 2003; Dewey *et al.*, 2004; Luan *et al.*, 2006). Sung *et al.* noted that *unf* mutants displayed axonal defects in EH neurons and the mushroom bodies and speculated that this might be the basis for the observed defects (Sung *et al.*, 2009). We checked the pattern of Bursicon α expressing neurons in *shlp*¹³¹ mutant CNSs of third instar larvae and we observed clear differences to *wildtype* control CNSs. The number of Bursicon α positive neurons was reduced (23 Bursicon α positive neurons at average) in *shlp*¹³¹ mutants when compared to controls (33 Bursicon α neurons at average). Therefore, an altered Burs expression pattern in the CNS might account for the observed wing expansion and cuticle phenotypes in the *shlp* mutant. We did not examine the pattern of other peptidergic neurons in the *shlp*¹³¹ mutant but to check for differences in subsets of these neurons would be a reasonable approach to figure out if the defect we observe is specific to Burs α expressing neurons or if it is a more general defect affecting different subtypes of neurons. Another interesting issue is our recent finding that *shlp* is expressed specifically in the larval brain. We did not detect *shlp* expression in Burs α positive cells but it is definitely necessary to re-examine the expression pattern of *shlp* mRNA in the larval CNS to get a better understanding of its function. Another important approach to figure out where exactly Shlp function is needed is a tissue-specific rescue of the wing expansion defect. For this, we will use a *Burs::GAL4* that is expressed in Bursicon neurons (Peabody *et al.*, 2008), and *GAL4-30A* that is expressed in wings (Kiger *et al.*, 2001) and express *UAS::Shlp* in the *shlp*¹³¹ mutant background. If it is possible to rescue the wing defect by expressing Shlp in Bursicon neurons, this would indicate that Shlp is specifically needed in Bursicon neurons for its role in wing unfolding.

A.3.4 Overexpression of Shlp-eGFP in flies mimics the defects seen in *shlp*¹³¹ mutant flies

An interesting finding is that UAS/GAL4 mediated overexpression of carboxy-terminally eGFP tagged Shlp (Shlp-eGFP) in the fly results in defects very similar to the defects observed in *shlp* mutant flies. When the strong ubiquitous *tub::GAL4* driver was used, wing expansion was blocked in all flies and all flies displayed cuticle defects. In contrast, ectopic expression of untagged Shlp did not result in any defects. Therefore the eGFP-tag at the carboxy-terminus of the Shlp amino acid sequence in the Shlp-eGFP construct seems to

confer this recombinant protein dominant negative properties. Remarkably when performing immunofluorescent staining with the anti-Shlp EP023003 antibody that was generated against a peptide consisting of the last 16 amino acids of Shlp on embryos or S2r cells expressing Shlp-eGFP, it was not possible to detect the protein (data not shown). When performing the same experiment on embryos or S2r cells ectopically expressing untagged Shlp protein, we were able to detect the protein. These results indicate that in the Shlp-eGFP construct the evolutionarily highly conserved intracellular carboxy-terminal region of Shlp is to some extent not accessible and this could contribute to the dominant negative effects we observed. But up to now it is not known in what molecular pathway Shlp could be involved.

A.3.5 Structure-function analysis of the Shlp protein

In order to characterize the function of the domains of Shlp we generated transgenic flies allowing UAS/GAL4 mediated expression of different N-terminally eGFP-tagged Shlp constructs. It is planned to express these constructs in the *shlp*¹³¹ mutant background in flies to check which of these constructs are able to rescue the wing and cuticle phenotypes. In first trial experiments we expressed *pUASp::eGFP-Shlp Δ C*, a construct lacking the last 22 carboxy-terminal amino acids of Shlp, and *pUASp::eGFP-Shlp Δ 589-596*, a construct lacking the last eight conserved residues, in flies using *tub::GAL4*. We hypothesized that if the C-terminus of Shlp might be critical for the function of the protein, we would observe similar defects by expression of these constructs as seen in flies ectopically expressing Shlp-eGFP. Surprisingly, expression of these constructs in flies did not result in wing or cuticle defects. Since we do not know the molecular pathways Shlp is involved in, it is difficult to speculate what might cause these differences. Further experiments are needed, especially aiming at identifying proteins that interact with Shlp, to be able to explain the observed dominant negative effect of Shlp-eGFP and to figure out in which pathways Shlp is involved.

A.3.6 Biochemical characterization of Shlp protein

A.3.6.1 Secretion of Shlp in *Drosophila* S2r cells

It has been suggested and also some experimental evidence is available that the mammalian Shlp homologue TIP is a secreted and glycosylated protein (Fiscella *et al.*, 2003). To test if Shlp has the same biochemical properties as TIP we performed biochemical assays. In *Drosophila* S2r cell culture cells we could demonstrate that an N-terminally eGFP-tagged Shlp is secreted in the cell culture medium. Overexpressing an untagged Shlp version in cells we could also demonstrate its secretion but it was far less efficiently secreted than the tagged

protein, although expression levels in the cells were comparable. Shlp is also endogenously expressed in S2r cells, but we could not detect secretion of the endogenous protein. Comparing the sizes of the secreted and cellular form of eGFP-Shlp, we detect a size difference of around 20 kDa. This implies that Shlp might need to get cleaved to be efficiently secreted. These results indicate that Shlp has the potential to be secreted but we do not know whether this is also relevant for its biological function. Therefore it would be very interesting to check if Shlp could be detected as a secreted protein in the haemolymph of flies by Western Blot analysis. With a similar approach Luan *et al.* analyzed Bursicon secretion (Luan *et al.*, 2006). Since we could not detect endogenous Shlp using the available anti-Shlp antibodies in Western Blots of protein extracts from embryos, larvae and fly heads, this only seems to make sense in extracts of flies overexpressing Shlp.

A.3.6.2 Glycosylation of Shlp

Fiscella *et al.* noted that they detected TIP in Western Blots at a position bigger than the predicted size (Fiscella *et al.*, 2003). They interpreted this size difference as a sign for glycosylation of the protein, since TIP has 12 predicted N-glycosylation sites. We detected 6 predicted N-glycosylation sites in the Shlp sequence and therefore we checked for N-glycosylation in a deglycosylation assay. After treatment with PNGase F Shlp-eGFP shifted to a position corresponding to approximately 100 kDa and therefore very close to the predicted size of 94 kDa. This result suggests that Shlp similar to its homologue TIP is glycosylated. The relevance of glycosylation for its biological function needs to be determined.

A.3.6.3 Screen for interaction partners of Shlp

To get insight into the biological function of Shlp in *Drosophila* it is necessary to identify proteins Shlp interacts with. Therefore, we undertook different approaches, but unfortunately none of them was successful up to now.

Most recently, we could reproducibly detect a protein band of 70 kDa in precipitates from pull down experiments with Shlp intra beads on embryonic protein lysates that was not present in precipitates from pull downs performed with control beads. This protein band was cut out from the gel and analyzed by mass spectrometry but unfortunately the protein amount was too low to confidently identify the corresponding protein or proteins. We will repeat these experiments with a good chance in identifying the precipitated protein and a potential interacting protein of Shlp.

A.3.7 Infection experiments to test a potential role of Shlp in immunity

TIP, the mammalian homologue of Shlp, has an influence on the mammalian immune system and is able to modulate immune responses (Fiscella *et al.*, 2003). Although the function of TIP in the mammalian immune system is not directly transferable to the *Drosophila* immune system, it was checked in collaboration with the group of Bruno Lemaitre if humoral immunity is impaired in flies mutant for *shlp*. Neither the response to Gram-negative nor to Gram-positive bacteria was affected as judged by the survival in response to infection with *Erwinia carotovora*, a Gram-negative bacterium, or *Enterococcus faecalis*, a Gram-positive bacterium. These results make it unlikely that *Shlp* influences Toll or Imd signaling.

We did not analyze if *Shlp* has a function in cellular immunity. Recently, *Shlp* was identified as one of 617 proteins that are enriched in *Drosophila* phagosomes (Stuart *et al.*, 2007). Phagosomes are organelles of phagocytic cells that are formed around internalized pathogens and aid in killing them by providing a highly hydrolytic environment (Stuart and Ezekowitz, 2008). *Drosophila* S2 cells demonstrate properties similar to mammalian macrophages and efficiently ingest particles and pathogens (Stuart and Ezekowitz, 2008). Therefore it would be interesting to test if RNAi mediated knock down of Shlp or overexpression of Shlp in *Drosophila* S2 cells influences their phagocytic activity. This experiment could help figuring out if the enrichment of Shlp in Phagosomes is of functional relevance.

B The role of vesicle trafficking for cell polarity of *Drosophila* neuroblasts

B Summary

Vesicle trafficking is crucial for the establishment and maintenance of cell polarity. Although this is a well established mechanism in epithelial cells, very little is known about the potential role of vesicle trafficking in the establishment and maintenance of polarity in the highly polarized neuronal stem cells of *Drosophila melanogaster* (*Drosophila*), the so-called neuroblasts (NBs). Many of the proteins that are involved in epithelial cell polarity are also required for NB polarity, the most prominent example being the highly conserved PAR/aPKC complex, which indicates that similar mechanisms may be involved. Therefore, we analyzed the role of vesicle trafficking for NB cell polarity. We studied the distribution of Bazooka (Baz), atypical Protein kinase C (aPKC) and Miranda (Mira), as key players of NB polarity, in NBs of embryos and larval brains that were mutant for different components of the endocytic and secretory pathway. While we could detect severe defects in the organization of the ectodermal epithelium of embryos that were mutant for *shibire*, a critical component for vesicle budding at the plasma membrane, and for *exo84*, a component of the exocyst complex, which is critical in polarized exocytosis, NB polarity appeared normal. Furthermore, we checked the distribution of polarity markers in larval NBs mutant for exocyst components, the Adaptor protein-2 (AP-2) complex component α -Adaptin, the early endosome component Rab5 and components of the Endosomal sorting complex required for transport (ESCRT) machinery. NB markers were distributed normally in mutant NBs, indicating that other mechanisms than in epithelial cells may apply to polarize the plasma membrane of NBs.

B.1 Introduction

In the present study I analyzed the influence of vesicle trafficking on the polarity of asymmetrically dividing neuronal stem cells of *Drosophila melanogaster* (*Drosophila*), the so-called neuroblasts (NBs). Therefore I will first give an introduction into the known mechanisms regulating asymmetric neuroblast (NB) divisions and then later give a short overview about so far known functions of vesicle trafficking in regulating cell polarity.

B.1.1 Cell polarity and asymmetric division of NBs

Cell polarity is a common feature of many cell types including epithelial cells and neuronal stem cells. During asymmetric cell division of some stem cells, cell polarity plays a crucial role. Examples of such highly polarized stem cells are the NBs of the *Drosophila* embryo and larva. NBs have been extensively studied and proven to be an excellent model system to study the mechanisms of cell polarization (Prehoda, 2009). Embryonic NBs give rise to the nervous system of the *Drosophila* larva while larval NBs give rise to the nervous system of the adult fly (Knoblich, 2008).

Asymmetric division of *Drosophila* NBs

NBs of the ventral neurogenic region (VNR) are specified in a monolayered epithelium, the neuroectodermal epithelium, and delaminate as individual cells. They enter into the interior of the embryo and are positioned between the epidermal epithelium and the mesoderm. Shortly after delamination, NBs start to divide asymmetrically into a larger NB and a smaller ganglion mother cell (GMC) (Fig. B.1-1). The NB repeatedly divides asymmetrically in a stem cell-like fashion, while the GMC divides only once more to produce either a pair of neurons or a pair of glia cells (Campos-Ortega, 1993; Wodarz and Huttner, 2003). During the first division after delamination the mitotic spindle rotates by 90°, leading to a perpendicular orientation to the plane of the overlying epithelium (Kaltschmidt *et al.*, 2000). In all following NB divisions the mitotic spindle is formed already aligned to a cortical polarity axis and therefore spindle rotation does not take place (Rebollo *et al.*, 2009).

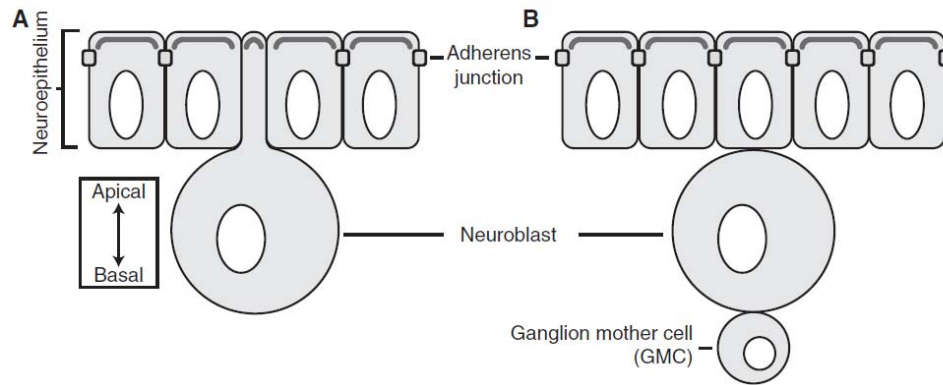


Figure B.1-1: An embryonic *Drosophila* neuroblast (NB). (A) An embryonic NB delaminates from the neuroectodermal epithelium where it is formed. After delamination the NB rounds up, grows in size and undergoes several rounds of asymmetric cell division. After each division a self-renewed NB is formed and a ganglion mother cell (GMC), which divides only once more to give rise to a pair of neurons or glia cells. From Prehoda (2009).

It is thought that certain aspects of epithelial polarity are inherited by the NBs and used to polarize the first mitotic division after delamination. This initial polarization directs the orientation of NB division and the unequal segregation of several proteins only to the GMC along an axis of polarity. Polarization is defined by the asymmetric localization of two protein complexes that localize in a crescent to the apical NB cortex. One complex, the PAR/aPKC complex, consists of the highly conserved proteins Bazooka (Baz, also known as Partitioning defective-3 (Par-3)), Partitioning defective-6 (Par-6) and atypical Protein kinase C (aPKC) (Schober *et al.*, 1999; Wodarz *et al.*, 1999; Wodarz *et al.*, 2000; Petronczki and Knoblich, 2001; Wodarz, 2005). The PAR/aPKC complex is involved in the regulation of most processes involving polarity (Suzuki and Ohno, 2006). The second complex contains Gai, a subunit of heterotrimeric G proteins, the GoLoco-motif proteins Partner of Inscutable (Pins) and locomotion defects (Loco), which act as guanine-nucleotide-dissociation inhibitors (GDIs) that stabilize Gai-GDP (Schaefer *et al.*, 2000; Schaefer *et al.*, 2001; Yu *et al.*, 2005), as well as the coiled-coil protein Mushroom body defective (Mud) (Bowman *et al.*, 2006; Izumi *et al.*, 2006; Siller *et al.*, 2006). The adaptor protein Inscuteable (Kraut *et al.*, 1996) links both protein complexes by interacting both with Baz and Pins (Schober *et al.*, 1999; Wodarz *et al.*, 1999; Schaefer *et al.*, 2000; Schaefer *et al.*, 2001).

Cell fate determinants and their adapter proteins

The apical protein complexes direct the basal segregation of the cell fate determinants Prospero (Pros), Brain tumor (Brat) and Numb and their adaptor proteins Miranda (Mira) and Partner of Numb (Pon) as well as the RNA binding protein Staufen (Rhyu *et al.*, 1994; Hirata

B Introduction

et al., 1995; Knoblich *et al.*, 1995; Spana and Doe, 1995; Ikeshima-Kataoka *et al.*, 1997; Shen *et al.*, 1997; Lu *et al.*, 1998; Matsuzaki *et al.*, 1998; Schuldt *et al.*, 1998; Bello *et al.*, 2006; Betschinger *et al.*, 2006; Lee *et al.*, 2006c). These proteins form a basal crescent in the NB that does not overlap with the crescent formed by the apical complexes.

Pros is a homeodomain transcription factor that is responsible for the cell fate difference, since *pros* mutants fail to express many GMC-specific markers and exhibit axonal defects (Doe *et al.*, 1991; Vaessin *et al.*, 1991; Hirata *et al.*, 1995; Knoblich *et al.*, 1995; Spana and Doe, 1995). *pros* mRNA is also segregated asymmetrically into the GMC because it associates with the RNA-binding protein Staufen (Matsuzaki *et al.*, 1998; Schuldt *et al.*, 1998). However, Staufen seems not to be required for cell-fate specification in NBs (Knoblich, 2008). In addition to Pros, Brat is required for proper fate specification of the GMC (Bello *et al.*, 2006; Betschinger *et al.*, 2006; Lee *et al.*, 2006c). It is a member of the evolutionarily conserved NHL (Ncl-1, HT2A and Lin41) domain family that generally seems to function in growth control (Slack and Ruvkun, 1998; Knoblich, 2008; Zhong and Chia, 2008). While fate transformations are limited in *brat* single mutant embryos, they are severe in *brat pros* double mutant embryos. This suggests that Brat and Pros might have partially redundant roles in specifying cell fate (Betschinger *et al.*, 2006). Numb is a phosphotyrosine-binding protein (Uemura *et al.*, 1989) that has been shown to act as a tissue-specific repressor of the Notch pathway (Schweisguth, 2004; Le Borgne *et al.*, 2005; Knoblich, 2008). It binds to the endocytic protein α -Adaptin (Berdnik *et al.*, 2002a) and it might influence the intracellular trafficking of Notch intermediates (Knoblich, 2008). While there are no obvious cell-fate changes in the progeny of embryonic NBs mutant for *numb*, *numb* mutant larval NBs overproliferate and form tumor like masses in the larval brain due to cell-fate transformations of GMCs into NBs (Lee *et al.*, 2006a; Wang *et al.*, 2006a).

The coiled-coil adaptor protein Mira binds to Pros, Brat and Staufen and mediates their asymmetric segregation during NB division (Ikeshima-Kataoka *et al.*, 1997; Shen *et al.*, 1997; Betschinger *et al.*, 2006; Lee *et al.*, 2006c). In *mira* mutants all three Mira binding partners become cytoplasmically localized and segregate equally into both daughter cells (Knoblich, 2008). In embryonic NBs Mira localizes to the apical cortex during interphase and becomes basally enriched during mitosis (Ikeshima-Kataoka *et al.*, 1997; Shen *et al.*, 1997). However, in larval NBs Mira never colocalizes with apical proteins but is rather both cytoplasmic and in a basal crescent during early prophase of mitosis (Slack *et al.*, 2006). The basal localization of Mira requires myosin II and IV as well as an intact actin cytoskeleton but the precise mechanism of basal localization is still not known (Barros *et al.*, 2003; Petritsch *et al.*, 2003;

Slack *et al.*, 2007). Fluorescence recovery after photobleaching (FRAP) analysis revealed that basal localization of Mira occurs mainly through passive diffusion throughout the cell rather than via active transport along the cortex (Erben *et al.*, 2008). A recent study suggested a role for the anaphase promoting complex/cyclosome (APC/C) and ubiquitinylation of Mira in the asymmetric localization of Mira to the NB cortex (Slack *et al.*, 2007). After segregation into the GMC, Mira is most likely degraded (Shen *et al.*, 1997; Matsuzaki *et al.*, 1998; Schuldt *et al.*, 1998), thereby allowing the release of Pros, Staufen and Brat.

The coiled-coil adaptor protein Pon binds to the cell fate determinant Numb and assists its asymmetric localization to the basal cortex (Lu *et al.*, 1998; Wang *et al.*, 2007). However Pon is not strictly required for Numb basal localization since Numb's cortical accumulation in NBs is delayed in metaphase but eventually is restored in anaphase and telophase (Wang *et al.*, 2007). Pon localization requires Myosin II and FRAP experiments revealed that basal localization of Pon occurs mainly along the NB cortex (Erben *et al.*, 2008). This is in contrast to the localization of Mira, which has been suggested to occur mainly through diffusion and indicates that different mechanisms are used for Pon and Mira localization (Erben *et al.*, 2008).

Coupling cortical polarity to asymmetric protein localization

How is cortical polarity coupled to basal Pon and Mira localization? The tumor suppressor protein Lethal giant larvae (Lgl) is a key player in this process. In NBs of *lgl* mutant embryos, localization of the PAR/aPKC complex is unaffected, while Miranda and Pon fail to localize to the basal cortex (Ohshiro *et al.*, 2000; Peng *et al.*, 2000; Betschinger *et al.*, 2003; Lee *et al.*, 2006b). Lgl is a key substrate for aPKC and in epithelial cells it is required to specify the basolateral domain and for restricting aPKC, Baz and Par-6 to the apical domain (Betschinger *et al.*, 2003; Plant *et al.*, 2003; Yamanaka *et al.*, 2003). Although it forms a complex together with aPKC and Par-6, it is distributed uniformly cortically in mitotic NBs (Betschinger *et al.*, 2003). By association with aPKC and Par-6, Lgl gets phosphorylated, which promotes an intramolecular interaction in Lgl that dissociates it from the cortex and displaces it into the cytosol (Betschinger *et al.*, 2003; Betschinger *et al.*, 2005). When a non-phosphorylatable Lgl (Lgl-3A) is overexpressed in embryonic NBs, it localizes exclusively to the cortex, while Mira is found all around the cortex and segregates into both daughter cells (Betschinger *et al.*, 2003). In contrast, overexpression of a mutant form of aPKC that is unable to bind to Par-6 and is no longer restricted to the apical cortex, causes partial displacement of Lgl from the cortex. As a result, Mira localizes to the cytoplasm (Betschinger *et al.*, 2003).

How does Lgl mediate basal recruitment of Pon and Mira in NBs? One possibility is that Lgl

B Introduction

could act by regulating vesicular trafficking. The homologues of Lgl in *Saccharomyces cerevisiae*, Sro7 and Sro77, associate with the t-SNARE (target-Soluble N-ethylmaleimide-sensitive-factor attachment receptor) Sec9 and aid in targeting vesicles to the plasma membrane (Lehman *et al.*, 1999). Therefore, Lgl could in analogy promote the delivery of Pon and Mira to the basal plasma membrane in NBs (Gönczy, 2008). It also has been suggested that Lgl might control basal localization of Pon and Mira by regulating myosin since Lgl binds to myosin II (Barros *et al.*, 2003), but experimental evidence for this is, just as for the role of Lgl in regulating vesicle trafficking, still missing.

Recently it has been shown that aPKC is able to phosphorylate cell fate determinants directly. aPKC is able to phosphorylate Numb and thereby Numb is released from the cortex into the cytosol (Smith *et al.*, 2007). Atwood *et al.* (2009) provide experimental evidence for a model in which aPKC directly phosphorylates Mira and thereby displaces Mira from the apical cortex in NBs. They further suggest that Lgl is not directly required for Mira localization but it is needed to negatively regulate aPKC function at the basal NB cortex (Atwood and Prehoda, 2009).

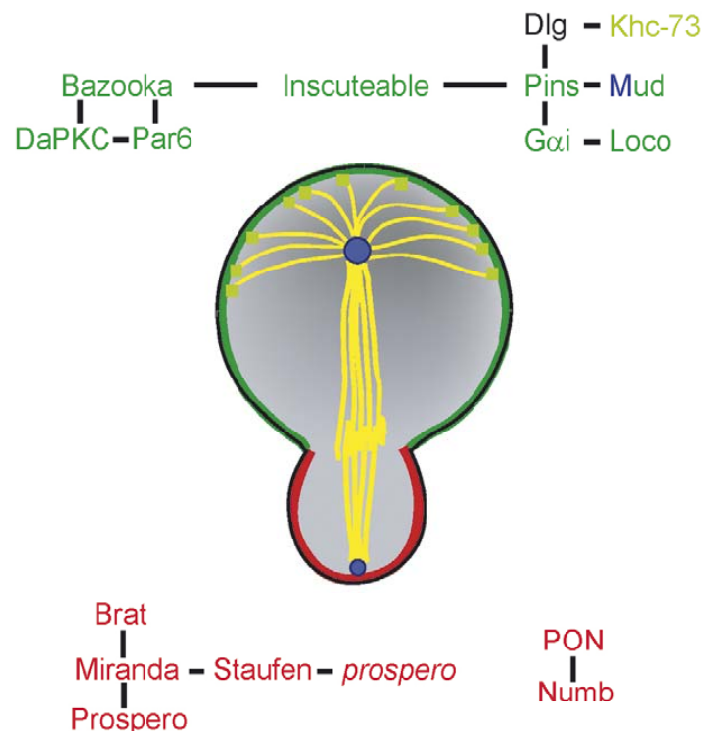


Figure B.1-2: Asymmetric division in *Drosophila* NBs. Two apically localized protein complexes are linked by Inscuteable. The evolutionarily conserved PAR/aPKC complex contains Bazooka, DaPKC and Par-6. DaPKC phosphorylates the tumour suppressor Lethal giant larvae (Lgl). This leads to the exclusion of basally localized proteins from the apical cortex. The second apical complex consists of the proteins Partner of Inscutabale (Pins), Gai and Locomotion defects (Loco). The Gai/Pins/LoCo complex regulates the orientation of the mitotic spindle to ensure that the cleavage plane is

perpendicular to the apicobasal polarity axis. Additionally, Pins can bind to Mushroom body defect (Mud), which is an essential component for proper spindle alignment, and Discs large (Dlg) as well as Kinesin Khc-73, which can induce spindle polarity. Basally, two protein complexes are localized. One contains the adaptor protein Miranda which mediates the basal localization of its binding partners, the homeodomain protein Prospero, Brain tumor (Brat) and Staufen, which is a RNA-binding protein that also binds *prospero* mRNA. The cell fate determinant Numb binds its adaptor protein Partner of Numb (Pon), which is needed for basal localization of Numb. Prospero, Brat and Numb segregate into the GMC, where they mediate differentiation and suppress self-renewal. From Zhong and Chia (2008).

Mitotic spindle orientation

To make sure that cell fate determinants are exclusively distributed to the GMC, the mitotic spindle has to be oriented orthogonally to the protein crescents. One key player in this process is the protein Inscuteable (Kraut *et al.*, 1996). Inscuteable localizes apically by binding to Baz and subsequently recruits Pins. Pins contains three so-called GoLoco domains in its C-terminus that bind Gai. This binding serves two functions (Nipper *et al.*, 2007): Binding to the first GoLoco domain recruits Pins to the plasma membrane. By binding to the second and third GoLoco, Gai changes the conformation of Pins. Thereby Pins switches to an active state in which Mud can bind to its N-terminus (Bowman *et al.*, 2006; Izumi *et al.*, 2006; Siller *et al.*, 2006). Mud is the *Drosophila* homologue of the microtubule and Dynein binding protein NuMA. In a simple model it has been suggested that Mud functions in providing a docking site for astral microtubules. By its apical concentration at the cortex it could attract one of the spindle poles and thereby tether the orientation of one spindle to the apical protein crescent (Bowman *et al.*, 2006). Another microtubule binding protein is implicated in NB polarity. The kinesin Khc-73 localizes to plus ends of microtubules and binds to an adaptor protein called Discs large (Dlg) at the cell cortex (Siegrist and Doe, 2005). Dlg binds to Pins and this collective binding leads to a clustering of apical polarity complexes over the spindle pole. This interaction is thought to account for the phenomenon called “telophase rescue” which occurs in many mutants affecting asymmetric cell division and describes the reestablishment of asymmetric protein localization defects during late stages of mitosis (Knoblich, 2008).

Larval NBs

Although most of the machinery for asymmetric division of embryonic NBs is also used in larval NBs there are several issues that make larval NBs different from embryonic NBs. Larval NBs have an embryonic origin: late in embryonic development, embryonic NBs become mitotically inactive and shrink in size (Hartenstein *et al.*, 2008). They start dividing during larval stages and until the third larval instar stage all NBs are mitotically active

B Introduction

(Hartenstein *et al.*, 2008). In contrast to the stereotyped orientation of the mitotic spindles during division of embryonic NBs, larval NBs do not show a fixed orientation of their mitotic spindles relative to the surface of the brain (Ceron *et al.*, 2001). Embryonic NBs give rise to the relatively simple nervous system of the larva and their capacity to self-renew is limited. In contrast to that, larval NBs give rise to thousands of neurons found in the central nervous system of the fly. Moreover, unlike embryonic NBs that become smaller with each division, larval NBs are able to regrow their size after each division and are able to divide several hundred times (Ito and Hotta, 1992). Several types of larval NBs can be identified based on their position within the central nervous system (Fig. B.1-3). In the ventral nerve chord 30 ventral nerve chord NBs per hemisegment divide repeatedly along an apical-basal axis to generate the neurons of the thoracic and abdominal ganglia (Truman and Bate, 1988). In each of the two brain lobes, roughly 85 central brain NBs are present that give rise to most of the neurons present in the adult brain (Ito and Hotta, 1992). These NBs of the central brain are heterogeneous regarding cell cycle length, number of divisions as well as cell lineage (Betschinger *et al.*, 2006; Bello *et al.*, 2008; Knoblich, 2008). Additionally the larval brain contains the mushroom body NBs and the optic lobe NBs. In each hemisphere only four mushroom body NBs give rise to 2500 neurons called Kenyon cells that are responsible for learning and memory (Ito and Hotta, 1992). The inner and outer proliferation centers, two multilayered epithelia, give rise to the optic lobe NBs (Fig. B.1-3) (White and Kankel, 1978; Egger *et al.*, 2007). While neuroepithelial cells divide symmetrically in parallel to the epithelial surface, NBs are generated on the rims of these neuroepithelia (Egger *et al.*, 2007). These cells lose their adherens junctions, start to express NB markers and divide asymmetrically and perpendicularly to the epithelial plane (Egger *et al.*, 2007). Optic lobe NBs give rise to the neurons of the visual processing centers in the adult fly brain.

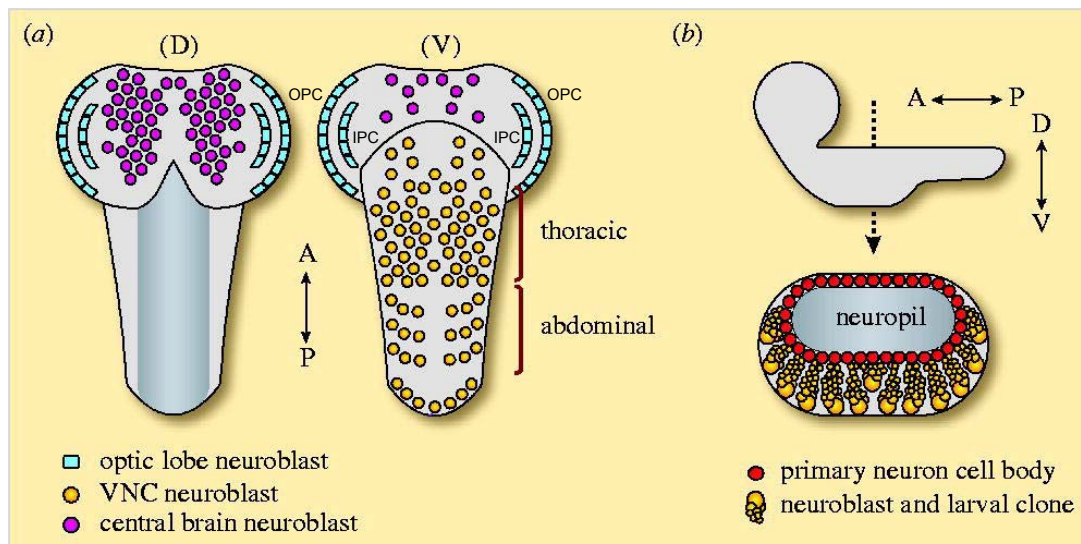


Figure B-1-3: Scheme of a third instar larval brain. (a) The left drawing represents a dorsal view (D); the right drawing a ventral view (V) of the larval brain. (b) A lateral view of the larval brain is shown on top with anterior (A) to the left, posterior to the right (P), dorsal to the top (D) and ventral to the bottom (V). OPC = outer proliferation center, IPC = inner proliferation center. The picture below represents a schematic cross section through the ventral nerve chord at the indicated position. From (Egger *et al.*, 2008).

B.1.2 Polarity and vesicle trafficking

Epithelial polarity

Epithelial cells are highly polarized as can be seen by the division of the membrane into an apical domain which faces the external environment and a basolateral domain which is in contact with the interstitial space of the body (Tepass *et al.*, 2001). These domains are separated by a subapical junctional complex which contains adherens junctions and encircles the cell just below the apical surface to bind to other cells (Nelson, 2003) (Fig. B.1-4). Epithelial cell polarity is established and maintained by the combined action of polarity complexes and the regulated endo- and exocytosis of these complexes (Leibfried and Bellaiche, 2007). The main complexes for establishment and maintenance of polarity comprise the Crumbs/Stardust/*Drosophila* Pals 1-associated tight junction protein (DPatj), the PAR/aPKC and the DE-Cadherin (DE-Cad)/*Drosophila* β -Catenin (Armadillo)/ α -Catenin complexes (Margolis and Borg, 2005). The DE-Cad/Armadillo/ α -Catenin complex promotes cell-cell adhesion by the homodimerization of DE-Cad monomers of adjacent cells and localizes mainly to adherens junctions. Polarity establishment depends on the mutually antagonistic activity of three protein complexes: The Crumbs/Stardust/Dpatj complex is recruited to the apical domain by the PAR/aPKC complex and counteracts the activity of the basolaterally localized Scribble/Discs large/Lethal giant larvae (Scrib/Dlg/Lgl) complex,

B Introduction

which in turn counteracts the activity of the PAR/aPKC complex (Bilder *et al.*, 2003; Johnson and Wodarz, 2003; Tanentzapf and Tepass, 2003). The PAR/aPKC complex is activated through the direct interaction of the small Ras-like GTPase Cell division cycle 42 (Cdc42) with Par-6, thereby aPKC is able to phosphorylate Lgl and restrict its activity to the basolateral membrane (Hutterer *et al.*, 2004). Armadillo is able to bind to the Par/aPKC complex via direct interaction with Baz. This interaction positions the PAR/aPKC complex to adherens junctions (Wei *et al.*, 2005; Morais-de-Sa *et al.*, 2010).

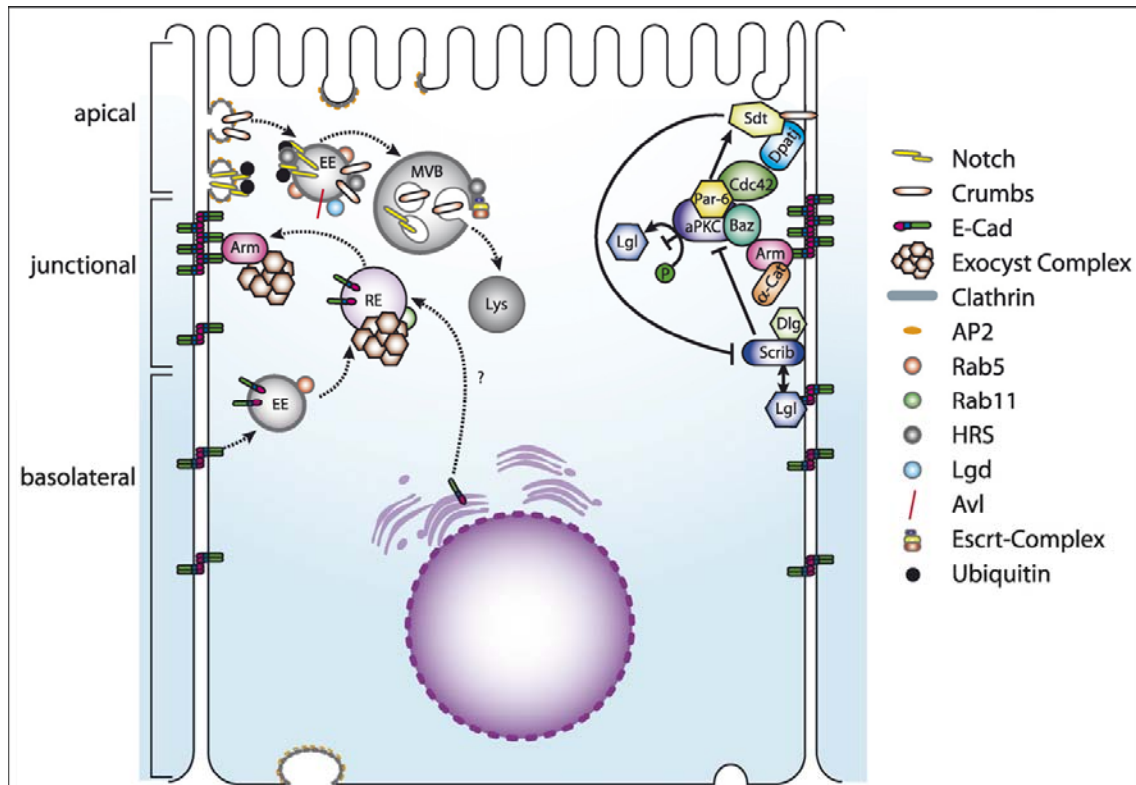


Figure B.1-4: An overview of polarity complexes and vesicular trafficking in polarized *Drosophila* cells. The plasma membrane in an epithelial cell can be subdivided into three distinct parts as indicated on the left side of the figure: An apical domain (apical) and a basolateral domain (basolateral), that are separated by the apical junctional complex (junctional). In the right part of the figure polarity complexes and their interactions that are required for establishment and maintenance of polarity are indicated. Establishment and maintenance of epithelial polarity depends on the mutually antagonistic activities of the Crumbs/Stardust/Dpatj, PAR/aPKC and Scribble/Disks large/Lethal giant larvae complexes. The transmembrane protein DE-Cadherin (E-Cad) localizes mainly to adherens junctions and is responsible for cell-cell adhesion. Armadillo (Arm) and α -Catenin can bind to E-Cad. Arm can bind to Baz and thereby aids in localizing the PAR/aPKC complex to adherens junctions. On the left side of the figure some of the different endosomal pathways and their role in cell polarity and signaling regulation are indicated. See main text for details. Protein internalization is triggered by clathrin-dependent and -independent pathways. Notch and Crumbs might get monoubiquitinated and subsequently endocytosed in Clathrin and Adaptor protein complex 2 (AP2) coated vesicles. Negative

(T) and positive (↑) genetic interactions are indicated. Abbreviations: Lys: lysosome, MVB: multivesicular bodies. From (Leibfried and Bellaiche, 2007).

The exocyst complex and cell polarity

As stated above most cells are polarized and have different plasma membrane domains with a distinct protein and lipid composition. The generation or maintenance of distinct plasma membrane domains depends on targeted exocytosis of transport vesicles from the biosynthetic pathway or the recycling endosome (Mostov *et al.*, 2003). The process of targeted exocytosis is highly regulated, but the precise mechanisms of regulation are still poorly understood. A protein complex which is involved in polarized cell surface delivery events in several cell types is the exocyst, also known as Sec6/8 complex (Wu *et al.*, 2008). The exocyst complex is involved in tethering, docking and fusion of post-Golgi vesicles with the plasma membrane (Wu *et al.*, 2008). The exocyst is an octameric complex composed of the subunits Sec3, Sec5, Sec6, Sec8, Sec10 Sec15, Exo70 and Exo84 and is conserved from yeast to mammals (Matern *et al.*, 2001). Initially the genes encoding the exocyst subunits were identified in a screen for mutants that cause a secretory defect in the budding yeast *Saccharomyces cerevisiae* (Novick *et al.*, 1980). Crystallographic studies revealed that the exocyst subunits are composed of structurally similar helical bundles, which form rod-like domains that might associate through an extensive network of interactions within the complex (Hamburger *et al.*, 2006; Munson and Novick, 2006). Although the importance of the exocyst in regulating exocytosis is clear, very little information is available about the mechanism by which it contributes to exocytosis in the context of cell polarity.

More recently, studies conducted on the mammalian and *Drosophila* components of the exocyst revealed that in contrast to the yeast exocyst complex which is required for all major secretory events, the metazoan exocyst seems to mediate more specialized functions. In neurons the exocyst has a role in neurite outgrowth and the targeting of receptors to the synapse but it is not generally required for neurotransmission (Vega and Hsu, 2001; Murthy *et al.*, 2003; Sans *et al.*, 2003). In mammalian Madin-Darby canine kidney (MDCK) epithelial cells it was shown that the exocyst is required for the transport of proteins to the basolateral, but not to the apical membrane (Grindstaff *et al.*, 1998). The exocyst has also been shown to be regulated by a number of small GTPases including members of the Rho and Rab family (Lipschutz *et al.*, 2000; Inoue *et al.*, 2003; Prigent *et al.*, 2003).

It was shown for the yeast exocyst complex that it is not only involved in all major secretory events, but each of the eight exocyst components is essential for targeted exocytosis (Finger and Novick, 1998; Hsu *et al.*, 2004). Genetic studies in *Drosophila* indicate that a significant

B Introduction

functional diversification of exocyst components may have taken place. While Sec5 is broadly required for exocytosis and survival in flies (Murthy *et al.*, 2003; Murthy and Schwarz, 2004), Sec10 appears to have an essential function only in hormone secretion, but is not generally required for exocytosis or neurotransmission (Andrews *et al.*, 2002). *sec6* mutations cause cell lethality and disrupt plasma membrane growth and in epithelial photoreceptor cells with reduced Sec6 function, apical exocytosis is disrupted (Beronja *et al.*, 2005). Additionally, it was shown that the exocyst forms a complex with the small GTPase Rab11, suggesting that the exocyst is a Rab11 effector.

Langvin *et al.* analysed the role of the exocyst in localization of the adherens junction protein *Drosophila* E-Cadherin (DE-Cad) in epithelial cells of the dorsal thorax of *Drosophila* pupae (Langevin *et al.*, 2005). They showed that loss of function of the exocyst subunits Sec5, Sec6 and Sec15 results in accumulation of DE-Cad in an enlarged Rab11 positive recycling endosomal compartment and inhibits DE-Cad delivery to the membrane. Furthermore, they could demonstrate that Sec15 and Sec10 interact with Rab11 and Armadillo (*Drosophila* β -Catenin). They suggested a model in which the exocyst is required for DE-Cad transport from recycling endosomes to the adherens junctions and thereby contributing to the maintenance of epithelial cell polarity.

A role of the exocyst in actively maintaining apical localization of the transmembrane protein Crumbs and thus for preserving epithelial polarity has been proposed (Blankenship *et al.*, 2007). The EGF-repeat transmembrane protein Crumbs plays a key role in specifying the apical plasma membrane domain in ectodermal epithelial cells (Wodarz *et al.*, 1995). In mutants for the exocyst subunit Exo84, loss of Crumbs is the earliest defect observed. In advanced stages of epithelial degeneration *Exo84* mutants also exhibit defects in trafficking of apical and junctional proteins like Baz and DE-Cad from an enlarged recycling endosomal compartment to the plasma membrane (Blankenship *et al.*, 2007).

These results from *Drosophila* and mammalian cells demonstrate a key role for the exocyst complex in diverse functions including the maintenance of epithelial polarity. But, the exocyst has also been shown to be required during the asymmetric division of the sensory organ precursor cells (SOPs) of the *Drosophila* pupa. SOPs give rise to the mechanosensory bristles of the *Drosophila* dorsal thorax. SOPs are a well established model for the role of Notch signaling in cell fate decisions. After SOP division, Notch and its ligand Delta are present in both daughter cell called pIIa and pIIb but the differential regulation of vesicle trafficking ensures that Notch is active in the pIIa but not in the pIIb cell (Emery and Knoblich, 2006). In SOPs mutant for the exocyst subunit Sec15 Notch signaling is impaired and proper cell fate

determination does not take place (Jafar-Nejad *et al.*, 2005). It has been proposed that defective recycling of the Notch ligand Delta from the recycling endosome is responsible for the defects in cell fate determination in the SOP lineage (Jafar-Nejad *et al.*, 2005).

A connection between the exocyst and the PAR/aPKC complex was shown recently, by demonstrating that the association of PAR-3 (the mammalian Baz homologue) with the exocyst is needed for the polarization of cultured rat neurons. This association is mediated by the Ras-like GTPase (Ral) isoform Ral A (Lalli, 2009).

In *Saccharomyces cerevisiae* (*S. cerevisiae*) an interaction between the exocyst complex component Exo84 and the yeast homologues of Lgl, Sro7 and Sro77 was shown (Zhang *et al.*, 2005). Furthermore it was demonstrated that this interaction is important for exocytosis and polarity, since *sro7* and *sro77* mutants showed defects in polarized secretion and polarity similar to defects of *exo84* mutants and *exo84* defects in secretion could be rescued by overexpressing Sro7. Since Lgl has been shown to have a crucial function in NB polarity, the question arises whether NB polarity could be regulated by exocyst function.

Endocytosis and cell polarity

Endocytosis has an important function in maintaining membrane composition in polarized cells. Several endosomal proteins have been implicated in the regulation of cell polarity. In genetic screens carried out in *Drosophila* components of the early endosomal and of the ESCRT (endosomal sorting complex required for transport) complex have been identified as regulators of epithelial cell polarization and proliferation through the regulation of endocytosis (Lu and Bilder, 2005; Moberg *et al.*, 2005; Thompson *et al.*, 2005; Vaccari and Bilder, 2005).

Lu and Bilder identified two core components of the vesicle trafficking machinery, Avalanche (Avl), a *Drosophila* Syntaxin, and Rab5, as regulator of epithelial cell polarity, both being proteins of the early endosomal compartment. Mutations in the genes encoding Avl and Rab5 lead to an expansion of the apical membrane domain as reflected by the mislocalization of aPKC, Crumbs or DE-Cad (Lu and Bilder, 2005). This polarity defect is accompanied by overproliferation, which results in the formation of neoplastic tumors. Crucial for the expansion of apical membrane in *avl* and *rab5* mutants is the apical accumulation of the transmembrane protein Crumbs. Crumbs accumulation is caused by a failure in endosomal entry and progression towards lysosomal degradation. Therefore, endocytic downregulation seems to be an important mechanism to ensure correct steady state levels of certain polarity regulators at the membrane (Lu and Bilder, 2005).

Loss of function of *Drosophila* Tumor susceptibility gene 101 (Tsg101, named Erupted (Ept)

B Introduction

in *Drosophila*) and Vps25 (Vps = vesicular protein sorting), components of the ESCRT-I and ESCRT-II complexes, respectively, leads to similar defects as observed in *avl* and *rab5* mutants. ESCRT complexes are required for the recruitment of monoubiquitinated proteins and their internalization into luminal vesicles of multivesicular bodies (Hurley and Emr, 2006). Epithelial cells mutant for *ept* and *vps25* lose apicobasal polarity and show extensive overproliferation (Moberg *et al.*, 2005; Thompson *et al.*, 2005; Vaccari and Bilder, 2005).

α -Adaptin is a component of the Adaptor protein (AP)-2 complex, a heterotetramer that functions as an adapter between the intracellular domain of transmembrane receptors destined for endocytosis and the endocytic machinery (Clague, 1998; Berdnik *et al.*, 2002b). In a study performed by Berdnik *et al.* it was shown that the cell fate determinant Numb binds to *Drosophila* α -Adaptin via the so called ear domain at α -Adaptin's C-terminus (Berdnik *et al.*, 2002b). Like Numb, α -Adaptin localizes asymmetrically in dividing SOPs and also segregates preferentially to the pIIb cell. In the pIIb cell Numb, which can also bind to Notch, is thought to enhance endocytosis of Notch via α -Adaptin and thereby reduces Notch signaling in the pIIb cell. This model is supported by the similar cell fate changes observed in *numb* and *α -adaptin* mutants that affect Numb binding (Berdnik *et al.*, 2002b; Emery and Knoblich, 2006). Recently, the PAR/aPKC complex has been implicated in direct control of endocytic trafficking. In a genetic screen for genes required in vesicle trafficking conducted in *Caenorhabditis elegans* (*C. elegans*) the PAR/aPKC complex was identified and the results further indicated that the PAR/aPKC complex acts on multiple steps in endocytosis (Balklava *et al.*, 2007).

B.1.3 Vesicle trafficking and asymmetric cell division of NBs

Cell polarity is regulated by conserved polarity complexes that localize asymmetrically to the plasma membrane. The evolutionarily conserved PAR/aPKC complex is crucial for the establishment and maintenance of polarity in epithelial cells and neuronal stem cells of *Drosophila*, the so-called NBs. Mainly in epithelial cells it has been shown that the appropriate regulation of vesicle trafficking is critical for adjusting the proper amount of polarity proteins at the membrane and that disruption of endosomal or secretory pathways can lead to loss of polarity. Recently, a role for the PAR/aPKC complex in regulating endocytosis was shown as well (Balklava *et al.*, 2007; Harris and Tepass, 2008). In NBs proper generation of distinct cortical apical and basal protein complexes during division is essential for asymmetric division. How the cortical association of these complexes is achieved is so far unknown. One possibility is that the cortical domains are established through polarized

vesicle trafficking to the plasma membrane of a so far unknown transmembrane protein. Therefore, it is obvious that vesicle trafficking might play, similar to its role in epithelial cell polarity for the establishment of polarity in NBs a crucial role. To test the role of endocytosis in NBs, we completely blocked clathrin-dependent and caveolae-dependent endocytosis in embryos and third instar larvae and analyzed the influence on NB polarity. We analyzed the polarity of NBs of embryos mutant for the exocyst component Exo84, which has been described to be crucial for epithelial polarity. Furthermore, we analyzed NB polarity of third instar larval brains in which the function of different endosomal proteins and exocyst subunits, with a known function in epithelial polarity, had been genetically disrupted.

B.2 Results

B.2.1 Influence of a general block of endocytosis on neuroblast cell polarity

Endocytosis plays an important role in in apico-basal polarity of epithelial cells (Lu and Bilder, 2005). *Drosophila* embryonic neuroblasts (NBs) develop from epithelial cells and also show a pronounced polarity. We therefore analyzed the role of endocytosis in NB cell polarity by completely blocking endocytosis during neurogenesis and NB delamination. To achieve a time specific block of endocytosis, we took advantage of a temperature sensitive allele of *shibire* (*shi*), the gene coding for the *Drosophila* GTPase Dynamin, named *shi^{ts1}*. Dynamin is essential for endocytosis of Clathrin-coated vesicles at the plasma membrane (Mettlen *et al.*, 2009). At the permissive temperature (22°C) *shi^{ts1}* embryos develop normally, but at the restrictive temperature (29°C) Dynamin is not functional and therefore endocytosis is blocked. Embryos were treated as described in Material and Methods 3.2.5. In brief, embryos from 30 min collections were given the possibility to develop for 6 h at 22°C and were then shifted to the restrictive temperature of 29°C for 1 h to block endocytosis at a time when NB delamination takes place. After that, embryos were immediately dechorionated and fixed. As a control, *shi^{ts1}* embryos were allowed to rear at 22°C for 7 h prior to fixation. To visualize apico-basal polarity, embryos were stained with the polarity markers Bazooka (Baz) and Miranda (Mira). As shown in Figure B.2-1, the morphology of *shi^{ts1}* embryos that were shifted for 1 h to the restrictive temperature was severely altered compared to control embryos. In control embryos, NBs were overlaid with a monolayered epithelium (Fig. B.2-1 A, A', white arrows). In embryos reared at the restrictive temperature a high number of NBs were exposed to the outside of the embryo (Fig. B.2-1 B, B', white arrows). While the neuroectodermal epithelium of control embryos formed a columnar and ordered monolayer with clear polarity (Fig. B.2-2 A, A''), the neuroepithelium of *shi^{ts1}* embryos, that had been shifted to the restrictive temperature, appeared unorganized and partially multilayered (Fig. B.2-2 B, B''). Some cells were rounded, had basal Miranda crescents and were not aligned with the other cells in the epithelium (Fig. B.2-2 A'', arrowhead). Baz still localized to adherens junctions in epithelial cells (Fig. B.2-2 B'', arrow). Surprisingly, polarity in dividing NBs was not affected by the block in endocytosis. Dividing NBs showed a clear apical Baz and basal Miranda crescent and spindle alignment relative to the crescents was normal. (Fig. B.2.2 B'', asterisk). Therefore, we conclude that a general block of endocytosis does affect NB position and epithelial organization but it does not affect NB polarity. Since *shi* has been described as a

neurogenic mutant (Poodry, 1990), it seems more likely that the effects we observe are caused by impaired cell fate decision than by disturbed polarity.

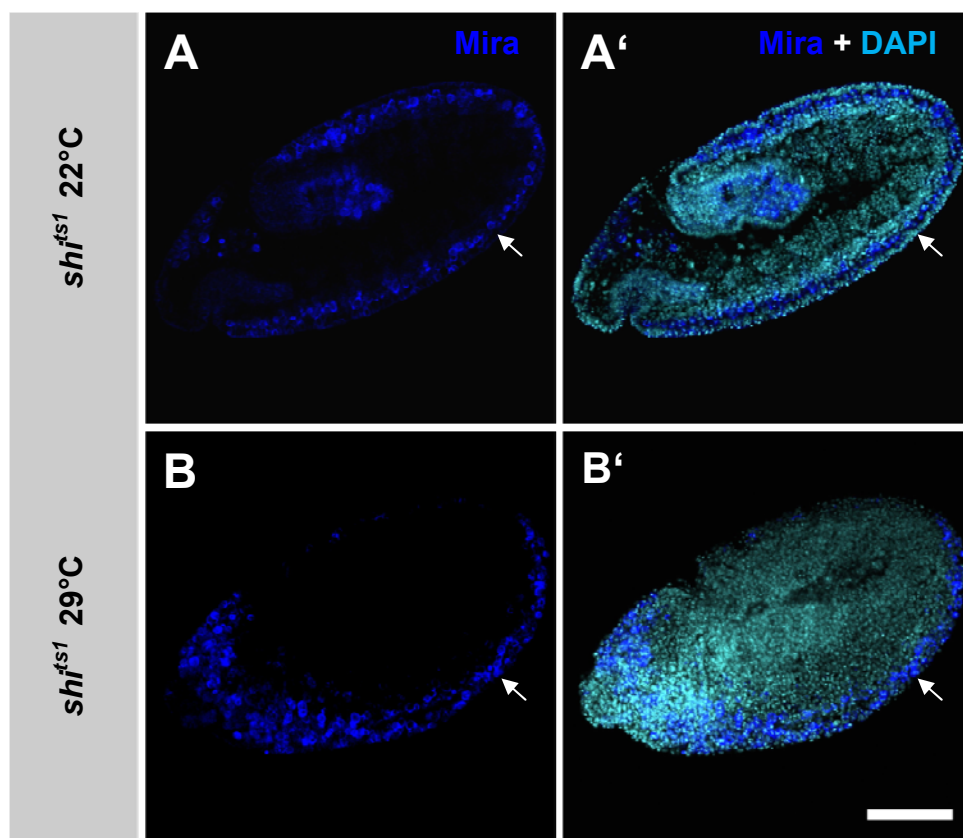


Figure B.2-1: Blocking endocytosis during early embryonic development leads to defects affecting NB position within the embryo. (A-A*) *shi^{ts1}* from 30 min egg collections were reared for 7 h at 22°C and then immediately fixed. NBs lie below an epithelial cell sheet (arrow). (B-B*) *shi^{ts1}* embryos from 30 min collections were reared for 6 h at 22°C and then shifted to 29°C before fixation. NBs can be found at the exterior of the embryo (arrow). Miranda is in blue and DAPI in turquoise. Scale bar is 100 μ m.

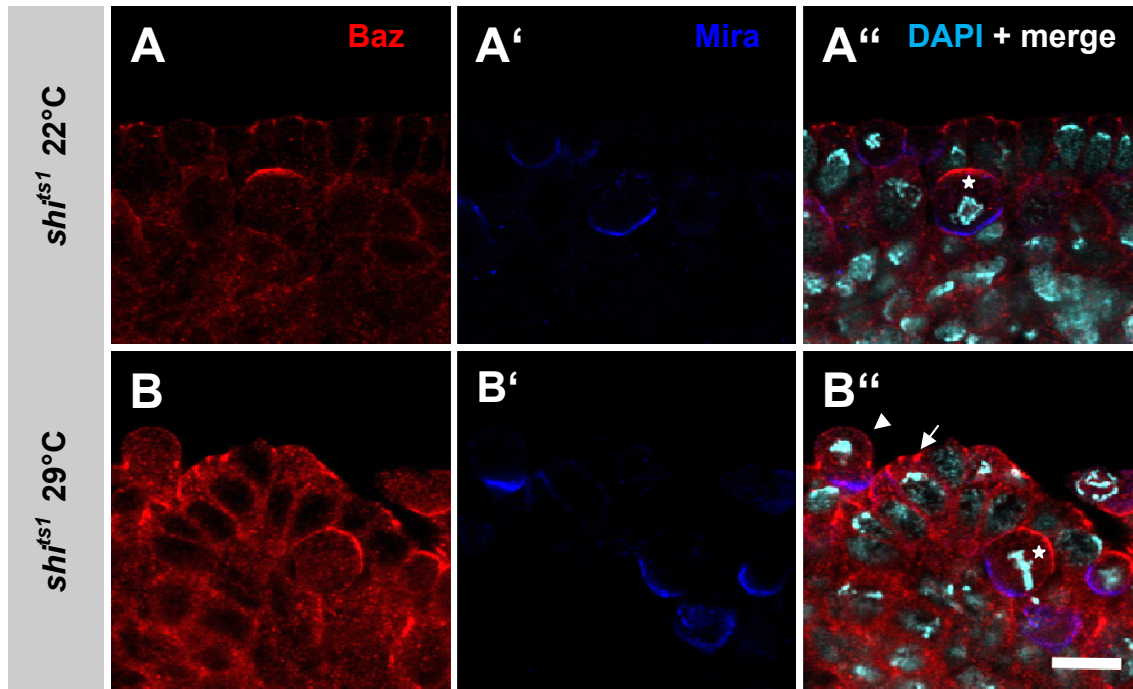


Figure B.2-2: Blocking endocytosis during early embryonic development leads to severe defects in epithelial architecture but NB polarity is not affected. (A-A'') *shl^{fs1}* from 30 min egg collections were reared for 7 h at 22°C and then fixed immediately. NB is marked with an asterisk. (B-B'') *shl^{fs1}* embryos from 30 min collections were reared for 6 h at 22°C and then shifted to 29°C before fixation. (B'') Cell with basal Miranda crescent at ectopic position is marked with an arrowhead. Baz accumulation in subapical region (arrow). Embryos are at stage 10. Baz is in red, Miranda is in blue and DAPI in turquoise. Scale bar is 10 μ m.

B.2.2 The influence of exocyst function on embryonic NB cell polarity

The octameric exocyst complex has a conserved role in the delivery of subcellular vesicles and their transmembrane cargo proteins to precise locations at the surface of polarized cells (Hsu *et al.*, 1999; Lipschutz and Mostov, 2002). Blankenship *et al.* have shown that the exocyst component Exo84 is required for the maintenance of epithelial polarity in the *Drosophila* embryo (Blankenship *et al.*, 2007). They demonstrated that localization of the transmembrane protein Crumbs to the apical surface is dependent on *exo84* function and loss of Crumbs from the apical surface is a major cause for defects in epithelial polarity. They could also show a cytoplasmic accumulation of apical and adherens junction proteins, including Baz, in an expanded Rab11 recycling endosome compartment by late embryonic stage 10. To analyze the influence of exocyst function on NB cell polarity, we used the *exo84^{omr}* allele (Blankenship *et al.*, 2007). Null mutations in other exocyst subunits cause developmental arrest in oogenesis (Murthy and Schwarz, 2004; Beronja *et al.*, 2005; Murthy *et al.*, 2005) and therefore make it impossible to analyze their function during embryonic

development. *exo84^{onr}* represents a hypomorphic allele of *exo84* and the availability of hemizygous *exo84^{onr}* females allows the generation of embryos that are maternally and zygotically mutant for *exo84^{onr}* by crossing them to *exo84^{onr}/TM3fz::lacZ* males (Blankenship *et al.*, 2007). We checked cell polarity by staining *exo84^{onr}* mutant embryos against the polarity markers Baz and Mira. *exo84^{onr}/TM3fz::lacZ* heterozygous control embryos showed normal polarity of the ectodermal epithelium and NBs (Fig. B.2-3 A-A''). *exo84^{onr}* mutant embryos in contrast exhibited severe defects of the ectodermal epithelium (Fig. B.2-3 B-B''). Baz was lost from adherens junctions and localized to large intracellular aggregates. Loss of Baz from its normal localization is also shown in Fig. B.2-4. While in control embryos Baz localized to adherens junctions, which can be seen by the characteristic honey-comb pattern (Fig. B.2-4 A-A''), in *exo^{onr}* mutants Baz accumulated in large cytoplasmic aggregates (Fig. B.2-4 B-B'', arrow). Embryonic NBs of *exo84^{onr}* mutants in contrast displayed normal distribution of Baz and Mira (Fig. B.2-3 B-B'', asterisk). Alignment of the mitotic spindle as judged by position and orientation of the chromosomes in metaphase was also normal. Occasionally, size of NBs was decreased in *exo84^{onr}* mutant embryos when compared with control embryos (Fig. B.2.3 B'', asterisk).

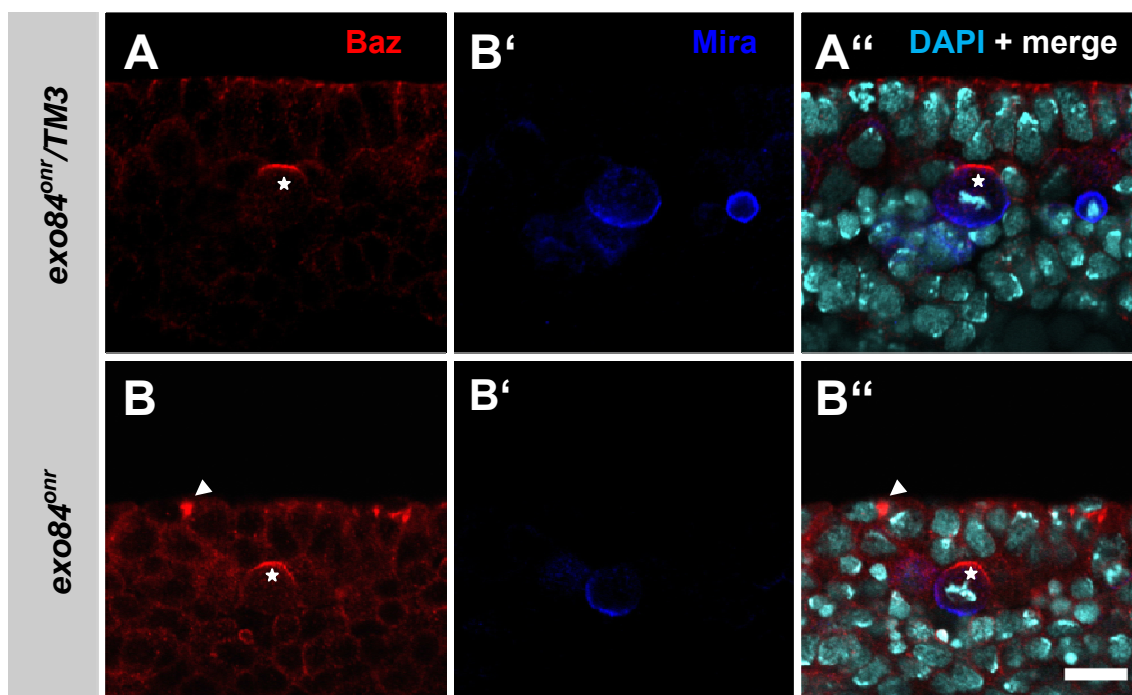


Figure B.2-3: While epithelial polarity is severely disrupted in *exo84^{onr}* mutants, NB polarity is still normal. (A-A'') embryos carrying a *wt* allele of *exo84* on the TM3 balancer chromosome were used as controls. (B-B'') *exo84^{onr}* mutant embryos display accumulation of Baz in intracellular aggregates (arrowhead). Asterisks mark dividing NBs during metaphase. Embryos are at stage 11. Baz is in red, Miranda is in blue and DAPI is in turquoise. Scale bar is 10 μ m.

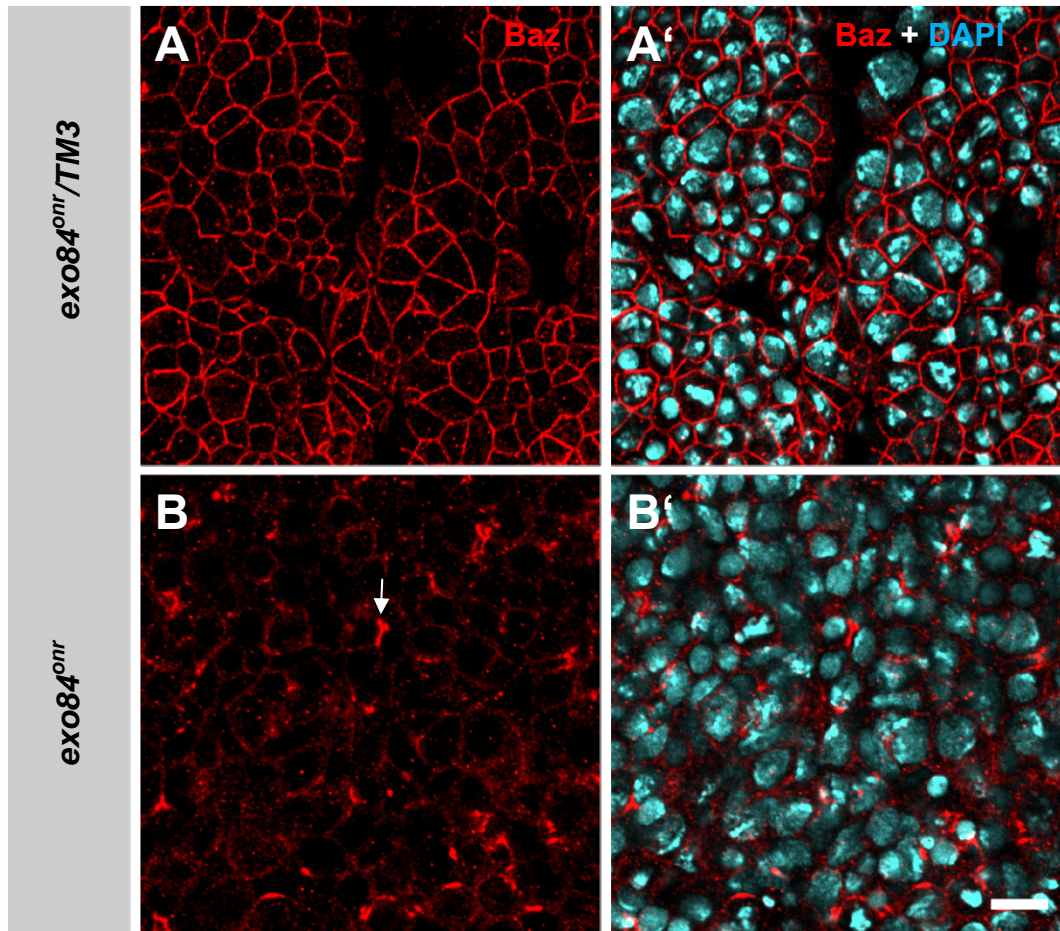


Figure B.2-4: Baz accumulates in intracellular aggregates in *exo84^{nr}* mutant embryos. (A and A') Baz localization in control embryos. (B and B') Baz localization in *exo84^{nr}* mutant embryos. Arrow points to a Baz aggregate. A-B' are top views at the level of adherens junctions of the embryonic ectodermal epithelium at stage 11. Baz is shown red, DAPI is shown in turquoise. Scale bar is 10 μ m.

B.2.3 The influence of a general block of endocytosis on larval NB polarity

To check the influence of a general block of endocytosis on larval NB polarity we used the *shi^{ts1}* allele. NBs delaminate from the embryonic neuroectoderm starting at stage 9 giving rise to the embryonic nervous system and then stop dividing at embryonic stage 15 to enter into a quiescent phase. During this phase NBs shrink in size and are mitotically inactive (Hartenstein *et al.*, 2008). NBs start dividing again during larval stages and until the third larval instar stage all NBs are mitotically active (Hartenstein *et al.*, 2008). To block endocytosis during third larval instar stage, we shifted larvae that were raised for 96 h at 22°C to 29°C for 6 h. After that time period larvae were directly dissected and fixed. As markers for NB polarity Baz and Mira were used. We then analyzed the polarity of central brain NBs by confocal microscopy. Central brain NBs are a heterogeneous group of NBs in the larval brain that give rise to most neurons in the adult brain (Ito and Hotta, 1992; Knoblich, 2008). Central brain NBs of *shi^{ts1}* mutant larvae raised at the permissive temperature showed normal NB

polarity during metaphase with a Baz crescent on one side of the cell opposed by a Miranda crescent on the other side of the cell. Spindle orientation relative to the two crescents also appears normal (Fig. B.2-5 A'', star). Central brain NBs of *shi^{ts1}* mutant larvae that had been shifted to the restrictive temperature of 29°C for 6 h showed the same polarity as NBs in control animals (Fig. B.2-5 B-B''). During metaphase Baz localized to one side of the NB plasma membrane with Mira localizing to the opposing side of the plasma membrane. We could not observe any influence on spindle orientation in dividing NBs either. Therefore we conclude that as far as examined in our experimental setup, a general block of endocytosis does not influence NB polarity.

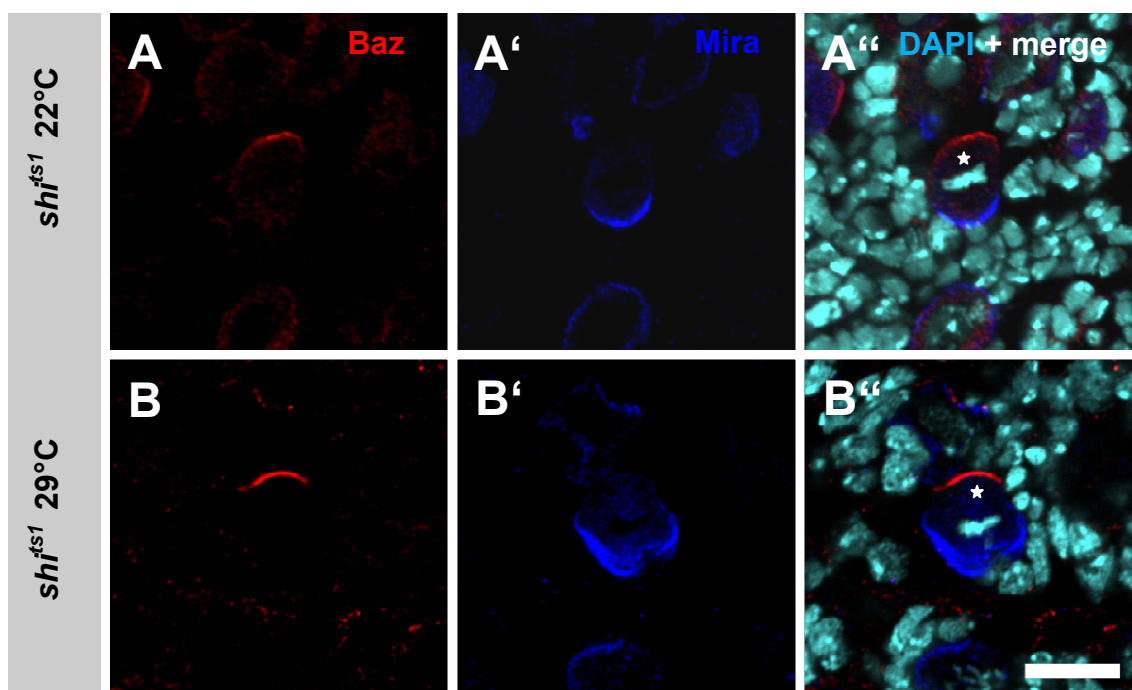


Figure B.2-5: Blocking endocytosis in L3 larvae does not affect NB cell polarity. After larval hatching larvae were allowed to develop at 22°C. Then control animals stayed at 22°C for 6 additional h while animals in which endocytosis should be blocked were shifted to 29°C for 6h. (A-A'') *shi^{ts1}* larva raised at the permissive temperature (22°C). (B-B'') *shi^{ts1}* larvae shifted to the restrictive temperature. Baz is shown in red, Mira is shown in blue and DAPI is shown in turquoise. Asterisks mark metaphase central brain NBs. Scale bar is 10 μ m.

B.2.4 Mosaic analysis with a repressible cell marker (MARCM) screen to analyze the influence of vesicle trafficking on NB polarity

Vesicle trafficking has been shown to be an important mechanism to regulate cell polarity in epithelial cells and the asymmetric division of sensory organ precursors (SOPs) of *Drosophila* pupae (Emery *et al.*, 2005; Lu and Bilder, 2005; Blankenship *et al.*, 2007; Leibfried and Bellaiche, 2007). Many null mutations in genes coding for the components of the vesicle

B Results

trafficking machinery cause either arrest during oogenesis if one removes the maternal gene product or die during early larval development when only the zygotic gene product is missing. This complicates the analysis of NB polarity in these mutants. Therefore, we generated positively labeled mutant clones containing single NBs in an otherwise *wildtype* larva by using mosaic analysis with a repressible cell marker (MARCM). Cell polarity of positively labeled central brain NBs was analyzed using the cell polarity markers Miranda and aPKC. Table B.2.1 summarizes the genes and alleles that were used in this candidate approach and the effect on Miranda and aPKC localization in NBs homozygous for the indicated alleles.

Table B.2-1: Candidate genes to study the role of polarized vesicle traffic during asymmetric NB divisions using MARCM. The first column lists the genes analysed in this study. The second column lists the used alleles. The third and fourth column summarizes the effect on Miranda and aPKC localization in NBs lacking the function of the indicated gene. “no clones obtainable” states that under the chosen experimental conditions no clones containing NBs homozygous for the indicated null alleles were recovered. The different color shading indicates the complex or endosomal compartment the gene product of the listed genes is found in: the Exocyst complex, the ESCRT complex, early endosomes and the AP2 complex.

Gene	Allele	Miranda localisation	aPKC localisation
<i>sec5</i>	<i>sec5^{E10}</i> (null)	normal	normal
<i>sec6</i>	<i>sec6^{Ex15}</i> (null)	normal	normal
<i>sec15</i>	<i>sec15¹</i> (null)	normal	normal
<i>vps25</i>	<i>vps25^{A3}</i> (null)	no clones obtainable	no clones obtainable
<i>erupted (tsg101)</i>	<i>ept²</i> (null)	no clones obtainable	no clones obtainable
<i>rab5</i>	<i>rab5²</i> (null)	normal	normal
<i>alpha-adaptin</i>	<i>ada^{ear4}</i>	normal	normal

First MARCM clones for the *FRT* chromosomes *FRT40A*, *FRT42D*, *FRT80B* and *FRT82B* were generated. The different mutant alleles analyzed in this study are all located on one of the above mentioned *FRT* chromosomes and therefore the clones generated for the *FRT* chromosomes served as *wildtype* controls for the different mutants. In Fig. B.2-6 A MARCM clone homozygous for *FRT42D* is shown. A wildtype clone usually contained one larger cell with a diameter of roughly 12 μm , the NB (Fig. B.2-6 A⁵, white asterisk), and a number of smaller progeny cells (Fig. B.2-6 A², smaller GFP positive cells). The NB was the only cell within the GFP-positive clone that expressed Mira localized in a cortical crescent opposite of the aPKC crescent during metaphase (Fig. B.2-6 A⁵, white asterisk). We noticed that cortical localization of aPKC and Mira at the opposing poles of the cell was apparent starting at prometaphase until anaphase (see chapter B.1 and (Slack *et al.*, 2006)). The mitotic spindle of *wildtype* NBs was aligned to the apical-basal axis of the cell which is defined by the aPKC

and Miranda crescents during metaphase/anaphase of the cell (Fig. B.2-6 A⁶, white arrow).

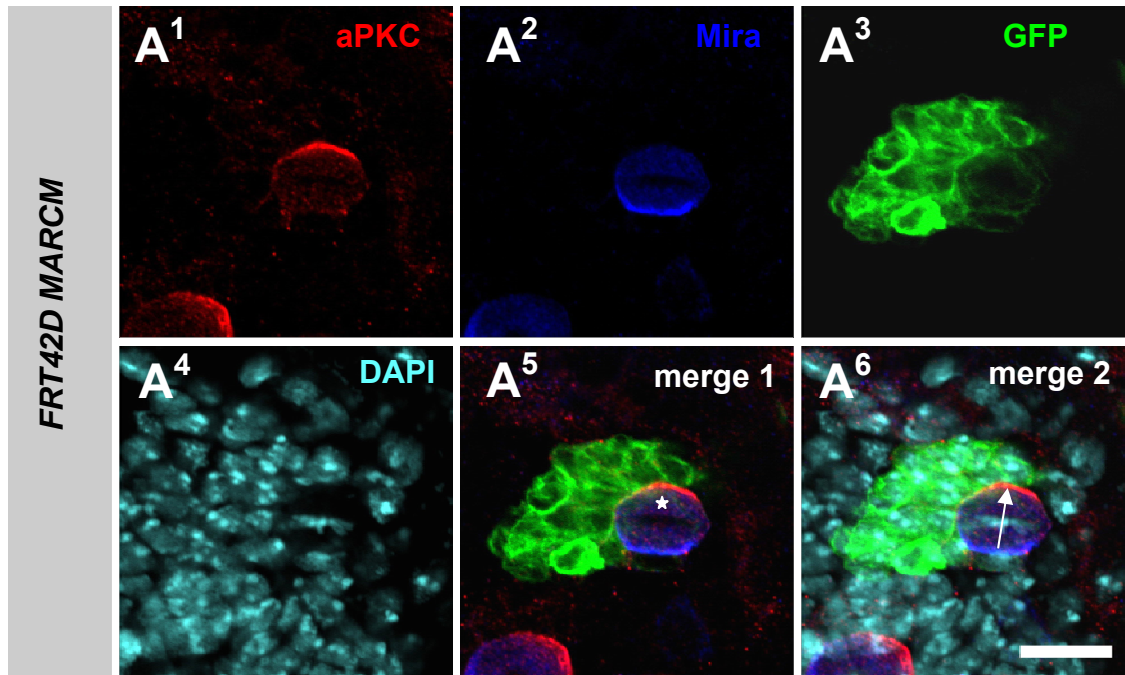


Figure B.2-6: Central brain NBs of *FRT42D* MARCM clones show wildtype polarity, spindle orientation and NB cell size. (A¹) aPKC (red) localization. (A²) Mira (blue) localization. (A³) GFP (green) marks the limits of the clone. (A⁴) DAPI (turquoise) localization. (A⁵) Merge of A¹-A³. A white asterisk marks the NB. (A⁶) Merge of all previous pictures. A white arrow indicates the orientation of the mitotic spindle. The shown NB is at metaphase. Scale bar is 10 μ m.

To analyze if it is possible to identify polarity defects with our experimental setup we generated MARCM clones homozygous for the amorphic *aPKC* allele *l(2)k06403* (Wodarz *et al.*, 2000). Loss of *aPKC* in embryonic and larval NBs leads to mislocalization of Mira to the whole NB cortex (Rolls *et al.*, 2003; Kim *et al.*, 2009). NBs in *aPKC*^{*k06403*} clones were lacking the aPKC crescent indicating that aPKC protein was absent (Fig. B.2-7 A⁵, white asterisk). In those NBs Mira was distributed all around the cell cortex (Fig. B.2-7 A² and A⁵). These results show that it is possible to discover polarity defects in NBs with our experimental setup.

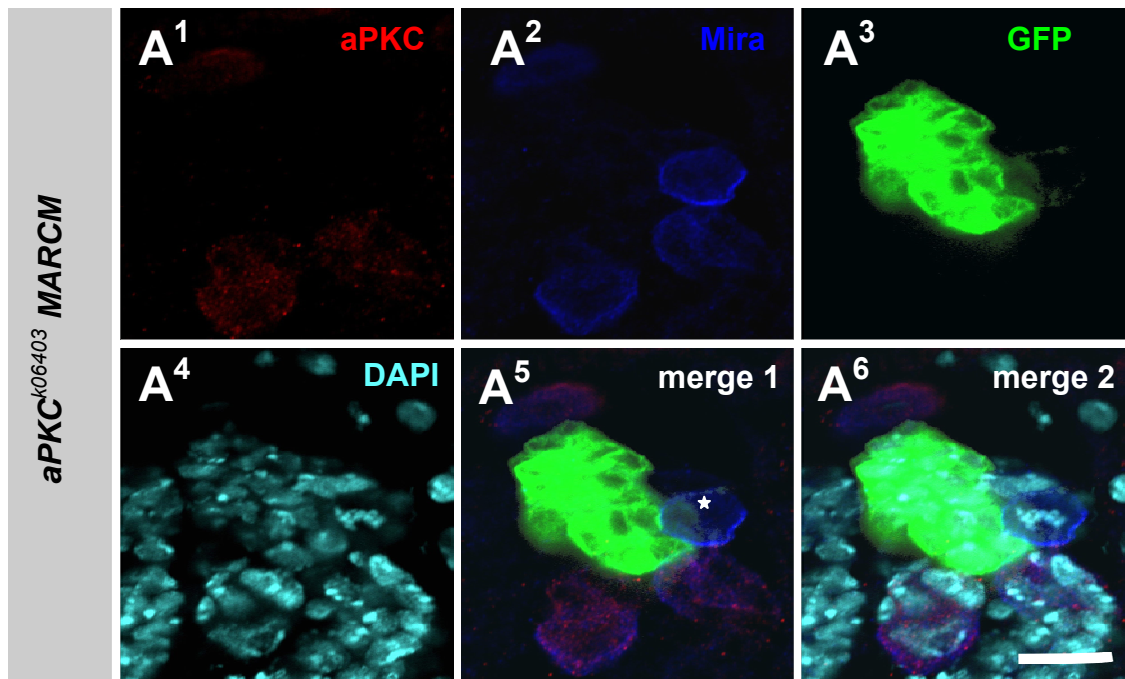


Figure B.2-7: In central brain NBs of *aPKC^{k06403}* MARCM clones, Miranda is distributed all around the cell cortex. (A¹) aPKC (red) localization. In *aPKC^{k06403}* MARCM clones aPKC is absent from the cell cortex. (A²) Miranda (blue) localization. Miranda localizes all around the cell cortex of the NB. (A³) GFP (green) marks the limits of the clone. (A⁴) DAPI (turquoise) localization. (A⁵) Merge of A¹-A³. A white asterisk marks the NBs. (A⁶) Merge of all previous pictures. The depicted NB is at metaphase. Scale bar is 10 μ m.

B.2.4.1 Role of exocyst function for larval NB polarity

The role of the exocyst subunit Exo84 for NB polarity was analyzed in embryos homozygous or hemizygous for *exo84^{onr}*. Polarity in these NBs was normal (see chapter B.2.2). *exo84^{onr}* represents a hypomorphic allele (Blankenship *et al.*, 2007) that might be partially functional. Null alleles are described for exocyst genes *sec5*, *sec6* and *sec15* (Murthy *et al.*, 2003; Beronja *et al.*, 2005; Mehta *et al.*, 2005; Murthy *et al.*, 2005). These alleles are homozygous lethal at the first or second instar stage. Therefore we generated positively labeled clones homozygous mutant for *sec5^{E10}* (Murthy *et al.*, 2003), *sec6^{Ex15}* (Murthy *et al.*, 2005) and *sec15¹* (Mehta *et al.*, 2005) to study their role in NB polarity in third instar larvae.

In NBs of MARCM clones homozygous for the *sec5^{E10}* mutant allele, aPKC and Mira were localized as in *wildtype* NBs (Fig. B.2-8 A⁵, white asterisk). NBs size was also normal and we did not detect defects in spindle alignment during mitosis (Fig. B.2-8 A⁶, white arrow). These results were counterintuitive due to the fact that loss of *sec5* function has been described to be cell lethal (Murthy *et al.*, 2003). One possibility is that Sec5 protein provided before mitotic recombination and generation of the clones is still present. It was not possible to rule out this option since staining performed with a mouse Sec5 antibody did not result in any significant

staining when performed on larval brains.

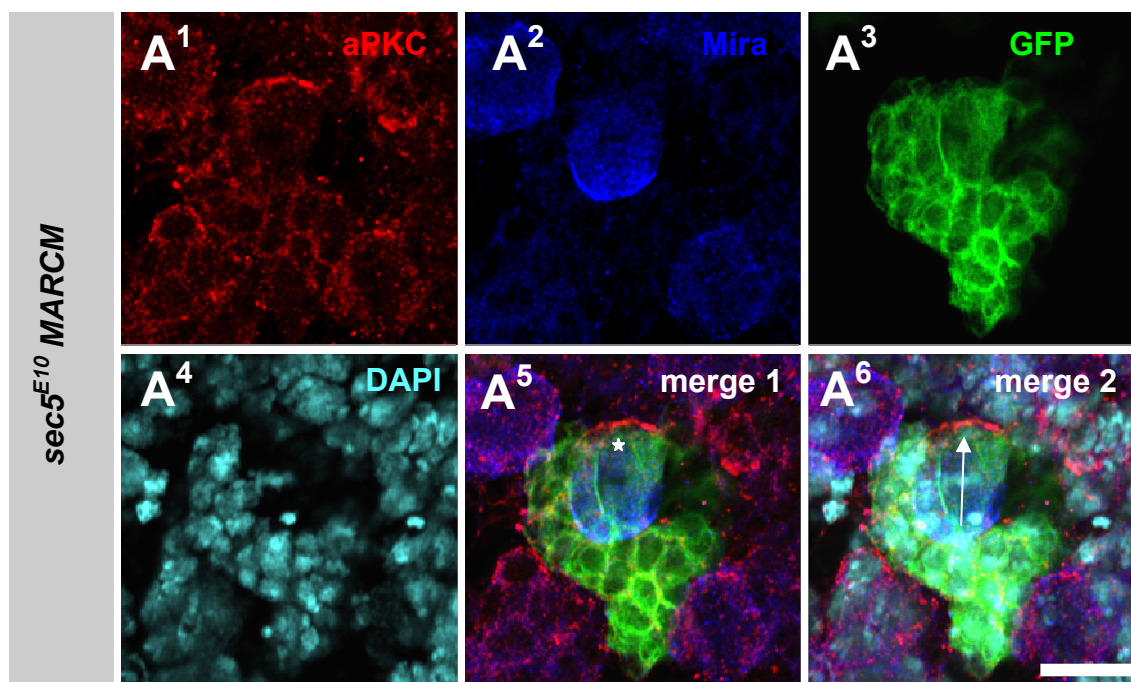


Figure B.2-8: Central brain NBs of *sec5^{E10}* MARCM clones show wildtype polarity, spindle orientation and NB cell size. (A¹) aPKC (red) localization. (A²) Miranda (blue) localization. (A³) GFP (green) marks the limits of the clone. (A⁴) DAPI (turquoise) localization. (A⁵) Merge of A¹-A³. A white asterisk marks the NB. (A⁶) Merge of all previous pictures. A white arrow indicates the orientation of the mitotic spindle. The depicted NB is at anaphase of mitosis. Scale bar is 10 μ m.

The localization of aPKC and Miranda in NBs of MARCM clones homozygous for *sec6^{ex15}* (Murthy *et al.*, 2005) was indistinguishable to that observed in *wildtype* NBs (compare Fig. B.2-9 with Fig. B.2-6). Starting at prometaphase aPKC localized to one side of the cortex while the opposite part of the cortex was occupied by Miranda (Fig. B.2-9 A¹, A² and A⁵). NB size was comparable to *wildtype* NB size.

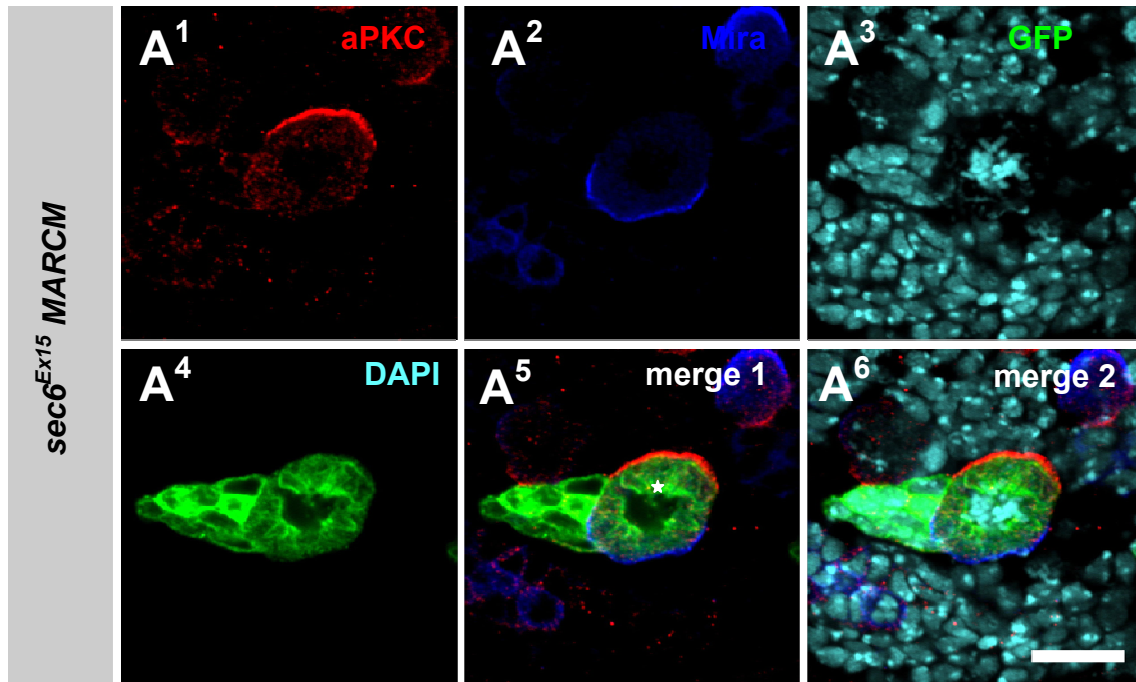


Figure B.2-9: Central brain NBs of $sec6^{Ex15}$ MARCM clones show *wildtype* polarity, spindle orientation and NB cell size. (A¹) aPKC (red) localization. (A²) Miranda (blue) localization. (A³) GFP (green) marks the limits of the clone. (A⁴) DAPI (turquoise) localization. (A⁵) Merge of A¹-A³. A white asterisk marks the NB. (A⁶) Merge of all previous pictures. A white arrow indicates the orientation of the mitotic spindle. The depicted NB is at prometaphase. Scale bar is 10 μ m

MARCM clones that were homozygous for the null allele of $sec15$, $sec15^l$, did not show obvious defects in polarity or cell size (Fig. B.2-10). In Fig. B.2-10 a $sec15^l$ clone is shown that contains an anaphase NB. aPKC localization (Fig. B.2-10 A¹) and Miranda localization was normal (Fig. B.2-10 A²). We also did not detect any abnormalities in cell size and spindle orientation (Fig. B.2-10 A⁵, white asterisk and A⁶, white arrow).

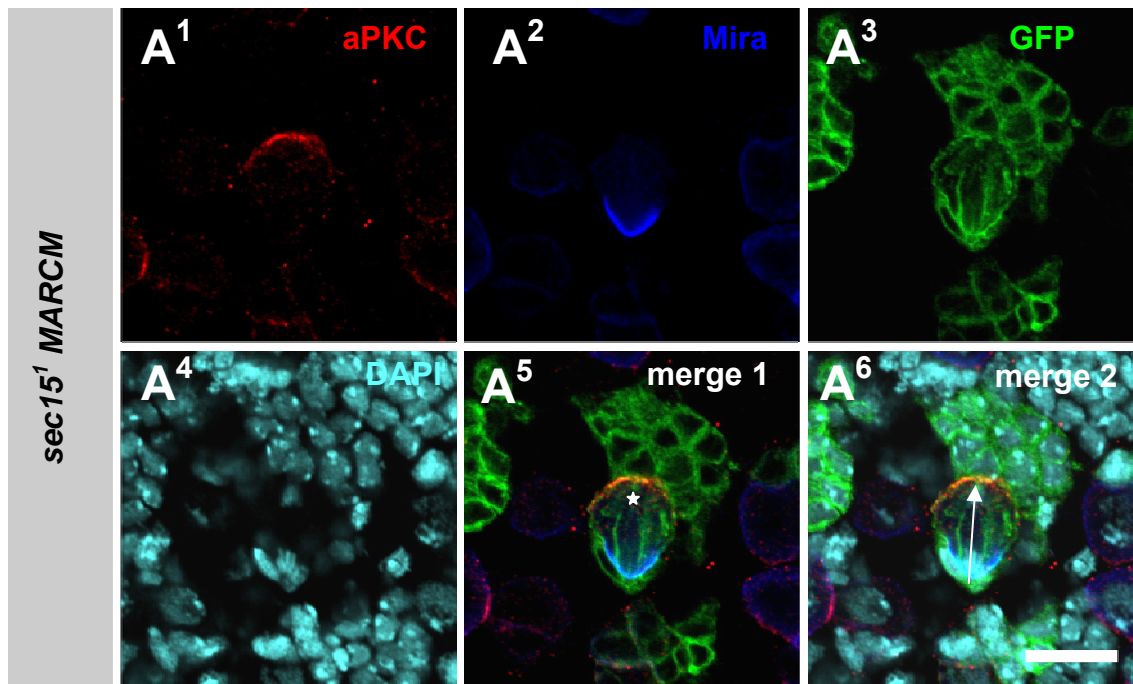


Figure B.2-10: Central brain NBs of *sec15*¹ MARCM clones show wildtype polarity, spindle orientation and NB cell size. (A¹) aPKC (red) localization. (A²) Miranda (blue) localization. (A³) GFP (green) marks the limits of the clone. (A⁴) DAPI (turquoise) localization. (A⁵) Merge of A¹-A³. A white asterisk marks the NB. (A⁶) Merge of all previous pictures. A white arrow indicates the orientation of the mitotic spindle. The depicted NB is at anaphase. Scale bar is 10 μ m.

B.2.4.2 Role of α -Adaptin function for larval NB polarity

Next we generated MARCM clones homozygous for α -adaptin^{ear4} (*ada*^{ear4}). *ada*^{ear4} is a mutation in α -adaptin, that specifically affects asymmetric cell divisions in sensory organ precursor cells (Berdnik *et al.*, 2002a). α -Adaptin is an essential component of the AP-2 complex, a heterotetramer that has a function as an adapter between the intracellular domain of transmembrane receptors destined for endocytosis and the endocytic machinery (Robinson, 1994; Clague, 1998; Berdnik *et al.*, 2002a). Analysis with polarity markers aPKC and Mira did not reveal any polarity defects (Fig. B.2-11). aPKC and Mira were localized to the opposing sides of the cell cortex during metaphase (Fig. B.2-11 A¹, A² and A⁵). We also did not detect alterations in cell size or spindle orientation when compared to *wildtype* NBs (Fig. B.2-11 A⁵, white asterisk and A⁶, white arrow).

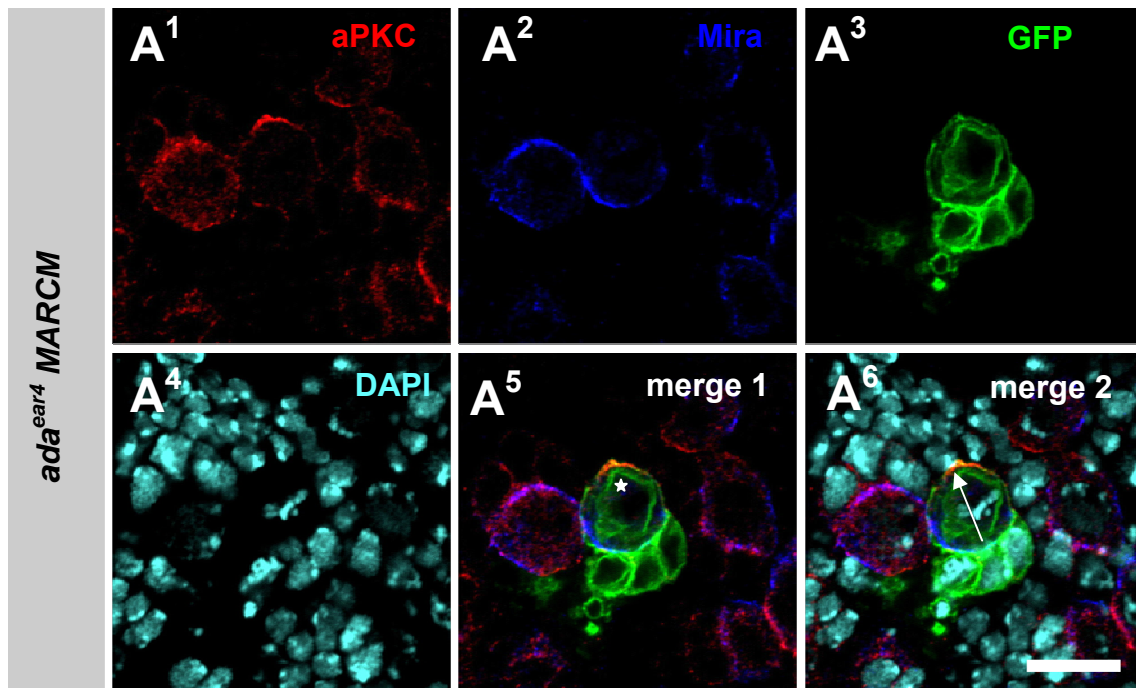


Figure B.2-11: Central brain NBs of *ada^{ear4}* MARCM clones show *wildtype* polarity, spindle orientation and NB cell size. (A¹) aPKC (red) localization. (A²) Miranda (blue) localization. (A³) GFP (green) marks the limits of the clone. (A⁴) DAPI (turquoise) localization. (A⁵) Merge of A¹-A³. A white asterisk marks the NB. (A⁶) Merge of all previous pictures. A white arrow indicates the orientation of the mitotic spindle. The depicted NB is at metaphase. Scale bar is 10 μ m.

B.2.4.3 Role of Rab 5 function for larval NB polarity

The small GTPase Rab5 has been shown to regulate the transport between the plasma membrane and early endosomes and has been shown to be involved in the control of apico-basal polarity of epithelial cells (Bucci *et al.*, 1994; Lu and Bilder, 2005). For that reason we checked if loss of Rab5 from larval NBs affected cell polarity. In MARCM clones homozygous for *rab5²*, a *rab5* null mutation, NBs had a normal distribution of aPKC and Miranda during mitosis (Fig. B.2-12 A¹ and A²). NB cell size and spindle orientation was not changed compared to the *wildtype* situation (Fig. B.2-12 A⁵, white star and A⁶, white arrow).

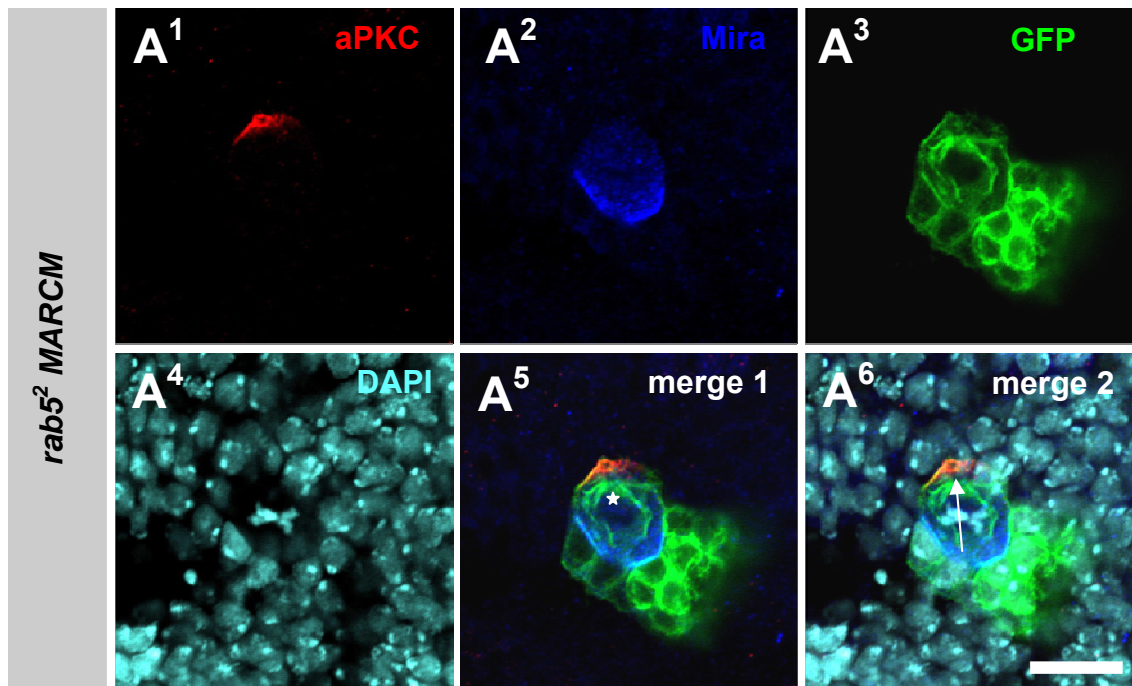


Figure B.2-12: Central brain NBs of *rab5²* MARCM clones show wildtype polarity, spindle orientation and NB cell size. (A¹) aPKC (red) localization. (A²) Miranda (blue) localization. (A³) GFP (green) marks the limits of the clone. (A⁴) DAPI (turquoise) localization. (A⁵) Merge of A¹-A³. A white asterisk marks the NB. (A⁶) Merge of all previous pictures. A white arrow indicates the orientation of the mitotic spindle. Depicted NB is at metaphase. Scale bar is 10 μ m.

B.2.4.4 Role of ESCRT function for larval NB polarity

Loss of *Drosophila* Tsg101 (Erupted) and Vps25 (Vps = vesicular protein sorting), components of the ESCRT (endosomal sorting complex required for transport)-I and ESCRT-II protein complexes, respectively caused loss of apico-basal polarity in the follicle cell epithelium of *Drosophila* and overproliferation (Moberg *et al.*, 2005; Vaccari and Bilder, 2005; Leibfried and Bellaiche, 2007). To analyze the role of these genes for polarity of larval NBs we generated MARCM clones homozygous for null alleles of *vps25* and *erupted* (*ept*), *vps25^{A3}* and *ept²*. We rarely observed small clones from these mutants but we never observed NBs in these clones (data not shown). It is possible that these clones result from inappropriate NB differentiation, but it is more likely that NB loss is caused by cell lethality of the mutations.

B.3 Discussion

Vesicle trafficking is crucial for the establishment and maintenance of cell polarity (Rodriguez-Boulán *et al.*, 2005). Although this is a well established mechanism in epithelial cells, very little is known about the potential role of vesicle trafficking in the establishment and maintenance of polarity in the highly polarized *Drosophila* neuroblasts (NBs). Many of the proteins that are involved in epithelial cell polarity are also required for NB polarity, the most prominent example being the PAR/aPKC complex, which indicates that similar mechanisms may be involved. Therefore, we analyzed the role of vesicle trafficking for NB cell polarity. We studied the distribution of Baz, aPKC and Mira, as key players of NB polarity, in NBs of embryos and larval brains that were mutant for different components of the endocytic and secretory pathway. While we could detect severe defects in the organization of the ectodermal epithelium of embryos that were mutant for *shibire*, a critical component for vesicle budding at the plasma membrane, and for *exo84*, a component of the exocyst complex, NB polarity appeared normal. Furthermore, we checked the distribution of polarity markers in larval NBs mutant for exocyst components, the AP2 complex component α -Adaptin, the early endosome component Rab5 and components of the ESCRT machinery. NB markers were distributed normally in mutant NBs indicating that other mechanisms than in epithelial cells may apply to polarize the plasma membrane of NBs.

B.3.1 Influence of a general block in endocytosis on embryonic and larval neuroblast cell polarity

We analyzed NB polarity in embryos homozygous mutant for *shi^{ts1}*, a temperature sensitive allele of *shibire* (*shi*), which encodes *Drosophila* Dynamin (Chen *et al.*, 1991; van der Blik and Meyerowitz, 1991). Dynamin is a GTPase that is required to pinch of endocytic vesicles at the plasma membrane (Takei and Haucke, 2001). In *shi^{ts1}* mutants endocytosis is blocked at a restrictive temperature of 29°C (Kosaka and Ikeda, 1983; Poodry, 1990). *shi^{ts1}* embryos, that were shifted to the restrictive temperature during NB delamination, exhibited severe defects in the organization of the ectodermal epithelium and the position and number of NBs. *shi^{ts1}* was originally described as a neurogenic mutant (Poodry, 1990). Neurogenic mutants are characterized by an expansion of the nervous system at the expense of epithelial epidermis (Poodry, 1990). In neurogenic mutants most ectodermal cells develop into neuroblasts, which leads to a strong overproliferation of neural tissue, while ventral and cephalic epidermis are missing (Campos-Ortega, 1993). The defects in epithelial organization, NB position and

number are therefore most likely to be caused by the neurogenic function of *shi* and do not point to a function of *shi* in polarity. Even though we observed severe defects in epithelial organization, NB number and position, the localization of Baz and Mira was normal in dividing NBs of *shi^{ts1}* embryos, in which Dynamin-dependent endocytosis was blocked. Chabu *et al.* analyzed the polarity of larval brain NBs homozygous for the *shi^{ts2}* temperature sensitive allele. In dividing NBs of *shi^{ts2}* larval brains, in which Dynamin function had been blocked by a temperature shift to the restrictive temperature, the localization of aPKC, Mira and Numb was normal (Chabu and Doe, 2008). Although one has to take into consideration that the study by Chabu *et al.* was conducted in larval NBs and cannot be directly applied to embryonic NBs, these results also suggest that Dynamin function and Dynamin-dependent endocytosis may not be required for proper polarization of dividing NBs.

We checked the influence of a general block of Dynamin-dependent endocytosis on larval NB polarity using the temperature-sensitive *shi^{ts1}* allele. NB polarity as judged by the localization of Baz and Mira in dividing NBs of larvae that had been shifted to the restrictive temperature to inhibit Dynamin function was indistinguishable to NB polarity of control animals. Our results confirm the findings by Chabu *et al.* and thereby further support the notion that Dynamin-dependent endocytosis might not be required for cortical polarization of dividing NBs.

B3.2 The influence of exocyst function on embryonic neuroblast cell polarity

In order to check whether loss of exocyst function influences NB cell polarity the distribution of the polarity markers Baz and Mira was examined in embryonic NBs that were maternally and zygotically mutant for *exo84^{onr}*. *exo84^{onr}* is a hypomorphic allele of *exo84* and a role for *exo84* function in cell polarity of the ectodermal epithelium of *Drosophila* embryos has been described before (Blankenship *et al.*, 2007). In *wildtype* embryos Baz, Crumbs, aPKC and DPatj localize to the apical margins of the lateral cell surfaces close to adherens junctions (Bhat *et al.*, 1999; Wodarz *et al.*, 1999; Wodarz *et al.*, 2000; Blankenship *et al.*, 2007). By contrast in *exo84^{onr}* mutants Baz, Crumbs and DPatj and also the adherens junction protein Armadillo accumulate in large aggregates at ectopic positions within the cells. The first protein to be mislocalized in *exo84^{onr}* zygotic and maternal mutant embryos is the transmembrane protein Crumbs at stage nine of embryonic development. At late stage 10 other apical and junctional proteins become mislocalized. Mislocalization of adherens junction proteins is probably a secondary effect of Crumbs mislocalization (Blankenship *et al.*, 2007). At later embryonic stages apical proteins, including Baz, and junctional proteins

accumulate in an enlarged Rab11 positive recycling endosome compartment, which is likely to be the result of defective trafficking from the late endosome to the plasma membrane caused by impaired exocyst function (Blankenship *et al.*, 2007). In our study Baz accumulated in cytoplasmic aggregates in ectodermal epithelial cells of *exo84^{onr}* embryos just as described before. Although we could confirm the defects in epithelial cell polarity, the distribution of Baz and Mira in NBs of *exo84^{onr}* mutants was normal. In the study by Blankenship *et al.* NB polarity was not examined. Epithelial polarity is initially set up correctly in *exo84^{onr}* mutants and the first defect that becomes obvious is the loss of Crumbs from the apical membrane at stage nine of embryonic development, mislocalization of Baz follows Crumbs mislocalization at late stage 10 as a consequence of a more general protein trafficking defect. Embryonic NBs inherit their polarity from the overlying epithelium, since proteins of the PAR/aPKC complex maintain their apical localization during delamination and form an apical crescent in NBs (Schober *et al.*, 1999; Wodarz *et al.*, 1999; Petronczki and Knoblich, 2001; Knoblich, 2008). Therefore, it is possible that polarity is initially correctly established and subsequently correctly inherited to the NB. In the NB Crumbs is not expressed and so far no transmembrane protein has been detected that specifically localizes to the apical crescent in NBs. Thus it is possible that other mechanism may apply to achieve cortical localization of the PAR/aPKC complex and other polarity proteins in NBs.

B.3.3 Mosaic analysis with a repressible cell marker (MARCM) screen to analyze the influence of vesicle trafficking on neuroblast polarity.

B.3.3.1 Role of exocyst function for larval neuroblast polarity

We generated MARCM clones for the exocyst subunits Sec5, Sec6 and Sec15 to examine the function of the exocyst complex for polarity of larval NBs. For these experiments we used the alleles *sec5^{E10}*, *sec6^{Ex15}* and *sec15^l*. All three alleles were described as null alleles (Murthy *et al.*, 2003; Mehta *et al.*, 2005; Murthy *et al.*, 2005). Clones of *sec5* and *sec6* null alleles in the *Drosophila* eye do not develop, indicating that both *sec5* and *sec6* are needed for cell viability (Murthy *et al.*, 2003; Beronja *et al.*, 2005). Loss of function of *sec15* in the *Drosophila* eye is not cell lethal in contrast to loss of *sec5* or *sec6* (Mehta *et al.*, 2005). Epithelial cells of the notum of *Drosophila* pupae that were mutant for *sec5^{E10}*, *sec6^{Ex15}* or *sec15^l* displayed enlarged Rab11 recycling endosomes in which DE-Cad and Arm accumulated (Langevin *et al.*, 2005). The localization of Crumbs and Baz was largely unaffected in *sec5^{E10}* mutant epithelial cells indicating that the exocyst preferentially affects the intracellular localization of

DE-Cad. Beronja *et al.* demonstrated that *sec6* is required for apical protein transport in photoreceptor cells of the *Drosophila* eye. As mentioned earlier, the exocyst, or at least the exocyst subunit Exo84, is mainly required for apical targeting of the Crumbs transmembrane protein from the recycling endosomal compartment (Blankenship *et al.*, 2007). All these data point to a function of the exocyst in targeting transmembrane proteins from the recycling endosomal compartment to the plasma membrane, but the specificity of the targeted proteins seems to vary depending on the cell type studied. Surprisingly, we did not detect any requirement for exocyst activity in larval NBs, as far as tested in our experimental settings. NBs of MARCM clones homozygous for *sec5^{E10}*, *sec6^{Ex15}* or *sec15^l* did not display any defects in the distribution of aPKC and Mira. We stained larval brains containing MARCM clones for *sec15^l* with an anti-Sec15 antibody and could show that Sec15 protein level was strongly reduced in the clones homozygous for *sec15^l* compared to the surrounding heterozygous tissue (data not shown). However, we cannot exclude the possibility that polarity in MARCM clones for *sec5^{E10}*, *sec6^{Ex15}* and *sec15^l* is rescued by remaining protein that was produced in the NB before clones were induced. The exocyst is a octameric complex. Therefore it is possible that functional redundancy between the different subunits could partially rescue the exocyst function. We did not check this possibility but it definitely would be interesting to check polarity in double mutants for the exocyst.

B.3.3.2 Role of α -Adaptin function for larval neuroblast polarity

The endocytic protein α -Adaptin is essential for asymmetric cell divisions of SOPs in the *Drosophila* pupa (Berdnik *et al.*, 2002b). In SOPs α -adaptin is asymmetrically segregated by interaction with Numb to the pIIb daughter cell, where it is required to repress Notch signaling possibly by mediating endocytosis of a Notch-interacting four pass transmembrane protein called Sanpodo and Notch itself (Hutterer and Knoblich, 2005; Emery and Knoblich, 2006). In this study we generated MARCM clones of the *ada^{ear4}* allele, which specifically affects asymmetric cell divisions in SOPs. In the *ada^{ear4}* allele the coding region for the so-called Ear domain of α -Adaptin is deleted and the mutant protein encoded by this allele is not able to bind to Numb (Berdnik *et al.*, 2002b). NBs in *ada^{ear4}* clones displayed normal distribution of Baz and Mira, indicating that NB polarity was not affected. Since we used a hypomorphic allele in this study that specifically affects the interaction between Numb and α -Adaptin, it is possible that the remaining truncated protein is functionally sufficient to mask potential effects of α -Adaptin loss of function on NB cell polarity. A feasible way to exclude this possibility would be to generate clones with other stronger *ada* alleles, like the amorphic

*ada*³ allele (Gonzalez-Gaitan and Jäckle, 1997). Since in the study of Berdnik *et al.* the *ada*³ allele did not lead to cell fate transformations and defects in asymmetric cell divisions of the SOP, presumably because of its general requirement for endocytosis and cell viability (Berdnik *et al.*, 2002b), a role of this allele in asymmetric cell division appears rather unlikely.

B.3.3.3 Role of Rab 5 function for larval neuroblast polarity

The small GTPase Rab5 controls epithelial polarity in epithelial cells of *Drosophila* by regulating endosomal entry of the apical transmembrane protein Crumbs (Lu and Bilder, 2005). Because of its role in controlling epithelial polarity, we investigated whether loss of Rab5 function in *rab5*² MARCM clones has an influence on NB polarity. aPKC and Mira were distributed normally in dividing NBs indicating that cell polarity was not affected. We cannot rule out the possibility that remaining Rab5 protein synthesized before clone induction is still present in the MARCM clones and masks effects of Rab5 loss on NB cell polarity.

B.3.3.4 Role of ESCRT function for larval neuroblast polarity

We generated MARCM clones in the larval brain for *vps25*^{A3} and *ept*². Both are null alleles of the corresponding genes *vps25* and *ept*, which code for components of the ESCRT-I and -II complexes, respectively (Leibfried and Bellaiche, 2007). We rarely observed only small clones from these mutants, but we never observed cells positive for Mira, indicating the absence of NBs in these clones. A possible explanation is that these clones result from premature NB differentiation caused by loss of *vps25* and *ept* gene function. Epithelial cells of *Drosophila* larval eye discs mutant for *vps25* or *ept* display loss of apicobasal polarity and are able to induce overproliferation of adjacent wildtype cells (Moberg *et al.*, 2005; Vaccari and Bilder, 2005). Although eye discs containing cells mutant for *vps25* or *ept* induce overproliferation of surrounding wildtype cells, the mutant cells themselves survive rather poorly, indicating that they are eliminated by cell competition, in which slow growing mutant cells are eliminated in the vicinity of wildtype cells (Moberg *et al.*, 2005). Although we did not detect any overproliferation defects in larval brains containing *vps25*^{A3} or *ept*² MARCM clones, it is likely that NB loss and small size of the clones is caused by cell competition with the surrounding wildtype cells. One possibility to enlarge the size of mutant clones offers the *Minute* technique (Blair, 2003). The presence of a chromosome harboring dominant *Minute* mutations slows down cell division rates. A slow growing homozygous mutant clone will therefore get a growth advantage because the surrounding heterozygous cells are impaired in their cell divisions. By introducing a chromosome harboring *Minute* mutations into our MARCM stocks it might be possible to obtain bigger *vps25*^{A3} or *ept*² mutant MARCM clones,

in which NB polarity could be analyzed.

B3.4 Does vesicle trafficking play a role in NB polarity?

Vesicle trafficking in epithelial cells regulates polarity mainly by controlling the protein levels of the transmembrane proteins Crumbs and DE-Cad. The epithelial defects observed in mutants for exocyst components or the endosomal machinery including Rab5, Avl, Tsg101 and Vps25 are all a result of defective trafficking of either Crumbs or DE-Cad. In NBs no asymmetrically localized transmembrane protein has been described so far except for one: Numb-interacting protein (NIP) is a multi-pass transmembrane protein that associates with the basal cortex of dividing NBs where it colocalizes with Numb. In *Drosophila* Schneider cells Numb and NIP colocalize at the plasma membrane and RNAi-mediated knockdown of NIP results in a release of Numb from the plasma membrane (Qin *et al.*, 2004). Whether NIP also plays a role in asymmetric cell division of NBs is still an open question, since so far no NIP loss of function mutant has been described and therefore phenotypic data are missing.

In our study, impaired vesicle trafficking did not influence NB polarity. We did not detect mislocalization of aPKC or Mira neither in mutants affecting polarized secretion nor in mutants affecting the endocytic pathway, which had been previously described to function in epithelial polarization.

How could polarity be established and maintained in NBs? One hint comes from a recent structure function analysis of Baz, the main scaffolding protein of the PAR/aPKC complex, in which it was shown that an evolutionary conserved region in the C-terminus of Baz is able to bind to phosphoinositide membrane lipids and is necessary and sufficient to localize Baz to the apical cell cortex in embryonic NBs (Krahn *et al.*, 2010). Therefore it is possible that polarity in NBs is not established through the polarized trafficking of transmembrane proteins to the NB cortex, but that the central regulator of polarity in NBs, the PAR/aPKC complex, achieves its apical cortical localization by direct association of the main scaffolding protein Baz with the plasma membrane.

Although the ability of Baz to directly associate with lipids of the plasma membrane may mark a corner stone for the establishment of NB polarity, it seems unlikely that it represents the only mechanism governing cell polarization in NBs. In a NB cell culture system for example, it has been shown that contact to epithelial cells is required to properly orient spindle orientation and PAR/aPKC complex localization during asymmetric cell NB divisions. While in isolated neuroblasts, GMCs bud off at random positions, in NBs that are in contact with epithelial cells, GMCs bud off oriented in only one direction indicating that extrinsic cues

coming from the epithelial cells might aid in orienting asymmetric divisions (Siegrist and Doe, 2006). One obvious explanation for these observations would be the involvement of a transmembrane protein that might integrate these extrinsic cues on NB polarity. But so far no candidate transmembrane protein that could fulfill this task has been identified.

This example illustrates that the exact mechanisms regulating NB polarity are still largely unknown and although the results of our study indicate that vesicle trafficking does not play a crucial role during NB polarization, it does not generally exclude the possibility that an involvement of vesicle trafficking may aid in the establishment of polarity due to the limitations of our experimental setup.

C Material and Methods

C.1 Chemicals and reagents

All chemicals were of analytical grade and were purchased from the following companies: *Acros*, Geel, Belgium; *Applichem GmbH*, Darmstadt; *Baker*, Deventer, Netherlands; *Biozym Scientific GmbH*, Hess. Oldendorf; *Biomol*, Hamburg; *Bio-Rad*, Munich; *Roche Diagnostics*, Mannheim; *Difco*, Detroit, USA; *Fluka*, Buchs, Switzerland; *Gibco/BRL Life Technologies*, Karlsruhe; *Grüssing*, Filsum; *Merck*, *Pharmacia/LKB*, Freiburg; *Reidel-de Haen*, Seelze; *Roth*, Karlsruhe; *Serva*, Heidelberg and *Sigma-Aldrich*, Steinheim.

Restriction enzymes, Polymerases and Ligases, as well as their corresponding buffers were purchased from *Roche Diagnostics*, Mannheim; *MBI Fermentas*, St. Leon Rot; *New England Biolabs*, Schwalbach/Taunus; *Promega*, Madison; *Genecraft*, Cologne and *Stratagene*, La Jolla, USA.

All solutions were prepared in distilled water and according to standard protocols from “Molecular Cloning: A Laboratory Manual” (Third Edition), Sambrook, J. et al. 2001 (Cold Spring Harbor Press) if not stated otherwise.

Sequencing of DNA was carried out in the Department of Developmental Biochemistry, AG, Pieler, GZMB Göttingen.

C.1.1 Microscopy and Image Acquisition

Samples were analyzed using a confocal laser scanning microscope (Carl Zeiss LSM510 Meta) and acquired images were further processed using Adobe Photoshop 7.0 or ImageJ (NIH). Wing preparations were imaged using a fluorescence microscope (Carl Zeiss Axio Imager).

C1.2 DNA sequence analysis

The DNA-Star software package was used for analysis of DNA sequences and the generation of gene maps on a Macintosh PowerPC (Apple).

C.2 Genetic methods

C.2.1 Fly breeding and fly stocks

The fly stocks used in this work were kept at 18°C, 25°C or 29°C on standard medium (Ashburner, 2004). For collection of embryos flies were kept in egg collection cages on apple

C Material and Methods

juice plates. To stimulate egg-laying, a small amount of yeast paste was applied at the centre of the apple juice plate.

Table C-1: Fly stocks used in this thesis. Stocks used in part A “Functional characterization of the gene *shlp* (CG7739) during development of *Drosophila*” are shaded blue, stocks used in part B “The role of vesicle trafficking for cell polarity of *Drosophila* neuroblasts” are shaded green. General stocks are shaded white.

Name	genotype	description	Reference, donor
<i>wild type</i>	+, +; +	Wild type stock	stock collection A. Wodarz
<i>w</i> ¹¹¹⁸	<i>w</i> ¹¹¹⁸ ; ;	1 st , 2 nd and 3 rd chromosome isogenic	Bloomington (Bl.) no. 5905
<i>w</i> ; ; <i>TM3ftz::lacZ/TM6b</i>	<i>w</i> ; ; <i>TM3P{ftz::lacZ}c</i> <i>e, Ser/TM6b, e, Tu,</i> <i>Ser</i> ¹	Double balancer stock for 3 rd chromosome	stock collection Wodarz, A.
<i>w</i> ; ; <i>Gla/CyOftz::lacZ</i>	<i>w</i> ; <i>Gla/CyO,</i> <i>P{ftz::lacZ}</i>	Glaced marker over CyO balancer carrying P-element that expresses β-galactosidase in the fushi tarazu pattern	stock collection Wodarz, A.
<i>w</i> ; <i>lf/CyO;</i> <i>MKRS/TM6b</i>	<i>w</i> ; <i>lf/CyO;</i> <i>MKRS/TM6b</i>	Irregular facettes marker on 2 nd chromosome over CyO balancer, MKRS marker over TM6b balancer	stock collection Wodarz, A.
<i>actin::Gal4</i>	<i>y</i> ¹ , <i>w</i> [*] ; <i>P{w[+mC]=Act5C-</i> <i>GAL4}25FO1/CyO,</i> <i>y</i> ⁺	Gal4 expression in the pattern of the actin gene. On 2 nd chromosome; homozygous lethal	Bl. no. 4414
<i>bursicon::Gal4</i>	<i>w</i> [*] ; <i>P{w[+mC]=burs-</i> <i>Gal4}P12</i>	Gal4 expression in the pattern of the <i>bursicon</i> gene. On 2 nd chromosome. homozygous viable	gift from White B.; (Peabody <i>et al.</i> , 2008)
<i>daughterless::Gal4</i>	<i>w</i> [*] ; <i>{w[+mW.hs]=GAL4</i> <i>-da.G32}UH1</i>	Gal4 expression in the pattern of the daughterless gene. On 3 rd chromosome. homozygous viable	Bl. no. 5460
<i>engrailed::Gal4</i>	<i>y</i> ¹ , <i>w</i> [*] ; <i>P{w[+mW.hs]=en2.</i> <i>4-Gal4}e16E,</i> <i>P{w[+mC]=UAS-</i> <i>FLP1.D}</i>	Gal4 expression in the pattern of the engrailed gene. On 2 nd chromosome. homozygous viable	Bl. no. 6356
<i>Gal4-30A</i>	<i>w</i> [*] ; <i>P{w[+mW.hs]=Gaw</i> <i>B}30A/CyO</i>	Gal4 expression in imaginal wing discs and wings	Bl. no. 1795; Brand, A.
<i>tubulin::Gal4</i>	<i>y</i> ¹ , <i>w</i> [*] ; <i>P{w[+mC]=tubP-</i> <i>GAL4}LL7/TM3, Sb</i> ¹	Gal4 expression in the pattern of the tubulin gene. On 3 rd chromosome. Homozygous lethal	Bl. no. 5138
<i>Δ2-3Ki</i>	<i>y</i> ¹ , <i>w</i> ¹ ; ; <i>Ki</i> ¹ , <i>P{ry[+t7.2]=Δ2-</i> <i>3}99B</i>	Transposase source on 3 rd chromosome	Bl. no. 4368
<i>P{EPgy2}CG7739</i> <i>EY14009</i>	<i>y</i> ¹ , <i>w</i> ⁶⁷⁶²³ ; ; <i>P{w[+mC]</i> <i>y[+mDint2]=EPgy2}</i> <i>CG7739[EY14009]</i>	P-element inserted in the 5' UTR of CG7739	Bl. no. 20903
<i>P{EP}CG7739</i> ^{GE2} <i>4395</i>	<i>y</i> , <i>w</i> ; ; <i>P{w[+mC]y[+mDint</i> <i>2]=EP}CG7739</i> <i>[GE24395]</i>	P-element inserted in the 5' UTR of CG7739	Bellen, H.
<i>shlp</i> ¹³¹	<i>w</i> ; ; <i>shlp</i> ¹³¹	Null allele of <i>shlp</i> , generated by P-element	this thesis

		excision	
<i>shlp</i> ⁵²	<i>w</i> ; ; <i>shlp</i> ⁵²	Null allele of <i>shlp</i> , generated by P-element excision	this thesis
<i>shlp</i> ⁷³	<i>w</i> ; ; <i>shlp</i> ⁷³	<i>Wild type</i> allele of <i>shlp</i> , generated by P-element excision	this thesis
<i>Df(3L)XG10</i>	<i>Df(3L)XG10/TM3, P{w[+mC.hs]=Thb8-lacZ}WD1, Sb¹, Ser¹</i>	Deficiency that includes <i>shlp</i> gene region	Bl. no. 6555 Großhans J.
<i>Df(3L)XG8</i>	<i>Df(3L)XG8/TM3, P{Thb8-lacZ}WD1, Sb¹, Ser¹</i>	Deficiency that includes <i>shlp</i> gene region	Bl. no. 6554 Großhans, J.
<i>w</i> ; <i>pUAS-CG7739(17)</i>	<i>w</i> ; <i>pUAS-CG7739(17)/CyO</i>	P-element based transgene. Expresses Shp under UAS control. On 2 nd chromosome.	thesis Egger-Adam, D.
<i>w</i> ; <i>pTWG-CG7739(18)</i>	<i>w</i> ; <i>pTWG-CG7739(18)</i>	P-element based transgene. Expresses a C-terminally GFP tagged Shp under UAS control. On 2 nd chromosome	this thesis
<i>w</i> ; ; <i>pTWG-CG7739(13)</i>	<i>w</i> ; ; <i>pTWG-CG7739(12)</i>	P-element based transgene. Expresses a carboxy-terminally GFP tagged Shp under UAS control. On 3 rd chromosome	this thesis
<i>w</i> ; <i>pPW-eGFP-CG7739(38)</i>	<i>w</i> ; <i>pPW-GFP-CG7739(38)</i>	P-element based transgene. Expresses an amino terminally GFP tagged Shp under UAS control. On 2 nd chromosome	this thesis
<i>w</i> ; <i>pPW-eGFP-CG7739ΔC(1)</i>	<i>w</i> ; <i>pPW-GFP-CG7739ΔC(1)</i>	P-element based transgene. Expresses a amino terminally GFP tagged Shp deletion construct lacking intracellular carboxy terminus under UAS control. On 2 nd chromosome	this thesis
<i>w</i> ; <i>pPW-eGFP-CG7739Δ589-596(4)</i>	<i>w</i> ; <i>pPW-GFP-CG7739Δ589-596/CyO</i>	P-element based transgene. Expresses a amino terminally GFP tagged Shp deletion construct lacking last eight carboxy terminal amino acids under UAS control. On 2 nd chromosome	this thesis
<i>w</i> ; <i>PW-eGFP-CG7739ΔTM+C</i>	<i>w</i> ; <i>PW-GFP-CG7739ΔTM+C/CyO</i>	P-element based transgene. Allows expression of amino terminally GFP tagged Shp deletion construct lacking transmembrane and intracellular domain under UAS control. On 2 nd chromosome	this thesis
<i>w</i> ; <i>pPW-eGFP-CG7739ΔexDom(4.1)</i>	<i>w</i> ; <i>pPW-GFP-CG7739ΔexDom(4.1)/CyO</i>	P-element based transgene. Expresses a amino terminally GFP tagged Shp deletion construct lacking extracellular domain under UAS control. On 2 nd	this thesis

C Material and Methods

		chromosome	
<i>w; pPW-CG7739</i>	<i>w; pPWCG7739/CyO</i>	P-element based transgene Expresses Shlp under UASp control. On 2 nd chromosome	this thesis
<i>w; pPW-CG7739Δ589-596</i>	<i>w; pPW-CG7739Δ589-596/CyO</i>	P-element based transgene. Expresses a Shlp deletion construct lacking the last eight carboxy terminal amino acids under UASp control. On 2 nd chromosome	this thesis
<i>w; pPW-CG7739ΔC/CyO</i>	<i>w; pPW-CG7739ΔC/CyO</i>	P-element based transgene. Expresses a Shlp deletion construct lacking the intracellular domain under UASp control. On 2 nd chromosome	this thesis
<i>w; pPW-CG7739ΔTM+C</i>	<i>w; pPW-CG7739ΔTM+C</i>	P-element based transgene. Expresses a Shlp deletion construct lacking last eight carboxy terminal amino acids under UAS control. On 2 nd chromosome	this thesis
<i>y, w; FRT40, sec5^{E10}/CyO y⁺</i>	<i>y, w; FRT40, sec5^{E10}/CyO y⁺</i>	Null allele of <i>sec5</i> recombined on FRT40A	Schwarz, T. (Murthy <i>et al.</i> , 2003)
<i>y, w; FRT40, sec5^{E13}/CyO y⁺</i>	<i>y, w; FRT40, sec5^{E13}/CyO y⁺</i>	Hypomorphic allele of <i>sec5</i> recombined on FRT40A	Schwarz, T. (Murthy <i>et al.</i> , 2003)
<i>w; FRT42D sec6^{Ex15}/CyO</i>	<i>w; FRT42D sec6^{Ex15}/CyO</i>	Null allele of <i>sec6</i> recombined on FRT42D	Schwarz, T. (Murthy <i>et al.</i> , 2005)
<i>w; FRT42D sec6^{Ex212}/CyO</i>	<i>w; FRT42D sec6^{Ex212}/CyO</i>	Hypomorphic allele of <i>sec6</i> recombined on FRT42D	Schwarz, T. (Murthy <i>et al.</i> , 2005)
<i>w; ; FRT82B, sec15¹</i>	<i>w; ; FRT82B, sec15¹</i>	Null allele of <i>sec15</i> recombined on FRT82B	Bellen, H. (Mehta <i>et al.</i> , 2005)
<i>w¹¹¹⁸, shi¹</i>	<i>w¹¹¹⁸, shi¹</i>	Temperature sensitive allele of <i>shibire</i> , protein inactive at ≥29°C	Bl. no. 7068; Bejsovec, A.
<i>onr¹⁴²⁻⁵/TM3, hb-lacZ</i>	<i>; ; onr¹⁴²⁻⁵/TM3, hb-lacZ</i>	Hypomorphic allele of <i>exo84</i>	Blankenship, TJ (Giansanti <i>et al.</i> , 2004; Blankenship <i>et al.</i> , 2007)
<i>Df(3R)Esp13/TM6 C, cu¹, Sb¹, Tb¹, ca¹</i>	<i>;;Df(3R)Esp13/TM6C, cu¹, Sb¹, Tb¹, ca¹</i>	Deficiency covering the <i>exo84</i> gene region	Bl. no. 5601
<i>elav::Gal4,UAS-mCD8::GFP, hsFLP</i>	<i>P{w[-mW.hs]=GawB}elav[C155], P{w[-mC]=UAS-mCD8::GFP.L}LL4, P{ry[-7.2]=hsFLP}1, w[*]</i>	Stock harbours three transgenes needed for MARCM: <i>elav::Gal4</i> drives expression in neuronal cells as well as in central brain neuroblasts. Mouse CD8::GFP is a GFP tagged	Bl. no. 5146; Luo, L.

		transmembrane protein that labels the cell membrane and the nuclear membrane. FLP recombinase is under the control of a heatshock promoter	
<i>upd/FM7; ; mirP⁺/TM3Sb</i>	<i>upd/FM7; ; mirP⁺/TM3Sb</i>	double balancer for 1 st and 3 rd chromosome	stock collection Vorbrüggen, G.
<i>w[*]; FRTG13, GAL80/CyO</i>	<i>w[*]; P{FRT(w^{hs})}G13, P{πM}45F, P{tubP-GAL80}LL2/CyO</i>	FRT, GAL80 stock for right arm of 2 nd chromosome	Bl. no. 5142; Luo, L.
<i>y¹, w[*]; GAL80, FRT40A /CyO</i>	<i>y¹, w[*]; P{tubP-GAL80}LL10 P{neoFRT}40A/CyO</i>	FRT, GAL80 stock for left arm of 2 nd chromosome	Bl. no. 5192; Luo, L.
<i>y¹, w[*]; GAL80, FRT80B</i>	<i>y¹, w[*]; P{tubP-GAL80}LL9 P{neoFRT}80B</i>	FRT, GAL80 stock for left arm of 3 rd chromosome	Bl. no. 5192; Luo, L.
<i>y¹, w[*]; FRT82B, GAL80</i>	<i>y¹, w[*]; P{neoFRT}82B P{tubP-GAL80}LL3</i>	FRT, GAL80 stock for right arm of 3 rd chromosome	Bl. no. 5135; Luo, L.
<i>ada^{ear4}, FRT40A</i>	<i>w; ada^{ear4}, FRT40A /CyO</i>	hypomorphic <i>ada^{ear4}</i> allele on FRT40A chromosome	(Berdnik <i>et al.</i> , 2002b)
<i>rab5², FRT40A</i>	<i>w; rab5², FRT40A</i>	amorphic <i>rab5²</i> allele on FRT40A chromosome	(Wucherpennig <i>et al.</i> , 2003)
<i>FRT42D, vps25^{A3}</i>	<i>w; FRT42D, vps25^{A3}/CyO</i>	amorphic <i>vps25^{A3}</i> allele on FRT42D chromosome	(Vaccari and Bilder, 2005)
<i>FRT80B, ept²</i>	<i>w; FRT80B, ept²/TM6B</i>	amorphic <i>ept²</i> allele on FRT80B	(Moberg <i>et al.</i> , 2005)

C.2.2 Generation of *shlp* mutant alleles by imprecise excision of P-elements

Deletion mutants for *shlp* were generated by P-element excision (Ashburner, 2004) of the P-elements P{EPgy2}EY14009 or P{EP}GE24395, inserted 111 bp (P{EPgy2}EY14009) or 103 bp (P{EP}GE24395) respectively in the 5'UTR upstream of the translational start site of the *shlp* gene. A crossing scheme for the generation of *shlp* mutant flies is shown in Fig. C1. In the F1 generation, males carrying both the P-element and the transposase source Δ 2-3 (*w/y; ; P{EP}GE24395 / Δ 2-3Ki*) were crossed to *w; ; TM3ftz::lacZ/TM6b* virgin females. White-eyed males, indicating the loss of the mini white gene by an excision event, were crossed against *w; ; TM3ftz::lacZ/TM6b* virgin females and after four days of mating genomic DNA was isolated from every single male and genotyped by PCR to identify excision chromosomes in which a part of the coding region of *shlp* was deleted (Fig. C1, red ellipse). The genotyping PCR was performed with three primers, one binding upstream of the

C Material and Methods

translational start site of the *shlp* gene, one binding the inverted repeats of the P-element and one binding of the translational start site of the *shlp* gene (Fig. C2). In case no excision occurred three fragments of different size were synthesized, one fragment of 580 bp (UP-primer + EY14009A), one fragment of 750 bp (UP-primer + EY14009B) and one fragment of 1330 bp (EY14009A + EY14009B) which served as an internal control for the PCR, since this product was synthesized using the balancer chromosome as template. PCR conditions were chosen as described in table C2. Candidates for an excision chromosome in which a part of the coding region of *shlp* was removed were chosen in the PCR screen by the absence of the 750 bp fragment. Offspring from every single cross that inherited the excision chromosome balanced over the TM6b balancer chromosome were mated to their siblings with the same genotype and a stock of every excision chromosome lacking a part of the coding region of *shlp* was established. The generated deletions were molecularly characterized by PCR amplification with primers located in the 5' and 3' flanking region. The PCR products were subsequently sequenced.

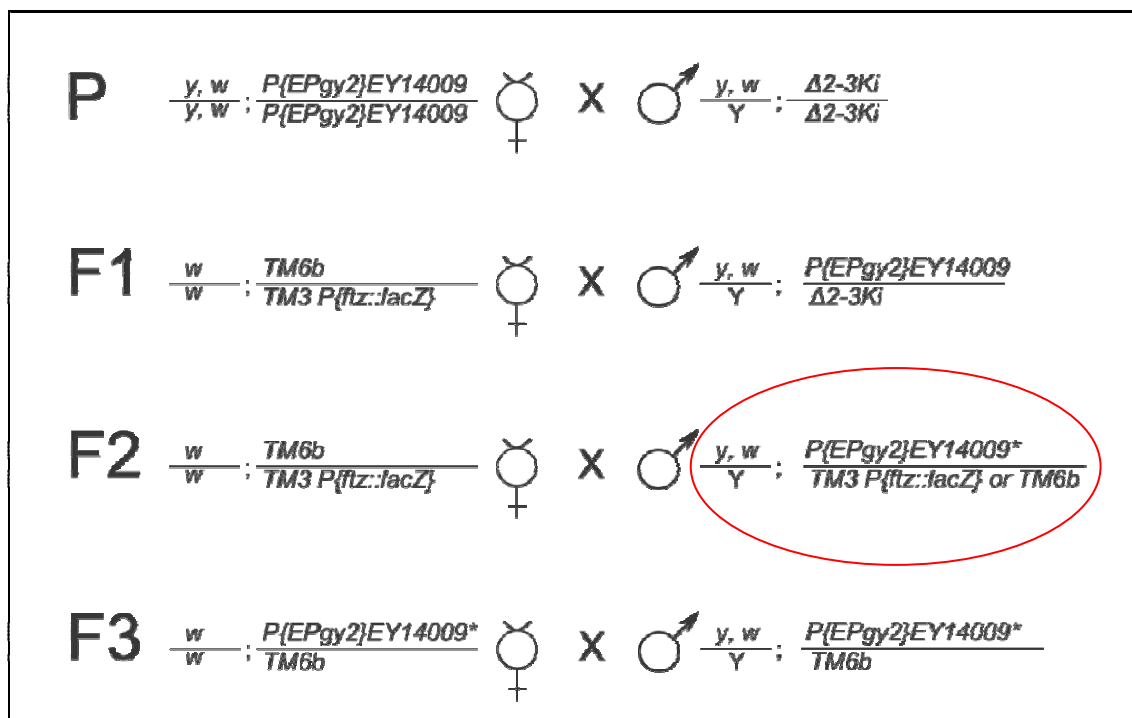


Figure C-1: Generation of flies mutant for *shlp* by imprecise P-element mobilization. See text for details. The mobilization scheme is shown for P{EPgy2}cEY14009. For P{EP}GE24395 the crossings were the same except for the starting P-element. Asterisk indicates that the P-element has been mobilized. Red ellipse marks the males that were used for genotyping.

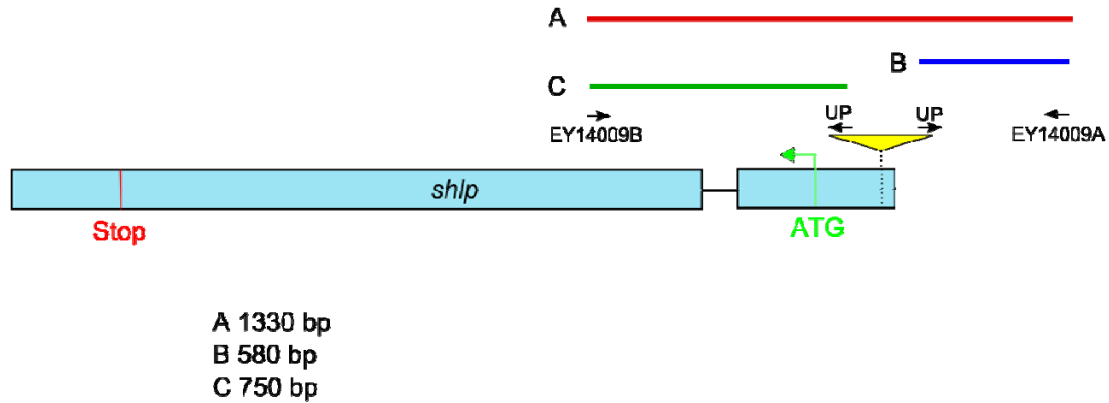


Figure C-2: Scheme of the *shlp* gene locus and position of primers used for genotyping PCR. Fragment A was synthesized using the *wildtype shlp* gene locus on the balancer chromosome as template, which lacks the P-element insertion. Fragment B was amplified using one primer (EY14009A) binding upstream of *shlp* and the UP-primer, which binds the inverted repeats of the P-element (yellow triangle) and fragment C was amplified using a primer (EY14009B) binding in the 2nd exon of *shlp* and the UP-primer. PCR screening was performed to identify P-element excisions where parts downstream of the P-element had been removed.

The original *shlp*¹³¹ and *shlp*⁵² alleles obtained by imprecise P-element excision were semi lethal with few adult escapers. Homozygous *shlp*¹³¹ mutant flies showed severe movement abnormalities. Lethality as well movement abnormalities were caused by two independent secondary mutations on the *shlp*¹³¹ and *shlp*⁵² chromosomes as revealed by complementation tests hemizygous over the deficiency *Df(3L)XG10* or *Df(3L)XG8* and by testing both alleles in trans. Therefore the chromosomes were crossed to isogenic third chromosomes and the chromosomes carrying the *shlp*¹³¹ or *shlp*⁵² mutation were allowed to recombine with the isogenic *wt* third chromosome in the female germ line to remove the secondary mutation. These females were crossed to *w/Y; TM3ftz::lacZ/TM6b* males and the offspring of this cross was established as an individual stock. Each stock was characterized by presence for the *shlp*¹³¹ or *shlp*⁵² by PCR and each stock tested for viability. Stocks that carried the mutant alleles were established and kept.

Table C-2: thermocycler program for genotyping PCR

	Temperature	Time
1	95°C	5 min
2	95°C	30 sec
3	50°C	30 sec
4	72°C	1 min 30 sec
5	repeat 2 to 4	34 cycles
6	4°C	∞

C.2.3 Generation of transgenic flies

Different *shlp* constructs were used to generate transgenic flies. For that 20 µg of plasmid was mixed with 5 µg of transposase DNA in 50 µl injection buffer containing 5 mM KCl, 0.1 mM sodium phosphate, pH 6.8 and centrifuged at 14000 rpm for 10 min. *white*⁻ flies were allowed to lay embryos on apple juice plates for 20 min at 18°C. The embryos were dechorionated, aligned on cover slips and immersed in 10S Voltalef oil (*Prolabo*, Paris, France). The plasmid mixture was injected into the pole cells at the posterior ends of the embryos using a micromanipulator (InjectMan NI2, *Eppendorf*, Hamburg, Germany). After injection, embryos were kept in 3S Voltalef oil at 18°C for 48 h before the hatched larvae were collected. Flies were single-crossed to *w*⁻; *Gla/CyO* flies for the selection of positive transgene insertion and further insertion site analysis.

C.2.4 Mosaic analysis with a repressible cell marker (MARCM) in *Drosophila* larval brains

The mosaic analysis with a repressible cell marker (MARCM) genetic system is a method that allows to positively label homozygous mutant cells in mosaic tissues (Lee and Luo, 2001; Wu and Luo, 2006). Figure C3 gives a schematic overview of this technique. Initially, animals are generated that are transheterozygous for a mutation and a transgene encoding the GAL80 protein which represses GAL4 mediated gene expression (Figure C3 B, unlabeled heterozygous parental cell). After replication (Fig. C3 B, unlabelled cell after replication), recombination is induced by activation of Flp recombinase (Fig. C3 B, unlabelled cell after recombination). The following division generates two distinct daughter cell types: cells homozygous for the mutation of interest lost the GAL80 repressor, leading to GAL4-mediated UAS-GFP reporter gene expression and thereby labeling these cells. *Wildtype* daughter cells are unlabelled due to GAL80-mediated repression of GAL4 activity.

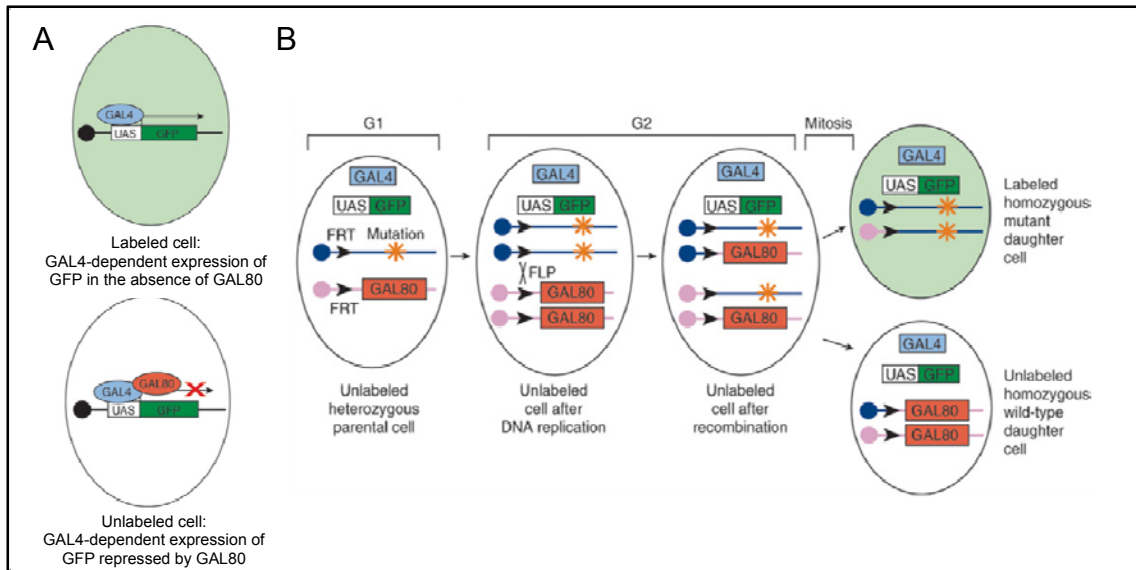


Figure C-3: Schematic representation of the GAL4-UAS system with GAL80 repressor and the mosaic analysis with a repressible cell marker (MARCM) genetic system. (A) In cells where GAL4 protein is present, UAS-GFP is expressed. If additionally the GAL80 protein is present, GAL4-mediated gene expression is repressed. Proteins are denoted by colored ovals, genes are represented by colored boxes in this scheme. (B) In the MARCM genetic system the GAL4-UAS system with GAL80 is combined with FLP recombinase mediated site-specific recombination to positively label only a small clonal population of wild-type or mutant cells. See text for details. Adapted from Wu and Luo, 2006.

We used the *elav::Gal4*, *UAS-mCD8::GFP*, *hsFLP* stock that harbors the *elav::Gal4* transactivator, the UAS-GFP marker and the FLP recombinase controlled by a heatshock promoter. All transgenes were inserted on the first chromosome as a starting stock to generate different “MARCM ready stocks” (see Fig. C4). The *elav::Gal4* has been previously used in a MARCM screen for novel mutations affecting neuroblast division (Slack *et al.*, 2006). Therefore it should be suitable for our MARCM with mutations affecting vesicle trafficking in larval brains. Since the different mutations we wanted to investigate are on the left and right arm of the second and third chromosome, the *elav::Gal4*, *UAS-mCD8::GFP*, *hsFLP* stock enables us to use the same GAL4 transactivator and the same *hsFLP* and therefore comparable experimental settings. Figures C4 and C5 summarize the crosses carried out to generate MARCM clones for mutations on the second and third chromosome.

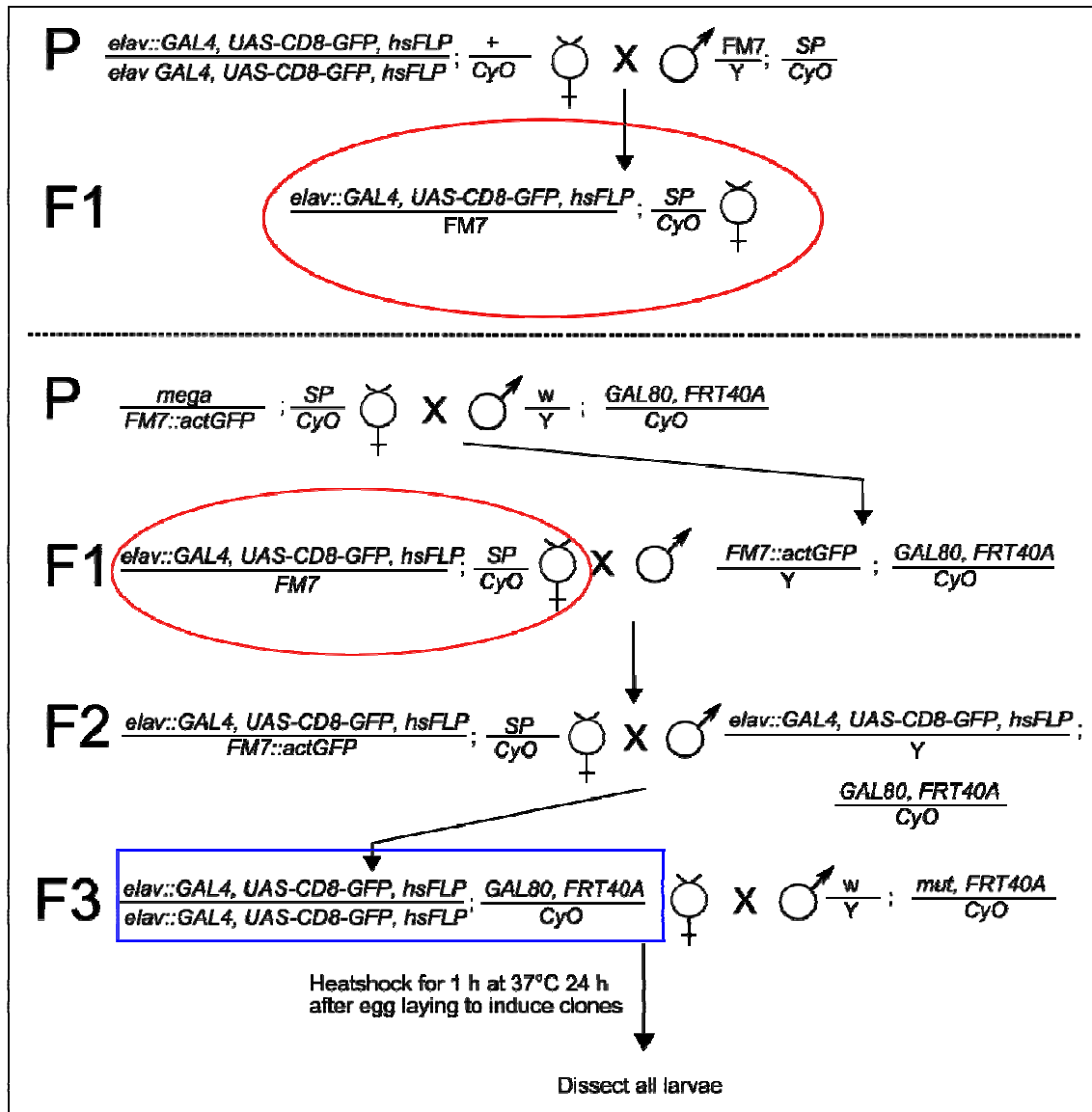


Figure C-4: Crosses to generate MARCM clones for genes on the left arm of the second chromosome. MARCM clones for genes on the right arm of the second chromosome were performed according to the same crossing scheme with the exception that *FRT42D*, *GAL80* was used instead of *GAL80*, *FRT40A*. Blue rectangle marks females that were used to generate “MARCM ready stocks” by crossing them to their sibling with the same genotype. *mut* is a recessive lethal mutation located on the *FRT40A* chromosome.

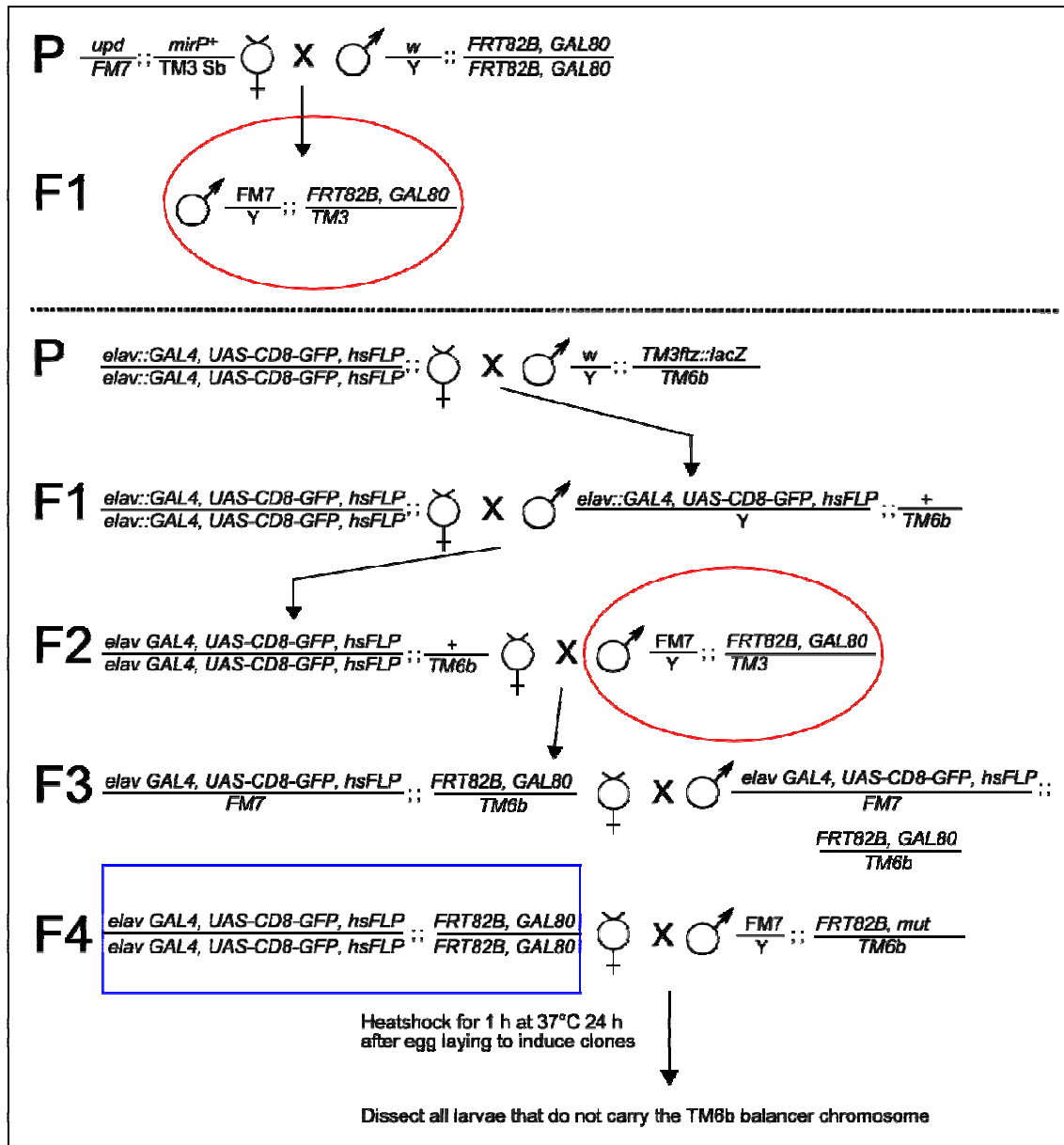


Figure C-5: Crosses to generate MARCM clones for genes on the right arm of the third chromosome. MARCM clones for genes on the left arm of the third chromosome were performed according to the same crossing scheme with the exception that *GAL80*, *FRT80A* was used instead of *FRT82B*, *GAL80*. Blue rectangle marks females that were used to generate “MARCM ready stocks” by crossing them to their sibling with the same genotype. *mut* is a recessive lethal mutation located on the *FRT82B* chromosome.

Dissected larvae were then fixed and stained as described in C.3.3 and images were analysed under a LSM510 confocal microscope (Carl Zeiss LSM510 Meta).

C.2.5 Generation of embryos maternally and zygotically mutant for *onion rings*¹⁴²⁻⁵ (*exo84^{onr}*)

To obtain maternally and zygotic *onion rings*¹⁴²⁻⁵ (*exo84^{onr}*) mutant embryos crosses were

C Material and Methods

performed as described in Blankenship *et al.* (Blankenship *et al.*, 2007) with the exception that the *onr*¹⁴²⁻⁵ was balanced over *TM3, ftz::lacZ* to facilitate genotyping by the *lacZ* expression pattern. Overnight embryo collections were fixed with 4 % formaldehyde and stained as described in C.3.2. Primary antibodies used were Baz N-term DE99646, Miranda DE02120 SA120 and β -Gal (JIE 7). Embryos hemizygous or homozygous for *exo84^{onr}* were identified by absence of *lacZ* staining.

C.2.6 Analysis of embryos lacking *shibire* gene function during neuroblast division

Embryos were laid by females homozygous for *shibire^{ts1}* for 30 min at 22°C. *shibire^{ts1}* is a temperature sensitive allele of *shibire* that is functional at 22°C and non functional at 29°C. Embryos were then allowed to develop at 22°C for 6 h and were then put to 29°C for 1 h or 3 h. After this period embryos were immediately fixed and stained as described in C.4.1. Primary antibodies used were Baz N-term DE99646 and Miranda DE02120 SA120.

C.2.7 Analysis of L3 larvae lacking *shibire* gene function during neuroblast division

Wandering L3 larvae were shifted to 29°C 96 h after larval hatching for 6 h and directly dissected and fixed and stained as described in C.3.2 and C.3.3.

C.3 Immunohistochemistry

C.3.1 Antibodies

Table C-3: Primary antibodies used in this thesis. "Not detected" is shortened to n.d.

Name	Organism	Epitope	Dilution		Reference
			Immunofluorescence	Western Blot	
Baz N-term DE99646	rabbit	aa 1-297 of Bazooka	1:1000	1:2000	(Wodarz <i>et al.</i> , 2000)
Baz N-term DE99647-1	rat	aa 1-297 of Bazooka	1:500	does not work	(Wodarz <i>et al.</i> , 1999)
Crumbs Cq4	mouse	Crumbs	1:20	n. d.	(Tepass <i>et al.</i> , 1990)
PKC ζ (C20)	rabbit	carboxy-terminal peptide (20aa) of rat PKC ζ	1:1000	1:1000	Santa Cruz #sc-216
CG7739 EP023003	rabbit	aa 582-596 at carboxy terminus of Shlp	1:250	1:500	D. Egger-Adam, PhD thesis
CG7739 EP023004	rabbit	aa 433-447 in extracellular region of Shlp	1:500	1:500-1:750	D. Egger-Adam, PhD thesis
CG7739 SAC115	guinea pig	GST fused to extracellular region (aa 21-551) of Shlp	1:500	1:500	this thesis
Miranda DE02120 SA120	guinea pig	Miranda (carboxy-terminus 13 aa)	1:1000	n. d.	unpublished, antibodies A. Wodarz

Par-6 DE02639 SA172	guinea pig	Par-6 (carboxy terminal region 16 aa)	1:1000	1:1000	D. Egger-Adam, PhD thesis
Pins	rabbit	Fusion protein of aa 98-516 of Pins with GST	1:1000	n. d.	(Yu <i>et al.</i> , 2000)
DE- Cadherin DCAD2	rat	Cadherin, DE-	1:50	1:100	(Oda <i>et al.</i> , 1994)
Discs Lage (Dlg) 4F3	mouse	Discs Large	1:20	n. d.	(Parnas <i>et al.</i> , 2001)
Actin	rabbit	Carboxy terminal fragment of Actin	n. d.	1:2000	Sigma-Aldrich A2066
m GFP Molecular Probes	mouse	GFP	1:1000	n. d.	Invitrogen Molecular Probes A11120
rb GFP Molecular Probes	rabbit	GFP	1:1000	1:1000	Invitrogen Molecular Probes A11122
m GFP Roche	mouse	GFP	n. d.	1:1000	Roche # 11814460001
C-Myc	mouse	C-Myc	n. d.	1:50	(Evan <i>et al.</i> , 1985)
m HA	mouse	HA epitope (aa YPYDVPDYA)	does not work	1:1000	Roche # 11583816001
rt HA	rat	HA epitope (aa YPYDVPDYA)	1:1000	does not work	Roche # 11867423001
Burs α	rabbit	Carboxy terminus of Bursicon α	1:2500	n. d.	(Luan <i>et al.</i> , 2006)
N-Hrs	guinea pig	amino-terminus of Hrs	1:150	n. d.	(Lloyd <i>et al.</i> , 2002)
Avl	chicken	aa 1-258 of Avl fused to GST	1:500	n. d.	(Lu and Bilder, 2005)
Rab5	rabbit	aa 11-28 of Rab5	1:1000	n. d.	(Tanaka and Nakamura, 2008)
Rab7	rabbit	aa 184-200 of Rab7	1:3000	n. d.	(Tanaka and Nakamura, 2008)
Rab11	rabbit	aa 177-191 of Rab11	1:8000	n. d.	(Tanaka and Nakamura, 2008)
Sec5 (22A2)	mouse	Sec5 fused to GST	1:100	n. d.	(Murthy <i>et al.</i> , 2003)
Sec6	guinea pig	aa 341-507 of Sec6	1:1000	n. d.	(Beronja <i>et al.</i> , 2005)
Sec8	guinea pig	aa 137-386 of Sec8	1:1000	n. d.	(Beronja <i>et al.</i> , 2005)
Sec15	guinea pig	aa 382-697 of Sec15	1:500	n. d.	(Mehta <i>et al.</i> , 2005)
β - Galactosid ase (JIE 7)	mouse	β -Galactosidase	1:50	n. d.	Developmental Studies Hybridoma Bank

Table C-4: Secondary antibodies used in this thesis

Name	conjugate	Dilution	Supplier
donkey- α -rabbit	Cy3	1:200	Dianova
goat- α -rabbit	Alexa 647	1:200	Dianova

C Material and Methods

donkey- α -mouse	Cy3, Cy2	1:200	Dianova
goat- α -mouse	Alexa 647	1:200	Dianova
goat- α -guinea pig	Alexa 647	1:200	Dianova
goat- α -rabbit	HRP	1:10000	Dianova
goat- α -mouse	HRP	1:10000	Dianova

C.3.2 Embryo fixation and immunofluorescent antibody staining

Embryos were fixed with different methods depending on the antibody used. If not indicated otherwise, embryos were fixed with 4% formaldehyde. For 4% formaldehyde fixation, embryos were dechorionated with a mixture of 50% Klorix bleach and 50% dH₂O for approximately 2 min and subsequently extensively washed with dH₂O. Embryos were transferred to a scintillation vial filled with a 1:1 mixture of 4 % formaldehyde fixation solution and heptane. Embryos were fixed for 20 min on a rocking platform. The lower aqueous phase was removed, 3 ml of methanol was added and the embryos were shaken vigorously for 30 s. Embryos that sank to the bottom were transferred to an Eppendorf tube and washed two times with methanol. Embryos were now ready for subsequent antibody staining or could be stored at -20°C up to several months.

Stefanini fixation was carried out like 4% formaldehyde fixation except that Stefanini solution (330 μ l 37% formaldehyde, 450 μ l 0,5 mM PIPES (pH 7.5), 45 μ l saturated picric acid) was used.

Strong fixation and methanol fixation were also used in this study as described elsewhere (McCartney *et al.*, 1999; Giet *et al.*, 2002).

Incubation of fixed embryos with primary and secondary antibodies was done according to standard procedures (Muller, 2008). In general, embryos were rehydrated and washed with PBT (PBS with 0,1 % Tween 20) and washed three times with 1 ml PBT for 20 min at room temperature. Thereafter embryos were blocked for 1 h at room temperature on a rocking platform in 500 μ l PBT containing 5% normal horse serum (NHS). Then they were incubated with primary antibodies diluted in 500 μ l PBT containing 5% NHS over night at 4°C on a rocking platform. On the next day embryos were washed three times with PBT for 20 min and afterwards incubated with the secondary antibodies diluted in *PBT containing 5% NHS for 2 h at room temperature on a rocking platform. After incubation with the secondary antibodies, embryos were washed again three times with PBT for 20 min. During the first washing step* 4',6-Diamidino-2-phenylindole (DAPI, Sigma Aldrich, Steinheim) was added at a dilution of 1:2000 of a 1 mg/ml stock. Embryos were mounted in Mowiol/Dabco (1,4-DIAZABICYCLO(2.2.2)OCTANE) on a glass slide. Dabco was used in the mounting

medium to prevent bleaching of the fluorescent labels.

Preparation of Mowiol/Dabco: 5g Evanol (Mowiol, Höchst) were dissolved in 20 ml PBS (pH 7,4), 10 ml of glycerin were added and stirred for 16 h. The solution was then centrifuged at 12000 rpm and the supernatant was collected. Dissolved Mowiol was aliquotted and stored at -20°C. Prior to mounting of samples a few crystals of Dabco were added and the Mowiol was rotated for at least 30 min.

C.3.3 Fixation and antibody staining on brains of wandering third instar larvae

Larval brains of wandering third instar larvae were dissected in PBS and then fixed in 4% formaldehyde in PBS (110 µl 37% formaldehyde solution in 890 µl PBS) for 20 min at room temperature on a rocking platform. The tissue was washed three times with PBT and thereafter permeabilized by treating with PBS containing 1 % Triton X-100 for 1 h at room temperature on a rocking platform. Subsequent steps were in analogy to the protocol for antibody staining of embryos (C.3.2).

C.3.4 Cell fixation and staining

Drosophila S2r cells were seeded on glass cover slips in six well plates. For some experiments cells were transfected with FuGene HD Transfection Reagent (*Roche Diagnostics*, Mannheim) and incubated at 25°C for 24 to 48 h. For fixation, the cells were carefully washed three times with 1 ml of PBS since the cells can easily be detached from the cover slip. Fixation solution containing 4 % formaldehyde in PBS was added into the well to fix the cells at room temperature for 10 min. Fixed cells were washed three times with PBT and subsequently blocked in blocking solution (PBT containing 5% normal horse serum) for 30 min. Thereafter cells were incubated with primary antibody in blocking solution for 1 h at room temperature. Then the cells were washed three times with PBT followed by incubation with the secondary antibody for 45 min at room temperature. Afterwards, cells were washed again three times with PBT and DAPI was added in the second washing step for DNA staining at a dilution of 1:2000. The cover slip was mounted in Mowiol/DABCO on a glass slide.

C.3.5 Fluorescent *in situ* hybridization (FISH) on embryos and brains of wandering third instar larvae

All steps are described for FISH on embryos. For FISH on brains of wandering third instar larvae all steps are according to the protocol for FISH on embryos except for fixation which is the same as in C.3.2.

C Material and Methods

FISH was performed according to the protocol from Lécuyer et al. (Lécuyer *et al.*, 2008) with minor modifications. For preparation of a Digoxigenin (DIG)-labelled RNA probe, 10 µg of template DNA was linearized in 20 µl final volume. The linearized template was then purified using the High Pure PCR Product Purification Kit (*Roche Diagnostics*), according to the manufacturer's instructions except for the elution volume which was adjusted to 20 µl instead of 50 µl.

In vitro transcription and incorporation of DIG was performed with the DIG RNA labeling kit (SP6/T7) (*Roche Diagnostics*) according to the manufacturer's instructions. The labeled probe was purified using the RNeasy mini kit (*Qiagen*). The purified DIG labeled probe was then mixed with Hybe-solution to a final volume of 2 ml. At this point the probe could be stored at -20°C. Fixation of embryos was performed as described in chapter C.3.2.

Incubation of embryos was carried out with 100 µl of DIG labeled probe in Hybe-solution at 56°C over night. Incubation with sheep anti-DIG-POD Fab fragments (*Roche Diagnostics*) was performed for two hours at room temperature in PBT containing 1% milk powder (PBTB) on a rocking platform. For protein-RNA co-staining the primary antibody for protein labeling was included in this incubation step. Signal amplification was performed with Tyramid Biotin (*Perkin Elmer*). Embryos were incubated with 150 µl Tyramid Biotin diluted 1:50 in amplification buffer at room temperature for 2 h in the dark under constant mixing. Next embryos were washed three times with PBT for 5 min. Then embryos were incubated with streptavidin Alexa 594 conjugate (*Invitrogen*) diluted 1:500 in PBT for 60 min on a rocking platform. After that embryos were washed six times for 10 min with PBS. In the first washing step DAPI at a dilution of 1:2000 was added. Embryos were then rinsed once with PBT and then mounted on a glass slide in Mowiol/DABCO.

C.3.6 DAPI staining of adult wings

Adult wings were dissected and fixed for 20 min in 0.5 ml of 4% formaldehyde in PBS/900 μ l heptane in 1.5 ml eppendorf tubes on a rocking platform. Wings were then washed in PBS containing 0.1 % Triton X-100 three times for 15 min. In the last washing step nuclei were counterstained by adding DAPI at a dilution of 1:2000. Wings were mounted on glass slides in Mowiol/DABCO.

C.4 Cell culture

C.4.1 Cell transfection

FuGene HD Transfection Reagent (*Roche Diagnostics*) was used for cell transfection according to the manufacturer's instructions. 2×10^6 S2r cells were resuspended in 2 ml of fresh *Drosophila* S2 medium supplemented with serum and antibiotics (*Invitrogen*). Resuspended cells were plated in one well of a 6-well plate. 2 mg of target plasmid was diluted in 100 μ l of sterile water. 4 μ l of FuGene transfection reagent was added into the plasmid solution and mixed for 10 sec. The mixture was incubated at room temperature for 15 min before added to the cell culture. Cells were harvested after 2-4 days if not indicated otherwise.

C.5 Molecular biology methods

C.5.1 List of plasmid vectors

Table C-4: plasmid vectors used in this thesis

Plasmid vectors	Purpose	Source
<i>pGEX-4T-1</i>	Expression of GST-fusion proteins in <i>E. coli</i>	<i>Amersham Pharmacia Biotech</i> , Buckinghamshire, England
<i>pENTR/D-TOPO</i>	Gateway cloning	Gateway pENTR™/D-TOPO® Cloning Kit, <i>Invitrogen</i>
<i>pAW</i>	Destination vector with an <i>actin::5c</i> promoter, no tag	<i>Drosophila</i> Gateway Vector Collection, Murphy Labor
<i>pPW</i>	Destination vector with <i>UASp</i> promoter, no tag	<i>Drosophila</i> Gateway Vector Collection, Murphy Labor
<i>pTWG</i>	Destination vector with <i>UASt</i> promoter, eGFP tag	<i>Drosophila</i> Gateway Vector Collection, Murphy Labor
<i>pTWH</i>	Destination vector with <i>UASt</i> promoter, HA tag	<i>Drosophila</i> Gateway Vector Collection, Murphy Labor

C.5.2 List of oligonucleotides

Table C-5: Primers/oligonucleotides used in this thesis

Name	Sequence 5' → 3'	Purpose
Cg7427rev1	GGCAGTGCAATGGTGAGTACTTC	Characterisation of P-excision lines
CG7427for2	TCAAGGATGGGCAGCTTGGTCTT	Characterisation of P-excision lines
CG7427for3	GTTTGTACTGTGCGAGGTCTGGT	Characterisation of P-excision lines
CG7427rev4	CGACTGGAAATTCGAGTTGGCCA	Characterisation of P-excision lines
UP-primer	GACGGGACCACCTTATGTTATTTTCATCATG	Characterisation of P-excision lines
Plac1	CACCCAAGGCTCTGCTCCCACAAT	Characterisation of P-excision lines
Pry4	CAATCATATCGCTGTCTCACTCA	Characterisation of P-excision lines
EY14009A	CGTATCGCACAGTTCGGTTAGGTT	Characterisation of P-excision lines
EY14009B	CTCCGTGGGTTCTGCTTGGTGTA	Characterisation of P-excision lines
CG7739EV+Stop_1901-20_rev	CTTACATTGCATCGAAATGG	Cloning of pEntr- <i>shlp</i> +stop
CG7739EV-Stop_1897-916_rev	CATTGCATCGAAATGGAATC	Cloning of pEntr- <i>shlp</i> -stop
CG7739EV_129-47_for	CACCATGACGAGATGCAGTCTTG	Cloning of pEntr- <i>shlp</i> -stop/ pEntr- <i>shlp</i> +stop
CG7739for1	TACACCAAGCAGAACCCACGGAG	Characterisation of P-excision lines
CG7739rev2	CCTGAGTAGTGGTACTGTAGGTG	Characterisation of P-excision lines
CG7739for3	CGGAATGACGAGATGCAGTCTTG	Characterisation of P-excision lines

CG7739for4	TGCCTGGTTATCGTCTTTAT	Characterisation of P-excision lines
CG7739rev5	GCATCTCTATTGATTCCATG	Characterisation of P-excision lines
revCG7739RISE	CACTCCTTGCCGTAATGGTT	Characterisation of P-excision lines
CG7739EV+Stop_1901-20_rev	CTTACATTGCATCGAAATGG	Characterisation of P-excision lines
GSP-CG7739Nested	CCTGCAAGCGTTCCTGTTTATCCTCG	5' RACE PCR
GSP-CG7739	GGGCGACCACCTTACATTGCATCGA	5'RACE PCR
forSP-CG7739	CACCATGACGAGATGCAGTCTTGTA	SP-GFP- <i>shlp</i> construct
forXba-CG7739	TGCTCTAGAAGTAATATCACTGATAAAGTTT	SP-GFP- <i>shlp</i> construct
forXho-GFP	CCGCTCGAGATGGTGAGCAAGGGCGAGGA	SP-GFP- <i>shlp</i> construct
revEco-CG7739	CCGGAATTCTTACATTGCATCGAAATGGA	SP-GFP- <i>shlp</i> construct
revEcoXba-GFP	CCGGAATTCGCTCTAGACGTGGACCGGTGCTTGACATA	SP-GFP- <i>shlp</i> construct
revEcoXho-SP	GAATCCCGCTCGAGGTCTGCAAAACTTTATCAGTG	SP-GFP- <i>shlp</i> construct
D1forEcoR1	CCGGAATTCAGTAATATCACTGATAAAGTT	pGEX4T1- <i>shlp</i> -exDom construct
D1revXho1	CCGCTCGAGCTACAGAATCAGTTTGCTAGGC	pGEX4T1- <i>shlp</i> -exDom construct
forCG7739RNAi	TTAATACGACTCACTATAGGGGAGAAGAGTAATGGCCCTGGACT	RNAi in S2 cells
revCG7739RNAi	TTAATACGACTCACTATAGGGGAGACACTCCTTGCCGTAATGGTT	RNAi in S2 cells
forEGFPRNAi	TTAATACGACTCACTATAGGGGAGAACGTAACGGCCACAAGTTC	RNAi in S2 cells control
revEGFPRNAi	TTAATACGACTCACTATAGGGGAGATGTTCTGCTGGTAGTGGTCCG	RNAi in S2 cells control

C Material and Methods

C-termOligo-for	GATCCAAGGAAAAGCGCGAGGATAAACA GGAACGCTTGCAGGAGTCTCACAGATTC CATTTTCGATGCAATGTAA	pGEX-4T-1- <i>shlp</i> -intra construct
C-termOligo-rev	AATTTTACATTGCATCGAAATGGAATCTGT GAGACTCCTGCAAGCGTTCCTGTTTATCC TCGCGCTTTTCCTTG	pGEX4T1- <i>shlp</i> -intra construct
CG7739 Δ Ctermfor	CTTGTGCTATATATCTAGGAAAAGCGCGA GGAT	Deletion of intracellular domain
CG7739 Δ Ctermrev	ATCCTCGCGCTTTTCCTAGATATATAGCAC AAG	Deletion of intracellular domain
CG7739 Δ exDomfor1	TCACGCCTAGCAAATCTAGACTGATGAGC GTCC	Deletion of extracellular domain of Shlp
CG7739 Δ exDomrev1	CGACGCTCATCAGTCTAGATTTGCTAGGC GTGA	Deletion of extracellular domain of Shlp
CG7739 Δ exDomfor2	CCTAGCAAACCTGATTTCTAGAAGCGTCGT GGCG	Deletion of extracellular domain of Shlp
CG7739 Δ exDomrev2	CGCCACGACGCTTCTAGAAATCAGTTTGC TAGG	Deletion of extracellular domain of Shlp
CG7739 Δ exDomfor3	AGCTTTTTGTCACGTCTAGAAAACCTGATT CTGA	Deletion of extracellular domain of Shlp
CG7739 Δ exDomrev3	TCAGAATCAGTTTTCTAGACGTGACAAAA AGCT	Deletion of extracellular domain of Shlp
CG7739 Δ HRFHFDAMfor	CGCTTGCAGGAGTCTTAGAGATTCCATTT CGAT	Deletion of last carboxy terminal amino acids of Shlp
CG7739 Δ HRFHFDAMrev	ATCGAAATGGAATCTCTAAGACTCCTGCA AGCG	Deletion of last carboxy terminal amino acids of Shlp
CG7739 Δ TM-Ctermfor	AGCAAACCTGATTCTGTAGAGCGTCGTGG CGCTG	Deletion of transmembrane and intracellular domain of Shlp
CG7739 Δ TM-Ctermrev	CAGCGCCACGACGCTCTACAGAATCAGT TTGCT	Deletion of transmembrane and intracellular domain of Shlp

C.5.3 Sequencing of plasmids and PCR products

For sequencing of plasmids or PCR products the following PCR reactions were set up using seqmix and seqbuffer (BigDye Terminator v1.1 kit, *Applied Biosystems*) :

Table C-7: PCR mix for sequencing

Sequencing of plasmids		Sequencing of PCR products	
300 ng	plasmid	20 – 30 ng	PCR product
8 pmol	primer	8 pmol	primer
1.5 µl	seqmix	1 µl	seqmix
1.5 µl	seqbuffer	1 µl	seqbuffer
add to 10 µl	ddH ₂ O	add to 10 µl	ddH ₂ O

Table C-8: PCR program for sequencing

Step	Temperature	Time
1	96°C	2 min
2	96°C	20 sec
3	55°C	30 sec
4	60°C	4 min
5	repeat step 2 – 4 26 times	
6	12°C	∞

C.5.4 Generation of *shlp* expression constructs

Cloning of pENTR-*shlp*-stop and pENTR-*shlp*+stop

Cloning of pENTR-*shlp*-stop and pENTR-*shlp*+stop was performed by Diane Egger-Adam. pENTR-*shlp*-stop was generated by cloning a PCR fragment amplified with the oligonucleotides CG7739EV_129-47_for and CG7739EV-Stop_1897-916_rev from embryonic cDNA into pENTR/D-TOPO using the pENTRTM/D-TOPO[®] cloning kit (*Invitrogen*) according to the manufacturer's instructions.

Generation of pTWG-*shlp* and pTWH-*shlp*

The insert from pENTR-*shlp*-stop was recombined into the destination vectors pTWG and pTWH (the *Drosophila* Gateway Vector Collection, Carnegie Institution of Washington, Baltimore, MD) to generate pTWG-*shlp* (*shlp* under UAS_t control with a carboxy terminal GFP tag) and pTWH-*shlp* (*shlp* under UAS_t control with a carboxy terminal hemagglutinin (HA) epitope tag) expression plasmids using the Gateway LR ClonaseTM II Enzyme Mix (*Invitrogen*, Groningen, Netherlands). The manufacturer's protocol was modified by using only ¼ of the reaction mix. In general, 50 ng ENTR-*shlp*-stop were mixed with 75 ng destination vector and 1 µl of TE-buffer, pH 8.0 in a total volume of 2 µl. Then 0.5 µl of LR

C Material and Methods

Clonase™ enzyme mix were added to the reaction and all further steps were conducted according to the standard protocol by the manufacturer.

Generation of pPW-*shlp*

pPW-*shlp* (*shlp* under UASp control without tag) was generated using pENTR-*shlp*+stop and pPW destination vector as described under “Generation of pTWG-*shlp* and pTWH-*shlp*”.

Cloning of pPW-SP-eGFP-*shlp*

Shlp has an amino-terminally located signal peptide that is needed to insert it correctly into the plasma membrane. To generate amino-terminally eGFP tagged Shlp that is targeted to the plasma membrane, it was therefore necessary to insert a signal peptide amino-terminally of the eGFP tag. This construct was created using a four step cloning strategy. First a fragment coding for the predicted Shlp signal peptide (SP) and the following 10 amino acids (base pairs (bp) 1 to 90 of *shlp* cDNA) flanked by a XhoI and a EcoRI restriction site, named SP-XhoI-EcoRI, a fragment coding for enhanced Green Fluorescent Protein flanked by a XhoI and aEcoRI restriction site, named XhoI-eGFP-XbaI-EcoRI and a fragment coding for Shlp excluding the SP (bp 61 to 1791 of *shlp* cDNA), flanked by a XbaI and a EcoRI restriction site, named XbaI-Shlp-EcoRI were amplified using Pfu polymerase (*Bioline*, Luckenwalde), pTWG-*shlp* as template and the following primers:

Table C-9: Fragments for pPW-SP-eGFP-*shlp* cloning generated by PCR amplification

Fragment	Primers
SP-XhoI-EcoRI	forSP-CG7739 and revEcoXho-SP
XhoI-eGFP-XbaI-EcoRI	forXho-GFP and revEcoXba-GFP
XbaI-Shlp-EcoRI	forXba-CG7739 and revEco-CG7739

The PCR mixture was adjusted according to the following standard reaction:

Table C-10: standard PCR reaction using Pfu polymerase

Reagent	volume
template DNA	x µl
forward primer	0.5 µl
reverse primer	0.5 µl
dNTP-mix 10 mM (dATP, dCTP, dGTP, dTTP)	2 µl
10x polymerase buffer	5 µl
Pfu polymerase	1 µl
fill up to 50 µl with dH ₂ O	x µl

The PCR program used was adjusted to the expected fragment length and annealing

temperatures according to the following standard program:

Table C-11: standard PCR program using Pfu polymerase

Step	Time	temperature
1 Denaturation	2 min	95°C
2 Denaturation	30 sec	95°C
3 Annealing	30 sec	50-70°C
4 Elongation	1.5 min per kB	72°C
5	repeat step 2-4 30 times	
6 final elongation	5 min	72°C
7	∞	4°C

Then the SP-XhoI-EcoRI fragment was cloned into the pENTRTM/D-TOPO[®] vector using the pENTR/D-TOPO cloning kit (*Invitrogen*) according to the manufacturer's instructions. Together with the SP fragment a XhoI and an EcoRI restriction site was introduced into the pENTRTM/D-TOPO[®] vector. The vector containing the SP-XhoI-EcoRI insert as well as the XhoI-eGFP-XbaI-EcoRI fragment that was amplified by PCR were digested with XhoI and EcoRI simultaneously and ligated according to standard protocols (Sambrook, J. et al., 2001). The resulting plasmid pENTR/D-TOPO-SP-eGFP-XbaI-EcoRI and the fragment XbaI-Shlp-EcoRI were then digested with XbaI and EcoRI and the cut fragments were ligated according to standard protocols (Sambrook, J. Et al., 2001) to generate the plasmid pENTR/D-TOPO-SP-eGFP-Shlp. The insert SP-eGFP-*shlp* was then recombined into the pAW (allowing transgene expression in *Drosophila* S2 and S2r cells under the control of an *actin::5C* promoter) and pPW (transgene expressed under UASp control) destination vector using the Gateway LR ClonaseTM II Enzyme Mix (*Invitrogen*) as described above. The pAW-SP-eGFP-*shlp* constructs was used for transfection of S2r cells and the pPW-SP-eGFP-*shlp* construct was used to generate transgenic flies (see C.2.7).

C.5.5 Generation of Shlp deletion constructs by site directed mutagenesis

Site directed mutagenesis was carried out using the Quickchange Site-Directed Mutagenesis Kit from *Stratagene*, LaJolla, USA according to the manufacturer's instructions to generate different deletion constructs of Shlp. As template for site directed mutagenesis pENTR-SP-eGFP-*shlp* and pENTR-*shlp*+stop were used. After successful mutagenesis as verified by sequencing, the constructs were recombined into the pPW destination vector using the Gateway LR ClonaseTM II Enzyme Mix (*Invitrogen*) as described above. Table C11 summarizes the primers used to generate Shlp constructs in which premature stop codons have been introduced into the coding sequence of the carboxy terminus of Shlp.

Table C-12: Primers used for deletion constructs of Shlp

Construct	primers	Deleted part in eGFP-Shlp/Shlp
pPW-SP-eGFP- <i>shlp</i> Δ589-596	CG7739ΔHRFHFDAMfor CG7739ΔHRFHFDAMrev	last 6 carboxy terminal amino acids
pPW-SP-eGFP- <i>shlp</i> ΔC	CG7739ΔCtermfor CG7739ΔCtermrev	last 22 carboxy terminal amino acids
pPW-SP-eGFP- <i>shlp</i> ΔTM+C	CG7739ΔTM-Ctermfor CG7739ΔTM-Ctermrev	transmembrane domain and carboxy terminus
pPW- <i>shlp</i> Δ589-596	CG7739ΔHRFHFDAMfor CG7739ΔHRFHFDAMrev	last 6 carboxy terminal amino acids
pPW- <i>shlp</i> ΔC	CG7739ΔCtermfor CG7739ΔCtermrev	last 22 carboxy terminal amino acids
pPW- <i>shlp</i> ΔTM+C	CG7739ΔTM-Ctermfor CG7739ΔTM-Ctermrev	transmembrane domain and carboxy terminus

A Shlp deletion construct lacking the coding region for the extracellular domain (pPW-SP-eGFP-*shlp*ΔexDom) was generated by introducing a second XbaI restriction site into the plasmid pENTR-SP-eGFP-*shlp* via site directed mutagenesis as described above. The primers used for mutagenesis were CG7739ΔexDomfor2 and CG7739ΔexDomrev2. Following successful mutagenesis, as verified by sequencing, the plasmid was digested using XbaI and the insert and the cut fragments were separated by gel electrophoresis. The digested fragment lacking the coding region for the extracellular domain of Shlp was then religated to generate pENTR-SP-eGFP-*shlp*ΔexDom. Thereafter the constructs was recombined into the pPW destination vector using the Gateway LR ClonaseTM II Enzyme Mix (*Invitrogen*) as described above. All deletion constructs described here were used to generate transgenic flies as described under C2.7.

C.5.6 Generation of pGEX-4T-1-*shlp*-exDom

A fragment encoding the extracellular domain of Shlp (bp 61 to 1791 of *shlp* cDNA) was amplified using the primers D1forEcoR1 and D1revXhoI according to standard procedures. The resulting fragment was separated on an agarose gel and the fragment was purified using the Nucleospin Extract Kit (*Macherey-Nagel*, Düren) according to the manufacturer's instructions. The purified fragment and the pGEX-4T-1 vector (*GE Healthcare*) were digested using EcoRI and XhoI and the purified fragments were ligated using standard protocols (Sambrook, J. et al. 2001). The resulting plasmid was sequenced and used for expression of Shlp-exDom in Bacteria (*E. coli* strain BL21).

C.5.7 Single fly genomic DNA preparation

One fly (preferentially male) was anesthetized, transferred to an Eppendorf tube and snap frozen in liquid nitrogen. 50 µl SB buffer (10 mM Tris pH 8.2, 1 mM EDTA, 2 mM NaCl), supplemented freshly with 0.5 µl proteinase K from a 20 mg/ml stock was added and the fly

homogenized by pipetting. The homogenate was incubated at 37°C for 20 min and after that proteinase K (*Fermentas*) was inactivated by heating to 95°C for 3 min. For PCR 5 µl of the homogenate was used.

C.5.8 Extraction of genomic DNA from flies

30 male flies were collected in one Eppendorf tube and snap frozen in liquid nitrogen. 400 µl of lysis buffer containing 100 mM Tris-HCl, pH 7.5, 100 mM EDTA, pH 8.0, 100 mM NaCl and 0.5% SDS was added into the tube. Frozen flies were homogenized using a biovortexer. The lysate was incubated at 65°C for 15-30 min. Afterwards, 228.4 µl of 5 M KAc and 571.6 µl of 6 M LiCl were added into the lysate and incubated on ice for 15 min before being centrifuged at 13,000 rpm for 15 min. 1 ml of the supernatant was transferred into a new tube. 600 µl of isopropanol was added and the mixture was centrifuged again at 13,000 rpm for 15 min. The DNA pellet was washed with 70% ethanol and dissolved in 150 µl of sterile water.

C.5.9 Long-template PCR

Expand Long Template PCR System (*Roche Diagnostics*) was used for the characterization of the exact deletion in *shlp* mutant alleles. Components of PCR reaction and thermal cycles were set up according to the manufacturer's instructions.

Table C-13: Polymerase chain reaction mix for long-template PCR

Components	Volume (µl)
ddH ₂ O	37.75
dNTPs (10 mM)	2.5
Primers (10 mM)	1.5+1.5
10×PCR buffer (MgCl ₂)	5
Template DNA	1 (≤500 ng)
Long template enzyme mix	0.75
Total	50

Table C-14: Conditions for long template PCR

temperature	time	cycles
94°C	2 min	1
94°C	10 sec	10
55°C	30 sec	
68°C	10 min	
94°C	15 sec	20

55°C	30 sec	
68°C	10 min+20 sec	
68°C	7 min	1
4°C	∞	1

C.6 Biochemical methods

C.6.1 Western Blot and Immunoprecipitation

Western Blot and immunoprecipitation were performed according to standard procedures (Wodarz, 2008).

C.6.2 Deglycosylation of Shlp-GFP

Embryos overexpressing Shlp-GFP (genotype: *w*; ; *da::Gal4, pTWG-shlp/TM6*) and embryos expressing Rngo-GFP (genotype: *w*; ; *da::Gal4, PTWG-rngo*) as a control were collected over night, dechorionated in Klorix bleach and washed extensively with water. Around 100 μ l of embryos of each genotype were homogenized in 500 μ l ice-cold RIPA buffer (50mM Tris-HCl, pH 7.5, 150 mM NaCl, 1% Igepal (*Sigma-Aldrich*), 0.5 % sodiumdesoxycholat, 0.1 % SDS and protease inhibitors) with a Dounce homogenizer. Protein lysates were incubated on ice for 30 min and then centrifuged at 14000 rpm for 15 min at 4°C. For each genotype two times 1000 mg of protein were diluted in wash buffer (10 mM Tris-HCl, 150 mM NaCl, 0,5 mM EDTA and protease inhibitors) to a final volume of 1000 μ l. Then 15 μ l of GFP-Trap[®] beads (*ChromoTek GmbH*) equilibrated with wash buffer were added to each of the protein lysates and the mixture was incubated for 2 h at 4°C with gentle end-over-end mixing. After incubation beads were collected by centrifugation at 2000 g for 2 min at 4°C and the supernatant was discarded. The beads were washed three times with wash buffer and then 3 μ l of 10x Glycoprotein Denaturing Buffer (5% SDS, 0.4 M DTT, supplied with PNGase F from *New England Biolabs*) were added to the beads and subsequently the mixture was heated to 95°C for 10 min. After that the following reagents, included in the PNGase F kit (*New England Biolabs*) were added: 4 μ l 10x, 10% NP-40 and 2 μ l of PNGase F. As a negative control PNGase was substituted with ddH₂O. After incubation for 1 h at 37°C, 20 μ l of 2x SDS sample buffer were added and the mixture was heated to 95°C for 10 min. Thereafter the beads were sedimented by centrifugation at 2700 g for 2 min and the supernatant was transferred to a fresh eppendorf tube. The samples were then separated by SDS-PAGE and subjected to Western Blot analysis.

C.6.3 Secretion assay in S2r cells

S2r cells were harvested by centrifugation at 1000 rpm for 6 min. Cells were washed three

times with 1 ml of *Drosophila* Schneider medium (Invitrogen) lacking serum and antibiotics. As negative control for later SDS page and Western Blot analysis 30 µl of serum and antibiotics free medium were taken. The cells were incubated at 25°C. At various time points samples were taken for Western Blot analysis. After 5 hours the cells were pelleted by centrifugation at 1000 rpm, for 6 min. The supernatant was transferred to a fresh eppendorf tube and kept on ice. The cells were lysed by resuspending in 100 µl of Ansgar lysis buffer (25 mM Hepes pH 7.5, 100 mM NaCl, 1 mM CaCl₂, 1 mM MgCl₂, 1 % Triton X-100 and protease inhibitor cocktail (Roche) and incubating for 20 min on ice. After incubation the lysate was centrifuged at 14000 rpm for 15 min at 4°C and the supernatant was transferred to a fresh eppendorf tube. The protein content was determined spectrometrically. The supernatant of the cells was transferred to ultracentrifugation tubes and subjected to centrifugation at 100000 g for 30 min, 4°C in a Beckmann Coulter Optima Max ultracentrifuge (Fullerton, California, USA) to pellet all remaining cell debris and the supernatant was then transferred to a new tube. 20 µl of the supernatant was subjected to SDS page and Western Blot analysis.

C.6.4 Purification of GST-Shlp-exDom for antibody production

The procedure describes the expression of the extracellular domain of Shlp including amino acids 21 to 551 as an amino-terminally GST-tagged fusion protein (GST-Shlp-exDom) in *E. coli*. 8 l of 2YTA medium was inoculated with 80 ml overnight culture of BL21 cells transformed with pGEX-4T-1-*shlp*exDom and incubated at 37 °C till the culture reached OD₆₀₀ 0.8. IPTG was added to a final concentration of 0.5 mM to induce the expression of GST-Shlp-exDom overnight at 17°C. Bacteria were harvested by centrifugation at 5,000 g for 15 min at 4°C. The pellet was resuspended in 200 ml 1×PBS with protease inhibitors and cells were lysed by high pressure homogenisation in a French press. 20% Triton-X100 was added to the lysate to a final concentration of 1%. The mixture was gently rotated for 30 min and centrifuged at 12,000 g for 10 min at 4°C. 1 ml of 50:50 slurry of glutathione-Sepharose beads (GE Healthcare) was added to the supernatant and rotated for 30 min at 4°C. The beads were sedimented and washed three times. The bound protein was eluted from the beads by elution buffer containing 20 mM reduced glutathione and 120 mM NaCl in 50 mM Tris-HCl, pH8.0. Eluted protein was snap frozen and stored at -70 °C for later use. The purified protein was then used to generate a polyclonal antibody in guinea pig. Immunization was conducted by Eurogentec, Seraing, Belgium following standard procedures.

C.6.5 Pull down with Shlp-intra beads

A peptide composed of the 22 carboxy terminal amino acids of Shlp (Shlp-intra, amino acid sequence: CVLYIKEKREDKQERLQESHRFHFDAM) was synthesized and coupled to agarose beads by the Proteomics group at the MPI for Experimental Medicine. As a control agarose beads were saturated with L-cysteine (control beads). Embryos were collected over night and dechorionated with Klorix bleach. Embryos were homogenized in lysis buffer (10 mM Tris-HCl, pH 7.5, 150 mM NaCl, 0.5 % Triton-X-100, 1 mM DTT and protease inhibitors) using a Dounce homogenizer. Lysates were incubated on ice for 30 min and subsequently centrifuged in a table top centrifuge at 14000 rpm for 15 min. The supernatant was then transferred to a fresh Eppendorf tube. Supernatant containing 1 mg of protein was adjusted to a final volume of 1 ml with wash buffer (10 mM Tris-HCl, pH 7.5, 150 mM, 1 mM DTT and protease inhibitors) and then 40 µl of control beads, washed once with wash buffer, were added. Protein lysates were pre-incubated with control beads for 1 h 30 min rotating head over head at 4°C. After that lysates were centrifuged for 2 min at 2700 g, 4°C to pellet the control beads and the supernatant was transferred to a fresh Eppendorf tube. 40 µl of Shlp-intra beads were washed once with wash buffer and then added to the pre cleared protein lysates. Binding to the beads was performed over night at 4°C rotating slowly head over head. As a control protein lysates were incubated with the same amount of pre incubated control beads in parallel. After that beads were washed five times with ice cold wash buffer. Then elution was performed with 40 µl of Shlp-intra peptide dissolved in wash buffer (1 µg peptide / µl) for 30 min at room temperature slowly shaking. Then beads were sedimented by centrifugation at 2700 g and the supernatant was transferred to a new Eppendorf tube. Subsequently 40 µl of 2x SDS sample buffer were added to the beads and the sample heated to 95°C for 7 min. Afterwards the sample was centrifuged at 2700 g and the supernatant was transferred to a fresh eppendorf tube. The samples were later analysed by SDS-PAGE using 10 % polyacrylamide gels followed by silver staining or colloidal coomassie staining. Colloidal coomassie staining was performed according to Neuhoff et al. (Neuhoff *et al.*, 1988). Silver staining was performed as follows: after SDS-PAGE the gel was incubated in fixer (40 % methanol, 10 % acetic acid in dH₂O) for 1 h, 30 min. Then the gel was washed twice in 50 % ethanol for 20 min. The gel was subsequently put in 0.8 mM Na₂S₂O₃ for 1 min followed by three washing steps in dH₂O each time for 20 sec. Thereafter the gel was incubated with silver nitrate solution (0.2 g AgNO₃, 0.05 ml 37 % formaldehyde solution in 100 ml dH₂O) for 20 min on ice. After three washing steps in dH₂O, each for 20 sec, the gel was incubated in developer solution (6 g Na₂CO₃, 0.05 ml 37 % formaldehyde solution).

Sufficient staining intensity was reached after one to three min, the maximum time for development was 15 min. The staining reaction was stopped by rinsing the gel once in dH₂O and then in fixing solution (40 % methanol, 10 % acetic acid in dH₂O).

C.7 Infection and Survival experiments

Infection and survival experiments to test if *shlp*¹³¹ mutant flies are susceptible to immune challenge were performed in the group of Bruno Lemaitre in Lausanne as previously described (Lemaitre *et al.*, 1997; Tzou *et al.*, 2002b; Pili-Floury *et al.*, 2004; Buchon *et al.*, 2009). In brief adult flies were pricked into the thorax with a sharpened tungsten needle (<0.2 mm) dipped into a concentrated bacterial pellet. Survival experiments were performed under the same conditions for each line tested. Three groups of 20 young adults from each line (for *shlp*¹³¹ only 14 adults) were challenged by pricking, then incubated at 29°C and transferred to fresh vials every three days. Flies that died within the first hour of challenge were not considered in the analysis.

D References

- Aggarwal, K., and Silverman, N.** (2008). Positive and negative regulation of the *Drosophila* immune response. *BMB Rep* *41*, 267-277.
- Altschul, S.F., Gish, W., Miller, W., Myers, E.W., and Lipman, D.J.** (1990). Basic local alignment search tool. *J Mol Biol* *215*, 403-410.
- Andersen, S.O.** (2010). Insect cuticular sclerotization: a review. *Insect Biochem Mol Biol* *40*, 166-178.
- Andrews, H.K., Zhang, Y.Q., Trotta, N., and Broadie, K.** (2002). *Drosophila* sec10 is required for hormone secretion but not general exocytosis or neurotransmission. *Traffic* *3*, 906-921.
- Ashburner, M., Golic, K.G., Hawley, R.S., ed. (2004). *Drosophila: a laboratory handbook*, 2nd edn (Cold Spring Harbor, New York, USA).
- Atwood, S.X., and Prehoda, K.E.** (2009). aPKC phosphorylates Miranda to polarize fate determinants during neuroblast asymmetric cell division. *Curr Biol* *19*, 723-729.
- Baker, J.D., McNabb, S.L., and Truman, J.W.** (1999). The hormonal coordination of behavior and physiology at adult ecdysis in *Drosophila melanogaster*. *J Exp Biol* *202*, 3037-3048.
- Baker, J.D., and Truman, J.W.** (2002). Mutations in the *Drosophila* glycoprotein hormone receptor, rickets, eliminate neuropeptide-induced tanning and selectively block a stereotyped behavioral program. *J Exp Biol* *205*, 2555-2565.
- Balklava, Z., Pant, S., Fares, H., and Grant, B.D.** (2007). Genome-wide analysis identifies a general requirement for polarity proteins in endocytic traffic. *Nat Cell Biol* *9*, 1066-1073.
- Barros, C.S., Phelps, C.B., and Brand, A.H.** (2003). *Drosophila* nonmuscle myosin II promotes the asymmetric segregation of cell fate determinants by cortical exclusion rather than active transport. *Dev Cell* *5*, 829-840.
- Bello, B., Reichert, H., and Hirth, F.** (2006). The brain tumor gene negatively regulates neural progenitor cell proliferation in the larval central brain of *Drosophila*. *Development* *133*, 2639-2648.
- Bello, B.C., Izergina, N., Caussinus, E., and Reichert, H.** (2008). Amplification of neural stem cell proliferation by intermediate progenitor cells in *Drosophila* brain development. *Neural Dev* *3*, 5.
- Belvin, M.P., Jin, Y., and Anderson, K.V.** (1995). Cactus protein degradation mediates *Drosophila* dorsal-ventral signaling. *Genes Dev* *9*, 783-793.
- Benton, R., and St Johnston, D.** (2003). A conserved oligomerization domain in *drosophila* Bazooka/PAR-3 is important for apical localization and epithelial polarity. *Curr Biol* *13*, 1330-1334.

- Berdnik, D., Torok, T., Gonzalez-Gaitan, M., and Knoblich, J.A.** (2002a). The endocytic protein alpha-Adaptin is required for numb-mediated asymmetric cell division in *Drosophila*. *Dev Cell* *3*, 221-231.
- Berdnik, D., Török, T., Gonzalez-Gaitan, M., and Knoblich, J.A.** (2002b). The endocytic protein alpha-Adaptin is required for numb-mediated asymmetric cell division in *Drosophila*. *Dev Cell* *3*, 221-231.
- Beronja, S., Laprise, P., Papoulas, O., Pellikka, M., Sisson, J., and Tepass, U.** (2005). Essential function of *Drosophila* Sec6 in apical exocytosis of epithelial photoreceptor cells. *J Cell Biol* *169*, 635-646.
- Betschinger, J., Eisenhaber, F., and Knoblich, J.A.** (2005). Phosphorylation-induced autoinhibition regulates the cytoskeletal protein Lethal (2) giant larvae. *Curr Biol* *15*, 276-282.
- Betschinger, J., Mechtler, K., and Knoblich, J.A.** (2006). Asymmetric segregation of the tumor suppressor brat regulates self-renewal in *Drosophila* neural stem cells. *Cell* *124*, 1241-1253.
- Betschinger, J., Mechtler, K., and Knoblich, J.A.** (2003). The Par complex directs asymmetric cell division by phosphorylating the cytoskeletal protein Lgl. *Nature* *422*, 326-330.
- Bhat, M.A., Izaddoost, S., Lu, Y., Cho, K.O., Choi, K.W., and Bellen, H.J.** (1999). Discs Lost, a novel multi-PDZ domain protein, establishes and maintains epithelial polarity. *Cell* *96*, 833-845.
- Bilder, D., Schober, M., and Perrimon, N.** (2003). Integrated activity of PDZ protein complexes regulates epithelial polarity. *Nat Cell Biol* *5*, 53-58.
- Blair, S.S.** (2003). Genetic mosaic techniques for studying *Drosophila* development. *Development* *130*, 5065-5072.
- Blankenship, J.T., Fuller, M.T., and Zallen, J.A.** (2007). The *Drosophila* homolog of the Exo84 exocyst subunit promotes apical epithelial identity. *J Cell Sci* *120*, 3099-3110.
- Bowman, S.K., Neumuller, R.A., Novatchkova, M., Du, Q., and Knoblich, J.A.** (2006). The *Drosophila* NuMA Homolog Mud regulates spindle orientation in asymmetric cell division. *Dev Cell* *10*, 731-742.
- Braun, A., Hoffmann, J.A., and Meister, M.** (1998). Analysis of the *Drosophila* host defense in domino mutant larvae, which are devoid of hemocytes. *Proc Natl Acad Sci U S A* *95*, 14337-14342.
- Bucci, C., Wandinger-Ness, A., Lutcke, A., Chiariello, M., Bruni, C.B., and Zerial, M.** (1994). Rab5a is a common component of the apical and basolateral endocytic machinery in polarized epithelial cells. *Proc Natl Acad Sci U S A* *91*, 5061-5065.
- Buchon, N., Poidevin, M., Kwon, H.M., Guillou, A., Sottas, V., Lee, B.L., and Lemaitre,**

D References

- B.** (2009). A single modular serine protease integrates signals from pattern-recognition receptors upstream of the *Drosophila* Toll pathway. *Proc Natl Acad Sci U S A* *106*, 12442-12447.
- Campos-Ortega, J.A.** (1993). Mechanisms of early neurogenesis in *Drosophila melanogaster*. *J Neurobiol* *24*, 1305-1327.
- Canalis, E., Economides, A.N., and Gazzerro, E.** (2003). Bone morphogenetic proteins, their antagonists, and the skeleton. *Endocr Rev* *24*, 218-235.
- Ceron, J., Gonzalez, C., and Tejedor, F.J.** (2001). Patterns of cell division and expression of asymmetric cell fate determinants in postembryonic neuroblast lineages of *Drosophila*. *Dev Biol* *230*, 125-138.
- Chabu, C., and Doe, C.Q.** (2008). Dap160/intersectin binds and activates aPKC to regulate cell polarity and cell cycle progression. *Development* *135*, 2739-2746.
- Chang, C.I., Pili-Floury, S., Herve, M., Parquet, C., Chelliah, Y., Lemaitre, B., Mengin-Lecreulx, D., and Deisenhofer, J.** (2004). A *Drosophila* pattern recognition receptor contains a peptidoglycan docking groove and unusual L,D-carboxypeptidase activity. *PLoS Biol* *2*, E277.
- Chen, M.S., Obar, R.A., Schroeder, C.C., Austin, T.W., Poodry, C.A., Wadsworth, S.C., and Vallee, R.B.** (1991). Multiple forms of dynamin are encoded by shibire, a *Drosophila* gene involved in endocytosis. *Nature* *351*, 583-586.
- Choe, K.M., Lee, H., and Anderson, K.V.** (2005). *Drosophila* peptidoglycan recognition protein LC (PGRP-LC) acts as a signal-transducing innate immune receptor. *Proc Natl Acad Sci U S A* *102*, 1122-1126.
- Choe, K.M., Werner, T., Stoven, S., Hultmark, D., and Anderson, K.V.** (2002). Requirement for a peptidoglycan recognition protein (PGRP) in Relish activation and antibacterial immune responses in *Drosophila*. *Science* *296*, 359-362.
- Clague, M.J.** (1998). Molecular aspects of the endocytic pathway. *Biochem J* *336* (Pt 2), 271-282.
- Clark, A.C., del Campo, M.L., and Ewer, J.** (2004). Neuroendocrine control of larval ecdysis behavior in *Drosophila*: complex regulation by partially redundant neuropeptides. *J Neurosci* *24*, 4283-4292.
- Davis, M.M., O'Keefe, S.L., Primrose, D.A., and Hodgetts, R.B.** (2007). A neuropeptide hormone cascade controls the precise onset of post-eclosion cuticular tanning in *Drosophila melanogaster*. *Development* *134*, 4395-4404.
- Dewey, E.M., McNabb, S.L., Ewer, J., Kuo, G.R., Takanishi, C.L., Truman, J.W., and Honegger, H.W.** (2004). Identification of the gene encoding bursicon, an insect neuropeptide responsible for cuticle sclerotization and wing spreading. *Curr Biol* *14*, 1208-1213.
- Doe, C.Q., Chu-LaGraff, Q., Wright, D.M., and Scott, M.P.** (1991). The prospero gene specifies cell fates in the *Drosophila* central nervous system. *Cell* *65*, 451-464.

- Egger-Adam, D.** (2005). Identifikation neuer Interaktionspartner des Bazooka Proteins in *Drosophila melanogaster*. Institut für Genetik, Heinrich-Heine Universität Düsseldorf *Dr. rer. nat.*, 168.
- Egger, B., Boone, J.Q., Stevens, N.R., Brand, A.H., and Doe, C.Q.** (2007). Regulation of spindle orientation and neural stem cell fate in the *Drosophila* optic lobe. *Neural Dev* 2, 1.
- Egger, B., Chell, J.M., and Brand, A.H.** (2008). Insights into neural stem cell biology from flies. *Philos Trans R Soc Lond B Biol Sci* 363, 39-56.
- Emery, G., Hutterer, A., Berdnik, D., Mayer, B., Wirtz-Peitz, F., Gaitan, M.G., and Knoblich, J.A.** (2005). Asymmetric Rab 11 endosomes regulate delta recycling and specify cell fate in the *Drosophila* nervous system. *Cell* 122, 763-773.
- Emery, G., and Knoblich, J.A.** (2006). Endosome dynamics during development. *Curr Opin Cell Biol* 18, 407-415.
- Erben, V., Waldhuber, M., Langer, D., Fetka, I., Jansen, R.P., and Petritsch, C.** (2008). Asymmetric localization of the adaptor protein Miranda in neuroblasts is achieved by diffusion and sequential interaction of Myosin II and VI. *J Cell Sci* 121, 1403-1414.
- Evan, G.I., Lewis, G.K., Ramsay, G., and Bishop, J.M.** (1985). Isolation of monoclonal antibodies specific for human c-myc proto-oncogene product. *Mol Cell Biol* 5, 3610-3616.
- Ewer, J., and Truman, J.W.** (1996). Increases in cyclic 3', 5'-guanosine monophosphate (cGMP) occur at ecdysis in an evolutionarily conserved crustacean cardioactive peptide-immunoreactive insect neuronal network. *J Comp Neurol* 370, 330-341.
- Fernandez, N.Q., Grosshans, J., Goltz, J.S., and Stein, D.** (2001). Separable and redundant regulatory determinants in Cactus mediate its dorsal group dependent degradation. *Development* 128, 2963-2974.
- Ferrandon, D., Imler, J.L., Hetru, C., and Hoffmann, J.A.** (2007). The *Drosophila* systemic immune response: sensing and signalling during bacterial and fungal infections. *Nat Rev Immunol* 7, 862-874.
- Ferrandon, D., Jung, A.C., Criqui, M., Lemaitre, B., Uttenweiler-Joseph, S., Michaut, L., Reichhart, J., and Hoffmann, J.A.** (1998). A drosomycin-GFP reporter transgene reveals a local immune response in *Drosophila* that is not dependent on the Toll pathway. *EMBO J* 17, 1217-1227.
- Finger, F.P., and Novick, P.** (1998). Spatial regulation of exocytosis: lessons from yeast. *J Cell Biol* 142, 609-612.
- Fiscella, M., Perry, J.W., Teng, B., Bloom, M., Zhang, C., Leung, K., Pukac, L., Florence, K., Concepcion, A., Liu, B., et al.** (2003). TIP, a T-cell factor identified using high-throughput screening increases survival in a graft-versus-host disease model. *Nat Biotechnol* 21, 302-307.
- Fraenkel, G., and Hsiao, C.** (1965). Bursicon, a hormone which mediates tanning of the

D References

cuticle in the adult fly and other insects. *J Insect Physiol* *11*, 513-556.

Fraenkel, G., and Hsiao, C. (1962). Hormonal and nervous control of tanning in the fly. *Science* *138*, 27-29.

Franc, N.C., Heitzler, P., Ezekowitz, R.A., and White, K. (1999). Requirement for croquemort in phagocytosis of apoptotic cells in *Drosophila*. *Science* *284*, 1991-1994.

Gammie, S.C., and Truman, J.W. (1999). Eclosion hormone provides a link between ecdysis-triggering hormone and crustacean cardioactive peptide in the neuroendocrine cascade that controls ecdysis behavior. *J Exp Biol* *202*, 343-352.

Giansanti, M.G., Farkas, R.M., Bonaccorsi, S., Lindsley, D.L., Wakimoto, B.T., Fuller, M.T., and Gatti, M. (2004). Genetic dissection of meiotic cytokinesis in *Drosophila* males. *Mol Biol Cell* *15*, 2509-2522.

Giet, R., McLean, D., Descamps, S., Lee, M.J., Raff, J.W., Prigent, C., and Glover, D.M. (2002). *Drosophila* Aurora A kinase is required to localize D-TACC to centrosomes and to regulate astral microtubules. *J Cell Biol* *156*, 437-451.

Gobert, V., Gottar, M., Matskevich, A.A., Rutschmann, S., Royet, J., Belvin, M., Hoffmann, J.A., and Ferrandon, D. (2003). Dual activation of the *Drosophila* toll pathway by two pattern recognition receptors. *Science* *302*, 2126-2130.

Gönczy, P. (2008). Mechanisms of asymmetric cell division: flies and worms pave the way. *Nat Rev Mol Cell Biol* *9*, 355-366.

Gonzalez-Gaitan, M., and Jäckle, H. (1997). Role of *Drosophila* alpha-adaptin in presynaptic vesicle recycling. *Cell* *88*, 767-776.

Gottar, M., Gobert, V., Matskevich, A.A., Reichhart, J.M., Wang, C., Butt, T.M., Belvin, M., Hoffmann, J.A., and Ferrandon, D. (2006). Dual detection of fungal infections in *Drosophila* via recognition of glucans and sensing of virulence factors. *Cell* *127*, 1425-1437.

Gottar, M., Gobert, V., Michel, T., Belvin, M., Duyk, G., Hoffmann, J.A., Ferrandon, D., and Royet, J. (2002). The *Drosophila* immune response against Gram-negative bacteria is mediated by a peptidoglycan recognition protein. *Nature* *416*, 640-644.

Grindstaff, K.K., Yeaman, C., Anandasabapathy, N., Hsu, S.C., Rodriguez-Boulan, E., Scheller, R.H., and Nelson, W.J. (1998). Sec6/8 complex is recruited to cell-cell contacts and specifies transport vesicle delivery to the basal-lateral membrane in epithelial cells. *Cell* *93*, 731-740.

Hamburger, Z.A., Hamburger, A.E., West, A.P., Jr., and Weis, W.I. (2006). Crystal structure of the *S.cerevisiae* exocyst component Exo70p. *J Mol Biol* *356*, 9-21.

Harris, K.P., and Tepass, U. (2008). Cdc42 and Par proteins stabilize dynamic adherens junctions in the *Drosophila* neuroectoderm through regulation of apical endocytosis. *J Cell Biol* *183*, 1129-1143.

Hartenstein, V., Spindler, S., Peraanu, W., and Fung, S. (2008). The development of the

Drosophila larval brain. *Adv Exp Med Biol* 628, 1-31.

Hirata, J., Nakagoshi, H., Nabeshima, Y., and Matsuzaki, F. (1995). Asymmetric segregation of the homeodomain protein Prospero during *Drosophila* development. *Nature* 377, 627-630.

Hoffmann, J.A. (2003). The immune response of *Drosophila*. *Nature* 426, 33-38.

Honegger, H.W., Dewey, E.M., and Ewer, J. (2008). Bursicon, the tanning hormone of insects: recent advances following the discovery of its molecular identity. *J Comp Physiol A Neuroethol Sens Neural Behav Physiol* 194, 989-1005.

Horodyski, F.M., Ewer, J., Riddiford, L.M., and Truman, J.W. (1993). Isolation, characterization and expression of the eclosion hormone gene of *Drosophila melanogaster*. *Eur J Biochem* 215, 221-228.

Hsu, S.C., Hazuka, C.D., Foletti, D.L., and Scheller, R.H. (1999). Targeting vesicles to specific sites on the plasma membrane: the role of the sec6/8 complex. *Trends Cell Biol* 9, 150-153.

Hsu, S.C., TerBush, D., Abraham, M., and Guo, W. (2004). The exocyst complex in polarized exocytosis. *Int Rev Cytol* 233, 243-265.

Hu, X., Yagi, Y., Tanji, T., Zhou, S., and Ip, Y.T. (2004). Multimerization and interaction of Toll and Spatzle in *Drosophila*. *Proc Natl Acad Sci U S A* 101, 9369-9374.

Hurley, J.H., and Emr, S.D. (2006). The ESCRT complexes: structure and mechanism of a membrane-trafficking network. *Annu Rev Biophys Biomol Struct* 35, 277-298.

Hutterer, A., Betschinger, J., Petronczki, M., and Knoblich, J.A. (2004). Sequential roles of Cdc42, Par-6, aPKC, and Lgl in the establishment of epithelial polarity during *Drosophila* embryogenesis. *Dev Cell* 6, 845-854.

Hutterer, A., and Knoblich, J.A. (2005). Numb and alpha-Adaptin regulate Sanpodo endocytosis to specify cell fate in *Drosophila* external sensory organs. *EMBO Rep* 6, 836-842.

Ikeshima-Kataoka, H., Skeath, J.B., Nabeshima, Y., Doe, C.Q., and Matsuzaki, F. (1997). Miranda directs Prospero to a daughter cell during *Drosophila* asymmetric divisions. *Nature* 390, 625-629.

Inoue, M., Chang, L., Hwang, J., Chiang, S.H., and Saltiel, A.R. (2003). The exocyst complex is required for targeting of Glut4 to the plasma membrane by insulin. *Nature* 422, 629-633.

Ito, K., and Hotta, Y. (1992). Proliferation pattern of postembryonic neuroblasts in the brain of *Drosophila melanogaster*. *Dev Biol* 149, 134-148.

Izumi, Y., Ohta, N., Hisata, K., Raabe, T., and Matsuzaki, F. (2006). *Drosophila* Pins-binding protein Mud regulates spindle-polarity coupling and centrosome organization. *Nat Cell Biol* 8, 586-593.

- Jafar-Nejad, H., Andrews, H.K., Acar, M., Bayat, V., Wirtz-Peitz, F., Mehta, S.Q., Knoblich, J.A., and Bellen, H.J.** (2005). Sec15, a component of the exocyst, promotes notch signaling during the asymmetric division of *Drosophila* sensory organ precursors. *Dev Cell* *9*, 351-363.
- Janeway, C.A., Jr., and Medzhitov, R.** (2002). Innate immune recognition. *Annu Rev Immunol* *20*, 197-216.
- Jang, I.H., Chosa, N., Kim, S.H., Nam, H.J., Lemaitre, B., Ochiai, M., Kambris, Z., Brun, S., Hashimoto, C., Ashida, M., et al.** (2006). A Spatzle-processing enzyme required for toll signaling activation in *Drosophila* innate immunity. *Dev Cell* *10*, 45-55.
- Jiang, H., and Kanost, M.R.** (2000). The clip-domain family of serine proteinases in arthropods. *Insect Biochem Mol Biol* *30*, 95-105.
- Johnson, K., and Wodarz, A.** (2003). A genetic hierarchy controlling cell polarity. *Nat Cell Biol* *5*, 12-14.
- Kaczanowski, S., and Zielenkiewicz, P.** (2003). A TIP on malaria (genomics). *Nat Biotechnol* *21*, 733.
- Kaltschmidt, J.A., Davidson, C.M., Brown, N.H., and Brand, A.H.** (2000). Rotation and asymmetry of the mitotic spindle direct asymmetric cell division in the developing central nervous system. *Nat Cell Biol* *2*, 7-12.
- Kambris, Z., Hoffmann, J.A., Imler, J.L., and Capovilla, M.** (2002). Tissue and stage-specific expression of the Tolls in *Drosophila* embryos. *Gene Expr Patterns* *2*, 311-317.
- Kaneko, T., Yano, T., Aggarwal, K., Lim, J.H., Ueda, K., Oshima, Y., Peach, C., Erturk-Hasdemir, D., Goldman, W.E., Oh, B.H., et al.** (2006). PGRP-LC and PGRP-LE have essential yet distinct functions in the *drosophila* immune response to monomeric DAP-type peptidoglycan. *Nat Immunol* *7*, 715-723.
- Kang, D., Liu, G., Lundstrom, A., Gelius, E., and Steiner, H.** (1998). A peptidoglycan recognition protein in innate immunity conserved from insects to humans. *Proc Natl Acad Sci U S A* *95*, 10078-10082.
- Kiger, J.A., Jr., Natzle, J.E., and Green, M.M.** (2001). Hemocytes are essential for wing maturation in *Drosophila melanogaster*. *Proc Natl Acad Sci U S A* *98*, 10190-10195.
- Kiger, J.A., Jr., Natzle, J.E., Kimbrell, D.A., Paddy, M.R., Kleinhesselink, K., and Green, M.M.** (2007). Tissue remodeling during maturation of the *Drosophila* wing. *Dev Biol* *301*, 178-191.
- Kim, S., Gailite, I., Moussian, B., Luschnig, S., Goette, M., Fricke, K., Honemann-Capito, M., Grubmuller, H., and Wodarz, A.** (2009). Kinase-activity-independent functions of atypical protein kinase C in *Drosophila*. *J Cell Sci* *122*, 3759-3771.
- Kim, T., and Kim, Y.J.** (2005). Overview of innate immunity in *Drosophila*. *J Biochem Mol Biol* *38*, 121-127.

- Kimura, K., Kodama, A., Hayasaka, Y., and Ohta, T.** (2004). Activation of the cAMP/PKA signaling pathway is required for post-ecdysial cell death in wing epidermal cells of *Drosophila melanogaster*. *Development* *131*, 1597-1606.
- Kimura, K.I., and Truman, J.W.** (1990). Postmetamorphic cell death in the nervous and muscular systems of *Drosophila melanogaster*. *J Neurosci* *10*, 403-401.
- Kingan, T.G., Cardullo, R.A., and Adams, M.E.** (2001). Signal transduction in eclosion hormone-induced secretion of ecdysis-triggering hormone. *J Biol Chem* *276*, 25136-25142.
- Knoblich, J.A.** (2008). Mechanisms of asymmetric stem cell division. *Cell* *132*, 583-597.
- Knoblich, J.A., Jan, L.Y., and Jan, Y.N.** (1995). Asymmetric segregation of Numb and Prospero during cell division. *Nature* *377*, 624-627.
- Knust, E., and Bossinger, O.** (2002). Composition and formation of intercellular junctions in epithelial cells. *Science* *298*, 1955-1959.
- Kocks, C., Cho, J.H., Nehme, N., Ulvila, J., Pearson, A.M., Meister, M., Strom, C., Conto, S.L., Hetru, C., Stuart, L.M., et al.** (2005). Eater, a transmembrane protein mediating phagocytosis of bacterial pathogens in *Drosophila*. *Cell* *123*, 335-346.
- Kosaka, T., and Ikeda, K.** (1983). Reversible blockage of membrane retrieval and endocytosis in the garland cell of the temperature-sensitive mutant of *Drosophila melanogaster*, shibirets1. *J Cell Biol* *97*, 499-507.
- Krahn, M.P., Klopfenstein, D.R., Fischer, N., and Wodarz, A.** (2010). Membrane targeting of Bazooka/PAR-3 is mediated by direct binding to phosphoinositide lipids. *Curr Biol* *20*, 636-642.
- Kraut, R., Chia, W., Jan, L.Y., Jan, Y.N., and Knoblich, J.A.** (1996). Role of inscuteable in orienting asymmetric cell divisions in *Drosophila*. *Nature* *383*, 50-55.
- Kuchinke, U., Grawe, F., and Knust, E.** (1998). Control of spindle orientation in *Drosophila* by the Par-3-related PDZ-domain protein Bazooka. *Curr Biol* *8*, 1357-1365.
- Lalli, G.** (2009). RalA and the exocyst complex influence neuronal polarity through PAR-3 and aPKC. *J Cell Sci* *122*, 1499-1506.
- Langevin, J., Morgan, M.J., Sibarita, J.B., Aresta, S., Murthy, M., Schwarz, T., Camonis, J., and Bellaiche, Y.** (2005). *Drosophila* exocyst components Sec5, Sec6, and Sec15 regulate DE-Cadherin trafficking from recycling endosomes to the plasma membrane. *Dev Cell* *9*, 365-376.
- Lanot, R., Zachary, D., Holder, F., and Meister, M.** (2001). Postembryonic hematopoiesis in *Drosophila*. *Dev Biol* *230*, 243-257.
- Le Borgne, R., Bardin, A., and Schweisguth, F.** (2005). The roles of receptor and ligand endocytosis in regulating Notch signaling. *Development* *132*, 1751-1762.

D References

- Lecuyer, E., Parthasarathy, N., and Krause, H.M.** (2008). Fluorescent in situ hybridization protocols in *Drosophila* embryos and tissues. *Methods Mol Biol* *420*, 289-302.
- Lee, C.Y., Andersen, R.O., Cabernard, C., Manning, L., Tran, K.D., Lanskey, M.J., Bashirullah, A., and Doe, C.Q.** (2006a). *Drosophila* Aurora-A kinase inhibits neuroblast self-renewal by regulating aPKC/Numb cortical polarity and spindle orientation. *Genes Dev* *20*, 3464-3474.
- Lee, C.Y., Robinson, K.J., and Doe, C.Q.** (2006b). Lgl, Pins and aPKC regulate neuroblast self-renewal versus differentiation. *Nature* *439*, 594-598.
- Lee, C.Y., Wilkinson, B.D., Siegrist, S.E., Wharton, R.P., and Doe, C.Q.** (2006c). Brat is a Miranda cargo protein that promotes neuronal differentiation and inhibits neuroblast self-renewal. *Dev Cell* *10*, 441-449.
- Lee, T., and Luo, L.** (2001). Mosaic analysis with a repressible cell marker (MARCM) for *Drosophila* neural development. *Trends Neurosci* *24*, 251-254.
- Lee, W.J., Lee, J.D., Kravchenko, V.V., Ulevitch, R.J., and Brey, P.T.** (1996). Purification and molecular cloning of an inducible gram-negative bacteria-binding protein from the silkworm, *Bombyx mori*. *Proc Natl Acad Sci U S A* *93*, 7888-7893.
- Lehman, K., Rossi, G., Adamo, J.E., and Brennwald, P.** (1999). Yeast homologues of tomosyn and lethal giant larvae function in exocytosis and are associated with the plasma membrane SNARE, Sec9. *J Cell Biol* *146*, 125-140.
- Leibfried, A., and Bellaiche, Y.** (2007). Functions of endosomal trafficking in *Drosophila* epithelial cells. *Curr Opin Cell Biol* *19*, 446-452.
- Leitinger, B., McDowall, A., Stanley, P., and Hogg, N.** (2000). The regulation of integrin function by Ca²⁺. *Biochim Biophys Acta* *1498*, 91-98.
- Lemaitre, B., Reichhart, J.M., and Hoffmann, J.A.** (1997). *Drosophila* host defense: differential induction of antimicrobial peptide genes after infection by various classes of microorganisms. *Proc Natl Acad Sci U S A* *94*, 14614-14619.
- Leulier, F., Rodriguez, A., Khush, R.S., Abrams, J.M., and Lemaitre, B.** (2000). The *Drosophila* caspase Dredd is required to resist gram-negative bacterial infection. *EMBO Rep* *1*, 353-358.
- Ligoxygakis, P., Pelte, N., Hoffmann, J.A., and Reichhart, J.M.** (2002). Activation of *Drosophila* Toll during fungal infection by a blood serine protease. *Science* *297*, 114-116.
- Lindebro, M.C., Poellinger, L., and Whitelaw, M.L.** (1995). Protein-protein interaction via PAS domains: role of the PAS domain in positive and negative regulation of the bHLH/PAS dioxin receptor-Arnt transcription factor complex. *EMBO J* *14*, 3528-3539.
- Lipschutz, J.H., Guo, W., O'Brien, L.E., Nguyen, Y.H., Novick, P., and Mostov, K.E.** (2000). Exocyst is involved in cystogenesis and tubulogenesis and acts by modulating synthesis and delivery of basolateral plasma membrane and secretory proteins. *Mol Biol Cell* *11*, 4259-4275.

- Lipschutz, J.H., and Mostov, K.E.** (2002). Exocytosis: the many masters of the exocyst. *Curr Biol* *12*, R212-214.
- Lloyd, T.E., Atkinson, R., Wu, M.N., Zhou, Y., Pennetta, G., and Bellen, H.J.** (2002). Hrs Regulates Endosome Membrane Invagination and Tyrosine Kinase Receptor Signaling in *Drosophila*. *Cell* *108*, 261-269.
- Locke, M.** (2001). The Wigglesworth Lecture: Insects for studying fundamental problems in biology. *J Insect Physiol* *47*, 495-507.
- Lu, B., Rothenberg, M., Jan, L.Y., and Jan, Y.N.** (1998). Partner of Numb colocalizes with Numb during mitosis and directs Numb asymmetric localization in *Drosophila* neural and muscle progenitors. *Cell* *95*, 225-235.
- Lu, H., and Bilder, D.** (2005). Endocytic control of epithelial polarity and proliferation in *Drosophila*. *Nat Cell Biol* *7*, 1232-1239.
- Lu, Y., Wu, L.P., and Anderson, K.V.** (2001). The antibacterial arm of the *drosophila* innate immune response requires an IkappaB kinase. *Genes Dev* *15*, 104-110.
- Luan, H., Lemon, W.C., Peabody, N.C., Pohl, J.B., Zelensky, P.K., Wang, D., Nitabach, M.N., Holmes, T.C., and White, B.H.** (2006). Functional dissection of a neuronal network required for cuticle tanning and wing expansion in *Drosophila*. *J Neurosci* *26*, 573-584.
- Luo, C.W., Dewey, E.M., Sudo, S., Ewer, J., Hsu, S.Y., Honegger, H.W., and Hsueh, A.J.** (2005). Bursicon, the insect cuticle-hardening hormone, is a heterodimeric cystine knot protein that activates G protein-coupled receptor LGR2. *Proc Natl Acad Sci U S A* *102*, 2820-2825.
- Maley, F., Trimble, R.B., Tarentino, A.L., and Plummer, T.H., Jr.** (1989). Characterization of glycoproteins and their associated oligosaccharides through the use of endoglycosidases. *Anal Biochem* *180*, 195-204.
- Margolis, B., and Borg, J.P.** (2005). Apicobasal polarity complexes. *J Cell Sci* *118*, 5157-5159.
- Matern, H.T., Yeaman, C., Nelson, W.J., and Scheller, R.H.** (2001). The Sec6/8 complex in mammalian cells: characterization of mammalian Sec3, subunit interactions, and expression of subunits in polarized cells. *Proc Natl Acad Sci U S A* *98*, 9648-9653.
- Matsuzaki, F., Ohshiro, T., Ikeshima-Kataoka, H., and Izumi, H.** (1998). miranda localizes staufer and prospero asymmetrically in mitotic neuroblasts and epithelial cells in early *Drosophila* embryogenesis. *Development* *125*, 4089-4098.
- McCartney, B.M., Dierick, H.A., Kirkpatrick, C., Moline, M.M., Baas, A., Peifer, M., and Bejsovec, A.** (1999). *Drosophila* APC2 is a cytoskeletally-associated protein that regulates wingless signaling in the embryonic epidermis [In Process Citation]. *J Cell Biol* *146*, 1303-1318.
- McLysaght, A., Hokamp, K., and Wolfe, K.H.** (2002). Extensive genomic duplication

D References

during early chordate evolution. *Nat Genet* 31, 200-204.

McNabb, S.L., Baker, J.D., Agapite, J., Steller, H., Riddiford, L.M., and Truman, J.W. (1997). Disruption of a behavioral sequence by targeted death of peptidergic neurons in *Drosophila*. *Neuron* 19, 813-823.

Mehta, S.Q., Hiesinger, P.R., Beronja, S., Zhai, R.G., Schulze, K.L., Verstreken, P., Cao, Y., Zhou, Y., Tepass, U., Crair, M.C., et al. (2005). Mutations in *Drosophila* *sec15* reveal a function in neuronal targeting for a subset of exocyst components. *Neuron* 46, 219-232.

Meister, M., Hetru, C., and Hoffmann, J.A. (2000). The antimicrobial host defense of *Drosophila*. *Curr Top Microbiol Immunol* 248, 17-36.

Mellman, I., and Nelson, W.J. (2008). Coordinated protein sorting, targeting and distribution in polarized cells. *Nat Rev Mol Cell Biol* 9, 833-845.

Mendive, F.M., Van Loy, T., Claeysen, S., Poels, J., Williamson, M., Hauser, F., Grimmlikhuijzen, C.J., Vassart, G., and Vanden Broeck, J. (2005). *Drosophila* molting neurohormone bursicon is a heterodimer and the natural agonist of the orphan receptor DLGR2. *FEBS Lett* 579, 2171-2176.

Meng, X., Khanuja, B.S., and Ip, Y.T. (1999). Toll receptor-mediated *Drosophila* immune response requires Dif, an NF-kappaB factor. *Genes Dev* 13, 792-797.

Mettlen, M., Pucadyil, T., Ramachandran, R., and Schmid, S.L. (2009). Dissecting dynamin's role in clathrin-mediated endocytosis. *Biochem Soc Trans* 37, 1022-1026.

Michel, T., Reichhart, J.M., Hoffmann, J.A., and Royet, J. (2001). *Drosophila* Toll is activated by Gram-positive bacteria through a circulating peptidoglycan recognition protein. *Nature* 414, 756-759.

Moberg, K.H., Schelble, S., Burdick, S.K., and Hariharan, I.K. (2005). Mutations in *erupted*, the *Drosophila* ortholog of mammalian tumor susceptibility gene 101, elicit non-cell-autonomous overgrowth. *Dev Cell* 9, 699-710.

Morais-de-Sa, E., Mirouse, V., and St Johnston, D. (2010). aPKC phosphorylation of Bazooka defines the apical/lateral border in *Drosophila* epithelial cells. *Cell* 141, 509-523.

Mostov, K., Su, T., and ter Beest, M. (2003). Polarized epithelial membrane traffic: conservation and plasticity. *Nat Cell Biol* 5, 287-293.

Moussian, B., and Roth, S. (2005). Dorsoventral axis formation in the *Drosophila* embryo--shaping and transducing a morphogen gradient. *Curr Biol* 15, R887-899.

Muller, H.A. (2008). Immunolabeling of embryos. *Methods Mol Biol* 420, 207-218.

Müller, H.A., and Wieschaus, E. (1996). *armadillo*, *bazooka*, and *stardust* are critical for early stages in formation of the zonula adherens and maintenance of the polarized blastoderm epithelium in *Drosophila*. *J Cell Biol* 134, 149-163.

Munson, M., and Novick, P. (2006). The exocyst defrocked, a framework of rods revealed.

Nat Struct Mol Biol *13*, 577-581.

Murthy, M., Garza, D., Scheller, R.H., and Schwarz, T.L. (2003). Mutations in the exocyst component Sec5 disrupt neuronal membrane traffic, but neurotransmitter release persists. *Neuron* *37*, 433-447.

Murthy, M., Ranjan, R., Deneff, N., Higashi, M.E., Schupbach, T., and Schwarz, T.L. (2005). Sec6 mutations and the *Drosophila* exocyst complex. *J Cell Sci* *118*, 1139-1150.

Murthy, M., and Schwarz, T.L. (2004). The exocyst component Sec5 is required for membrane traffic and polarity in the *Drosophila* ovary. *Development* *131*, 377-388.

Naitza, S., Rosse, C., Kappler, C., Georgel, P., Belvin, M., Gubb, D., Camonis, J., Hoffmann, J.A., and Reichhart, J.M. (2002). The *Drosophila* immune defense against gram-negative infection requires the death protein dFADD. *Immunity* *17*, 575-581.

Natzle, J.E., Kiger, J.A., Jr., and Green, M.M. (2008). Bursicon signaling mutations separate the epithelial-mesenchymal transition from programmed cell death during *Drosophila* melanogaster wing maturation. *Genetics* *180*, 885-893.

Nelson, W.J. (2003). Adaptation of core mechanisms to generate cell polarity. *Nature* *422*, 766-774.

Neuhoff, V., Arold, N., Taube, D., and Ehrhardt, W. (1988). Improved staining of proteins in polyacrylamide gels including isoelectric focusing gels with clear background at nanogram sensitivity using Coomassie Brilliant Blue G-250 and R-250. *Electrophoresis* *9*, 255-262.

Nipper, R.W., Siller, K.H., Smith, N.R., Doe, C.Q., and Prehoda, K.E. (2007). Galphai generates multiple Pins activation states to link cortical polarity and spindle orientation in *Drosophila* neuroblasts. *Proc Natl Acad Sci U S A* *104*, 14306-14311.

Novick, P., Field, C., and Schekman, R. (1980). Identification of 23 complementation groups required for post-translational events in the yeast secretory pathway. *Cell* *21*, 205-215.

Oda, H., Uemura, T., Harada, Y., Iwai, Y., and Takeichi, M. (1994). A *Drosophila* homolog of cadherin associated with armadillo and essential for embryonic cell-cell adhesion. *Dev Biol* *165*, 716-726.

Ohshiro, T., Yagami, T., Zhang, C., and Matsuzaki, F. (2000). Role of cortical tumour-suppressor proteins in asymmetric division of *Drosophila* neuroblast. *Nature* *408*, 593-596.

Park, J.H., Schroeder, A.J., Helfrich-Forster, C., Jackson, F.R., and Ewer, J. (2003). Targeted ablation of CCAP neuropeptide-containing neurons of *Drosophila* causes specific defects in execution and circadian timing of ecdysis behavior. *Development* *130*, 2645-2656.

Park, Y., Filippov, V., Gill, S.S., and Adams, M.E. (2002). Deletion of the ecdysis-triggering hormone gene leads to lethal ecdysis deficiency. *Development* *129*, 493-503.

Parnas, D., Haghghi, A.P., Fetter, R.D., Kim, S.W., and Goodman, C.S. (2001). Regulation of postsynaptic structure and protein localization by the Rho-type guanine nucleotide exchange factor dPix. *Neuron* *32*, 415-424.

- Peabody, N.C., Diao, F., Luan, H., Wang, H., Dewey, E.M., Honegger, H.W., and White, B.H.** (2008). Bursicon functions within the *Drosophila* CNS to modulate wing expansion behavior, hormone secretion, and cell death. *J Neurosci* 28, 14379-14391.
- Pearson, A.M., Baksa, K., Ramet, M., Protas, M., McKee, M., Brown, D., and Ezekowitz, R.A.** (2003). Identification of cytoskeletal regulatory proteins required for efficient phagocytosis in *Drosophila*. *Microbes Infect* 5, 815-824.
- Peng, C.Y., Manning, L., Albertson, R., and Doe, C.Q.** (2000). The tumour-suppressor genes *lgl* and *dlg* regulate basal protein targeting in *Drosophila* neuroblasts. *Nature* 408, 596-600.
- Petritsch, C., Tavosanis, G., Turck, C.W., Jan, L.Y., and Jan, Y.N.** (2003). The *Drosophila* myosin VI *Jaguar* is required for basal protein targeting and correct spindle orientation in mitotic neuroblasts. *Dev Cell* 4, 273-281.
- Petronczki, M., and Knoblich, J.A.** (2001). *DmPAR-6* directs epithelial polarity and asymmetric cell division of neuroblasts in *Drosophila*. *Nat Cell Biol* 3, 43-49.
- Pili-Floury, S., Leulier, F., Takahashi, K., Saigo, K., Samain, E., Ueda, R., and Lemaitre, B.** (2004). In vivo RNA interference analysis reveals an unexpected role for GGBP1 in the defense against Gram-positive bacterial infection in *Drosophila* adults. *J Biol Chem* 279, 12848-12853.
- Plant, P.J., Fawcett, J.P., Lin, D.C., Holdorf, A.D., Binns, K., Kulkarni, S., and Pawson, T.** (2003). A polarity complex of *mPar-6* and atypical PKC binds, phosphorylates and regulates mammalian *Lgl*. *Nat Cell Biol* 5, 301-308.
- Ponting, C.P., and Aravind, L.** (1997). PAS: a multifunctional domain family comes to light. *Curr Biol* 7, R674-677.
- Poodry, C.A.** (1990). *shibire*, a neurogenic mutant of *Drosophila*. *Dev Biol* 138, 464-472.
- Prehoda, K.E.** (2009). Polarization of *Drosophila* neuroblasts during asymmetric division. *Cold Spring Harb Perspect Biol* 1, a001388.
- Prigent, M., Dubois, T., Raposo, G., Derrien, V., Tenza, D., Rosse, C., Camonis, J., and Chavrier, P.** (2003). ARF6 controls post-endocytic recycling through its downstream exocyst complex effector. *J Cell Biol* 163, 1111-1121.
- Qin, H., Percival-Smith, A., Li, C., Jia, C.Y., Gloor, G., and Li, S.S.** (2004). A novel transmembrane protein recruits *numb* to the plasma membrane during asymmetric cell division. *J Biol Chem* 279, 11304-11312.
- Rebollo, E., Roldan, M., and Gonzalez, C.** (2009). Spindle alignment is achieved without rotation after the first cell cycle in *Drosophila* embryonic neuroblasts. *Development* 136, 3393-3397.
- Rhyu, M.S., Jan, L.Y., and Jan, Y.N.** (1994). Asymmetric distribution of *numb* protein during division of the sensory organ precursor cell confers distinct fates to daughter cells. *Cell*

76, 477-491.

Riddiford, L.M. (1993). Hormone receptors and the regulation of insect metamorphosis. *Receptor* 3, 203-209.

Rizki, R.M., and Rizki, T.M. (1984). Selective destruction of a host blood cell type by a parasitoid wasp. *Proc Natl Acad Sci U S A* 81, 6154-6158.

Robertson, H.M., Navik, J.A., Walden, K.K., and Honegger, H.W. (2007). The bursicon gene in mosquitoes: an unusual example of mRNA trans-splicing. *Genetics* 176, 1351-1353.

Robinson, M.S. (1994). The role of clathrin, adaptors and dynamin in endocytosis. *Curr Opin Cell Biol* 6, 538-544.

Rodriguez-Boulan, E., Kreitzer, G., and Musch, A. (2005). Organization of vesicular trafficking in epithelia. *Nat Rev Mol Cell Biol* 6, 233-247.

Rolls, M.M., Albertson, R., Shih, H.P., Lee, C.Y., and Doe, C.Q. (2003). Drosophila aPKC regulates cell polarity and cell proliferation in neuroblasts and epithelia. *J Cell Biol* 163, 1089-1098.

Rutschmann, S., Jung, A.C., Hetru, C., Reichhart, J.M., Hoffmann, J.A., and Ferrandon, D. (2000a). The Rel protein DIF mediates the antifungal but not the antibacterial host defense in Drosophila. *Immunity* 12, 569-580.

Rutschmann, S., Jung, A.C., Zhou, R., Silverman, N., Hoffmann, J.A., and Ferrandon, D. (2000b). Role of Drosophila IKK gamma in a toll-independent antibacterial immune response. *Nat Immunol* 1, 342-347.

Sans, N., Prybylowski, K., Petralia, R.S., Chang, K., Wang, Y.X., Racca, C., Vicini, S., and Wenthold, R.J. (2003). NMDA receptor trafficking through an interaction between PDZ proteins and the exocyst complex. *Nat Cell Biol* 5, 520-530.

Schaefer, M., Petronczki, M., Dorner, D., Forte, M., and Knoblich, J.A. (2001). Heterotrimeric G proteins direct two modes of asymmetric cell division in the Drosophila nervous system. *Cell* 107, 183-194.

Schaefer, M., Shevchenko, A., and Knoblich, J.A. (2000). A protein complex containing Inscuteable and the Galpha-binding protein Pins orients asymmetric cell divisions in Drosophila. *Curr Biol* 10, 353-362.

Scheiffele, P., Peranen, J., and Simons, K. (1995). N-glycans as apical sorting signals in epithelial cells. *Nature* 378, 96-98.

Schmucker, D., Clemens, J.C., Shu, H., Worby, C.A., Xiao, J., Muda, M., Dixon, J.E., and Zipursky, S.L. (2000). Drosophila Dscam is an axon guidance receptor exhibiting extraordinary molecular diversity. *Cell* 101, 671-684.

Schober, M., Schaefer, M., and Knoblich, J.A. (1999). Bazooka recruits Inscuteable to orient asymmetric cell divisions in Drosophila neuroblasts. *Nature* 402, 548-551.

D References

- Schuck, S., and Simons, K.** (2004). Polarized sorting in epithelial cells: raft clustering and the biogenesis of the apical membrane. *J Cell Sci* *117*, 5955-5964.
- Schuldt, A.J., Adams, J.H., Davidson, C.M., Micklem, D.R., Haseloff, J., St Johnston, D., and Brand, A.H.** (1998). Miranda mediates asymmetric protein and RNA localization in the developing nervous system. *Genes Dev* *12*, 1847-1857.
- Schultz, J., Milpetz, F., Bork, P., and Ponting, C.P.** (1998). SMART, a simple modular architecture research tool: identification of signaling domains. *Proc Natl Acad Sci U S A* *95*, 5857-5864.
- Schweisguth, F.** (2004). Regulation of notch signaling activity. *Curr Biol* *14*, R129-138.
- Shen, C.P., Jan, L.Y., and Jan, Y.N.** (1997). Miranda is required for the asymmetric localization of Prospero during mitosis in *Drosophila*. *Cell* *90*, 449-458.
- Siegrist, S.E., and Doe, C.Q.** (2006). Extrinsic cues orient the cell division axis in *Drosophila* embryonic neuroblasts. *Development* *133*, 529-536.
- Siegrist, S.E., and Doe, C.Q.** (2005). Microtubule-induced Pins/Galphai cortical polarity in *Drosophila* neuroblasts. *Cell* *123*, 1323-1335.
- Siller, K.H., Cabernard, C., and Doe, C.Q.** (2006). The NuMA-related Mud protein binds Pins and regulates spindle orientation in *Drosophila* neuroblasts. *Nat Cell Biol* *8*, 594-600.
- Silverman, N., Zhou, R., Stoven, S., Pandey, N., Hultmark, D., and Maniatis, T.** (2000). A *Drosophila* IkappaB kinase complex required for Relish cleavage and antibacterial immunity. *Genes Dev* *14*, 2461-2471.
- Slack, C., Overton, P.M., Tuxworth, R.I., and Chia, W.** (2007). Asymmetric localisation of Miranda and its cargo proteins during neuroblast division requires the anaphase-promoting complex/cyclosome. *Development* *134*, 3781-3787.
- Slack, C., Somers, W.G., Sousa-Nunes, R., Chia, W., and Overton, P.M.** (2006). A mosaic genetic screen for novel mutations affecting *Drosophila* neuroblast divisions. *BMC Genet* *7*, 33.
- Slack, F.J., and Ruvkun, G.** (1998). A novel repeat domain that is often associated with RING finger and B-box motifs. *Trends Biochem Sci* *23*, 474-475.
- Smith, C.A., Lau, K.M., Rahmani, Z., Dho, S.E., Brothers, G., She, Y.M., Berry, D.M., Bonneil, E., Thibault, P., Schweisguth, F., et al.** (2007). aPKC-mediated phosphorylation regulates asymmetric membrane localization of the cell fate determinant Numb. *EMBO J* *26*, 468-480.
- Spana, E.P., and Doe, C.Q.** (1995). The prospero transcription factor is asymmetrically localized to the cell cortex during neuroblast mitosis in *Drosophila*. *Development* *121*, 3187-3195.
- Springer, T.A.** (1997). Folding of the N-terminal, ligand-binding region of integrin alpha-subunits into a beta-propeller domain. *Proc Natl Acad Sci U S A* *94*, 65-72.

- Stoven, S., Ando, I., Kadalayil, L., Engstrom, Y., and Hultmark, D.** (2000). Activation of the *Drosophila* NF-kappaB factor Relish by rapid endoproteolytic cleavage. *EMBO Rep* 1, 347-352.
- Stroschein-Stevenson, S.L., Foley, E., O'Farrell, P.H., and Johnson, A.D.** (2006). Identification of *Drosophila* gene products required for phagocytosis of *Candida albicans*. *PLoS Biol* 4, e4.
- Stuart, L.M., Boulais, J., Charriere, G.M., Hennessy, E.J., Brunet, S., Jutras, I., Goyette, G., Rondeau, C., Letarte, S., Huang, H., et al.** (2007). A systems biology analysis of the *Drosophila* phagosome. *Nature* 445, 95-101.
- Stuart, L.M., and Ezekowitz, R.A.** (2008). Phagocytosis and comparative innate immunity: learning on the fly. *Nat Rev Immunol* 8, 131-141.
- Sudo, S., Avsian-Kretchmer, O., Wang, L.S., and Hsueh, A.J.** (2004). Protein related to DAN and cerberus is a bone morphogenetic protein antagonist that participates in ovarian paracrine regulation. *J Biol Chem* 279, 23134-23141.
- Sun, H., Bristow, B.N., Qu, G., and Wasserman, S.A.** (2002). A heterotrimeric death domain complex in Toll signaling. *Proc Natl Acad Sci U S A* 99, 12871-12876.
- Sun, H., Towb, P., Chiem, D.N., Foster, B.A., and Wasserman, S.A.** (2004). Regulated assembly of the Toll signaling complex drives *Drosophila* dorsoventral patterning. *EMBO J* 23, 100-110.
- Sung, C., Wong, L.E., Chang Sen, L.Q., Nguyen, E., Lazaga, N., Ganzer, G., McNabb, S.L., and Robinow, S.** (2009). The unfulfilled/DHR51 gene of *Drosophila melanogaster* modulates wing expansion and fertility. *Dev Dyn* 238, 171-182.
- Suzuki, A., and Ohno, S.** (2006). The PAR-aPKC system: lessons in polarity. *J Cell Sci* 119, 979-987.
- Takehana, A., Katsuyama, T., Yano, T., Oshima, Y., Takada, H., Aigaki, T., and Kurata, S.** (2002). Overexpression of a pattern-recognition receptor, peptidoglycan-recognition protein-LE, activates imd/relish-mediated antibacterial defense and the prophenoloxidase cascade in *Drosophila* larvae. *Proc Natl Acad Sci U S A* 99, 13705-13710.
- Takehana, A., Yano, T., Mita, S., Kotani, A., Oshima, Y., and Kurata, S.** (2004). Peptidoglycan recognition protein (PGRP)-LE and PGRP-LC act synergistically in *Drosophila* immunity. *EMBO J* 23, 4690-4700.
- Takei, K., and Haucke, V.** (2001). Clathrin-mediated endocytosis: membrane factors pull the trigger. *Trends Cell Biol* 11, 385-391.
- Tanaka, T., and Nakamura, A.** (2008). The endocytic pathway acts downstream of Oskar in *Drosophila* germ plasm assembly. *Development* 135, 1107-1117.
- Tanentzopf, G., and Tepass, U.** (2003). Interactions between the crumbs, lethal giant larvae and bazooka pathways in epithelial polarization. *Nat Cell Biol* 5, 46-52.

- Tauszig, S., Jouanguy, E., Hoffmann, J.A., and Imler, J.L.** (2000). Toll-related receptors and the control of antimicrobial peptide expression in *Drosophila*. *Proc Natl Acad Sci U S A* *97*, 10520-10525.
- Tepass, U., Tanentzapf, G., Ward, R., and Fehon, R.** (2001). Epithelial cell polarity and cell junctions in *Drosophila*. *Annu Rev Genet* *35*, 747-784.
- Tepass, U., Theres, C., and Knust, E.** (1990). crumbs encodes an EGF-like protein expressed on apical membranes of *Drosophila* epithelial cells and required for organization of epithelia. *Cell* *61*, 787-799.
- Thompson, B.J., Mathieu, J., Sung, H.H., Loeser, E., Rorth, P., and Cohen, S.M.** (2005). Tumor suppressor properties of the ESCRT-II complex component Vps25 in *Drosophila*. *Dev Cell* *9*, 711-720.
- Togel, M., Pass, G., and Paululat, A.** (2008). The *Drosophila* wing hearts originate from pericardial cells and are essential for wing maturation. *Dev Biol* *318*, 29-37.
- Truman, J.W.** (1996). Ecdysis control sheds another layer. *Science* *271*, 40-41.
- Truman, J.W., and Bate, M.** (1988). Spatial and temporal patterns of neurogenesis in the central nervous system of *Drosophila melanogaster*. *Dev Biol* *125*, 145-157.
- Tzou, P., De Gregorio, E., and Lemaitre, B.** (2002a). How *Drosophila* combats microbial infection: a model to study innate immunity and host-pathogen interactions. *Curr Opin Microbiol* *5*, 102-110.
- Tzou, P., Reichhart, J.M., and Lemaitre, B.** (2002b). Constitutive expression of a single antimicrobial peptide can restore wild-type resistance to infection in immunodeficient *Drosophila* mutants. *Proc Natl Acad Sci U S A* *99*, 2152-2157.
- Uemura, T., Shepherd, S., Ackerman, L., Jan, L.Y., and Jan, Y.N.** (1989). numb, a gene required in determination of cell fate during sensory organ formation in *Drosophila* embryos. *Cell* *58*, 349-360.
- Uvila, J., Parikka, M., Kleino, A., Sormunen, R., Ezekowitz, R.A., Kocks, C., and Ramet, M.** (2006). Double-stranded RNA is internalized by scavenger receptor-mediated endocytosis in *Drosophila* S2 cells. *J Biol Chem* *281*, 14370-14375.
- Vaccari, T., and Bilder, D.** (2005). The *Drosophila* tumor suppressor vps25 prevents nonautonomous overproliferation by regulating notch trafficking. *Dev Cell* *9*, 687-698.
- Vaessin, H., Grell, E., Wolff, E., Bier, E., Jan, L.Y., and Jan, Y.N.** (1991). prospero is expressed in neuronal precursors and encodes a nuclear protein that is involved in the control of axonal outgrowth in *Drosophila*. *Cell* *67*, 941-953.
- van der Blik, A.M., and Meyerowitz, E.M.** (1991). Dynamin-like protein encoded by the *Drosophila* shibire gene associated with vesicular traffic. *Nature* *351*, 411-414.
- Van Loy, T., Van Hiel, M.B., Vandersmissen, H.P., Poels, J., Mendive, F., Vassart, G., and**

- Vanden Broeck, J.** (2007). Evolutionary conservation of bursicon in the animal kingdom. *Gen Comp Endocrinol* *153*, 59-63.
- Van Loy, T., Vandersmissen, H.P., Van Hiel, M.B., Poels, J., Verlinden, H., Badisco, L., Vassart, G., and Vanden Broeck, J.** (2008). Comparative genomics of leucine-rich repeats containing G protein-coupled receptors and their ligands. *Gen Comp Endocrinol* *155*, 14-21.
- Vega, I.E., and Hsu, S.C.** (2001). The exocyst complex associates with microtubules to mediate vesicle targeting and neurite outgrowth. *J Neurosci* *21*, 3839-3848.
- Vie, A., Cigna, M., Toci, R., and Birman, S.** (1999). Differential regulation of *Drosophila* tyrosine hydroxylase isoforms by dopamine binding and cAMP-dependent phosphorylation. *J Biol Chem* *274*, 16788-16795.
- Wang, H., Ouyang, Y., Somers, W.G., Chia, W., and Lu, B.** (2007). Polo inhibits progenitor self-renewal and regulates Numb asymmetry by phosphorylating Pon. *Nature* *449*, 96-100.
- Wang, H., Somers, G.W., Bashirullah, A., Heberlein, U., Yu, F., and Chia, W.** (2006a). Aurora-A acts as a tumor suppressor and regulates self-renewal of *Drosophila* neuroblasts. *Genes Dev* *20*, 3453-3463.
- Wang, L., Weber, A.N., Atilano, M.L., Filipe, S.R., Gay, N.J., and Ligoxygakis, P.** (2006b). Sensing of Gram-positive bacteria in *Drosophila*: GGBP1 is needed to process and present peptidoglycan to PGRP-SA. *EMBO J* *25*, 5005-5014.
- Watson, F.L., Puttmann-Holgado, R., Thomas, F., Lamar, D.L., Hughes, M., Kondo, M., Rebel, V.I., and Schmucker, D.** (2005). Extensive diversity of Ig-superfamily proteins in the immune system of insects. *Science* *309*, 1874-1878.
- Weber, A.N., Tauszig-Delamasure, S., Hoffmann, J.A., Lelievre, E., Gascan, H., Ray, K.P., Morse, M.A., Imler, J.L., and Gay, N.J.** (2003). Binding of the *Drosophila* cytokine Spatzle to Toll is direct and establishes signaling. *Nat Immunol* *4*, 794-800.
- Wei, S.Y., Escudero, L.M., Yu, F., Chang, L.H., Chen, L.Y., Ho, Y.H., Lin, C.M., Chou, C.S., Chia, W., Modolell, J., et al.** (2005). Echinoid is a component of adherens junctions that cooperates with DE-Cadherin to mediate cell adhesion. *Dev Cell* *8*, 493-504.
- White, K., and Kankel, D.R.** (1978). Patterns of cell division and cell movement in the formation of the imaginal nervous system in *Drosophila melanogaster*. *Dev Biol* *65*, 296-321.
- Wilcockson, D.C., and Webster, S.G.** (2008). Identification and developmental expression of mRNAs encoding putative insect cuticle hardening hormone, bursicon in the green shore crab *Carcinus maenas*. *Gen Comp Endocrinol* *156*, 113-125.
- Williams, M.J.** (2007). *Drosophila* hemopoiesis and cellular immunity. *J Immunol* *178*, 4711-4716.
- Wodarz, A.** (2008). Extraction and immunoblotting of proteins from embryos. *Methods Mol Biol* *420*, 335-345.
- Wodarz, A.** (2005). Molecular control of cell polarity and asymmetric cell division in

D References

Drosophila neuroblasts. *Curr Opin Cell Biol* 17, 475-481.

Wodarz, A., Hinz, U., Engelbert, M., and Knust, E. (1995). Expression of crumbs confers apical character on plasma membrane domains of ectodermal epithelia of Drosophila. *Cell* 82, 67-76.

Wodarz, A., and Huttner, W.B. (2003). Asymmetric cell division during neurogenesis in Drosophila and vertebrates. *Mech Dev* 120, 1297-1309.

Wodarz, A., Ramrath, A., Grimm, A., and Knust, E. (2000). Drosophila atypical protein kinase C associates with Bazooka and controls polarity of epithelia and neuroblasts. *J Cell Biol* 150, 1361-1374.

Wodarz, A., Ramrath, A., Kuchinke, U., and Knust, E. (1999). Bazooka provides an apical cue for Inscuteable localization in Drosophila neuroblasts. *Nature* 402, 544-547.

Wu, H., Rossi, G., and Brennwald, P. (2008). The ghost in the machine: small GTPases as spatial regulators of exocytosis. *Trends Cell Biol* 18, 397-404.

Wu, J.S., and Luo, L. (2006). A protocol for mosaic analysis with a repressible cell marker (MARCM) in Drosophila. *Nat Protoc* 1, 2583-2589.

Wu, L.P., and Anderson, K.V. (1998). Regulated nuclear import of Rel proteins in the Drosophila immune response. *Nature* 392, 93-97.

Wucherpfennig, T., Wilsch-Brauninger, M., and Gonzalez-Gaitan, M. (2003). Role of Drosophila Rab5 during endosomal trafficking at the synapse and evoked neurotransmitter release. *J Cell Biol* 161, 609-624.

Yamanaka, T., Horikoshi, Y., Sugiyama, Y., Ishiyama, C., Suzuki, A., Hirose, T., Iwamatsu, A., Shinohara, A., and Ohno, S. (2003). Mammalian Lgl forms a protein complex with PAR-6 and aPKC independently of PAR-3 to regulate epithelial cell polarity. *Curr Biol* 13, 734-743.

Yoshida, H., Kinoshita, K., and Ashida, M. (1996). Purification of a peptidoglycan recognition protein from hemolymph of the silkworm, *Bombyx mori*. *J Biol Chem* 271, 13854-13860.

Yu, F., Morin, X., Cai, Y., Yang, X., and Chia, W. (2000). Analysis of partner of inscuteable, a novel player of Drosophila asymmetric divisions, reveals two distinct steps in inscuteable apical localization. *Cell* 100, 399-409.

Yu, F., Wang, H., Qian, H., Kaushik, R., Bownes, M., Yang, X., and Chia, W. (2005). Locomotion defects, together with Pins, regulates heterotrimeric G-protein signaling during Drosophila neuroblast asymmetric divisions. *Genes Dev* 19, 1341-1353.

Zettervall, C.J., Anderl, I., Williams, M.J., Palmer, R., Kurucz, E., Ando, I., and Hultmark, D. (2004). A directed screen for genes involved in Drosophila blood cell activation. *Proc Natl Acad Sci U S A* 101, 14192-14197.

Zhang, X., Wang, P., Gangar, A., Zhang, J., Brennwald, P., TerBush, D., and Guo, W.

(2005). Lethal giant larvae proteins interact with the exocyst complex and are involved in polarized exocytosis. *J Cell Biol* 170, 273-283.

Zhao, T., Gu, T., Rice, H.C., McAdams, K.L., Roark, K.M., Lawson, K., Gauthier, S.A., Reagan, K.L., and Hewes, R.S. (2008). A *Drosophila* gain-of-function screen for candidate genes involved in steroid-dependent neuroendocrine cell remodeling. *Genetics* 178, 883-901.

Zhong, W., and Chia, W. (2008). Neurogenesis and asymmetric cell division. *Curr Opin Neurobiol* 18, 4-11.

Zhou, R., Silverman, N., Hong, M., Liao, D.S., Chung, Y., Chen, Z.J., and Maniatis, T. (2005). The role of ubiquitination in *Drosophila* innate immunity. *J Biol Chem* 280, 34048-34055.

Danksagung

Herzlich bedanken möchte ich mich bei Prof. Dr. Andreas Wodarz, unter dessen Anleitung diese Arbeit angefertigt wurde. Seine Betreuung und ständige Ansprechbarkeit haben sehr zum Gelingen dieser Arbeit beigetragen. Ich möchte mich bei ihm auch für die gute Arbeitsatmosphäre und für die Möglichkeit zur Teilnahme an wissenschaftlichen Konferenzen bedanken.

Herrn Prof. Dr. Ernst Wimmer danke ich für die bereitwillige Übernahme des Zweitgutachtens und zahlreiche hilfreiche Kommentare bei meinen Fortschrittsberichten.

Ich danke auch Herrn Dr. Olaf Jahn für die massenspektrometrische Analysen und Prof. Bruno Lemaitre für die Durchführung der Tests zur humoralen Immunität.

Ein großes Dankeschön geht an alle „Stammzellen“:

Ich danke Tobi für den großartigen Polymerase Song, der es eines Tages noch bis zur Grand Prix Endauscheidung schaffen wird, Gang für seine Gelassenheit und witzigen, staubtrockenen Kommentare, Mona für ihre immense Hilfe während meiner Doktorarbeit und die Bereitschaft zu meist nicht all zuerst gemeinten ermahnenenden Worten, Hamze für gute Laune, die tollste Frisur der gesamten Abteilung und spaßige Gitarrensessions, Ieva für ihr unverkennbares Lachen und gelegentliche gedankliche Ausflüge in die unendlichen Weiten des Absurden, Michael für das Aushelfen mit Fiegenstocks, Katja für kuriose Einfälle und die Erweiterung meines Laborjargon Fachvokabulars, Sascha für coole Sprüche auf dem Fliegenkisten, Claudia für ihre enorme Unterstützung durch ihre Arbeit, Patricia für ihre preußische Art, Engagement und Hilfsbereitschaft, Carmen für unglaublich schnell gesprochen Sätze und Soya für ihren Optimismus und echte wissenschaftliche Neugierde.

Ich möchte mich auch bei den „Dobbelsteins“ für eine angenehme Arbeitsatmosphäre bedanken, ganz besonders jedoch bei Ulli, für nette Gespräche und bei Fred fürs allwöchentliche Fußballspielen.

Für die langjährige Freundschaft möchte ich mich bei Philipp F., Martin, Arne und Philipp B. bedanken.

Karen, vielen Dank für Deine Unterstützung und die schöne gemeinsame Zeit!

Mein ganz besonderer Dank geht an meine Familie. Es ist schön zu wissen, dass Ihr immer für mich da seid!

Curriculum Vitae

Nils Halbsgut

* 19.08.1979 in Lüneburg, Germany

Personal address

Ostlandweg 10
D-37075 Göttingen, GERMANY
Tel.: +49-551-2503891

e-mail: nhalbsg1@gwdg.de

Working address

Georg August University of Göttingen
Department of Stem Cell Biology
Justus-von-Liebig Weg 11
D-37077 Göttingen, GERMANY
Tel.: +49-551-39-13721

Education

- | | |
|-------------------|---|
| 05/2006 – now | Doctoral thesis in the Department of Stem Cell Biology, Georg August University of Göttingen
Title: “ Functional characterization of the gene <i>schlappohr</i> (CG7739) during development of <i>Drosophila</i> ” |
| 10/2005 – 12/2005 | Doctoral thesis at the Interfaculty Institute for Biochemistry, Eberhard Karls University Tübingen |
| 05/2004 – 03/2005 | Diploma thesis at the Max Planck Institute for Biophysical Chemistry, Göttingen, Department of Molecular Developmental Biology
Title: „Charakterisierung von <i>sarcoglycan</i> δ von der Fruchtfliege <i>Drosophila melanogaster</i> “ |
| 10/2000 – 03/2005 | Studies in biology at the University of Göttingen
Degree: Diploma in biology

Major subject: Developmental Biology
Minor subjects: Genetics and Zoology |
| 07/1999 – 06/2000 | Alternative civilian service at the Lebenshilfe gGmbH, Lüneburg |
| 06/1999 | Abitur (German high school diploma) |
| 08/1992 – 06/1999 | Bernhard Riemann Gymnasium, Scharnebeck |

Practical Training

- | | |
|--------------|---|
| 01 – 03/2006 | Internship in the editorial office at the Institute for Scientific Film (IWF) in Göttingen |
| 05 – 06/2004 | Lab rotation at the Max Planck Institute for Biophysical Chemistry, Department of Molecular Developmental Biology |

Teaching

- 06/2006, 05/2007, 05/2008, 10/2009 Supervision of short methods course for the Göttingen Graduate School for Neurosciences and Molecular Biosciences (GGNB)
Topic: "Confocal microscopy of whole mount preparations of *Drosophila* embryos"
- 03 – 04/2007 Supervision of a lab rotation project for the MSc/PhD Program in Molecular Biology
Topic: "Characterization of the function of CG7739, a potential new interaction partner of *Drosophila* PAR-3/ Bazooka in a *Drosophila* tissue culture system"
- 11/2006, 11/2007, 11/2008, 11/2009 Supervision of a course for the MSc/PhD Neuroscience Graduate Program
Topic: "Development of the Insect Nervous System"

Transferable skills

- 07/2008 Organization of the annual meeting of the Göttingen Center for Molecular Biosciences (GZMB Sommerfest)

Poster

Nils Halbsgut and Andreas Wodarz, Role of polarized vesicle trafficking during asymmetric cell division of *Drosophila* neuroblasts, 16th international society of developmental biologists congress, Edinburgh, September 2009; 18th Gesellschaft für Entwicklungsbiologie (GfE) meeting, Hannover, March 2009; SFB 523 "Protein and membrane transport between cellular compartments" Symposium, Göttingen, April 2008;

Nils Halbsgut, Diane Egger-Adam and Andreas Wodarz, Functional characterisation of CG7739 – a new potential interaction partner of Bazooka (Par-3), 6th GfE school, Günzburg, September 2006; 17th GfE meeting, Marburg, March 2007

Talks

CG7739, a novel *Drosophila* transmembrane protein with microtubule binding properties?
SFB523 retreat Schloss Ringberg, Tegernsee, October 2007